Spring 2020

NOVEL TOPOLOGIES IN POLYCYCLIC AROMATIC HYDROCARBONS: A STUDY OF TRIANGULENES AND OTHER MOLECULAR SHAPES

Carter James Holt
University of New Hampshire, Durham

NOVEL TOPOLOGIES IN POLYCYCLIC AROMATIC HYDROCARBONS: A STUDY OF TRIANGULENES AND OTHER MOLECULAR SHAPES

BY

CARTER J. HOLT

B.S., California State University, Chico, 2015

DISSERTATION

Submitted to the University of New Hampshire

in Partial Fulfillment of

the Requirements for the Degree of

Doctor of Philosophy

in

Chemistry

May, 2020

This dissertation has been examined and approved in partial fulfillment of the requirements for the degree of Doctor of Philosophy in Chemistry by:

Dissertation Director, Richard P. Johnson, Professor of Chemistry

Arthur Greenberg, Professor of Chemistry

Erik Berda, Professor of Chemistry

Glen P. Miller, Professor of Chemistry

Karsten Pohl, Professor of Physics

April 29, 2020

Original approval signatures are on file with the University of New Hampshire Graduate School.

DEDICATION

To my darling, my sweetness, my love.

Who helped me in every way imaginable. Even from 2,670 miles away.

ACKNOWLEDGEMENTS

First, I would like to express my sincerest gratitude to my PI and mentor, Richard Johnson, who has been a constant support system for me since day one of my graduate program. It was with his guidance and confidence in me that I was able to push past the seemingly insurmountable barriers of graduate research. From his daily check-ins, to general life advice, to discussions about new beers, there was never a time when he seemed unapproachable.

To my committee members, who have all taken time out of their busy schedules to assist me through this process and lend me valuable insights, thank you.

Past and present Johnson group members, who helped me get started in an unfamiliar lab and kept me happy every day at work. We were always a small group, but also the best group. (Unofficial Johnson group members included).

Cindi, Laura, Kristen, and the UIC, thank you all for working your magic and keeping this department running as smoothly as it does.

To Sarah, my best friend and lifetime partner, thank you for always being there for me and never letting me give up on my passions. You've always helped me see the light in this world, and our shared experiences are something I will cherish forever. Our next big life adventure awaits.

To my parents, brother, and family, thank you all for helping me get to this point in my life. Your constant support throughout the years has enabled me to set up my best possible future.

Lastly, I would like to thank the National Science Foundation for funding to make this research possible. Some computational data was obtained through the use of Extreme Science and Engineering Discovery Environment (XSEDE), which is supported by National Science Foundation grant number ACI-1053575.

TABLE OF CONTENTS

LIST OF SCHEMES

LIST OF FIGURES

LIST OF TABLES

ABSTRACT

NOVEL TOPOLOGIES IN POLYCYCLIC AROMATIC HYDROCARBONS:

A STUDY OF TRIANGULENES AND OTHER MOLECULAR SHAPES

by

Carter J. Holt

University of New Hampshire, May 2020

Triangulenes are the homologous series of triangle-shaped polycyclic aromatic hydrocarbons, first contemplated by chemists nearly 100 years ago. Computational models predict that triangulenes will be polyradicals, with high-spin electronic ground states. Recent technological advances have allowed the molecular-scale synthesis and on-surface characterization of the first three members of this series using atomic force microscopy techniques. In this work, a short and scalable synthesis of the [3]triangulene ring system was developed. Cascade cyclization of a tetra-benzyl alcohol precursor in trifluoromethanesulfonic acid solution gave the planar and three-fold symmetrical 4,8,12-trihydro[3]triangulenium carbocation. This new species has been characterized by NMR (nuclear magnetic resonance) and optical spectroscopies and is highly fluorescent. Quenching of the cation into basic solutions or by hydride transfer from triethylsilane provides access to stable dihydro and tetrahydro[3]triangulenes. Quenching with triethylamine gave isomerically pure 1,8-dihydrotriangulene, a known precursor to [3]triangulene. These neutral species interconvert with carbocations in a complex series of proton and hydride transfers. The presence and distribution of these cationic intermediates are determined by acid concentration and time spent in solution. With the help of density functional theory (DFT) calculations, a logical pathway to each isomer was proposed through a series of proton and hydride transfers.

This route provides several important [3]triangulene precursors. Preliminary experiments designed to generate [3]triangulene in the solution phase were performed. Reaction of 1,8-dihydrotriangulene with p-chloranil in solution was followed by NMR, optical spectroscopy, and LDI-TOF (laser-desorption-ionization time-of-flight) spectrometry. These experiments provided evidence for the formation and rapid oligomerization of [3]triangulene, consistent with the expectation of its high-spin ground state. The electrochemistry of 1,8-dihydrotriangulene was investigated for the first time. Experiments to date demonstrate a complex series of redox and chemical processes.

A related series of topologically interesting structures can be conceptually derived from triangulene by carving out one side and the center ring, or from phenalene by growing rings along two ring faces. When flipped on end, the resulting structure is V-shaped; herein, we refer to these structures as "victorenes." Viewed as phenalenyl homologues, the victorenes should not have a simple Kekulé aromatic structure. Also by analogy to the phenalenyl ring system, both the cations and anions in this series are likely to be aromatic. These structures are predicted by our DFT computations to be chiral, with low barriers to interconversion of enantiomers. A new and general synthetic route to victorenes was developed that allowed the preparation of two [3]victorene ketone derivatives. Slight modification of this route enabled the incorporation of substituents that block the reactive sites and afforded clean intramolecular cyclization to several hydro[3]victorenes. The relative free energies of hydro[3]victorenes were calculated using DFT and matched well with the experimental observations. Generation of the first victorenium cations was achieved in a TfOD/DCE-d_4 solution, with successful observation by ^{1}H NMR.

General Introduction

This dissertation is comprised of three separate chapters: (I) synthesis of 1,8-dihydrotriangulene and batch synthesis of triangulene, (II) electrochemistry of 1,8-dihydrotriangulene, and (III) the victorene series. Each chapter is self-contained with its own introduction, research objective, results and discussion, and conclusion. Additional projects not included in the content of this dissertation include efforts towards the mono-protection of 9,10-anthraquinone, generation and substitution of the triangulene dianion, and flow chemistry experiments for the optimization of mono-organolithium addition to 9,10-anthraquinone.

Chapter I. Synthetic Approaches to the Triangulene Ring System

Introduction

The History of Triangulene

Triangular-shaped hydrocarbons are a relatively rare class of polycyclic aromatic hydrocarbons (PAHs), and due to their unique topologies, there is no Kekulé-style resonance structure that can be drawn for them. Instead, they are predicted to exist with high-spin ground states (S ≥ 1/2) (Figure 1), both classically[1] and quantum mechanically.[2] These high-spin ground states make this class of molecules good candidates for applications in molecular spintronic devices[3,4] and possibly as qubits for quantum computers.[5] Structure **2,** known commonly as “Clar’s Hydrocarbon," is part of a broader set of homologues of [*n*]triangulenes starting with the well-known and studied phenalenyl radical[6–8] (**1**) up to “π-extended” triangulenes[9,10] (**3** and **4**). The numbering system for **2** is shown in Figure 1.

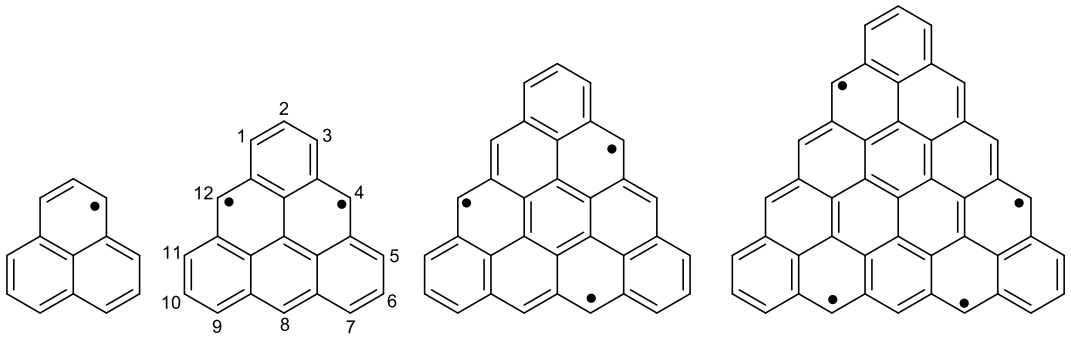

Figure 1: The [n]triangulene series (*n* = rings on a side).

Erich Clar is often cited as the father of triangulene chemistry; however, it was Weiß and Korczyn who synthesized the first triangulene 30 years before Clar’s seminal work.[11] This

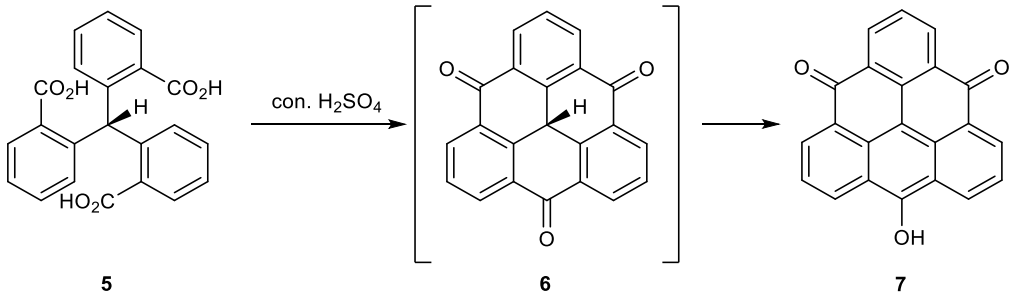

5 6 7

Scheme 1: First synthesis of triangulene core by Weiß and Korczyn.

synthesis involved the cyclization of the tricarboxylic acid (**5**) to give what was believed to be a triketone derivative of triangulene (**6**). In later attempts at repeating this chemistry reported by Bushby, it became evident that Weiß and Korczyn more likely isolated the diketone isomer (**7**)[12] (Scheme 1); nevertheless, this was the first reported synthesis of the triangulene core. Although this synthesis has been modified throughout the years, it remains the most common method for generating dihydrotriangulene, a known triangulene precursor.[13] Years later, using the same route as Weiß and Korczyn, Clar and Stewart attempted the synthesis of the [3]triangulene (**2**) in order to assess its molecular stability.[14,15] They were able to generate the 4,8-triangulenedione (**8**) successfully and, after subsequent reduction, 4,8-dihydrotriangulene (**9**) for the first time. All attempts to convert dihydrotriangulene to triangulene (**2**) led to immediate and complete polymerization (Scheme 2). The property of high-spin ground states that makes

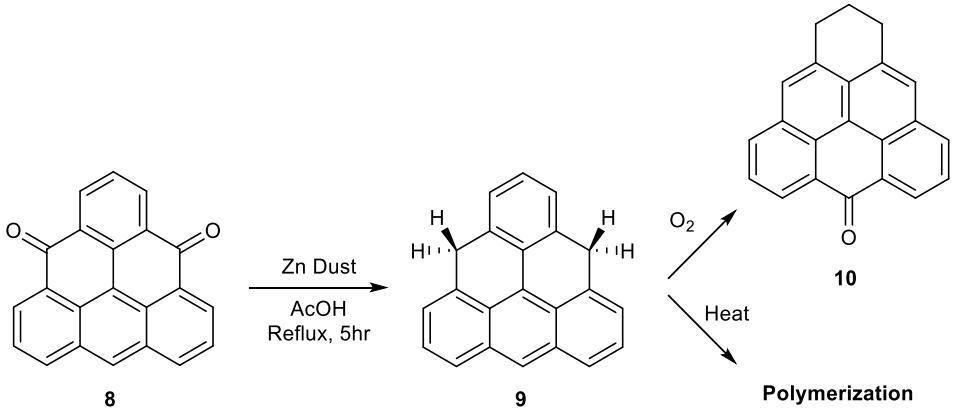

8 9 10

Scheme 2: Clar synthesis of 4,8-dihydrotriangulene (**9**) and olympicene ketone (**10**).

triangulene so attractive is also what makes it exceedingly difficult to isolate by conventional means due to its propensity towards polymerization and reaction with oxygen. Even the dihydro precursor **9** proved challenging to work with because it readily oxidizes in air to give a ketone (**10**). This rapid oxidation is similar to the air oxidation of 1*H*-phenalene (**11**) to phenalenone (**12**)[8] (Scheme 3), but much more complicated. The process involves a rearrangement as well as an oxidation; however, no mechanism of this pathway was provided. In Clar's research, the primary evidence to support the formation of these compounds was optical spectroscopy and

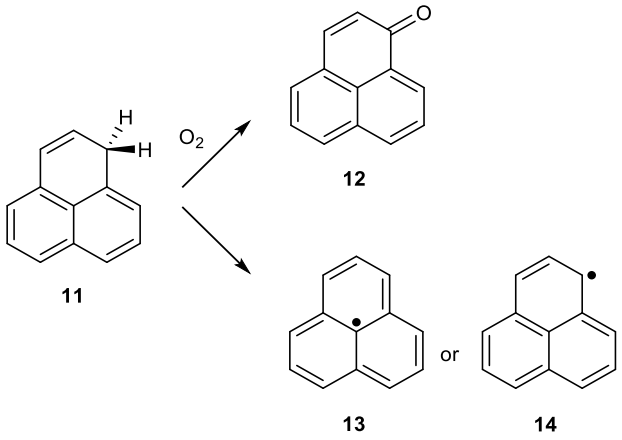

Scheme 3: Oxidation of 1H-phenalene to phenalenone and the phenalenyl radical.

elemental analysis since NMR was not yet available. This enhanced reactivity towards oxygen comes from the open-shell character of these compounds. The phenalenyl radical is surprisingly persistent, lasting months in degassed solution;[16] this is believed to support radical character localized at the central carbon[1]. Triangulene is theorized to exist as a diradical because no Kekulé style resonance structure can be drawn for it, unlike molecules such as benzene or naphthalene in which all carbon-carbon double bonds are accounted for. This property can be seen more clearly in Figure 3,[12] which compares triangulene to an isomer that can be described classically in terms of Kekulé structures. Here it can be seen how large a role topology plays in whether or not a structure can be represented classically. In the case of triangulene, a pair of electrons reside in non-bonding orbitals giving rise to its triplet ground state.

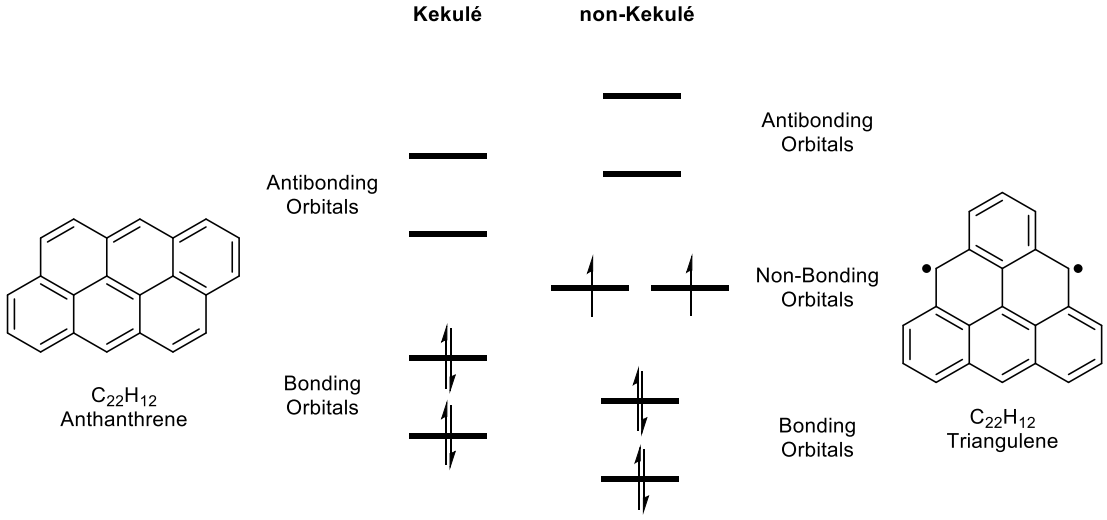

Figure 2: Comparison of the π-MOs of a Kekulé and a non-Kekulé system.

Triangulenes can be oxidized or reduced to make their respective dications and dianions. The dianion has been synthesized and observed by ^{1}H NMR spectroscopy, but the dication remains elusive.[17] In this NMR experiment, Murata *et al.* removed two protons from 1,8-dihydrotriangulene (**16**) using *n*-butyllithium in d_8-THF to give the fully aromatic triangulenyl dianion (**17**). The spectrum supports D_{3h} symmetry, indicating that the charges are fully delocalized throughout the triangulene structure (Scheme 4). Quenching of the reaction with D_2O led to clean conversion to the 1,8-dideuterotriangulene. Attempts at synthesizing the triangulenyl dication were unsuccessful, but the authors were able to generate the 4,8-dihydroxytriangulenyl dication (**15**) by the reaction of diketone **8** with D_2SO_4.

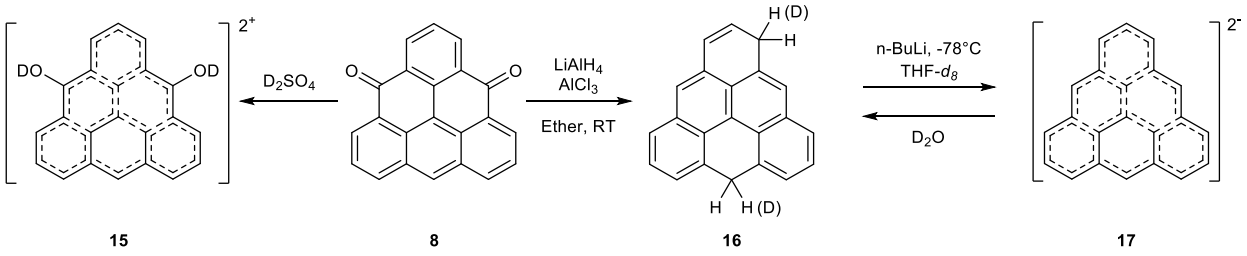

Scheme 4: NMR experiments for the triangulene dianion and dihydroxy dication.

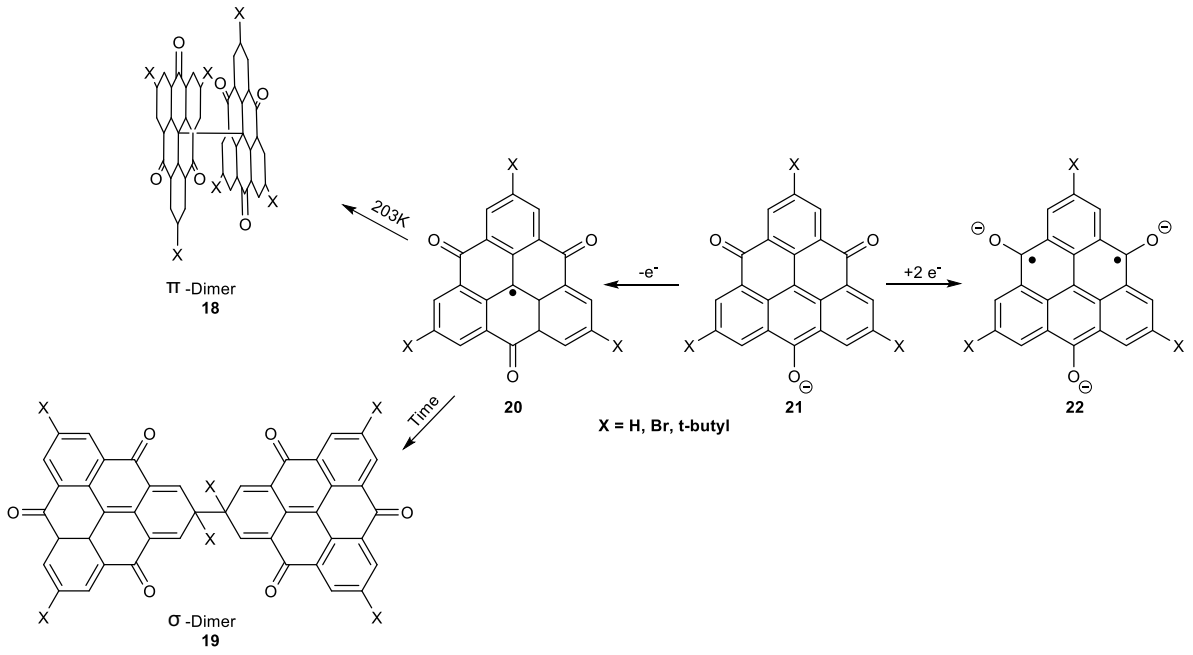

Scheme 5: Generation of tri-tertbutyl-triangulene diradical and subsequent oligomerization

Additional studies of substituted triangulene's radical properties have been reported by Bushby[12,18] and later by Morita[19–21]. In the former studies, the researchers synthesized a trioxotriangulene salt (**21,** X=H) using a modified Weiß/Korczyn route, that simplified the longer route described by Clar and Stewart.[14] Through cyclic voltammetry, the trioxotriangulene underwent successive one-electron reductions to give the diradical (**22**). These reductions were completely reversible, and each intermediate was chemically stable, being able to withstand slow sweep rates (ca. 10min), provided that the atmosphere was rigorously purged of oxygen. A follow-up EPR experiment of the diradical gave a spectrum indicating 3-fold symmetry in the molecular structure and confirmed the triplet ground state making this the first example of a non-Kekulé polynuclear aromatic.

Three years later, the Morita group began studies into the properties of substituted dioxophenalenyl radicals.[22] In this work, the radicals generated were only stable when di- and tri-tert-butyl substituents were installed in order to block the reactive sites. Samples were found to be stable over weeks but decomposed in a matter of days when exposed to air. As an

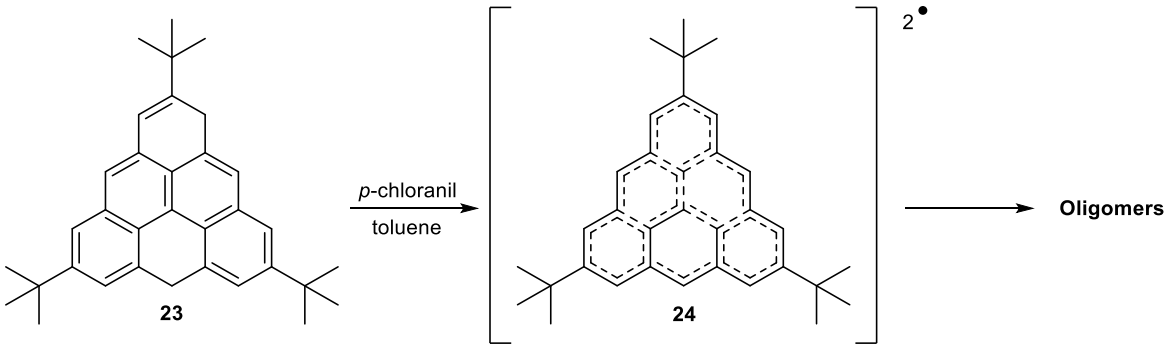

Scheme 6: Generation of tri-tertbutyl-triangulene diradical and subsequent oligomerization.

extension of this work, the Morita group synthesized a tri-tert-butyl triangulene (**23**) in order to probe its radical characteristics. The tert-butyl groups were placed on the apex carbons of dihydrotriangulene which, according to computations, are nodal points in the nonbonding molecular orbitals. In this way, the substituents had minimal electronic contributions to the core structure while reducing reactivity at the 4-, 8-, and 12-positions (Scheme 6). When this compound was exposed to an excess of *p*-chloranil in degassed toluene, initial EPR evidence suggested the formation of a radical cation of the dihydrotriangulene. However, as the temperature was increased from 253K to 273K, the emergence of a triplet diradical was observed (Scheme 6). This confirmed triangulene's predicted triplet ground state (**24**). When the sample was held at room temperature longer, the observed triplet ground state disappeared due to oligomerization at the highly reactive sites, indicating kinetic instability of the triplet ground state. Combining this work with that of Bushby, the Morita group synthesized tri-tert-butyl- and tri-bromo-trioxotriangulenes (**21**, X = t-butyl, Br) (Scheme 5).[20] With both compounds, a radical species was made that was stable in air at temperatures above 250°C. Crystallographic data showed a 1-dimensional columnar packing structure due to π-π stacking. CV analysis of the tri-substituted trioxyl anions showed oxidation to a centralized neutral radical and reduction to give the trianionic diradical. Seven years later, the Morita group repeated this same CV experiment on Bushby's unsubstituted trioxotriangulene and were able to observe the formation of the monoradical, which had not been previously reported.[19] As with the other trioxotriangulenes, the

unsubstituted radical was air-stable at temperatures up to 240°C in the solid state. In solution, however, the radical was observed to be in equilibrium with a π-dimer (**18**). EPR experiments indicated the observed resonance of the radical throughout the π-system occurred with three-fold symmetry. This observation decreased in intensity as the sample was cooled to lower temperatures due to the formation of the π-dimer. Further evidence for the dimeric structure was provided in a temperature-dependent NMR study in which the dimer was observable at low temperatures but disappeared as the sample was warmed to room temperature due to the formation of the paramagnetic species. σ-Dimerization of the radical was observed as well (**19**, X = H), but only after several days in a degassed solution. All of these studies suggest that trioxotriangulene radicals are much more stable than their hydrocarbon counterparts. A significant amount of this additional stability comes from the fact that the oxygen substituted triangulenes delocalize the radical further from what was already a highly delocalized system.

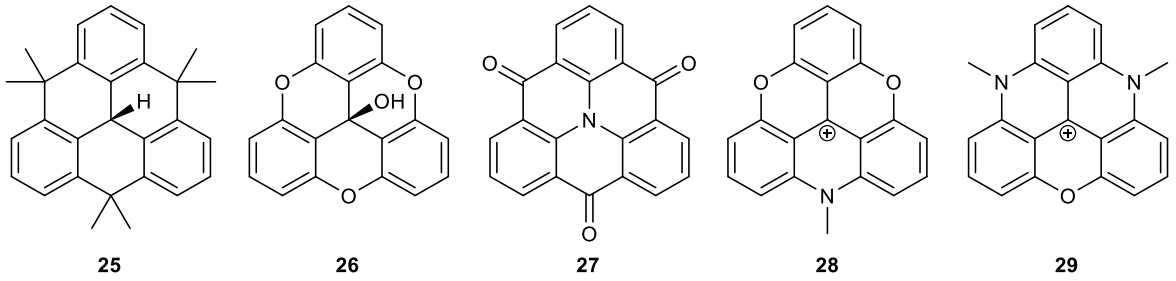

25 **26** **27** **28** **29**

Figure 3: Substituted and heterocyclic triangulenes.

Additionally, computations predict the highest spin density to be located on the central carbon making the periphery carbons less reactive. This is not the case with hydrocarbon only triangulene radicals whose highest calculated electron density resides on the periphery of the molecule.[7] It is because of this that hydrocarbon analogues have to be heavily substituted in order to prevent oligomerization (**23**, **25**).[21,23] Another option is to synthesize heterocyclic triangulenes (**26-29**), which are in general much more kinetically stable (Figure 3).[24–29]

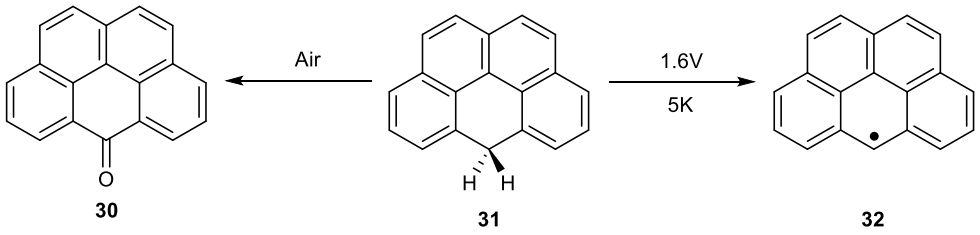

Scheme 7: Air oxidation of olympicene and generation of the olympicenium radical via removal of hydrogen atom.

The first synthesis of the unsubstituted triangulene diradical was reported by researchers at IBM using atomic force microscopy techniques.[13,30] The groundwork for this experiment was initially laid in 2009, where the team developed a new method for noncontact atomic force microscopy (NC-AFM) using a CO-functionalized tip on the microscope.[31] This type of functionalization increased the contrast of the AFM image and allowed for the atomic resolution of pentacene on top of a Cu(111) surface. Using this same technique, the IBM group was able to visualize and distinguish between isomers of hydro-olympicene (**31**) and its ketone (**30**).[32] They took the method one step further and applied a voltage to the methylene region of the molecule and were able to remove a hydrogen atom allowing for the first observation of the olympicenium radical (**32**) (Scheme 7). Two years later this method was applied to dihydrotriangulene, and after the removal of two successive hydrogen atoms, the first-ever observation of triangulene was realized (Scheme 8).[13] The AFM image confirmed triangulene's three-fold symmetric structure (Figure 4) and after comparing to simulated molecular orbitals, STM imaging confirmed the molecule as an open-shell triplet, nearly 100 years after the first

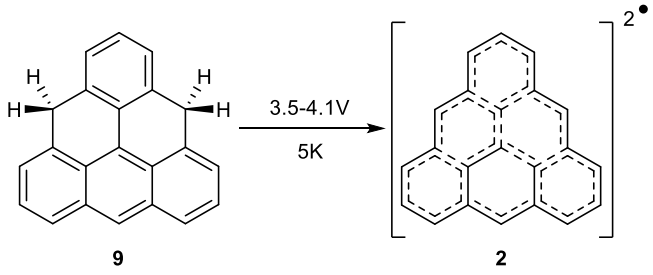

Scheme 8: Generation of triangulene diradical via removal of two hydrogen atoms.

triangulene was synthesized.[11] Following their lead, other research groups have used these techniques very recently to synthesize and visualize [4]-[9] and [5]-triangulenes[10] (**3, 4**) confirming their high-spin ground states containing three and four unpaired electrons, respectively (Figure 4). These recent advances have once again brought triangulenes into the spotlight, and questions of their stability and applications can finally be investigated.

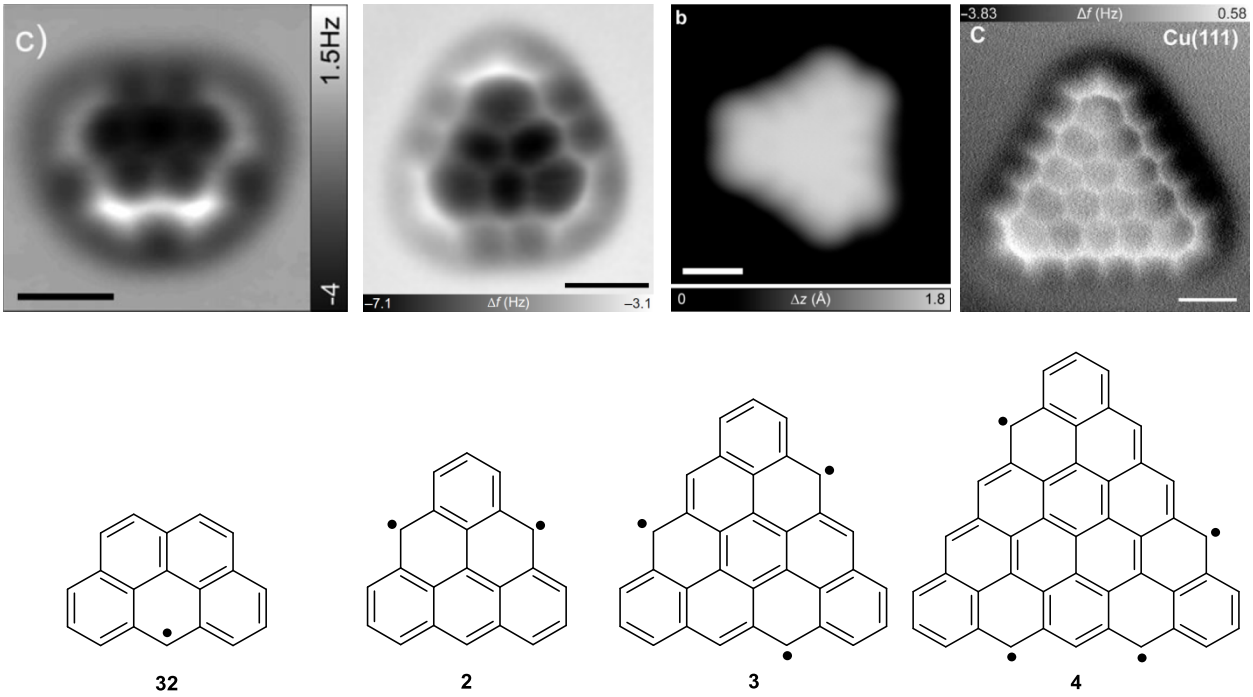

Figure 4: AFM images of olympicene and triangulene radicals. From Su, J. et al. Sci. Adv. 2019, 5, 1–6. Reprinted with permission from AAAS..

Research Objective

With the resurgence of interest in the triangulene molecular system, a more efficient route to its dihydro precursor must be developed. The present research aimed to provide a more straightforward synthesis of this precursor that can be modified for the incorporation of substituents to the periphery. Through DFT computations, we obtain a detailed understanding of the potential mechanisms involved in this fascinating system, which are further supported through experimentation. Efforts towards the solution-phase generation of triangulene provide insights into how this species reacts and can be tuned to reduce its reactivity.

Results and Discussion

Initial Routes to Dihydrotriangulene

Despite several drawbacks, the Weiß/Korczyn route to triangulenes (Scheme 9) is still the most widely used pathway in the field. This synthesis has been modified and improved throughout the years,[12,13] but still involves six linear steps and has an overall yield of only 5%. Furthermore, the final reaction, reduction of the triangulene diketone **8** to dihydro triangulene **9**, has only been performed on a milligram scale and gives a mixture of isomers that cannot be separated. For a molecular system with so much potential in the field of materials chemistry, this is an unacceptable outcome. An improved synthesis of triangulene precursors is necessary in order to further its study.

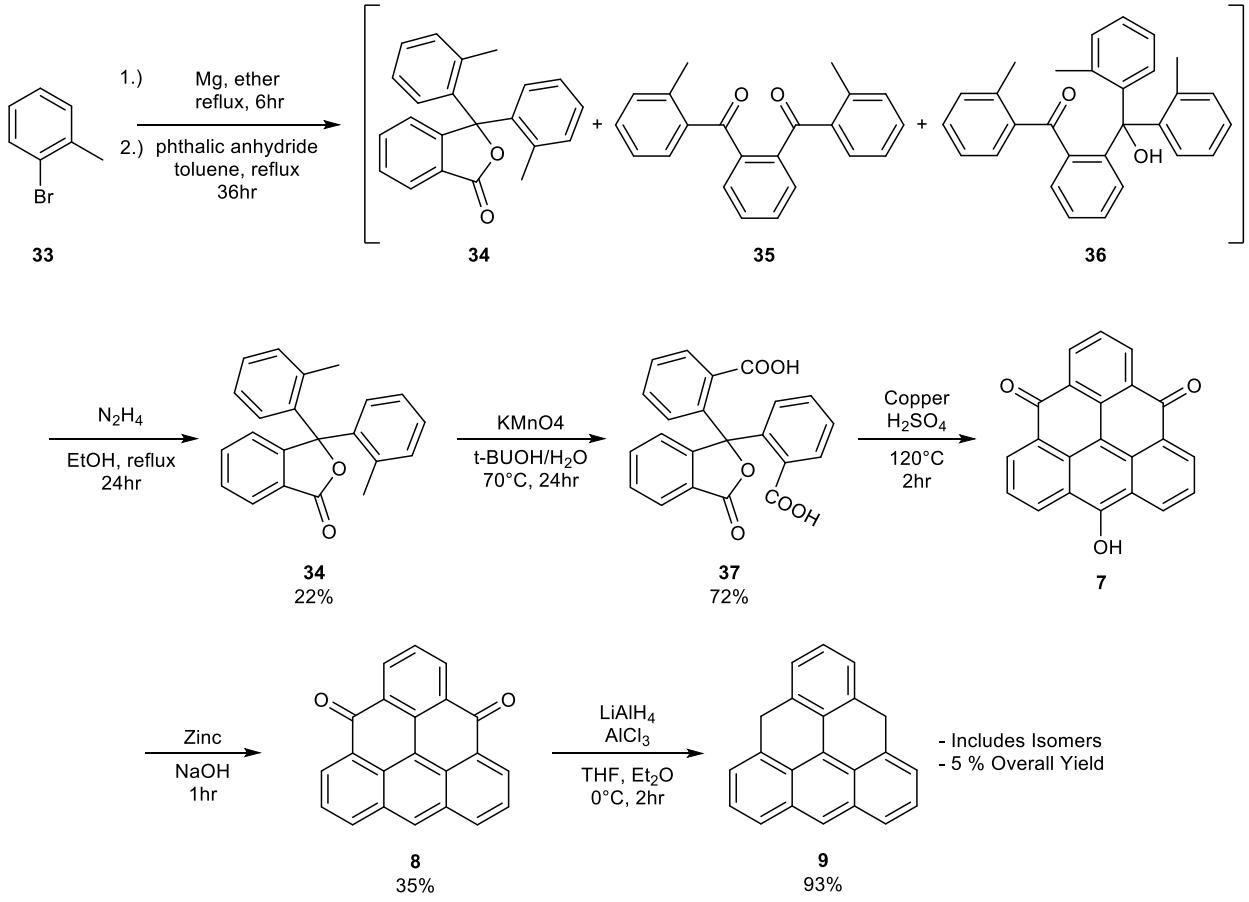

Scheme 9: Most common synthetic route to triangulenes.

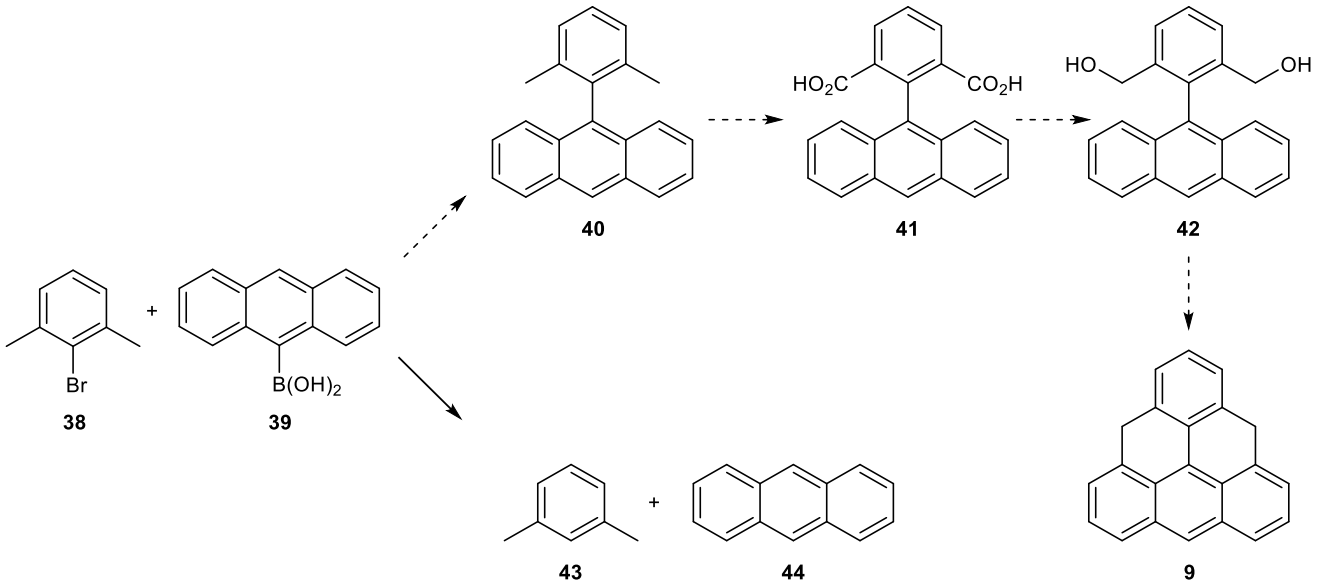

Scheme 10: Attempted synthesis of 9-(2,6-dimethylphenyl)anthracene via Suzuki coupling.

The first synthetic pathway that we proposed in order to improve the synthesis of dihydrotriangulene (Scheme 10) involved the coupling of 2-bromo-m-xylene (**38**) to 9-anthraceneboronic acid (**39**). From there, the methyl groups were to be oxidized to carboxylic acids (**41**) and ultimately converted to a diol (**42**) as a dihydrotriangulene precursor. This route failed. All attempts at the Suzuki coupling reaction were unsuccessful due to complete protodeboronation and protodebromination giving xylene (**43**) and anthracene (**44**) as the only products. In the literature, the coupling of bulky aryl groups to 9-anthraceneboronic acid involves the use of exotic catalysts to facilitate the process (Scheme 11).[33–35] Although these catalysts are claimed to work very well for the exact reaction we intended to perform (86 – 98% yield), none of them is commercially available, and their syntheses are long and challenging. It became clear that this route would not be successful without the use of these special catalysts.

The next route chosen involved organolithium chemistry in performing the coupling step (Scheme 12). This chemistry was modeled after work done by the Miller group,[36] but a mono-addition was implemented instead of a di-addition. In order to facilitate mono-addition, the

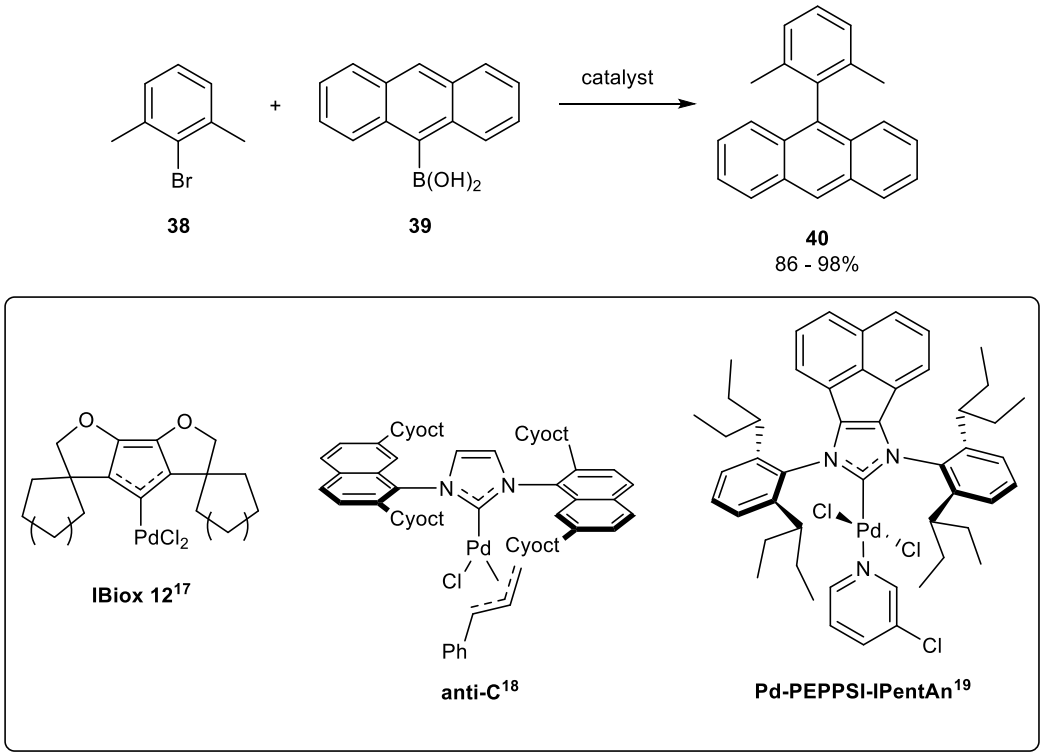

Scheme 11: Synthesis of 9-(2,6-dimethylphenyl)anthracene with catalysts.

organolithium reagent was generated and transferred dropwise *via* cannula to a dilute solution of a 2-fold excess of 9,10-anthraquinone to give the mono-substituted ketone (**45,** 26%). From there, the ketone needed to be reduced in order to perform the reductive aromatization step. Initially, $NaBH_4$ was used for the reduction, but this showed little to no conversion to the desired diol. Conversely, $LiAlH_4$ gave quantitative conversion to the diol (**46,** 100%). From there, the diol was reductively aromatized using NaI and $NaH_2PO_2 \bullet H_2O$ in refluxing acetic acid to give the fully aromatic mono-substituted adduct (**40**, 30%). Unfortunately, all attempts at oxidizing the methyl substituents to carboxylic acids (**41**) failed, either giving back starting material or insoluble products. Further attempts at substituting the methyl groups involved NBS bromination to give the dibenzyl bromide (**47**). However, the bromination only occurred at the 10-anthracenyl position (**48**, 90%) instead of the benzyl position. This result implies that ionic bromination is favored over free radical bromination for this system.

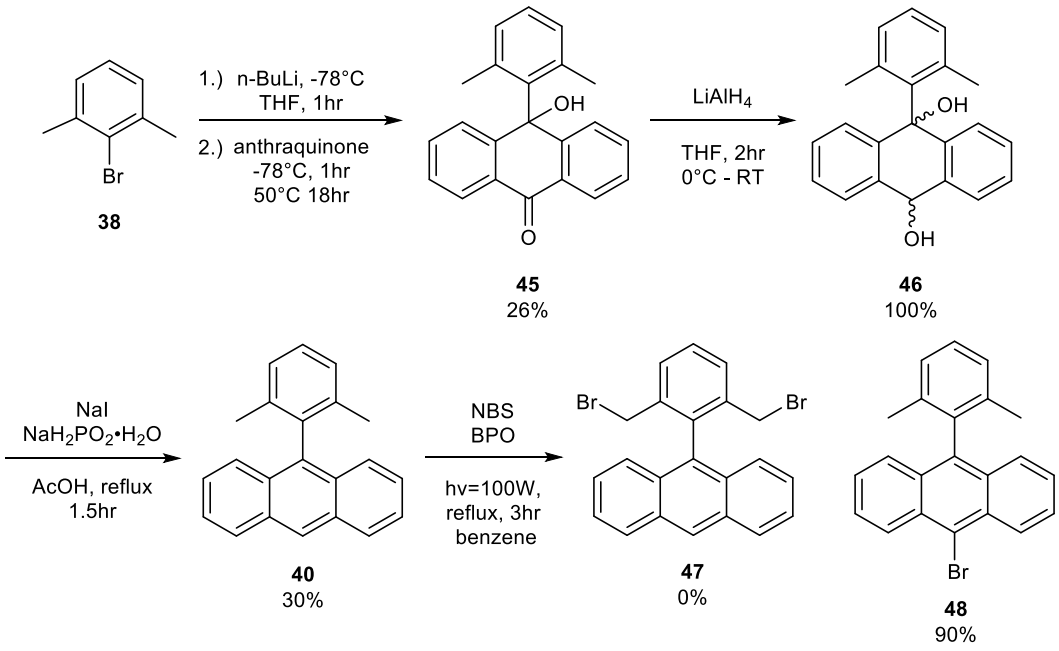

Scheme 12: Attempted synthesis of triangulenes through mono-organolithium addition and NBS bromination.

In order to bypass the difficulties encountered with post-synthetic modification of the benzyl groups, the route was modified again to have the benzyl alcohols pre-installed during the initial coupling reaction. This chemistry would require the synthesis of 2-bromo-1,3-benzenedimethanol (**51**) and subsequent protection in order to withstand the organolithium reaction conditions. The synthesis of the diol was carried out following a literature procedure[37] (Scheme 13) beginning with the oxidation of commercially available 2-bromo-m-xylene (**38**) to

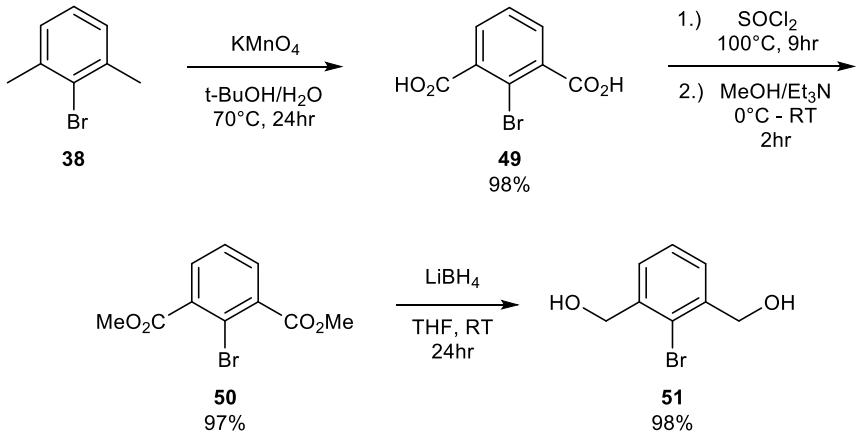

Scheme 13: Synthesis of 2-bromo-1,3-benzenedimethanol.

the dicarboxylic acid (**49,** 98%). This was followed by conversion to the methyl diester (**50**, 97%) using thionyl chloride, followed by MeOH/Et_3N. The diester was finally reduced to the diol using $LiBH_4$ (**51**, 98%). There are many options for alcohol protecting groups; however, few meet the necessary requirements of the desired chemistry.[38] Ideally, the diol would be protected in high yield (>90%), be stable under strongly nucleophilic conditions, resist decomposition under strongly acidic conditions, and finally be removed quantitatively.

The first protecting group used was the THP-ether. In a model experiment, an excess of THP-protected alcohol (**52**) was used to afford a mixture of diastereometric spirocycles (**53**, 38%) in a 1:3 ratio (Scheme 14). The mixture of spirocycles was reacted with polyphosphoric acid in the microwave in an attempt to induce cyclization. This type of cyclization was expected to yield two potential regioisomers (**54** and **55**); however, only regioisomer **54** was observed in 20% isolated yield. This compound has been previously reported using a different route.[39,40]

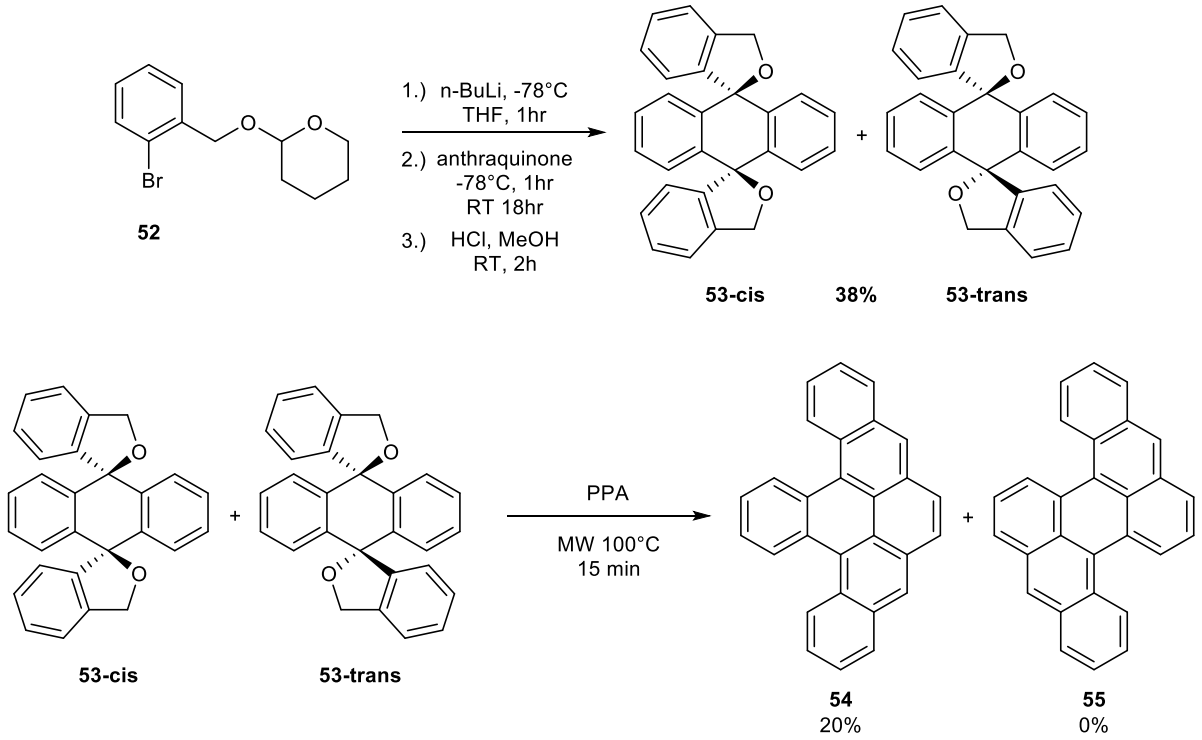

Scheme 14: Synthesis and cyclization of spirocycles.

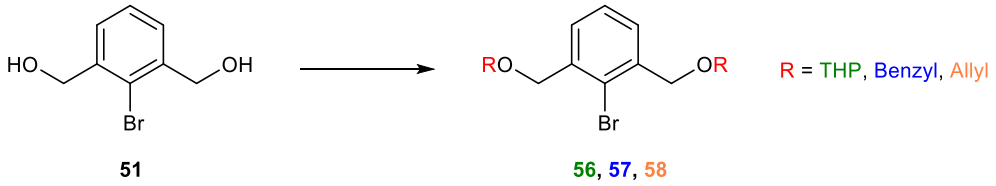

Scheme 15: Ether protection of bromobenzyl diol.

R Group	Protection >90% Yield	Organolithium Stability	Acid Stability at RT	Deprotection >80% Yield
THP Ether	✓	✗	✗	✗
Benzyl Ether	✗	✓	✓	✗
Allyl Ether	✓	✓	✓	✓

Table 1: Reaction summary of protected diols.

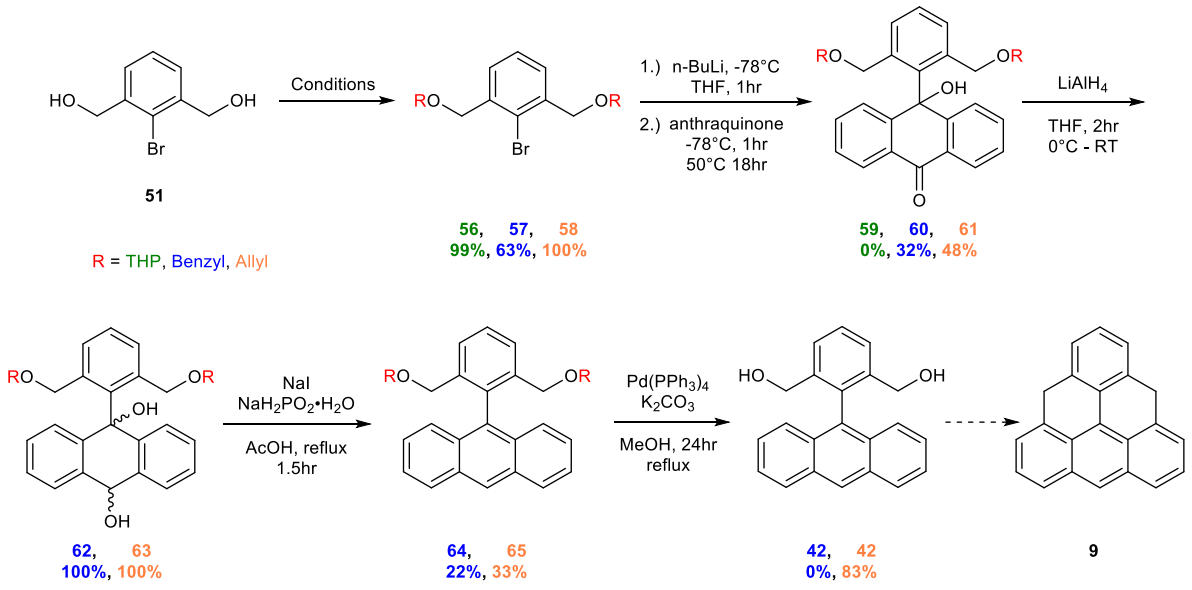

Scheme 16: Mono-organolithium addition of allyl-protected diol towards triangulene.

The ether was then easily installed on the diol using 3,4-dihydropyran and catalytic *p*-TsOH to give the THP-protected diol (**56**, 99%). The monoaddition to anthraquinone was carried out, but no ketone (**59**) was observed (Scheme 16). Due to the acid sensitivity of the THP-protecting group, the benzyl ether protecting group was used next. This protecting group can

withstand conditions of pH=1 at ambient temperature[38], making it a better candidate. This was installed using a Williamson ether synthesis approach to give the benzyl protected diol (**57**, 63%). The protecting group remained intact for the mono-addition reaction as well as the acidic quench to give the ketone (**60**, 32%). This was subsequently reduced to give the diol (**62**, 100%). Surprisingly, the benzyl ether protecting group remained attached, even under the reductive aromatization conditions, which involves refluxing acetic acid, to give the fully aromatic diprotected diol (**64**, 22%). A typical procedure for removing benzyl ether protecting groups is to use palladium-catalyzed hydrogenation;[41] however, several attempts using this method failed, giving back starting material. This, combined with the fact that acidic removal of the protecting group was not an option, led to the need for yet another protecting group.

For this, the allyl ether was chosen; this meets all of the necessary requirements (Table 1) despite being acid-sensitive at temperatures higher than 100°C.[38] The protection was carried out using a modified procedure for the allyl-protection of benzyl alcohols.[42] The procedure needed to be modified due to issues with the solubility of the diol, which ultimately led to low yields of the protected product (**58**, >50%). The key was to use sonication to facilitate the dissolution of the diol. Using this technique, the di-protection proceeded quantitatively and only required room temperature conditions instead of the reflux referenced in the procedure. Even though allyl-ethers are typically acid labile at elevated temperatures, in this case, they behaved just like the benzyl ether. They withstood all reaction conditions to give the fully aromatic allyl-protected diol (**65**, 33%), Scheme 16. The deprotection was again modeled after a literature procedure for similar benzyl alcohols[43] and used $Pd(PPh_3)_4$ with K_2CO_3 in refluxing methanol to give the aromatic diol (**42**, 83%). All cyclization attempts with **42** led to complex oligomerized product mixtures. Even though the preliminary goal of generating the aromatic diol was reached, the ultimate goal of creating a more efficient synthesis of dihydrotriangulene was not. This route involves eight linear steps, has a 13% overall yield, and a cyclization that led to a complex

mixture of products. It is because of this that a fourth and final route was planned to optimize the synthesis of dihydrotriangulene.

Cascade Cyclizations Towards Dihydrotriangulene

The idea was to take advantage of triangulene's 3-fold symmetry and install this in the first step (Scheme 17). This was possible through the condensation of three equivalents of allyl-protected bromobenzyl alcohol (**66**) with diethyl carbonate to give the allyl-protected triarylmethanol (**67**, 95%). From here, the compound was either deprotected directly to give the tetraol (**68**, 85%) or reduced and then deprotected to give the triol (**70**, 67%). Purification of these alcohols by chromatography proved difficult due to their high polarity; however, they were easily isolated by suspension in a hexanes/DCM mixture to give a precipitate that was filtered and rinsed with hexanes to give the desired products. Both of these alcohols are new compounds and have potential applications on their own as polymer scaffolds, as building

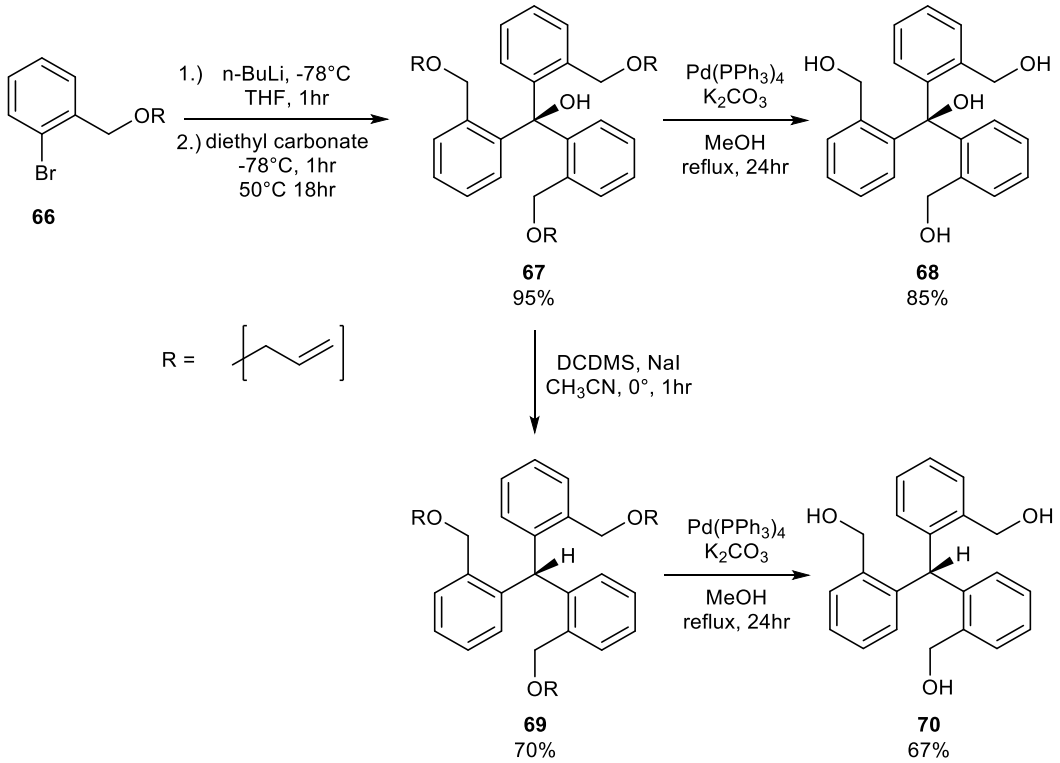

Scheme 17: Condensation of protected bromobenzyl alcohol towards triangulene precursors.

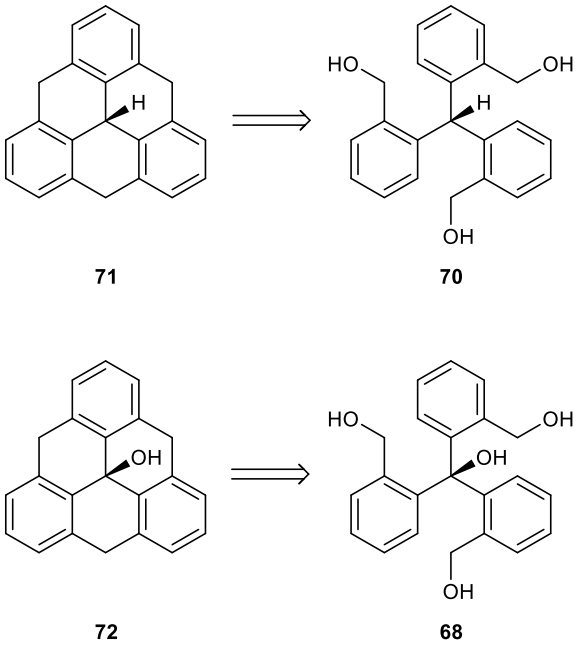

Figure 5: Retrosynthetic approach to triangulenes from alcohol precursors.

blocks in porous organic cages, or as new ligands. However, in this research, they were envisioned as potential precursors to triangulenes (**71** and **72**) (Figure 5).

The next synthetic challenge was cyclization. Preliminary attempts to cyclize tetraol **68** were carried out using Lewis-acids which are known to facilitate benzyl cation formation and subsequent intramolecular cyclization, including $FeCl_3$,[44] $AgSbF_6$,[45] and BF_3•Et_2O.[46] However, in all cases incomplete cyclizations and complex oligomeric product mixtures were observed, with low mass recoveries.

In a unique experiment, tetraol **68**, dissolved in DCM, was added dropwise to a refluxing biphasic mixture of DCE, water (10% v/v) and polyphosphoric acid (1% v/v) (Scheme 18). After the reaction was quenched, the only product observed was an off-white solid identified as spirocycle (**73**, 97%). This observation implies initial ionization of the central carbon atom and capture of the resultant cation by a proximate benzyl alcohol.

The key to complete cyclization was provided by an NMR experiment in which the tetraol was dissolved in DCE-d_4 and 1M TfOD to give a dark green solution. NMR analysis was carried

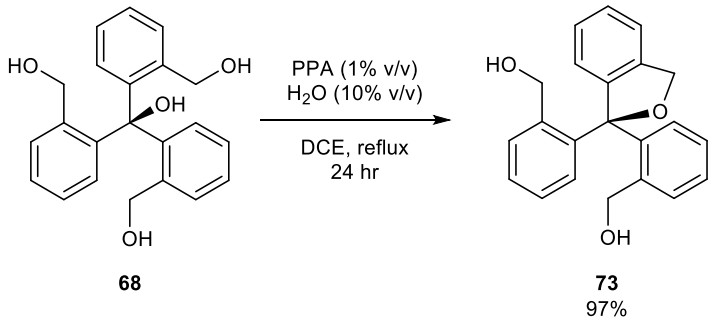

Scheme 18: Acid-catalyzed cyclization of tetraol to give spirocycle (**73**).

out immediately at room temperature to show very simple ^{1}H and ^{13}C spectra, with three unique hydrogens and six unique carbons, Figure 10. These data support the formation of the highly symmetrical 4,8,12-trihydro[3]triangulenium ion (**74**) (Scheme 19). DFT computations using the ωB97X-D/6-31G* level of theory predict this structure to have D_{3h} symmetry, and the calculated chemical shift of the central cation (173.8 ppm) is in good agreement with the experimental value (168.7 ppm). It should be noted that when triol (**70**) or spirocycle (**73**) were used in the same experiment, the same cation was observed, indicating a similar mechanism of cyclization. In all cases, samples of the cation were stable for over 24 hours in DCE-*d*$_4$/TfOD solution.

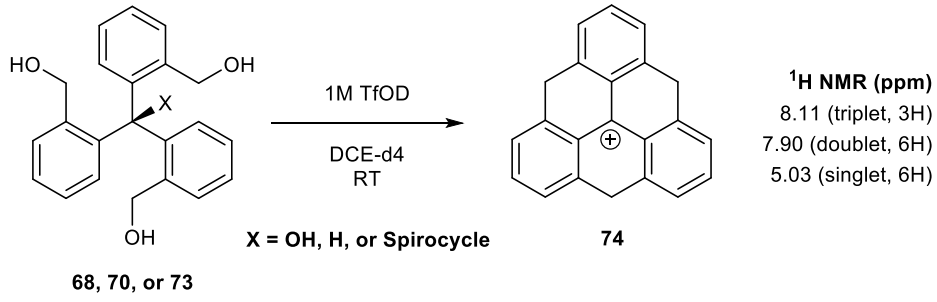

Scheme 19: NMR experiment for cyclization of alcohol precursors.

UV-vis experiments carried out in collaboration with Katelyn Wentworth provided more evidence for the proposed structure of **74**. The spectrum showed a pair of absorption bands (λ_{max} = 404.5 and 463.5 nm) (Figure 6). This can be compared to the well-known triphenylmethyl cation (**75**), which also has two has two absorption bands with λ_{max} = 411.5 and 433.5 nm.

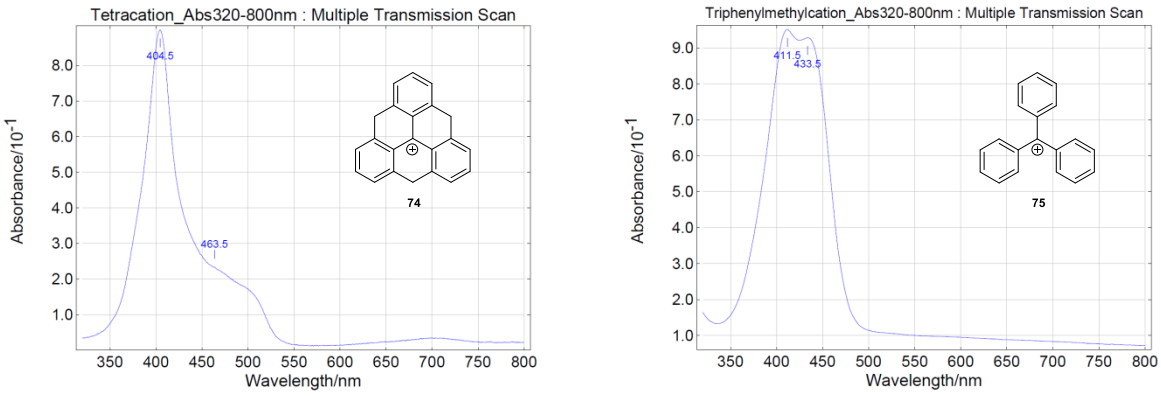

Figure 6: Absorption spectra for triangulene cation (**74**) and trityl cation (**75**).

The red shift of **74** relative to **75** can be explained by enhanced conjugation of the triangulene system due to its planar structure. This is not found in the trityl cation **75**, which adopts a propeller conformation.[47] In both cases, the two absorption bands arise from excitations to the LUMO from pairs of degenerate bonding orbitals. Computations accurately predict the relative intensities of these absorption bands but overestimate their excitation energies. This has previously been observed for carbocations of PAHs[48].

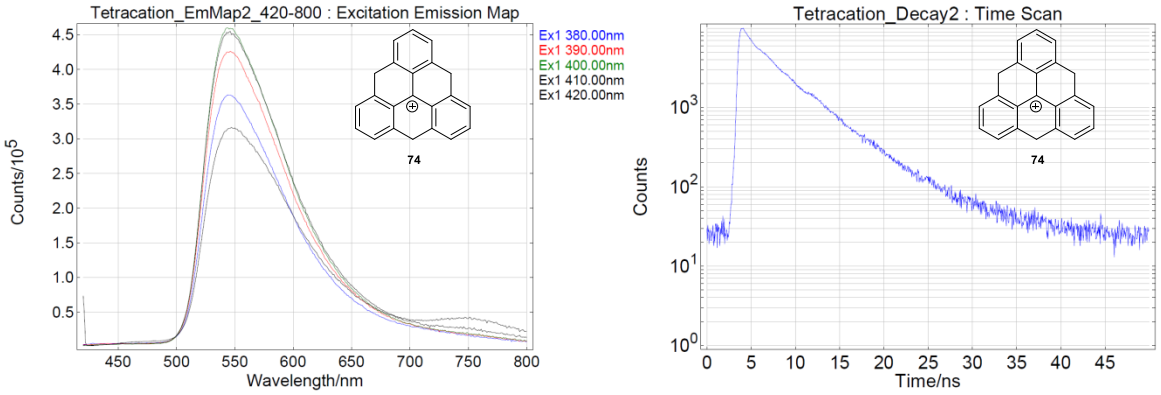

Figure 7: Emission map scan of triangulene cation (left) and fluorescence lifetime experiment (right).

The solutions used in the UV-Vis measurements were also used for fluorescence. The cuvette was placed in the spectrofluorometer, and an emission map scan was run using five wavelengths. These wavelengths were chosen based on the λ_{max}, this wavelength, and 10 nm

and 20 nm above and below it (Figure 7). The wavelength producing the maximum emission was used for generating the reported emission scan (Figure 7). For emission measurements, the sample was loaded into the instrument with a light blocker behind it, and a 405 nm laser was used as a light source. A lifetime measurement was run over 45 min. Following the acquisition of data, an IRF function was added by generating an experimental deconvolution fit. Tau values were guessed for a polynomial series to generate the lowest value X^2 for the best fit. This study gave a fluorescence lifetime of ~5 ns for the triangulenium cation and showed significantly stronger fluorescence relative to the trityl cation, (Figure 8). Enhanced fluorescence emission is attributed to the rigidity of the triangulenium cation induced by its more planar structure. The observed fluorescence lifetime is lower than that found for similar heterocyclic triangulenium salts (~20 ns),[27] but could be improved by the addition of substituents.[24]

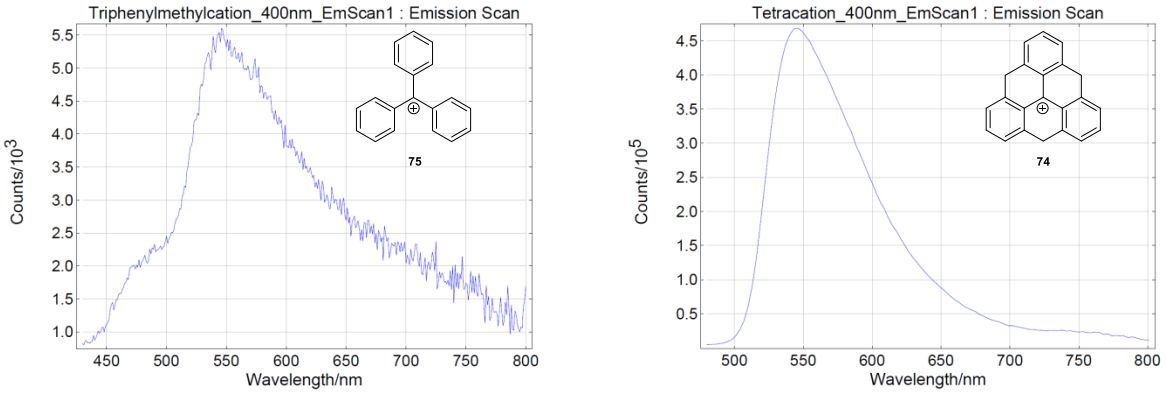

Figure 8: Emission scans comparing trityl cation (**75**) (left) and triangulene cation (**74**) (right).

With the triangulenium cation fully characterized, the next goal was to quench the cation and optimize the synthesis of dihydrotriangulene. To accomplish this, a variety of quenching conditions were used (Scheme 20), to give di- and tetrahydrotriangulenes (Table 2). The initial quenching conditions involved adding a solution of the cation (**74**) into saturated aqueous $NaHCO_3$. After purification, the product was found to contain tetrahydrotriangulene (**76**, 27%) and dihydrotriangulene (**16**, 53%), with the remaining 20% believed to be a complex mixture of

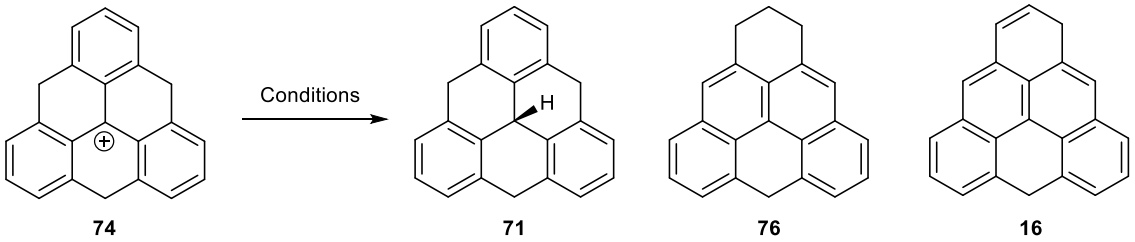

Scheme 20: Cation conversion to dihydro- and tetrahydrotriangulenes.

Reduction Conditions	71	76	16	Total Yield
Et_3SiH/DCM	38%	9%	49%	96%
sat. $NaHCO_3$	-	27%	53%	80%
Et_3N/DCM	-	-	66%	66%

Table 2: Isolated yields of dihydro- and tetrahydrotriangulenes

oligomeric products. Formation of the tetrahydrotriangulene **76** was unexpected. This novel compound resembles olympicene (**31**) in structure[32] but has an additional saturated ring on top. The di- and tetrahydrotriangulenes are isolable through column chromatography, but only with difficulty and often more than one column. A different quenching reagent was required in order to generate the dihydrotriangulene selectively. For this, a dilute solution of triethylamine in DCM was used. The rationale was to exclude aqueous solvents which can facilitate rearrangements and thus give unwanted side products. These quenching conditions were selective for generating 1,8-dihydrotriangulene (**16**) exclusively in 66% isolated yield. 1,8-Dihydrotriangulene is a known compound,[17] but has only been made previously using the Clar route[14] through reduction of the diketone precursor (**8**). In modern attempts of this synthesis, researchers are only able to achieve a 5% overall yield on a milligram scale to give a mixture of inseparable isomers in six linear steps.[13] Our synthesis involves four steps with an overall yield of 53% to give one isomer exclusively, and it can be run on a multi-gram scale, making it the current best synthesis of 1,8-dihydrotriangulene, a known triangulene precursor. Furthermore, our route provides a unique opportunity for facile substitution of triangulenes at the 4,8,12-positions by the

addition of organolithium reagents to the trialdehyde (**77**) before cyclization (Scheme 21). This is easily made by oxidation of **70** with PCC.

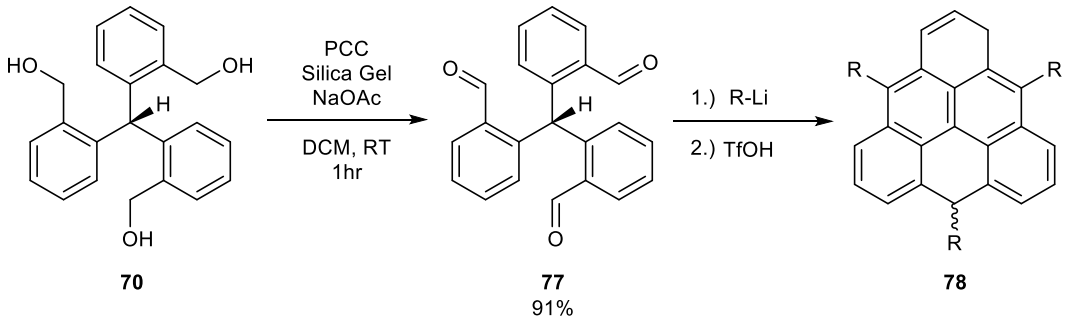

70 **77** 91% **78**

Scheme 21: Oxidation of triol (**70**) for facile substitution of triangulenes.

In a third quenching experiment using triethylsilane, a mixture of three triangulenes was observed with an isolated yield of 96%. In this case, the olympicene-like triangulene (**76**, 9%) and 1,8-dihydrotriangulene (**16**, 49%) were formed in addition to a new tetrahydrotriangulene (**71**, 38%) all of which were separable by column chromatography. DFT calculations predict this structure to be moderately bowl-shaped (Figure 9). ^{1}H NMR supports the proposed structure with the central methine hydrogen appearing as a quartet (J = 5.5 Hz) due to long-range coupling with the three pseudoaxial methylene protons. Similar ^{5}J homoallylic coupling has been observed in 1,4-cyclohexadienes.[49]

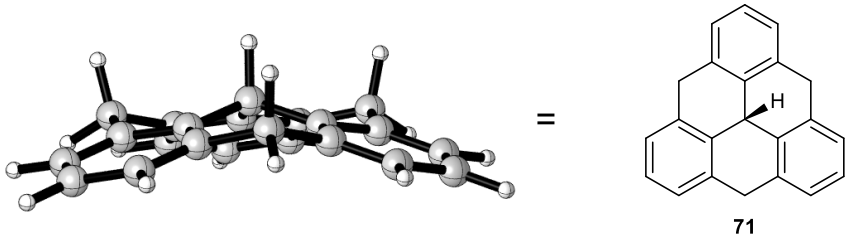

71

Figure 9: Bowl-shaped tetrahydrotriangulene (**71**).

Dihydrotriangulenes are known to readily undergo air oxidation,[13,14] but their oxidation products have not been well-characterized, and the oxidation of tetrahydrotriangulene (**76**) has not been previously studied. In a simple experiment, a pure sample of **76** was dissolved in DCE

and allowed to stir while being exposed to air overnight. The characteristic yellow-green color of the tetrahydrotriangulene changed to bright red (Scheme 22), indicating that oxidation had taken place. ^{1}H NMR analysis of the crude reaction mixture showed the formation of the olympicene ketone (**10**) in a 1:5 ratio relative to its tetrahydrotriangulene precursor as well as a complex mixture of decomposition products. Surprisingly, this same ketone was described by Clar as an oxidation product of 4,8-dihydrotriangulene (**9**); however, no mechanistic rationale of this product formation was provided.[14] Similarly, we find that a triangulene diketone (**79**) can be synthesized from dihydrotriangulene (**16**) by simple exposure to air. This is a slow process, with only low conversion over 24 hours. In an unusual reaction, this can be prepared more efficiently using an excess of TEMPO as an oxidant to give the diketone as a dark red solid (44%), (Scheme 23).

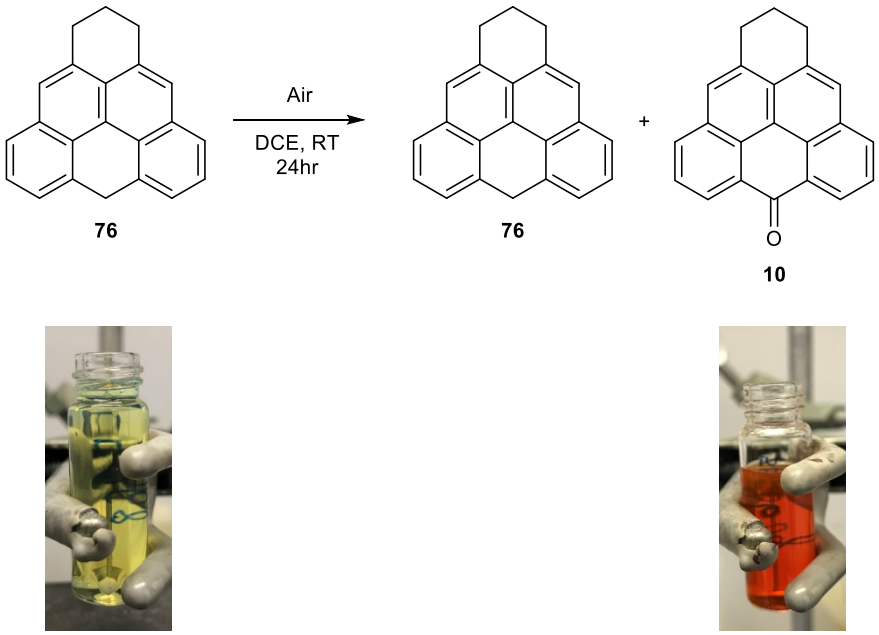

Scheme 22: Air oxidation of olympicene tetrahydrotriangulene (**76**) to olympicene ketone (**10**).

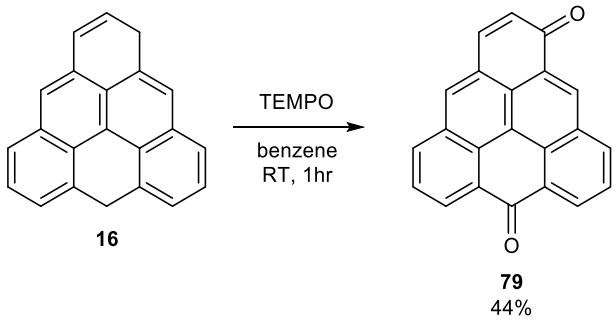

16

79
44%

Scheme 23: TEMPO oxidation dihydrotriangulene to diketone (**79**)

Experimental and Computational Models for Triangulene Interconversions in Acidic Media

The formation of the olympicene-like tetrahydrotriangulene (**76**) cannot be explained using a simple rearrangement mechanism because it is not isomeric with dihydrotriangulene. Therefore, a more intricate pathway to the observed products must be envisioned. The triangulenium cation (**74**) is the expected product from the complete cyclization of the tetraol (**68**). Scheme 24 shows the likely interconversions involved in going from the central triangulenium cation (**74**) to the olympicene tetrahydrotriangulene (**76**) through a series of proton and hydride transfers. In this scheme, isomers are labeled and color-coded in order to make comparisons easier. All free energy calculations were performed using the IEFPCM(DCE)/B3LYP/6-31+G(d,p) level of theory using both Spartan[50] and Gaussian 09.[51]

Starting with triangulenium cation (**74**), simple hydride addition gives the bowl-shaped tetrahydrotriangulene (**71**). In the other direction, initial deprotonation gives 4,8-dihydrotriangulene (**9**) which, through the loss of a hydride, gives C4 protonated triangulene (**80**). Hydride addition to this gives the observed neutral 1,8-dihydrotriangulene (**16**). Protonation of the vinyl carbon gives a high energy intermediate cation (**81**) which, after hydride addition, gives the neutral olympicene tetrahydrotriangulene (**76**). This neutral species can undergo one final loss of hydride to give the olympicenium cation (**82**). When comparing the relative free energies of neutral $C_{22}H_{16}$ isomers, it becomes clear that the bowl-shaped tetrahydrotriangulene

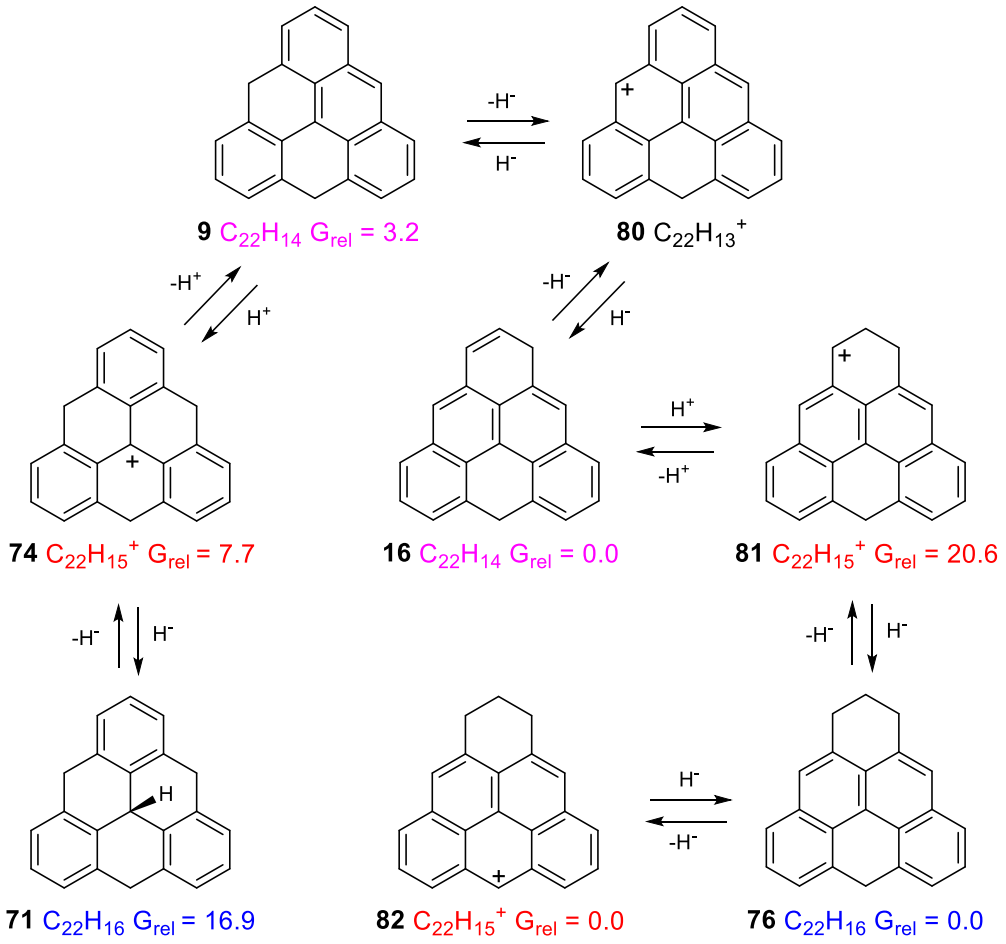

Scheme 24: Interconversions of neutral and cationic triangulene species, with relative free energies (kcal/mol).

(**71**) is not the thermodynamically favored product and should rearrange to the more stable olympicene tetrahydrotriangulene (**76**). Despite this, the bowl-shaped tetrahydrotriangulene is observed experimentally. Structure **71** is likely the kinetic product of hydride addition to **74**. Another factor is that the reaction must go through high energy cationic intermediate (**81**) to get to **76**. 1,8-dihydrotriangulene (**16**) cannot be compared to these compounds because they are not isomeric; however, it must be relatively stable because it is the major product in all experiments tested. Surprisingly, 4,8-dihydrotriangulene (**9**) was not observed in any experiments. This isomer is predicted to be relatively close in energy to 1,8-dihydrotriangulene (ΔG = 3.2 kcal/mol). 4,8-Dihydrotriangulene (**9**) is likely too acid-sensitive to be observed in this experiment because of facile protonation to the anthracene group.

NMR Experiments for Further Mechanistic Understanding

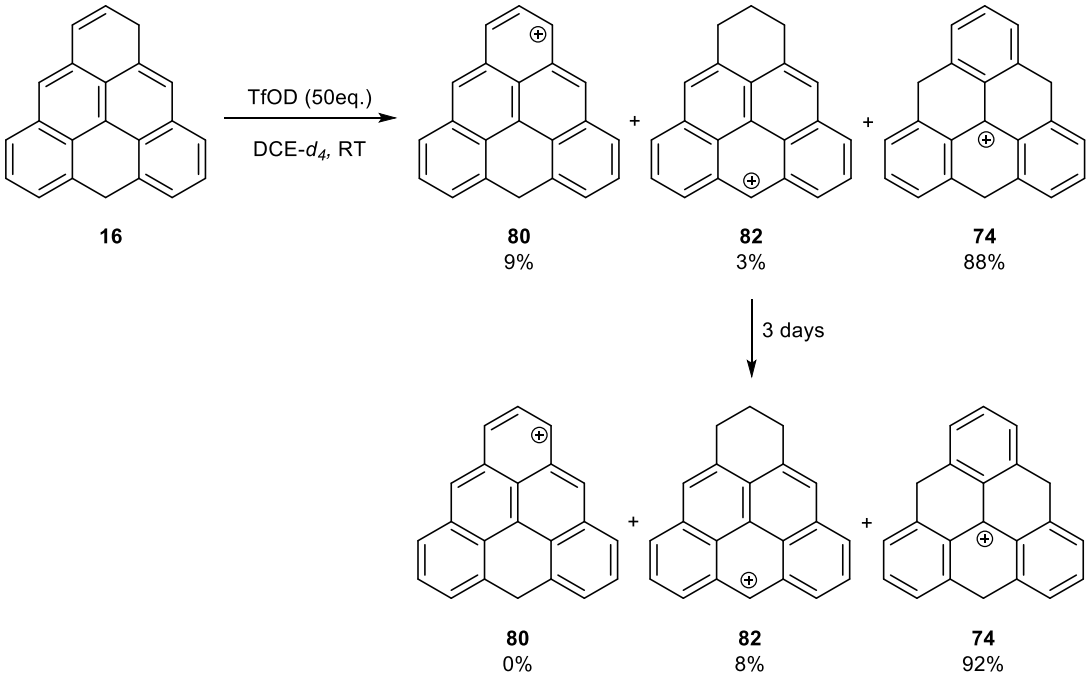

Scheme 25: Triangulene cation distribution in 50eq. TfOD.

More in-depth NMR experiments revealed that when neutral dihydrotriangulene (**16**) was exposed to deuterated triflic acid (Scheme 25), a variety of cationic intermediates could be observed. Furthermore, the presence and relative amounts of these intermediates were found to be dependent on both the concentration of triflic acid as well as time spent in solution. For example, when dihydrotriangulene (**16**) was reacted with a large excess of TfOD (50 eq.), the initial product mixture contained protonated triangulene (**80**, 9%), olympicenium cation (**82**, 3%), and triangulenium cation (**74**, 88%) as the major product (Scheme 25). When this same solution was held at room temperature for three days, the protonated triangulene (**80**) disappeared, and only cations (**82,** 8%) and (**74**, 92%) remained.

When dihydrotriangulene (**16**) was reacted with only 5 eq. of TFOD the initial product mixture did not contain any protonated triangulene (**80**), but instead only showed cations (**82**, 60%) and (**74**, 40%). When this solution was held at room temperature for three days, the triangulenium cation **74** disappeared, and only the olympicenium cation **82** remained (Scheme

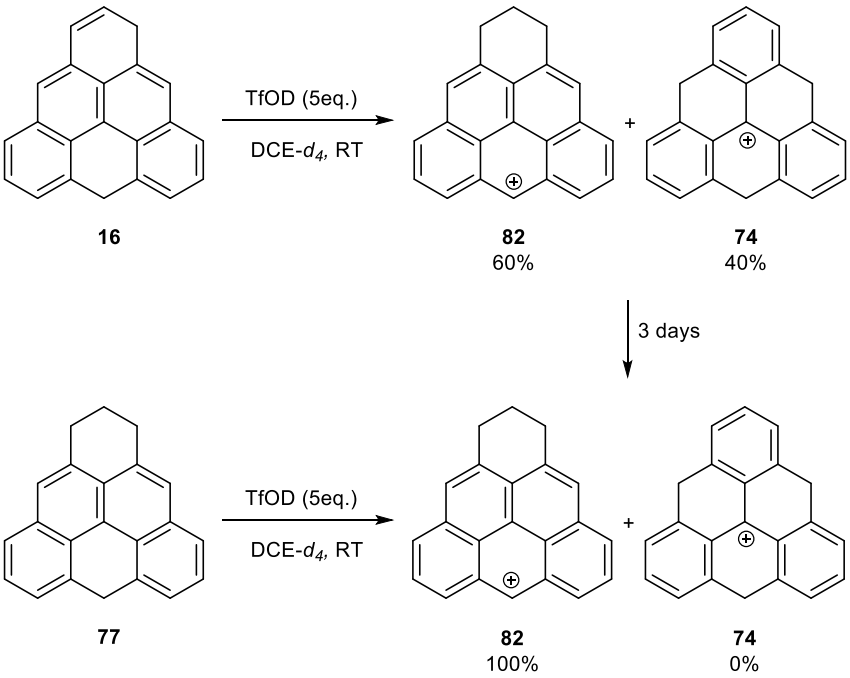

Scheme 26: Triangulene cation distribution in 5eq. TfOD.

26). The same olympicenium cation can be made quantitatively by the reaction of neutral triangulene **76** with triflic acid and is stable in solution for over two months. During the same two month period, a pure solution of the cation (**74**) converted ca. 66% to the olympicenium cation (**82**). This is consistent with calculations that predict the olympicenium cation (**82**) as the most stable $C_{22}H_{15}^{+}$ isomer. A summary of these results is provided in Table 3. The identity of these cationic intermediates is supported by NMR DFT calculations at the ωB97X-D/6-31G* level of theory, which match well with experimental results (Figures 10 – 13 and Tables 4 - 8).

	Days	**Relative % by ^{1}H NMR**		
		80	**82**	**74**
50 eq. TfOD	0	9 %	3 %	88 %
	3	-	8 %	92 %
	60	-	66 %	34 %
5 eq. TfOD	0	-	60 %	40 %
	3	-	100 %	-
	60	-	100 %	-

Table 3: Relative amounts of triangulene cations determined by ^{1}H NMR.

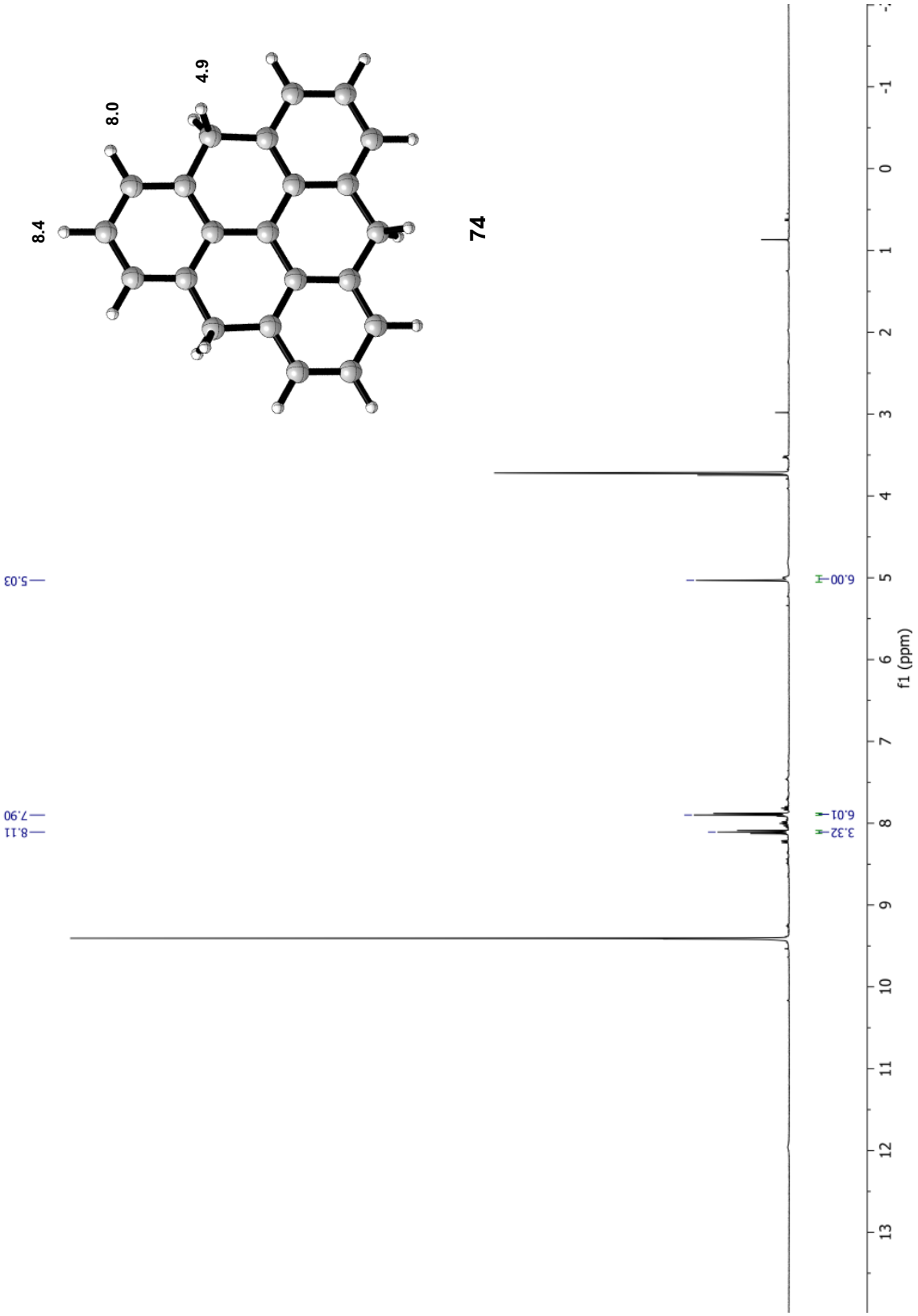

Figure 10: ^{1}H NMR of triangulene cation (**74**) compared to computations.

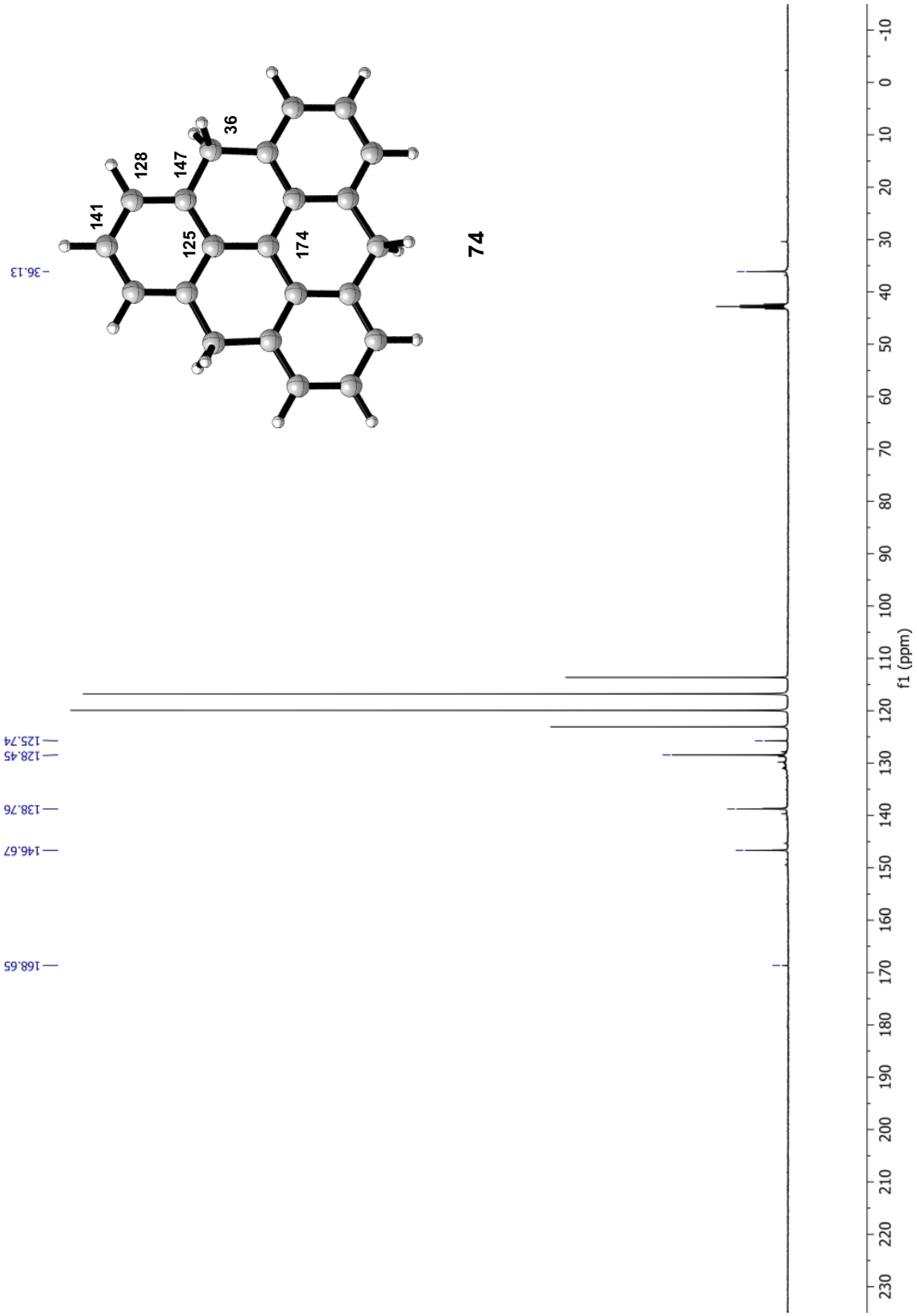

Figure 11: ^{13}C NMR of triangulene cation (**74**) compared to computations.

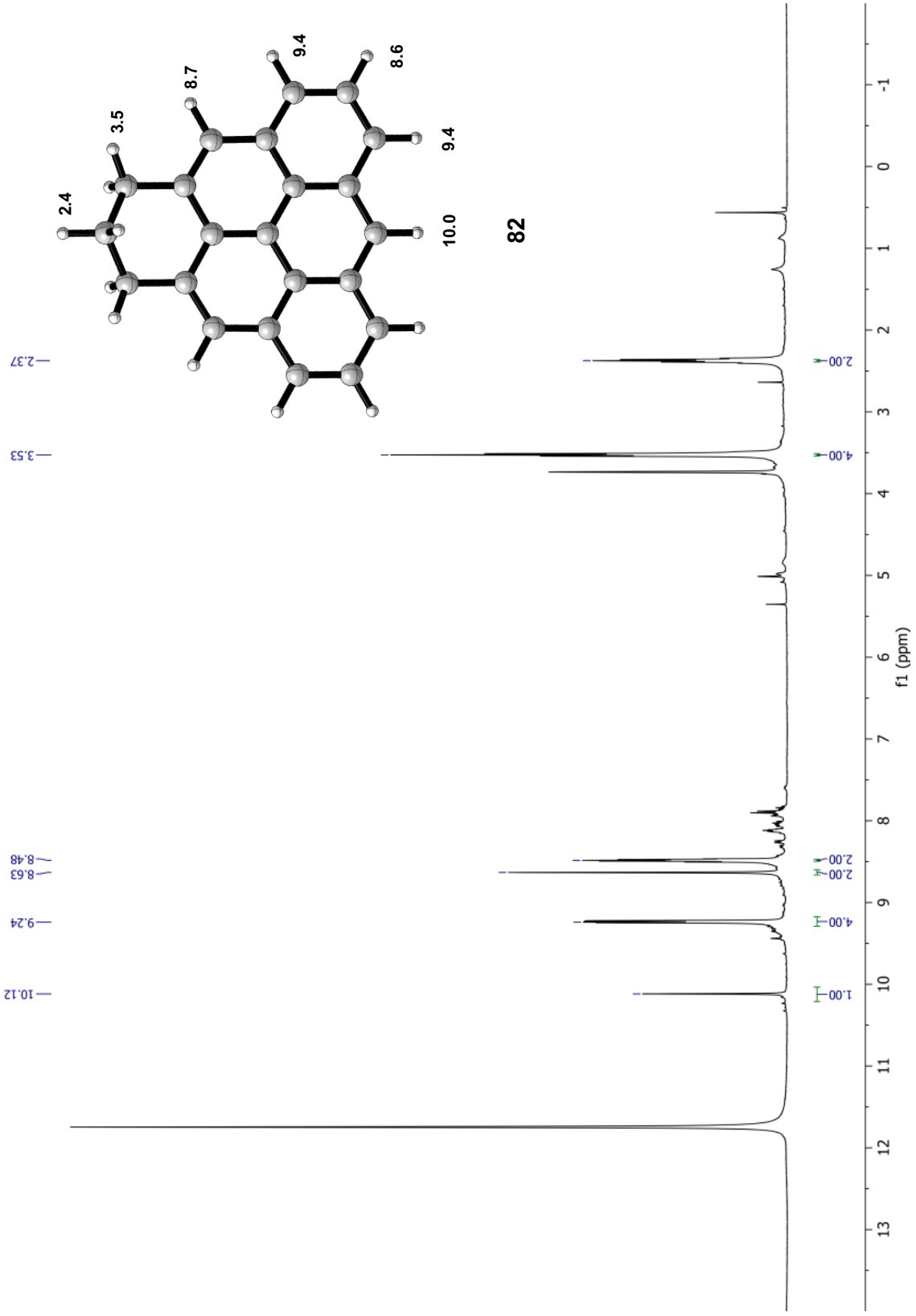

Figure 12: ^{1}H NMR of triangulene cation (**82**) compared to computations.

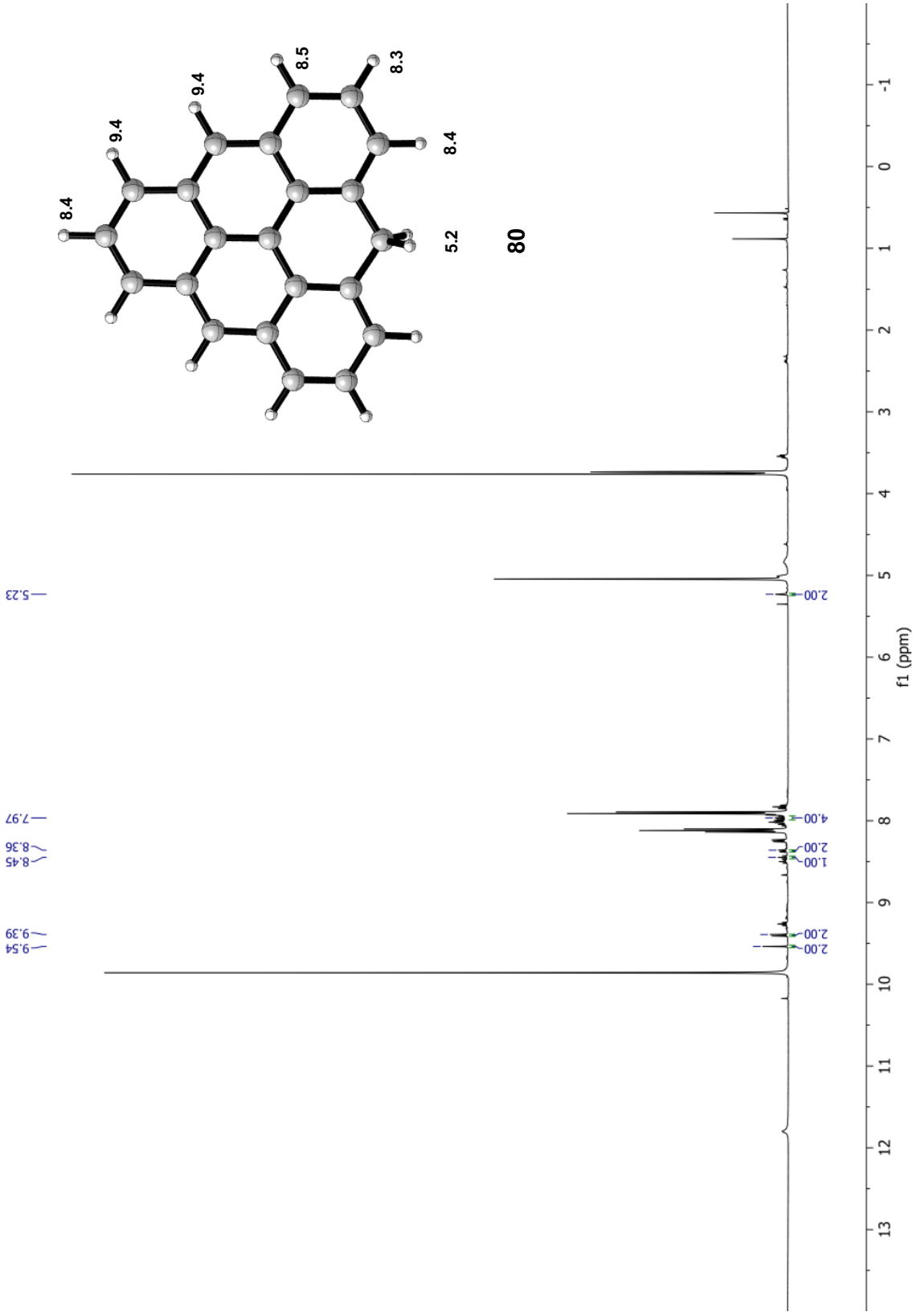

Figure 13: ^{1}H NMR of triangulene cation (**80**) compared to computations

δ (ppm) exp.	δ (ppm) cal.	m	#H	Assignment	Δδ (ppm)
8.12	8.43	t	3	A	0.31
7.90	8.01	d	6	B	0.11
5.05	4.90	s	6	C	0.15

Table 4: Comparison of ^{1}H NMR results for triangulene cation **76**.

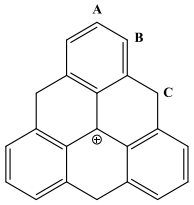

76

δ (ppm) exp.	δ (ppm) cal.	Assignment	Δδ (ppm)
168.7	173.8	F	5.2
146.7	147.8	C	1.1
138.8	141.4	A	2.6
128.5	128.4	B	0.0
123.1	124.5	E	1.4
36.1	35.5	D	0.6

Table 5: Comparison of ^{13}C NMR results for triangulene cation **76**.

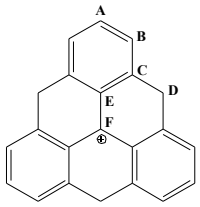

76

δ (ppm) exp.	δ (ppm) cal.	m	#H	Assignment	Δδ (ppm)
10.18	10.03	s	1	G	0.15
9.27	9.36	d	2	D	0.09
9.27	9.35	d	2	F	0.08
8.67	8.74	s	2	C	0.07
8.50	8.65	t	2	E	0.15
3.54	3.58	t	4	B	0.04
2.38	2.39	p	2	A	0.01

Table 6: Comparison of ^{1}H NMR results for triangulene cation **82**.

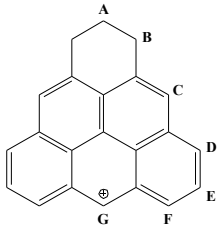

82

δ (ppm) exp.	δ (ppm) cal.	Assignment	Δδ (ppm)
157.2	162.5	M	5.3
149.7	152.5	F	2.8
145.6	148.0	H	2.4
140.8	145.6	I	4.8
138.9	141.1	C	2.2
135.2	137.8	D	2.6
131.2	130.0	G	1.2
130.8	129.2	E	1.6
130.2	128.7	L	1.5
128.7	125.0	K	3.7
123.3	123.4	J	0.1
30.9	30.7	B	0.2
22.4	21.4	A	1.0

Table 7: Comparison of ^{13}C NMR results for triangulene cation **82**.

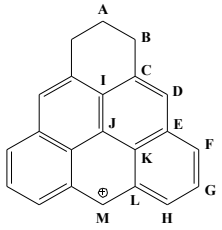

82

δ (ppm) exp.	δ (ppm) cal.	m	#H	Assignment	Δδ (ppm)
9.54	9.41	s	2	C	0.13
9.40	9.39	d	2	B	0.01
8.45	8.41	t	1	A	0.04
8.37	8.51	d	2	D	0.14
8.02	8.47	d	2	F	0.45
7.96	8.31	t	2	E	0.35
5.23	5.23	s	2	G	0.00

Table 8: Comparison of ^{1}H NMR results for triangulene cation **80**.

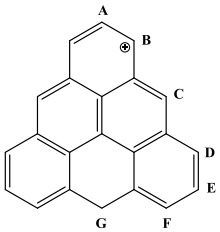

80

Computational Study of Triangulene Isomers

Although the NMR experiments and cation quenching experiments were able to identify several triangulene species, there are many more that remain elusive. Computations were once again used in order to help understand why these compounds were not observed. The results from these studies are summarized in Figures 14-19, where the relative free energies for each isomeric species of protonated and neutral triangulene can be compared. In each figure, aromatic cores are highlighted to help qualitatively rationalize their relative stabilities. For all experiments to date, no pentahydrotriangulene cations (PHCs) were ever observed. In order for any of these species to exist, a neutral tetrahydrotriangulene (THT) (Figure 15) would have to be protonated to give the respective cation. A comparison of these PHCs can be seen (Figure 14), where the two highest energy species PHC1 and PHC2 involve protonation of the bowl-shaped THT1 (**71**) to give an allylic cation. This type of protonation is disfavored because it breaks the aromaticity of one of the benzene rings and isolates the cation. The lowest energy isomer is PHC4, which involves the protonation of THT4 (**76**). This again disrupts the aromaticity of the aromatic core, but in this case, the cation can be stabilized by the benzene/naphthalene rings that remain. Even so, this cation is not observed experimentally, indicating that protonation of THTs is a disfavored process; instead, hydride removal to give trihydrotriangulene cations (THCs) (Figure 16), is much more favored.

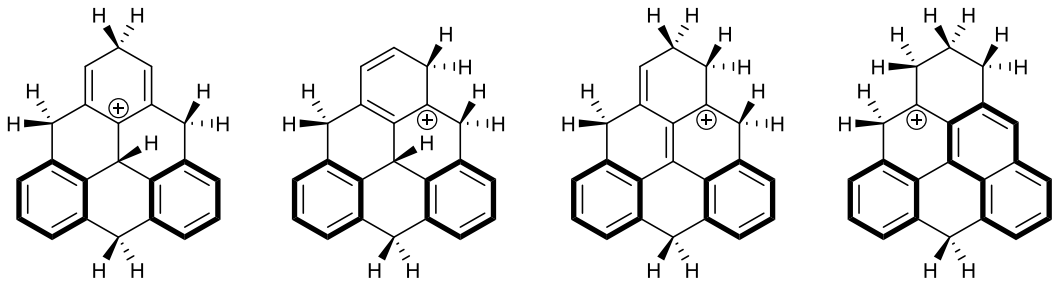

PHC1$^+$ 30.8 **PHC2$^+$** 25.9 **PHC3$^+$** 14.1 **PHC4$^+$** 0.0

Figure 14: Relative free energies of pentahydrotriangulene cations (kcal/mol).

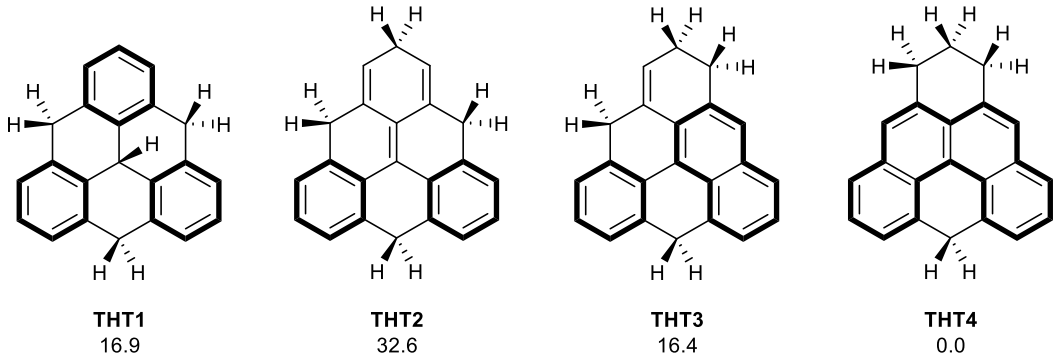

Figure 15: Relative free energies of tetrahydrotriangulenes (kcal/mol).

When comparing the relative energies of tetrahydrotriangulenes (Figure 15), the highest energy species is THT2. This involves hydride addition to the apex carbon of THC1 to give only two isolated benzene rings in the product. The only two THTs observed experimentally were THT1 (**71**) and THT4 (**76**). Although THT3 is slightly lower in energy relative to THT1, it can only be formed by protonation at the 4-position of the anthracene core of 4,8-dihydrotriangulene to give THC 2. This is much less favored than protonation at the 10-position to give THC1. The bowl-

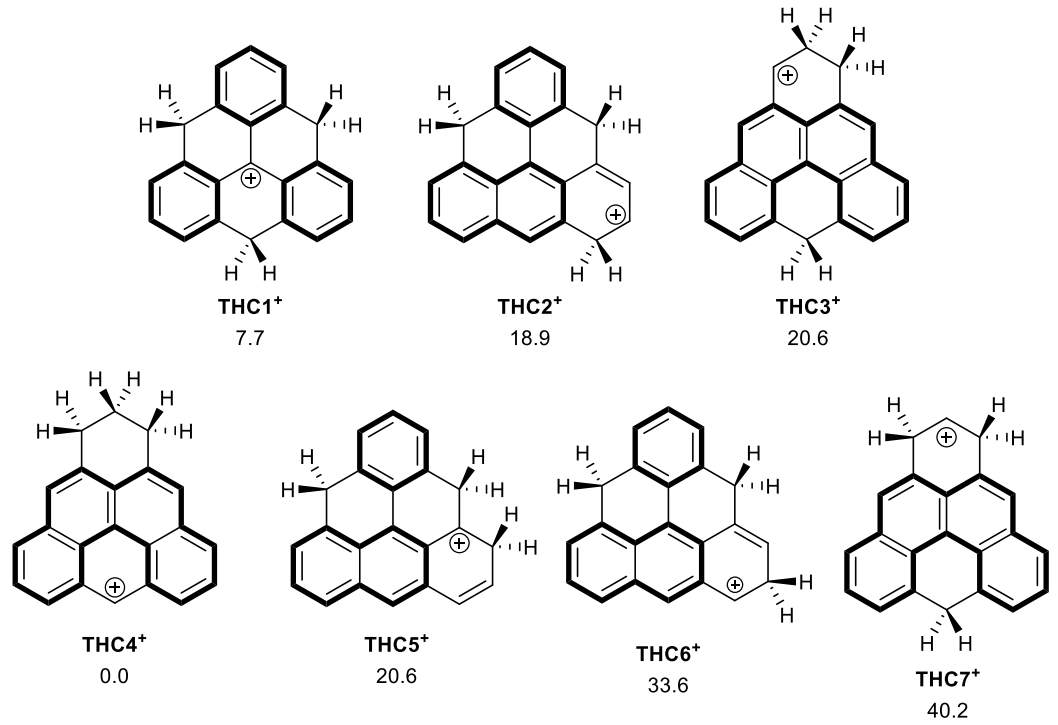

Figure 16: Relative free energies of trihydrotriangulene cations (kcal/mol).

shaped THT1 (**71**) is 16.9 kcal/mol higher in energy than the relatively flat olympicene THT4 (**76**). The observed difference in energy is caused by a combination of reduced aromaticity and the ring strain induced in THT1 that is not found in THT4. These factors are what make the bowl-shaped triangulene challenging to synthesize and isolate experimentally.

The two lowest energy trihydrotriangulene cations THC1 (**74**) and THC4 (**82**) are the only two observed experimentally. THC1 is the initial product observed from the cyclization of the tetraol (**68**) in triflic acid but is slowly converted to THC4 over time, indicating that this cation is a thermodynamic sink. THC7 is the highest energy isomer because it is the only species that has an isolated cation devoid of resonance stabilization. The remaining THCs are relatively high in energy due to unfavorable protonation sites of the anthracene core (THC2 and THC5), or protonation of the comparatively stable 1,8-dihydrotriangulene (THC3). The latter is involved in the proposed mechanism for the interconversions of triangulene cations and neutral species (Scheme 24) and is likely the reason the conversion of THC1 (**74**) to the more stable THC4 (**82**) is slow.

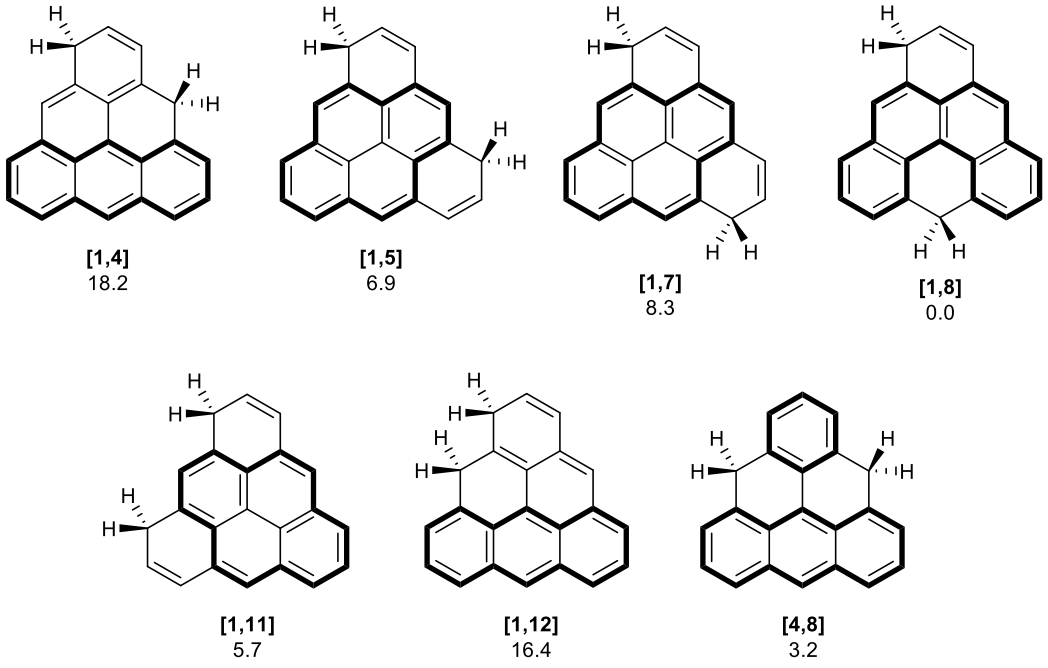

Figure 17: Relative free energies of dihydrotriangulenes (kcal/mol).

The nomenclature for dihydrotriangulenes (Figure 17) is in reference to the numbering system of triangulene (Figure 18, left), and indicates which positions are protonated. Certain combinations of protonation sites lead to open-shell species (Figure 18, right); however, only combinations that give closed-shell species were considered. The relative energies of these isomers can be compared qualitatively by the type of aromatic core they possess. For example, isomers with an anthracene core are highest in energy followed by those with a pyrene core. The lowest energy isomers [1,8]- and [4,8]-dihydrotriangulene (**16** and **9**) have olympicene and benzene/anthracene cores, respectively, and are the only isomers that have been observed.[13,15]

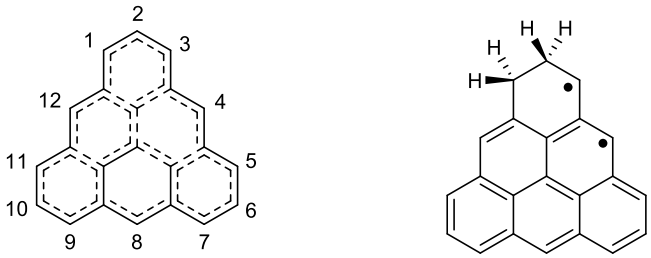

Figure 18: Numbering scheme for triangulenes and open-shell dihydro triangulene.

There are only two closed-shell isomers of monohydrotriangulene, and they are very similar in energy with a difference of ~2 kcal/mol (Figure 19). Surprisingly, only MHC1 (**80**) was observed experimentally, which is also used as part of the interconversions (Scheme 24). This is the only case in which the lowest energy isomer was not observed experimentally; however, they are very close in energy. Comparing the relative energies of triangulene isomers helps

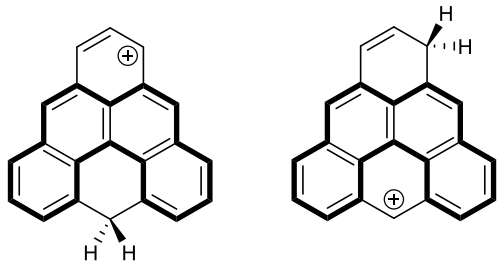

Figure 19: Relative free energies of monohydrotriangulene cations (kcal/mol).

explain why only specific isomers are observed experimentally and why others are too high in energy to be formed or are so unstable that they are not observed in the lifetime of the experiment.

Experimental Studies of Triangulene in Solution

The diradical of unsubstituted triangulene has only been isolated on a surface using microscopy techniques,[13] and there is limited information regarding its generation and properties in solution. In order to investigate these properties further, an NMR experiment was set up in which a solution of 1,8-dihydrotriangulene (**16**) in $CDCl_3$ was oxidized with *p*-chloranil (Scheme 27). Upon addition of the oxidant, the bright yellow-green solution instantly turned dark blue. The sample was then immediately analyzed by ^1H NMR to show the complete disappearance of starting material and the formation of reduced p-chloranil (**83**) as the sole material in solution.

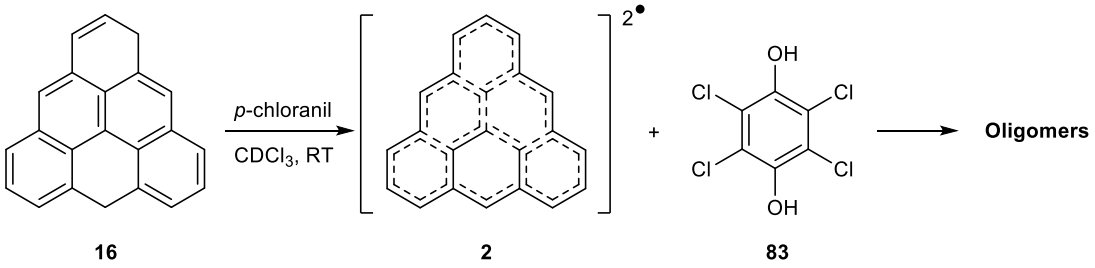

Scheme 27: Chemical oxidation of dihydrotriangulene and formation of oligomers.

This sample was condensed to give a black solid, which was subsequently analyzed by LDI-TOF spectrometry. The sample was dissolved at 1 mg/mL in dichloromethane and deposited neat on a polished steel MALDI plate. The LDI analysis was carried out on a rapifleX TOF/TOF mass spectrometer (performed by Dr. Sergei Dikler, Bruker Scientific, LLC, Billerica, MA). The spectra were acquired in reflector mode with 4000 laser shots per spectrum in the mass range 0-2200 Da to give a complex spectrum shown in Figure 20. This is believed to represent higher-order oligomeric products of triangulene.

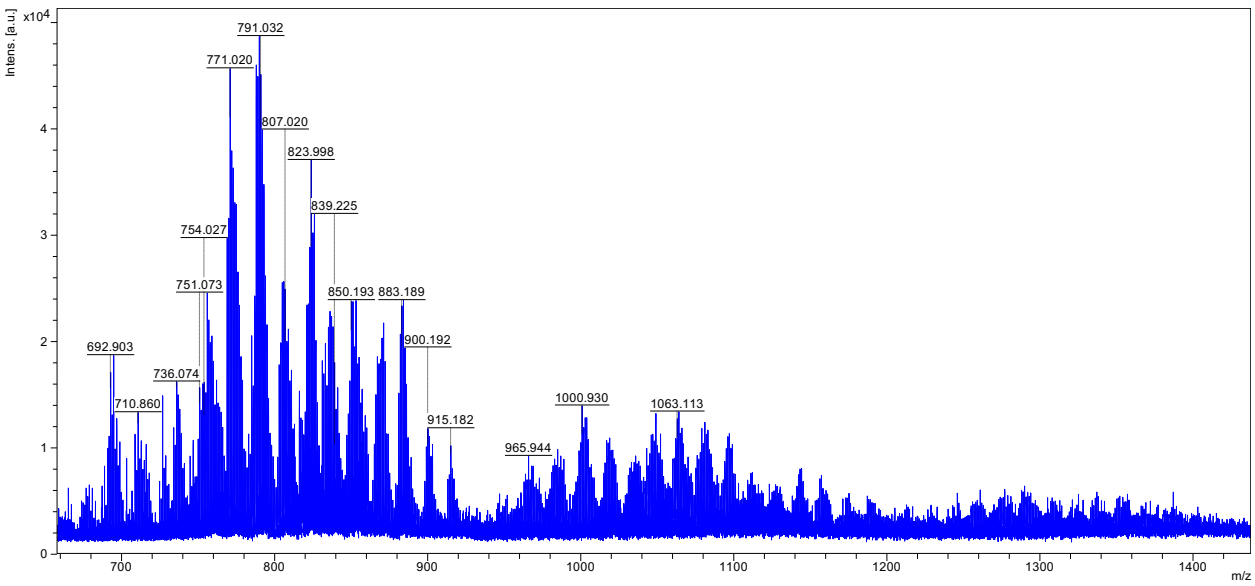

Figure 20: LDI-TOF spectrum showing complex mixture of higher order oligomers.

In a second study, the oxidation of 1,8-dihydrotriangulene (**16**) was monitored by UV-vis spectroscopy. Pure samples of dihydrotriangulene and *p*-chloranil in DCM were analyzed individually (Figure 21). In the case of dihydrotriangulene, there can be seen two large absorbance bands (λ_{max} = 258 and 318 nm), as well as several vibrational bands ranging from 380 to 482 nm, as is typical for polycyclic aromatic hydrocarbons.[14] *p*-Chloranil on its own only has two broad absorbance bands (λ_{max} = 300 and 374 nm).

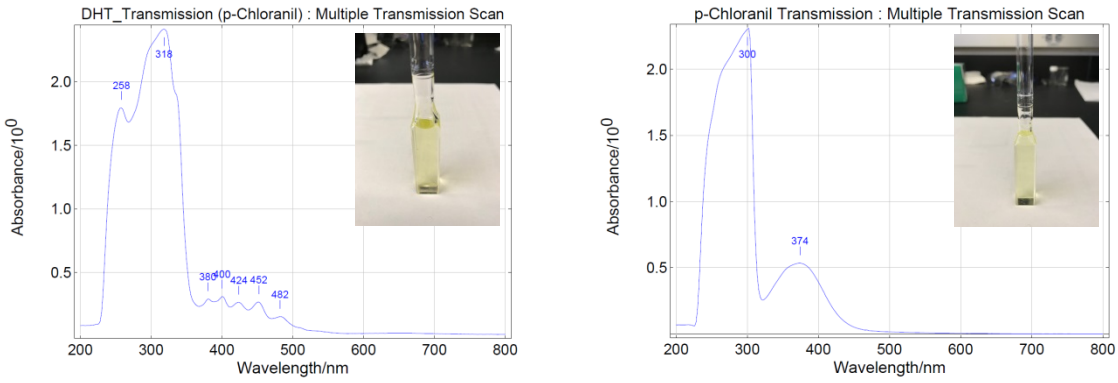

Figure 21: Transmission spectrum of dihydrotriangulene (left) and *p*-chloranil (right) in DCM.

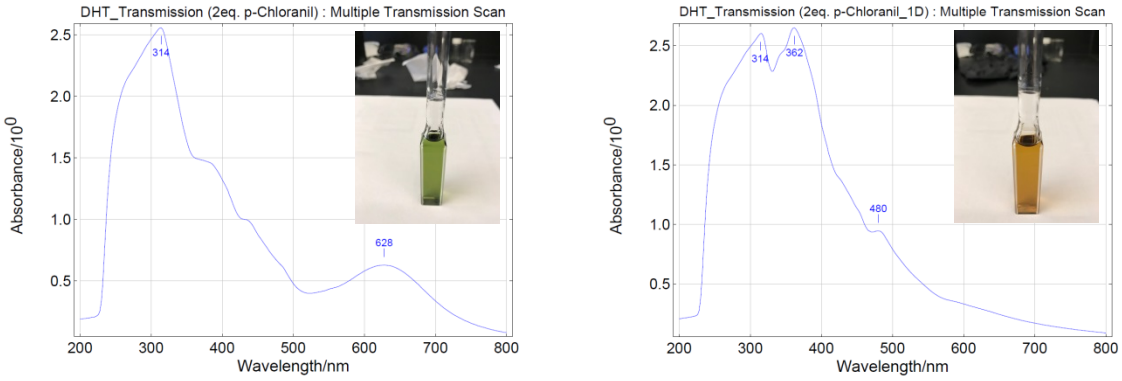

Figure 22: Transmission spectrum of oxidized 1,8-dihydrotriangulene (left) and after one day (right) in DCM.

When the two were combined a dark green solution resulted and a new broad band at 628 nm was observed (Figure 22). This new band is not likely to be the triangulene diradical but more likely some form of radical cation intermediate. When the solution is left to stand overnight, the color turned brown, and the intermediate peak disappeared. These preliminary results support the idea that triangulene is a highly reactive species that requires some method of chemical taming in order for it to be observed in solution.

Efforts Towards the Synthesis of Bitriangulenes

4,4'-Fusion of two [3]triangulens would yield bitriangulenes. Preliminary calculations support a twisted geometry and a high-spin quintet ground state with four unpaired electrons. We have made progress towards the synthesis of bitriangulenes. Using a route similar to what was initially proposed for the synthesis of triangulene, bis-organolithium addition of the allyl-protected diol **58** to bianthrone could be an easy way to generate tetraol (**89**), as a bitriangulene precursor (Scheme 29). In theory, an acid-catalyzed cyclization of the tetraol would give the bitriangulene after quenching. Rearrangements of the triangulene core are likely to occur, prompting the question of which bitriangulene isomer will be favored. DFT calculations predict a non-planar ground state geometry, which should help in the solubility of the hydrocarbon and intermediates. The tetraol precursor was synthesized beginning with a literature procedure for

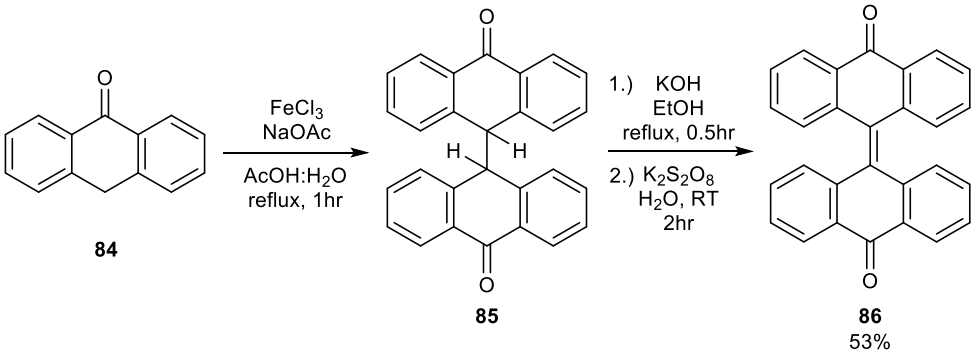

Scheme 28: Synthesis of bianthrone.

the two-step synthesis of bianthrone (**86**, 53%) from 9-anthrone (**84**) (Scheme 28).[52]

From there, an excess of lithiated allyl-protected diol (**58**) was added (Scheme 29) to afford a mixture of diol stereoisomers (**87**). This was subjected to the reductive aromatization conditions to give the bianthracene core (**88**, 41%), then deprotected to give the desired tetraol (**89**, 46%). At this point, we are unable to complete work on this chemistry. DFT computations using the IEFPCM(DCE)/B3LYP/6-31+G(d,p) level of theory predict the aromatic dication (**91**) as a ground state triplet and is 8.7 kcal/mol lower in energy than the singlet dication. Because of this, cyclization of the tetraol with triflic acid is likely to cause oligomerization of the product. To prevent this, the reactive cites could be blocked with bulky substituents. This could be accomplished by PCC oxidation of tetraol **89**, followed by addition of an organolithium reagent and cyclization to give hydrobitriangulene precursors. The hydro precursors could be a cleaner way to observe the cation in solution. They should be more soluble than the tetraol, and the cyclization and cation formation occurs in two separate steps which should limit oligomer formation.

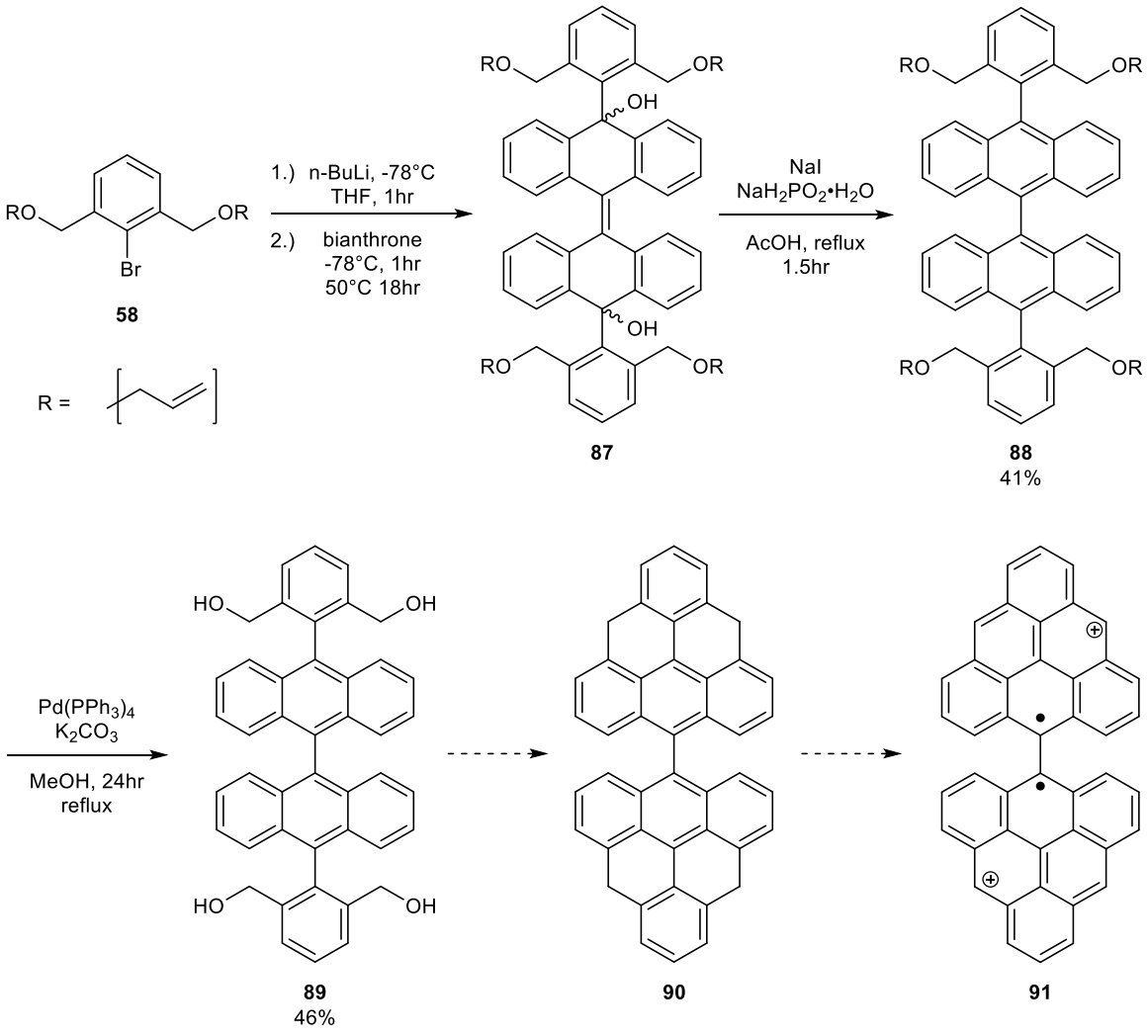

Scheme 29: Synthetic route towards bitriangulene.

Conclusions

This work describes an efficient synthesis of 1,8-dihydrotriangulene (**16**), a known-triangulene precursor, that is scalable to multi-grams and selective for only one isomer. Through acid-catalyzed NMR experiments, several cationic intermediates of triangulene were identified that have not been previously observed. The structures of these intermediates were supported by DFT computations and provided some mechanistic insight for how these unprecedented interconversions occur. In addition, a novel bowl-shaped tetrahydrotriangulene was synthesized by the capture of the triangulene cation with triethyl silane. Solution phase experiments for the

oxidation of dihydrotriangulene with *p*-chloranil gave a product that was initially NMR-silent, and analysis of the reaction mixture by LDI-TOF spectrometry indicates the formation of higher molecular weight triangulene oligomers. These results support the formation of a highly reactive paramagnetic intermediate that is kinetically unstable in solution. Additionally, a potential bitriangulene precursor was synthesized and characterized.

Chapter II. Electrochemical Study of Dihydrotriangulene

Introduction

Although the synthesis of dihydrotriangulene (**16**) has been known for years[14] there have been no studies into its electrochemistry. Examples in the literature only cover substituted versions of trioxotriangulenes (Scheme 5).[12,18–20] In these studies, four reversible redox waves were observed, including the formation of a trianionic diradical (**22**) and a central radical (**20**).

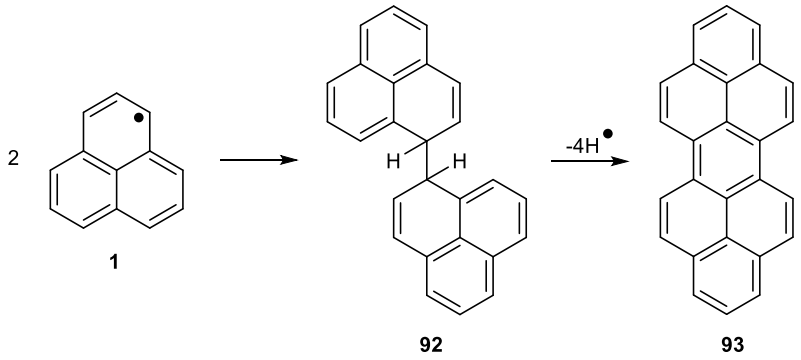

Scheme 30: σ-Dimerization of the unsubstituted phenalenyl radical (**1**).

The central radical was found to be in equilibrium with a π-dimer (**18**), but no polymerization was observed. σ-Dimerization of this radical is only observed after several weeks in solution. Similarly, the phenalenyl radical is known to dimerize to peropyrene (**93**) through a σ-dimerization pathway (Scheme 30).[16,53–55] Formation of the π-dimer for the phenalenyl radical is

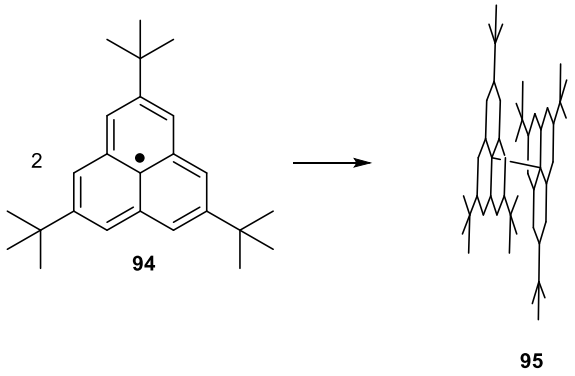

Scheme 31: π-Dimerization of the substituted phenalenyl radical (**94**)

only observed when the apex positions are heavily substituted with tert-butyl groups (Scheme 31).[56] The dimer formation was confirmed using cold-spray ionization MS as well as temperature-dependent NMR, which showed well-resolved peaks at 180 K. These findings, as well as computational models,[57,58] imply that the mode of dimerization observed is dependent on the degree of substitution in the phenalenyl system.

Other PAHs such as naphthalene and phenanthrene undergo single irreversible oxidations, due to the formation of a dimer. In contrast, pyrene readily oligomerizes, as evident by a significant increase in current and a lowering of pH.[59] Similar modes of dimerization and polymerization are possible in unsubstituted triangulene, but only computational models are available as evidence.[60,61] The most reactive sites of triangulene are the α- and γ- positions (Figure 23), which makes them the most likely sites for dimer/oligomerization. DFT computations suggest that σ-dimers are more stable than π-dimers by ~6 kcal/mol, and of the possible options the γγ-dimer is lowest in energy. Furthermore, the most stable singly-bound σ-dimer has a low-lying triplet state (2.5kcal/mol), which would facilitate the oligomerization of triangulene.

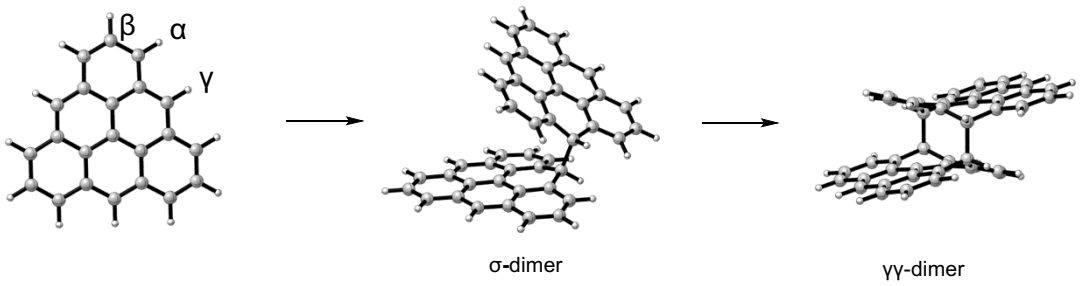

Figure 23: σ-dimerization of the triangulene diradical.

Research Objective

With pure samples of 1,8-dihydrotriangulene, the electrochemical properties of this fascinating molecule can be probed for the first time. This work aims to understand the types of redox reactions dihydrotriangulene undergoes. In order to support these claims, DFT

computations run at the IEFPCM(acetonitrile)/B3LYP/6-31+G(d,p) level of theory are used to compare the relative energies for a variety of triangulene species and likely intermediates.

Results and Discussion

Electrochemistry of Dihydrotriangulene

One of the major advantages of our synthetic route to dihydrotriangulene (DHT) is that one isomer can be preferentially made when triethylamine is used as the quenching reagent (Table 2). This is not true of any other current synthesis, which typically generates an inseparable mixture of 1,8- and 4,8-dihydrotriangulenes. The following electrochemical experiments were done in collaboration with Zane Thistleford. A pure sample of 1,8-dihydrotriangulene was prepared inside a glovebox to avoid oxidation. The sample was diluted to 1 mM in degassed anhydrous acetonitrile with 0.1 M n-Bu_4PF_6 as the supporting electrolyte under an atmosphere of N_2. The electrochemical apparatus contained a glassy carbon working electrode, sheathed platinum wire counter electrode, and a 0.01 M Ag/Ag+ pseudo reference electrode with ferrocene added as an internal reference.

The sample was analyzed first using linear sweep voltammetry (LSV) both in the positive (0 – +2 V) and negative (0 – -2 V) directions (Figure 24). This type of experiment involves changing the potential between the working electrode and reference electrode linearly in time while measuring current. Oxidation and reduction events are observed when the current

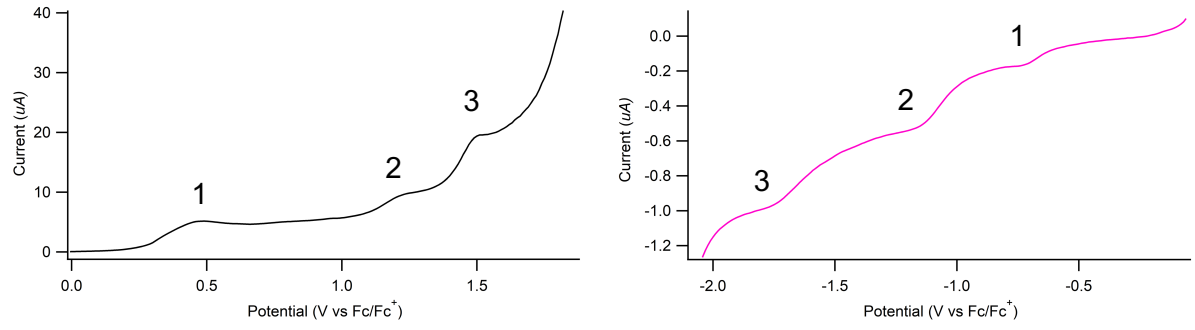

Figure 24: Oxidation LSV (left) and reduction LSV (right).

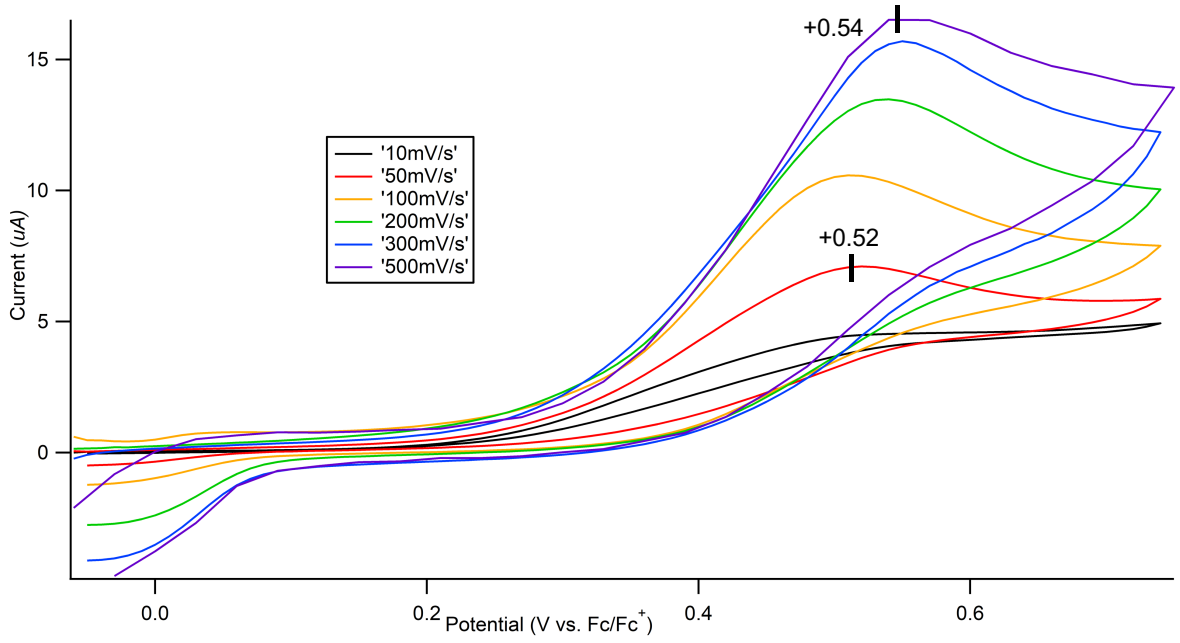

Figure 25: Scan rate dependence of 1st reduction

changes relative to the starting potential. In each LSV, three clear redox events were observed.

When the potential was swept from 0.0 – +0.8 V, the first oxidation event is seen more clearly (Figure 25). The oxidation is irreversible and the anodic peak potential (E_{PA}) varied from +0.52 V to +0.54 V when the scan rate was increased from 10 mV/s to 500 mV/s. The oxidation observed is likely the removal of a hydrogen atom and electron from DHT to give the aromatic mono-hydrotriangulene (MHT) cation. The two locations in dihydrotriangulene where removal of a hydrogen atom is likely to occur are the 1- and 8-methylene hydrogens. DFT computations

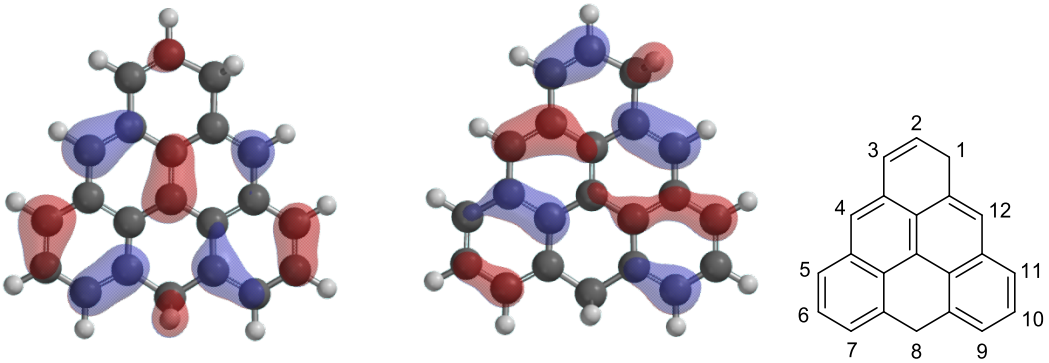

Figure 26: HOMO (left) and HOMO (-1) (center) of DHT with a numbering scheme (right).

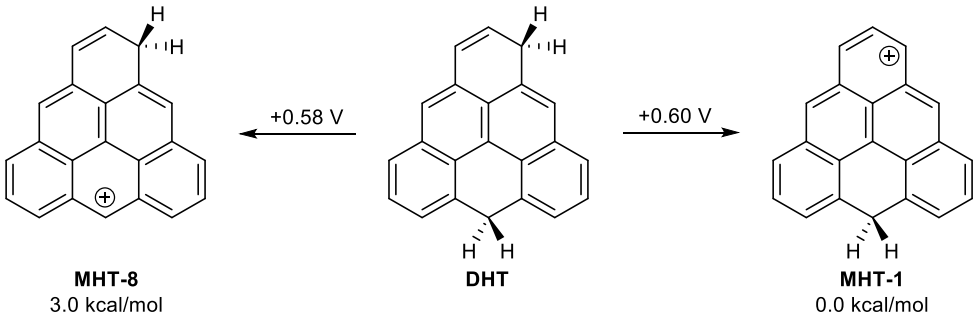

Scheme 32: Removal of a hydrogen atom at 1- or 8-position to give MHT cations.

predict the HOMO of DHT partially localized on the methylene hydrogen in the 8-position (Figure 26), making this hydrogen atom most likely to be removed first and therefore, the kinetic product. The HOMO (-1) is 0.1 eV lower in energy partially localized on the methylene hydrogen in the 1-position. The MHT cations that are produced by oxidation of DHT have an energy difference of 3.0 kcal/mol favoring removal of the 1-hydrogen, making it the thermodynamic product (Scheme 32). The observed shift in E_{PA} is caused by the removal of the 8-hydrogen versus the 1-hydrogen, which should require a higher potential to remove. When the scan rate is slow (50 mV/s) the hydrogen in the 8-position is removed first favoring the kinetic product when the scan rate is increased to 500 mV/s the higher potentials allow for removal of the 1-hydrogen to give the thermodynamic product.

There are two possible pathways to get to the MHT cation: a concerted pathway in which the hydrogen atom and electron are removed simultaneously, which is called a proton-coupled electron transfer (PCET), or a stepwise route in which these two events occur separately as electron then chemical reactions (EC) (Scheme 33). The fact that the oxidation event is irreversible even at higher scan rates suggests the PCET mechanism for hydrogen removal. Additionally, the DHT radical cation is 173 kcal/mol higher in energy than the neutral DHT and is not likely to be stable. When the scan window is expanded (-0.2 – +0.8 V), the reduction of the MHT cation is observed at -0.05 V (Figure 27). This reduction peak is not observed when the maximum potential is set to +0.25 V (or) before the MHT cation is formed, indicating that this is

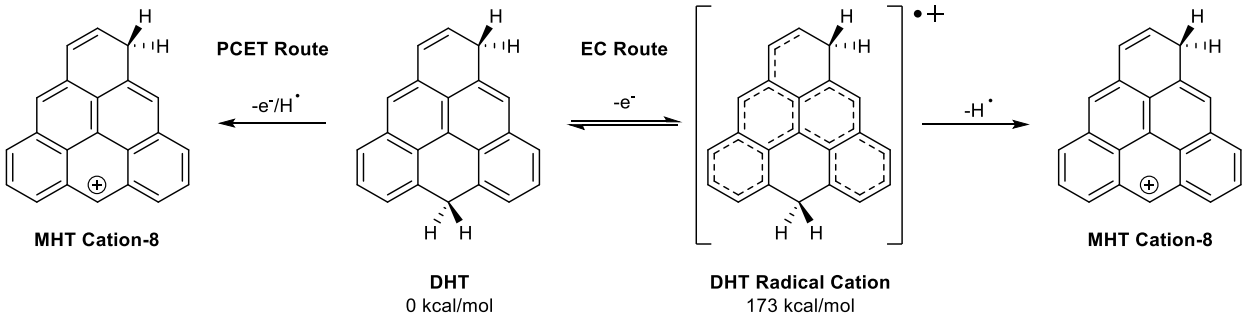

Scheme 33: PCET vs EC routes to MHT cation.

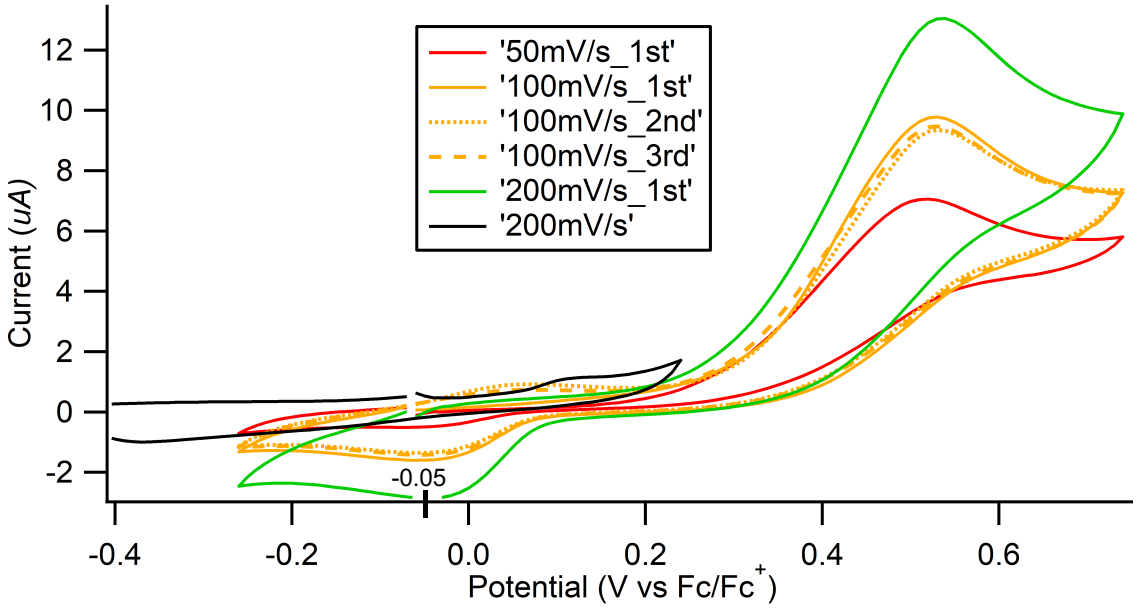

Figure 27: Formation of MHT cation and reduction to MHT radical.

a reduction of the newly formed MHT cation to give the MHT radical. Because this reduction is not reversible, it implies that the MHT radical reacts too quickly to be oxidized on the reverse sweep, likely due to the formation of a dimer. Oxidation of the dimer is not observed within this scan window.

The second oxidation event occurs at +1.24 V (Figure 28) and is again irreversible. Regardless of which MHT cation is formed in the first oxidation, the HOMO of each show localization of electron density on the remaining methylene hydrogen (Figure 29). Therefore, the

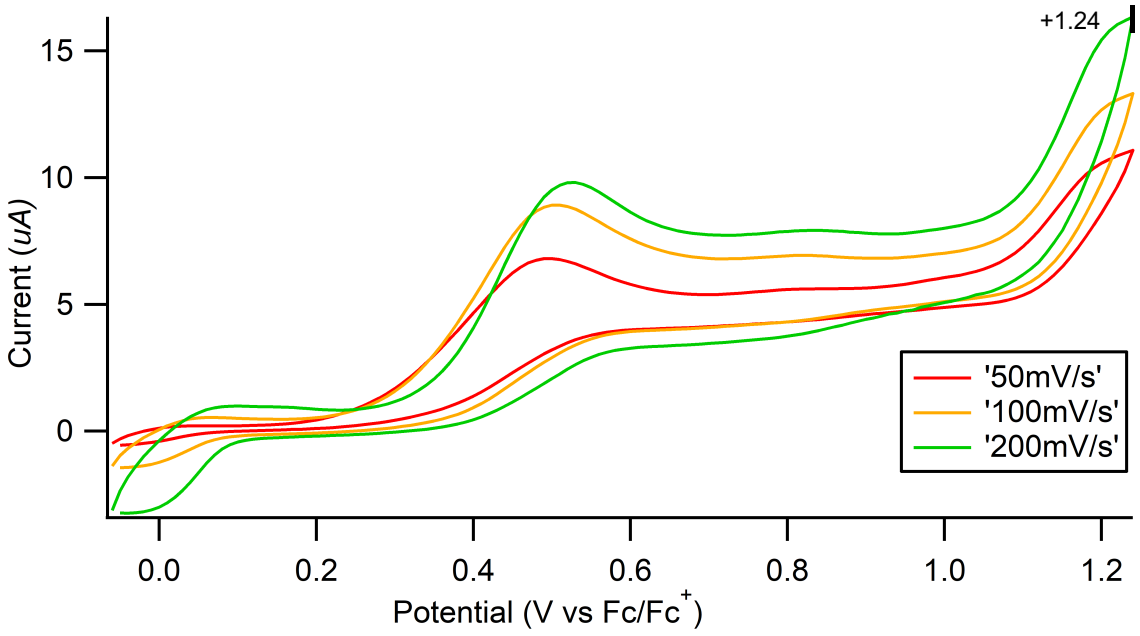

Figure 28: Second oxidation of DHT

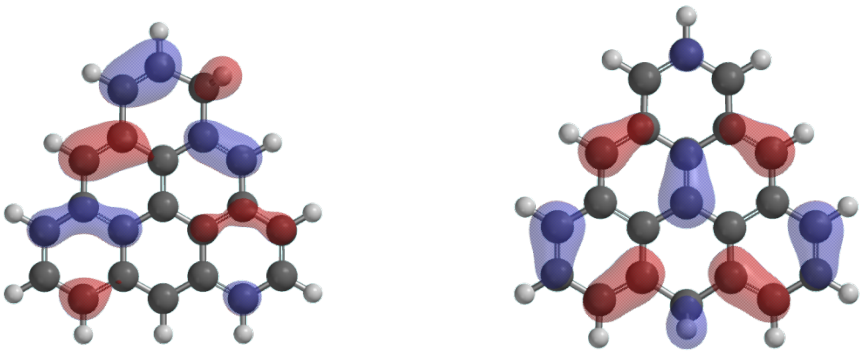

Figure 29: HOMO of MHT-1 (left) and MHT-8 (right).

second oxidation is expected to be the removal of this hydrogen atom to give the triangulene radical cation (Scheme 34). This generated species is expected to be highly reactive and likely dimerizes immediately.

Based on relative peak height, the third oxidation is a 2-electron irreversible oxidation at +1.54 V (Figure 30). This event can be explained by oxidation to the triangulene dication. The oxidation can happen in one of two ways: direct oxidation of the triangulene

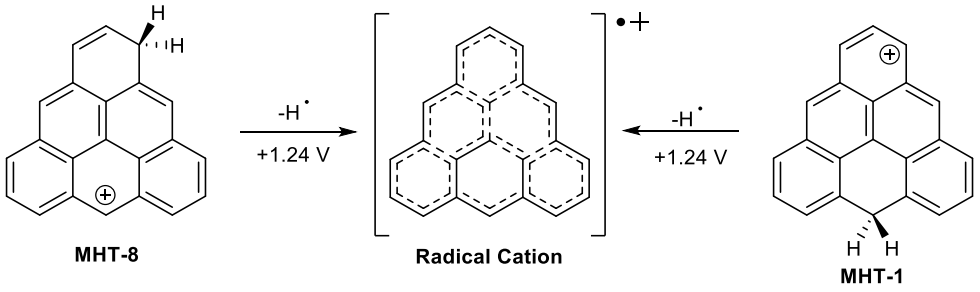

Scheme 34: Oxidation of MHT cations to triangulene radical cation.

radical cation or by the formation of a dication dimer intermediate, which is then oxidatively cleaved. Both pathways ultimately end up with the triangulene dication (Scheme 35).

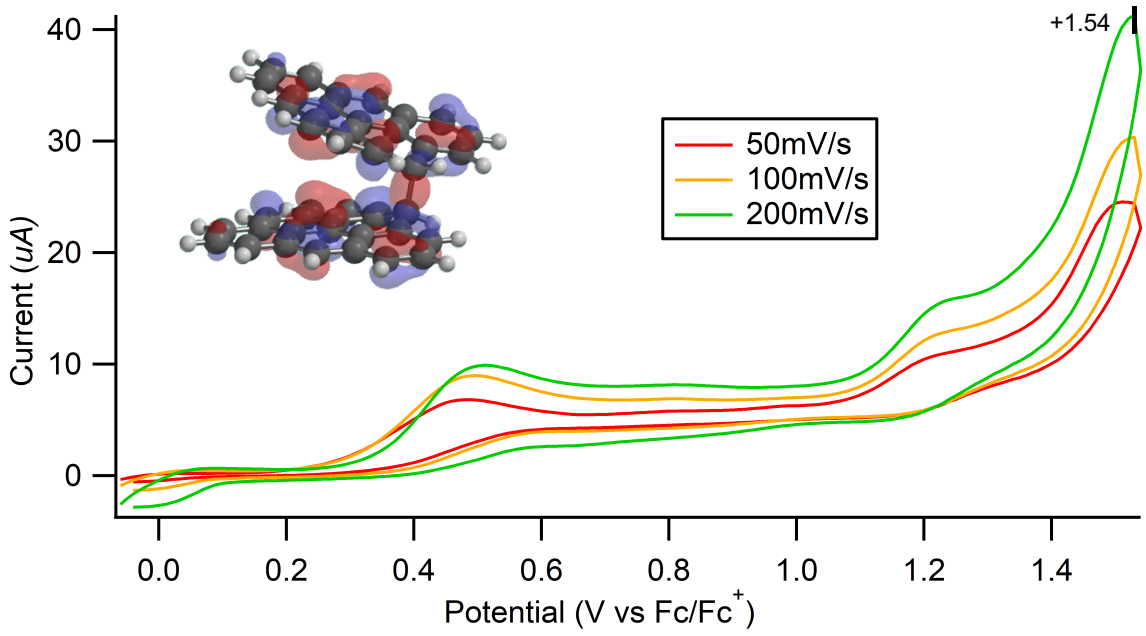

Figure 30: Third oxidation of DHT and HOMO of triangulene dimer dication.

The direct oxidation pathway is only a 1-electron oxidation, which should be reversible. Oxidation of the dication dimer is a 2-electron process and is not expected to be reversible, making this the more likely path to the triangulene dication. The HOMO of the dimer shows electron density in the dimer bond (Figure 30) and is likely where the electrons are removed. In either case, the dication that is formed does not persist long enough for its reduction to be observed. It is 240 kcal/mol higher in energy than the radical cation and is chemically unstable.

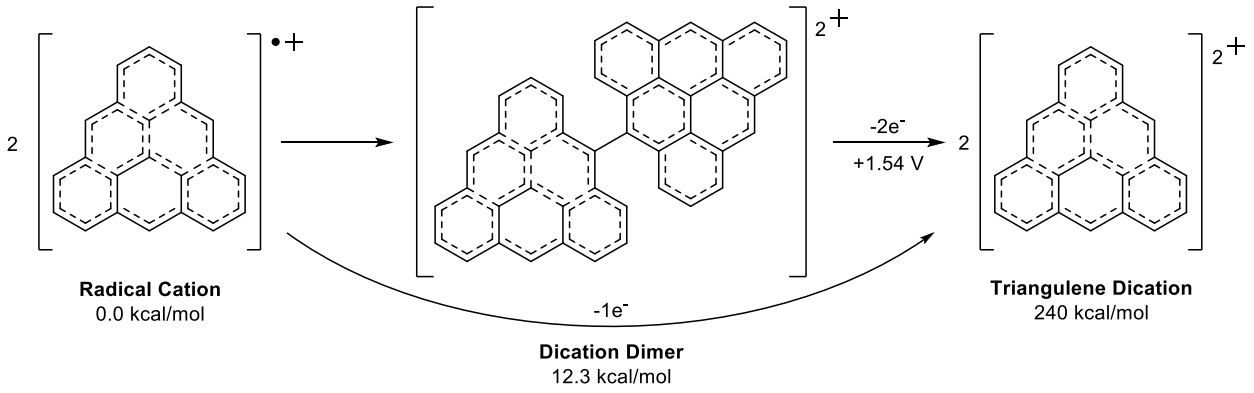

Scheme 35: Formation and 2e- oxidation of triangulene dimer.

The first reduction of DHT (Figure 31) appears as a broad peak on the first scan (-0.71 V) but increases in intensity on the second and third scans. Two oxidations are observed when the potential is swept in the opposite direction, which again sharpens and intensifies with successive scans. On the second and third scans, a 2e- reduction is observed at -0.61 V. The first reduction can be explained by the addition of an electron into DHT to give the radical anion (Scheme 36). Computations show the HOMO and the HOMO (-1) of the DHT radical anion on

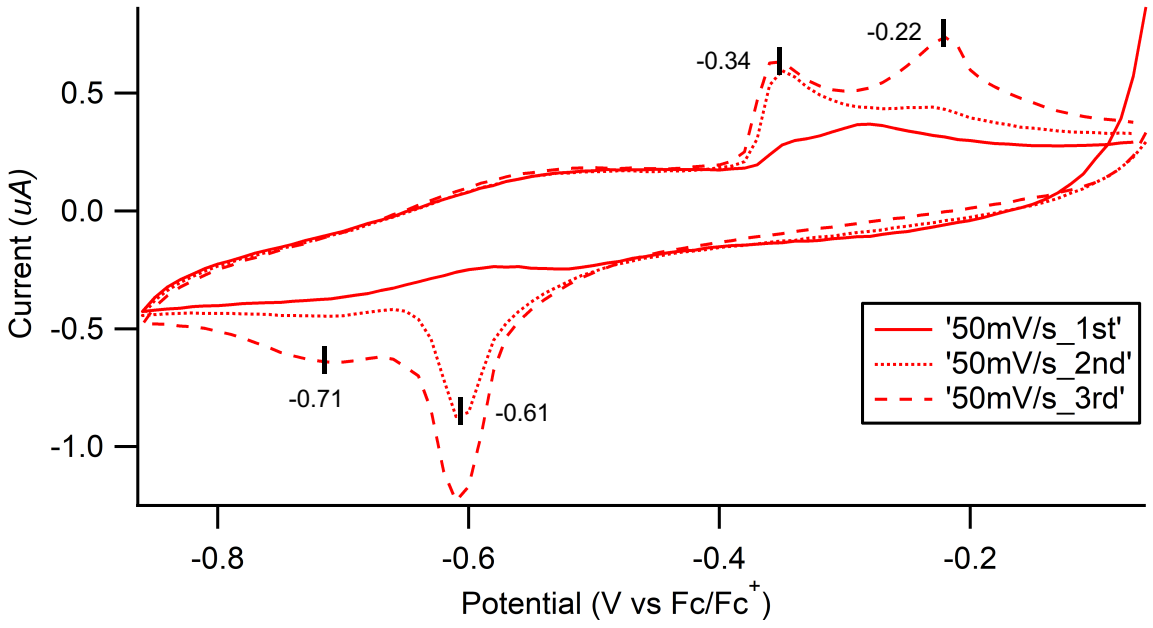

Figure 31: First reduction of DHT.

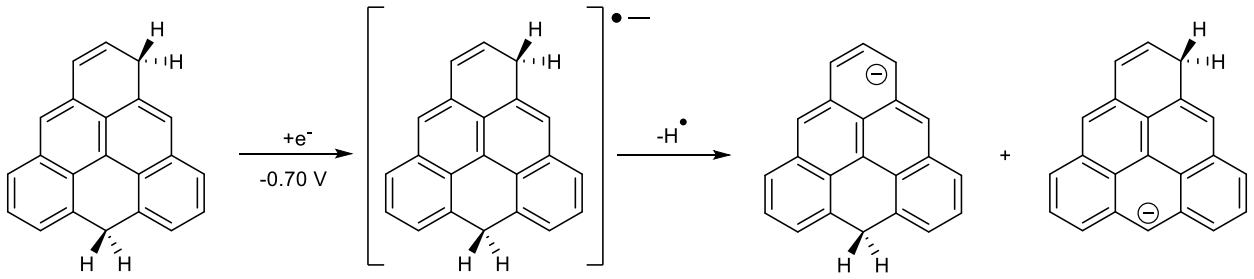

Scheme 36: Reduction of DHT to MHT anions.

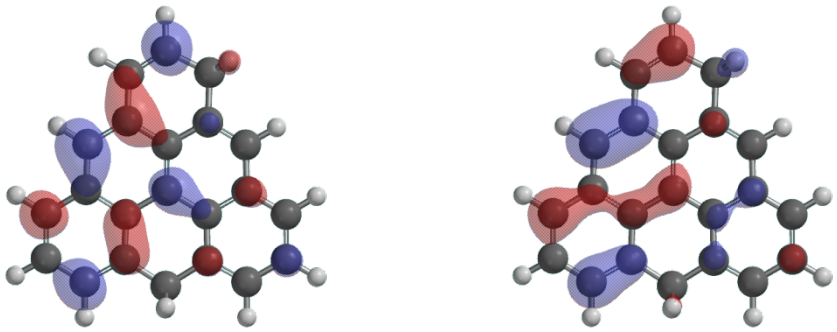

Figure 32: HOMO (left) and HOMO (-1) (right) of the DHT radical anion.

the methylene in the 1-position. This weakens the C-H bond, and the hydrogen atom is lost to give the MHT anion. Because these two events occur as separate steps the loss of the hydrogen atom occurs *via* an EC mechanism. The MHT anion is then oxidized to give the MHT radical as an intermediate species (Scheme 37). The radical readily dimerizes and is seen as two oxidation peaks (-0.34 V and -0.22 V). There are two oxidation peaks observed because the two dimers that can form have an energy difference of 4.7 kcal/mol. The formation of the more stable 1,1-dimer is observed at -0.34 V, and the 8,8-dimer formation is observed at the more positive potential of -0.22 V. On the second and third scans, the sharp $2e^-$ reduction at -0.61V represents cleavage of the dimer to give back the MHT anion. The LUMOs of each dimer are at +0.4 eV and therefore are expected to be reduced at the same potential.

The second reduction of DHT occurs at -1.21 V and is irreversible (Figure 33). This reduction is caused by the addition of an electron into the MHT anion followed by loss of a hydrogen atom to give the triangulene dianion, which is expected to be an irreversible process

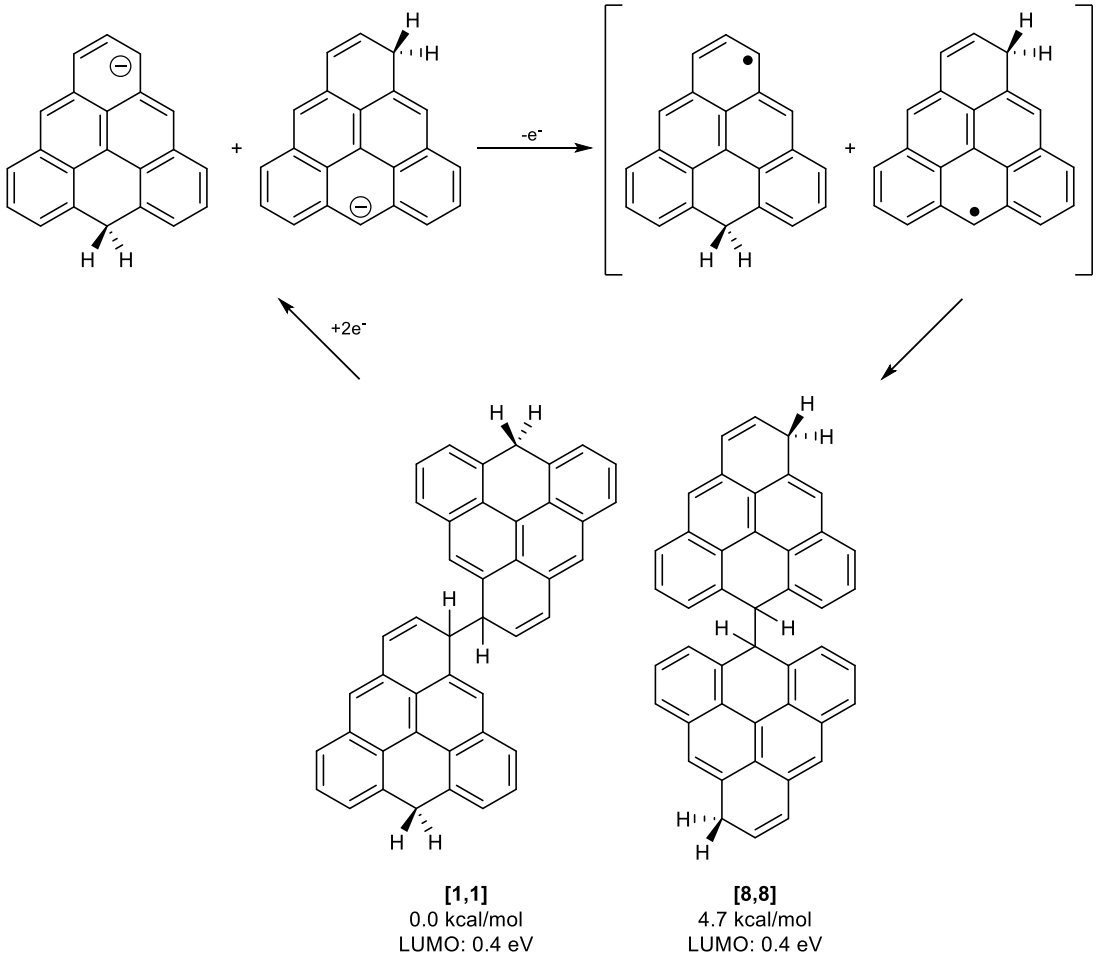

Scheme 37: Oxidation of MHT anions and 2e- reduction of dimers.

(Scheme 38). This likely follows a PCET mechanism for hydrogen atom removal, but no scan rate dependence study was done to confirm this.

It is unclear what the third reduction at -1.80 V represents. In the LSV scan (Figure 24) this reduction can be seen very clearly. However, after further scans, this reduction becomes much broader and less apparent (Figure 33). It is possible that this is an impurity or reduction of

some dimeric species still in solution. Under these experimental conditions, the formation of the triangulene diradical was not observed.

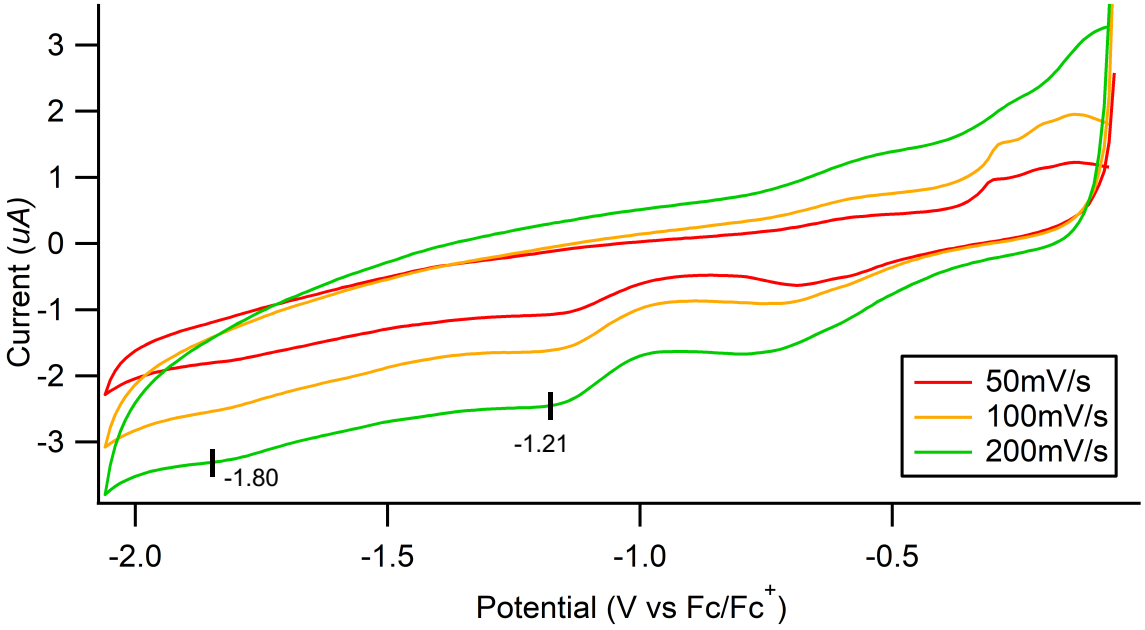

Figure 33: Second reduction of DHT.

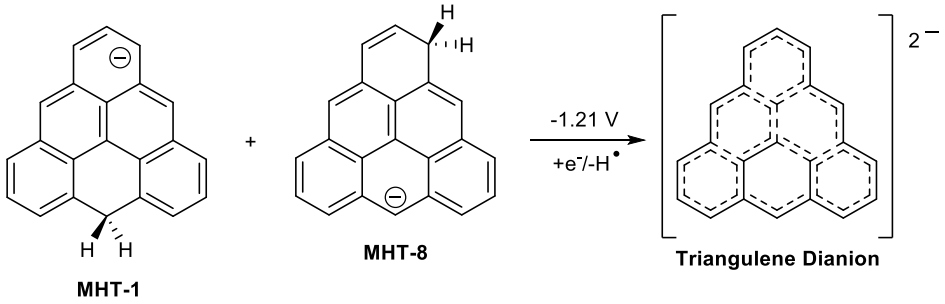

Scheme 38: Reduction of MHT anions to triangulene dianion.

Conclusions

The electrochemical properties of 1,8-dihydrotriangulene have been explored for the first time. This study revealed several redox events, all of which were found to be irreversible. This indicates that the intermediates formed are too reactive to be observed on the reverse sweep or that they undergo a chemical change that is not reversible by electrochemical means. The

assignments of these events are supported by DFT computations, which help identify which pathways are most favorable and, therefore, most likely to occur. In order to assign each event with confidence, additional experiments would be required. These could include simultaneous UV-vis monitoring of the redox processes, concentration-dependence experiments, and SEM analysis of the working electrode post-experiment to see if any oligomeric product is generated.

Chapter III. The Victorene Series

Introduction

As our triangulene project evolved, we envisioned a related series of topologically interesting structures which can be conceptually derived from phenalene by growing rings along two faces, or from triangulene by carving out one side and the center ring. This concept is illustrated in Figure 34 starting with [4]triangulene and removing two carbons and three rings. When flipped on end, the resulting structure is V-shaped; herein, we refer to these structures as "victorenes". Viewed as phenalenyl homologues, the victorenes should not have a simple Kekulé aromatic structure. As illustrated for [3]victorene (**96**), the odd carbon marked by an asterisk can either be a methylene, radical, cation or anion. Also by analogy to phenalenyl, both the cations and anions in this series are likely to be aromatic. The structure can be symmetrical or unsymmetrical, as illustrated for structures **96** – **99**. It is also noteworthy that victorenes will

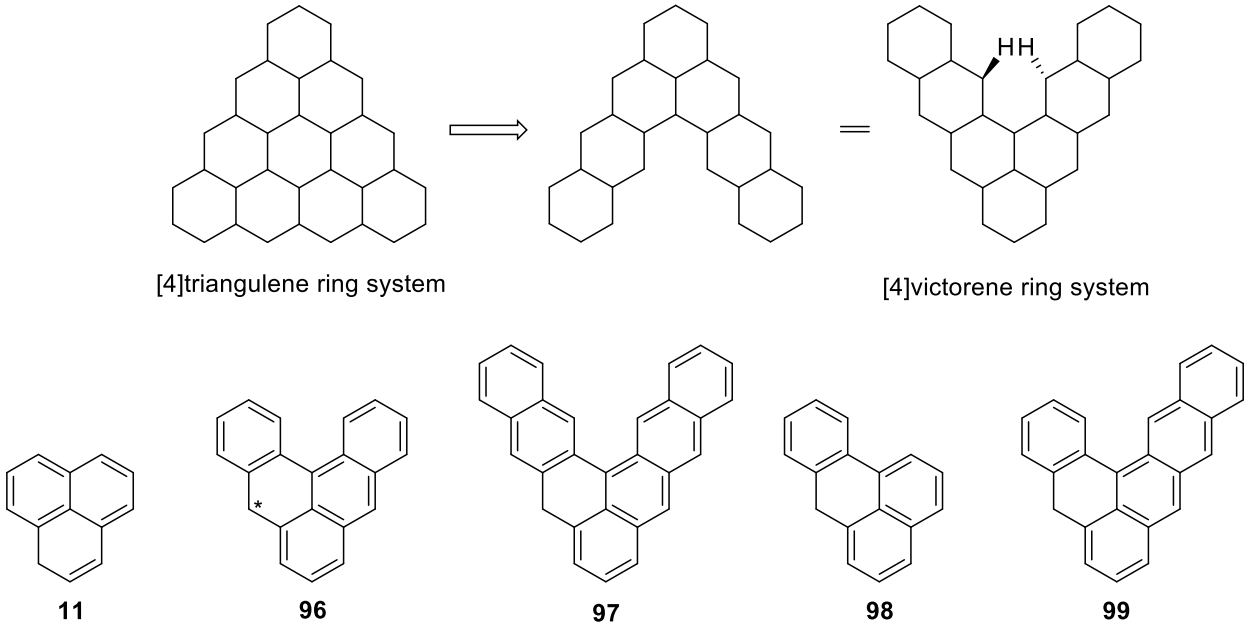

Figure 34: The [n]victorene series.

possess non-planar geometries due to crowding of the internal hydrogen atoms. This will lead to restricted rotation and give inherent chirality to the structure.[62,63] This feature makes victorenes physical properties and characteristics similar to that of helicenes and should lead to enhanced solubility relative to planar PAH molecules[64,65] A strategy for creating a larger barrier to racemization is shown below.

Little is known about the victorene ring system. In the most recent study, the potential for open-shell character was exploited in the synthesis of **102.** A 90 degree clockwise rotation shows that this is a benzannelated [3]victorene (Scheme 39).[63]

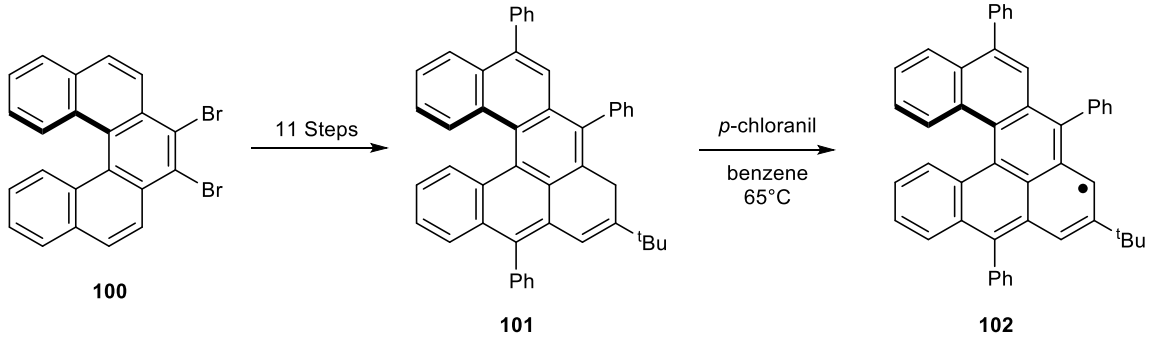

Scheme 39: Synthesis of chirally pure helicene radical (**102**)

In this study, an enantiopure helicene (**100**) was used as the starting material in order to preserve chirality in the final product. This was the first example of a neutral open-shell hydrocarbon that possesses helical chirality. The compound had to be heavily substituted in order to avoid dimerization, which was observed even in the monosubstituted product. To date, there is very little known about the victorene series, and aside from the first unsymmetrical example in the series (**98**), which has been well-studied, only the [3]victorene (**96**) has been synthesized. This compound was first described by Scholl in 1931,[66] but was first synthesized by Clar and Stewart in 1952. They synthesized it by reduction of its ketone precursor in 8% overall yield.[67] Samples from this study were provided to further assess the compound's electrochemical and optical properties in a separate experiment.[68] The only other reference to this compound's synthesis is from a Korean patent where it was one out of more than 500

compounds allegedly prepared to determine their electroluminescent properties.[69] It should be noted that the researchers in this study did not investigate hydrocarbon (**97**) on its own, but instead substituted it further for testing. In no experiments were [3]victorene's NMR properties given, nor its cationic properties explored. Only minimal computational details of the [3]victorene cation species are known, where its electronic properties were compared the phenalenyl cation.[70] This unique class of molecules and contorted PAHs, in general, have potential for use in applications such as asymmetric catalysis,[71,72] polarized light-emitting diodes,[73,74] field-effect transistors,[75,76] and as semiconductors.[77]

The fusion of two victorenes yields a more ordinary Kekulé aromatic structure. Most research has focused on the synthesis and applications of a fused divictorene, which can also be thought of as a tribenzopyrene (Figure 35). This compound is unique in that it possesses two regioisomers that are the product of syn- versus anti-addition to the anthracene core. Clar performed the first synthesis of the syn-regioisomer **54** in 1951, but only with a 0.5% overall yield.[39] Forty-three years later, a new synthetic route was applied to gain an increase in overall yield to 21%. In addition, this same route was attempted for the synthesis of [3]victorene (**96**) but ultimately failed.[40] In that time, there were several studies run to assess the physical

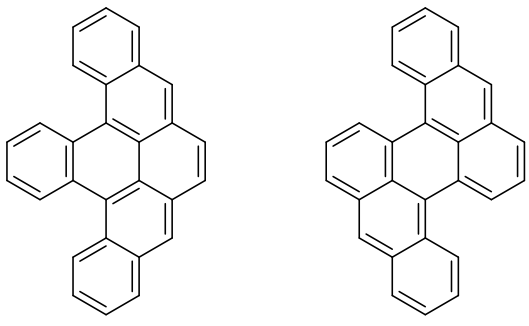

Figure 35: Syn- and anti-regioisomers of fused divictorenes.

properties of the syn-tribenzopyrene (**54**) primarily using optical spectroscopy[78–81] or computations,[82] and it was discovered as a byproduct from the pyrolysis of anthracene.[83] An in-

depth computational study of the syn-regioisomer compared the energy differences of distortions from C_{2v} symmetry to either C_2 or C_s symmetries.[62] Both were found to be significantly lower in energy than the C_{2v} geometry: ΔE C2v → C2 = -14.5 kcal/mol and ΔE C2v → Cs = -19.1 kcal/mol, but the C_s geometry was favored by 4.6 kcal/mol. A C_s symmetric transition state has been proposed as the favored route for racemization of some helicenes as well.[84,85]

Research Objective

There are very few examples of victorenes in the literature, which is surprising for such an interesting molecular structure. The goal of this work was to devise a synthesis that makes [3]victorenes and derivatives more readily accessible. Ideally, this synthesis would be modular in order to facilitate the incorporation of functional groups to the victorene core to tune its properties. In this work, the cationic properties of these victorenes are studied both experimentally by ^{1}H NMR and computationally.

Results and Discussion

Synthesis of Victorenes

Initial studies of the victorene system focused on the synthesis of unsymmetrical victorene (**98**). This was accomplished through Suzuki coupling of 2-bromobenzyl alcohol (**103**) to 1-naphthylboronic acid (**104**) to give the alcohol precursor directly (**105**, 82%) (Scheme 40). The alcohol was cyclized using $FeCl_3$ to give a dark green solution which, after chromatography was found to be a mixture of 5- and 6-membered ring regioisomers (**106** and **98**) in a 2:1 ratio respectively, as determined by ^{1}H NMR. The regioisomers were not separable by chromatography, and investigation of the victorene cation was not possible. The 5-memebered ring product **106** can be made exclusively by reaction of alcohol **105** with PPA in the microwave. DFT calculations predict the 5-membered ring product as being the favored product. The barrier

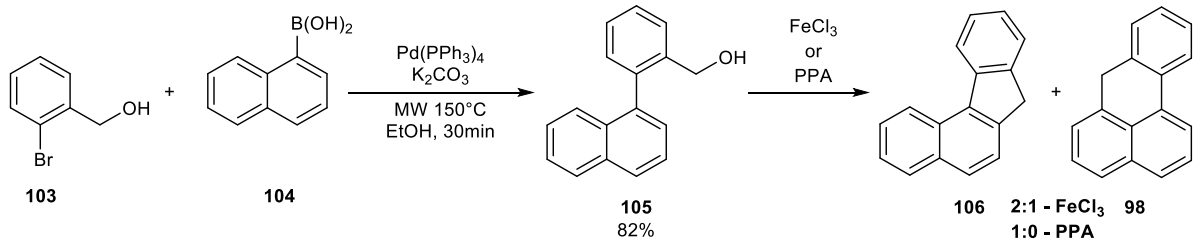

Scheme 40: Unsymmetrical victorene synthesis

to cyclization of the benzyl cation to give the 5-membered ring regioisomer is 1.85 kcal/mol lower in energy than that of the 6-membered ring isomer, and the cationic products are nearly the same in energy, (Figure 36).

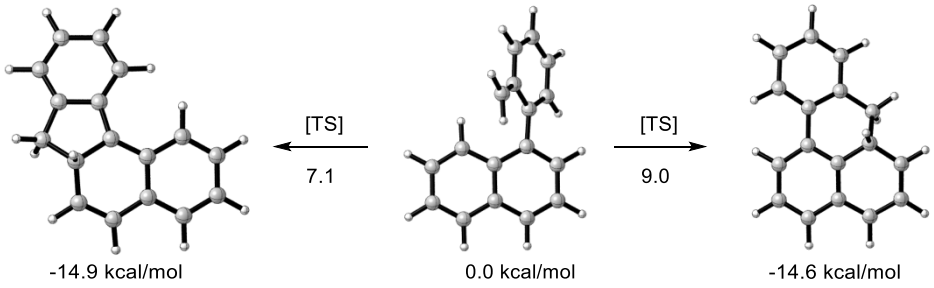

Figure 36: Barriers to cationic cyclization of 5- and 6-membered rings [IEFPCM(DCE)/B3LYP/6-31+G(d,p)].

According to computations, the victorenes should possess the property of helical chirality in their ground state, much like helicenes. DFT computations predict the barrier to racemization of the [3]victorene cation (**96**) as only 4.1 kcal/mol going through a C_{2v} transition state (Figure 37). With this very low barrier the enantiomers will interconvert at room temperature. However, a benzo[3]victorene cationic derivative (**107**) has a transition state that is significantly more

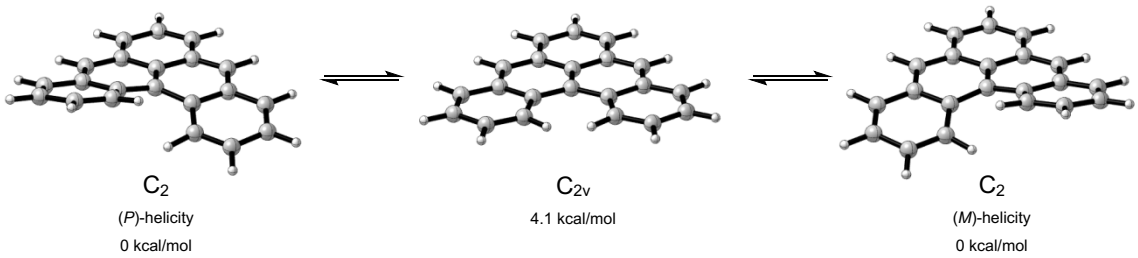

Figure 37: Racemization of [3]victorene cation (**96**) [IEFPCM(DCE)/B3LYP/6-31+G(d,p)].

contorted, leading to a much higher barrier to racemization of 24.5 kcal/mol (Figure 38). At room temperature (298K), a half-life of 29 h is predicted for racemization. These barriers to racemization can be compared to [4]- and [5]-helicene. [4]-Helicene has a racemization barrier of 3.5 kcal/mol going through a C_{2v} transition state, and [5]-Helicene has a racemization barrier of 22.7 kcal/mol going through a C_s transition state (Figure 39).[85]

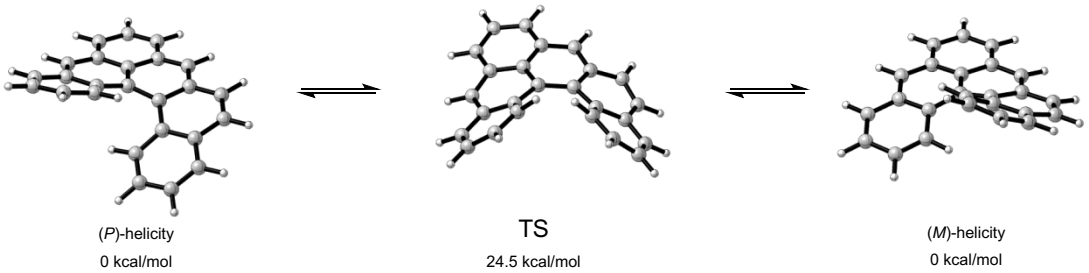

Figure 38: Racemization of benzo[3]victorene cation (**107**) [IEFPCM(DCE)/B3LYP/6-31+G(d,p)].

Preliminary attempts to synthesize these [3]victorenes once again used Suzuki coupling, but in this case, 9-anthraceneboronic acid was used. The coupling reaction failed, and only protodeboronated and protodebromonated products were observed. These same results were found in the initial route for triangulene (Scheme 10).

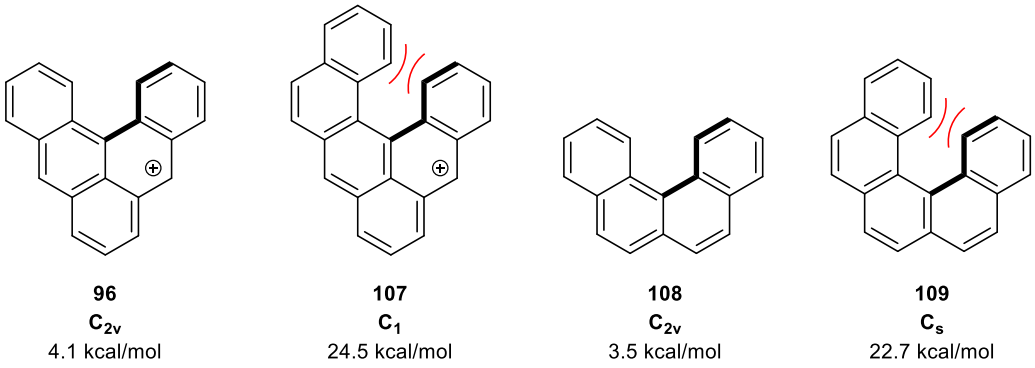

Figure 39: Predicted barrier to racemization of victorenes versus helicenes.

In order to generate the [3]victorene alcohol precursors, a new route was devised that started with mono-organolithium additions of the allyl-protected bromobenzyl alcohols (**66** and **113**). The allyl-protected alcohol **113** was prepared in three steps (Scheme 41), beginning with

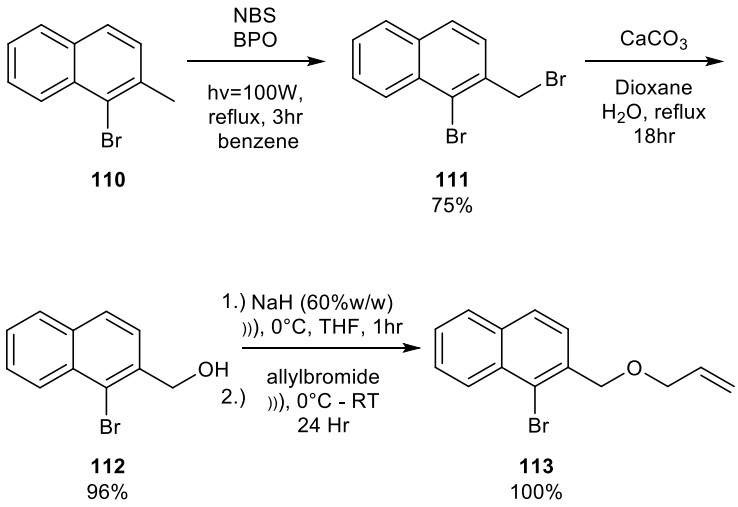

Scheme 41: Synthesis of allyl-protected bromo naphthalene methanol (**113**).

the NBS bromination of 1-bromo-2-methylnaphthalene (**110**) in 75% yield followed by conversion to the alcohol using $CaCO_3$ (**112**, 96%), and finally reaction with allyl bromide to give the allyl-protected alcohol (**113**, 100%). This, along with allyl-protected bromobenzyl alcohol (**66**) were added to anthraquinone to give the [3]victorene (**114**, 48%, black) and benzo[3]-

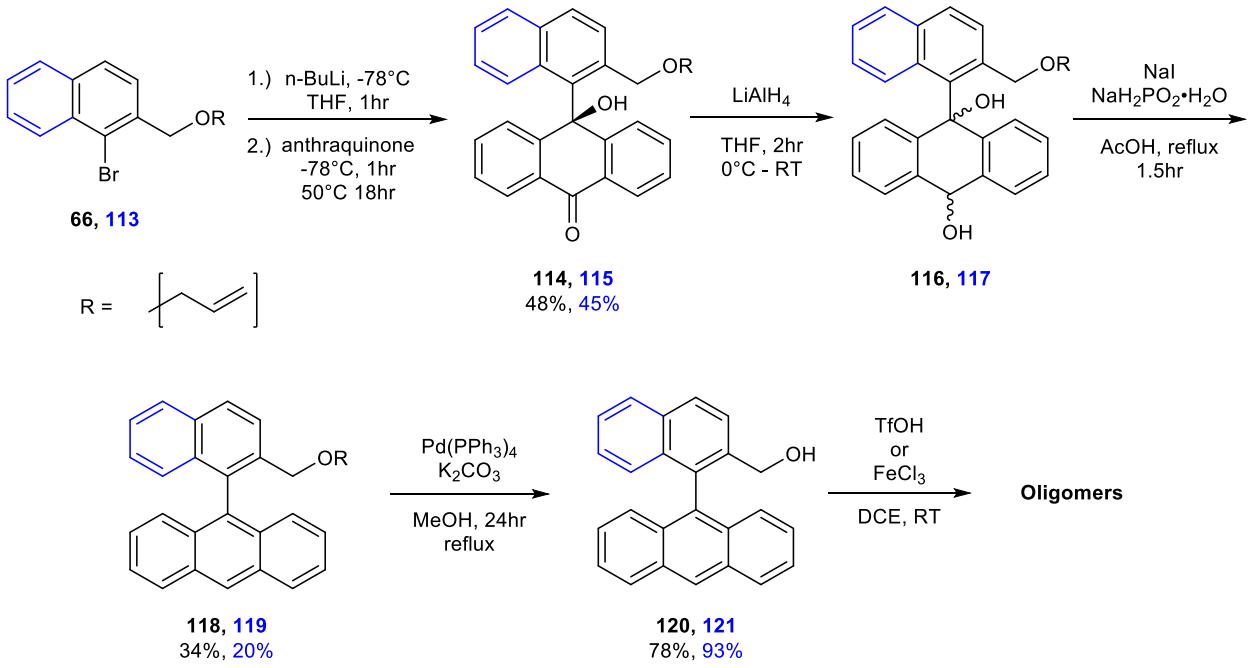

Scheme 42: Attempted [3]victorene and benzo[3]victorene synthesis.

victorene (**115**, 45%, blue) aryl ketones, Scheme 42. The ketones were reduced to give a mixture of diastereomers (**115** and **116**), reductively aromatized to give the anthracene core (**118**, 34% and **119**, 20%), and deprotected to give the alcohol precursors (**120**, 78%, **121**, 93%).

Again, Lewis-acids known to facilitate benzyl cation formation and subsequent intramolecular cyclization were used,[44–46] but only oligomeric products and decomposed starting materials were observed. The same was true when PPA and TfOH were used to promote the cyclization. Anthracene is known to readily polymerize in acidic and Lewis-acidic media[86] (Scheme 43), which is what seems to be happening in the victorene precursor as well since it contains an anthracene core. In light of this, we envisioned a different route through the intramolecular cyclization of an aldehyde precursor to yield a ketone which would effectively block the reactive methylene site.

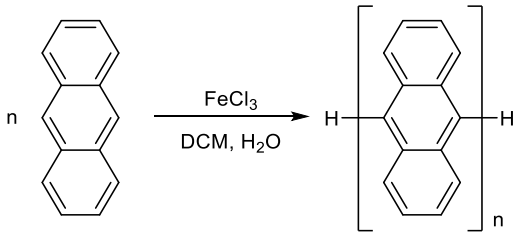

Scheme 43: Polymerization of anthracene under Lewis-acidic conditions.

This type of cyclization has been accomplished in similar biaryl systems through the generation and cyclization of an acyl radical formed using tBuOOH,[87] $K_2S_2O_8$,[88] or hypervalent iodine.[89] However, before the cyclization conditions could be tested, the aldehyde precursor needed to be synthesized. This was accomplished through PCC oxidation of alcohols (**120** and **121**) to give aldehydes (**122**, 67% and **123**, 65%). Surprisingly, a moderate amount of spirocyclic product was also formed in the oxidation (**124**, 31% and **125**, 35%) indicating that over oxidation was occurring (Scheme 44). This type of oxidation is known to occur with acenes to quinones under strongly oxidative conditions using chromium oxide.[90]

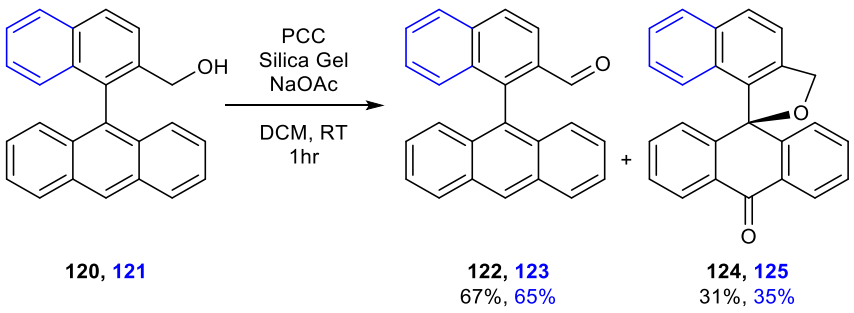

Scheme 44: PCC-oxidation of aryl alcohols **120** and **121**.

Nevertheless, the desired aldehydes **122** and **123** were isolable through chromatography and used for subsequent cyclization. The route chosen for the intramolecular cyclization involved a catalytic amount of ferrocene and an excess of tBuOOH to give the corresponding ketones in low yields (**126**, 36% and **127**, 32%). This reaction is believed to pass through acyl radical intermediates. Although the cyclization did not occur with an optimal yield, it did provide a proof of concept that the ketone could be isolated without a large degree of oligomerization. The idea was to reduce the ketone to the methylene and study its cationic properties, but so little of the product was isolated that this experiment was never run.

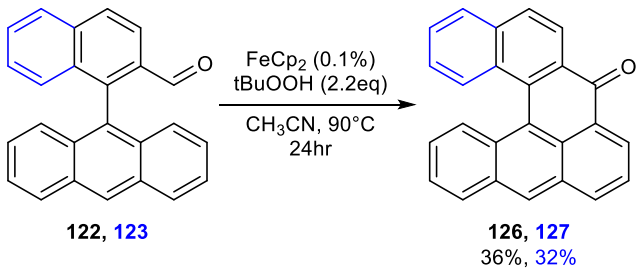

Scheme 45: Intramolecular cyclization of aldehydes **122** and **123**.

Another way to inhibit oligomerization of the anthracene core is to block this position with a substituent. Ideally, this substituent would not have a significant electronic contribution to the victorene core, so its cationic properties can be studied unperturbed. For this, the phenyl

substituent was chosen. DFT calculations predict little electronic involvement of the phenyl substituents because they are almost perpendicular to the victorene ring system.

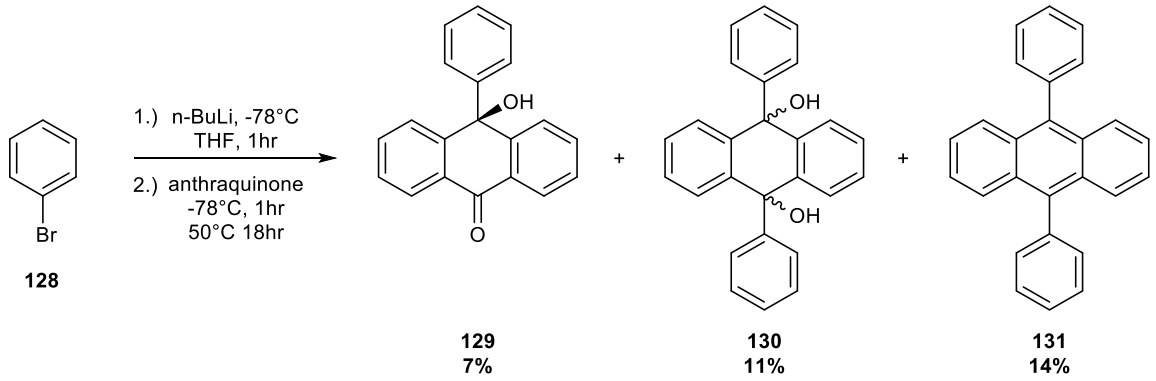

128 **129** 7% **130** 11% **131** 14%

Scheme 46: Mono-addition of phenyl-lithium.

Initially, the mono-addition of phenyl-lithium to anthraquinone was attempted in the first step, but only a 7% yield of mono-addition product (**129**) was isolated, instead preferring double addition to give diol (**130**, 11%) and 9,10-diphenylanthracene (**131**, 14%) (Scheme 46). However, when the bulkier allyl-protected bromobenzyl alcohols (**66** and **113**) were added first (Scheme 47), mono-addition to anthraquinone is preferred (**114**, 40%, **115**, 45%). After the first organolithium addition, an excess of phenyl-lithium was added to give diols (**132** and **133**), which were used without purification in the subsequent reductive aromatization to give the fully aromatic compounds (**134,** 40% and **135**, 24%). These were efficiently deprotected using the standard palladium-catalyzed conditions to give each alcohol (**136**, 80% and **137**, 88%). The alcohols were then oxidized to their respective aldehydes using PCC (**138**, 65% and **139**, 50%). Surprisingly, a small amount of spirocycles (**140**, 9% and **141**, 22%) formed even though a phenyl substituent blocks the 10-anthracenyl position. The spirocycles were easily removed *via* chromatography, and the pure aldehydes were used in the final organolithium addition of phenyl lithium to give the diphenyl alcohol precursors in excellent yields (**142**, 95% **143**, 97%).

An NMR experiment was conducted where the diphenyl[3]victorene precursor (**142**) was combined with 10 eq. of TfOD to generate the victorenium cation (**144**) *in situ*. The resulting spectrum was a complex mixture that contained peaks indicating the formation of the desired

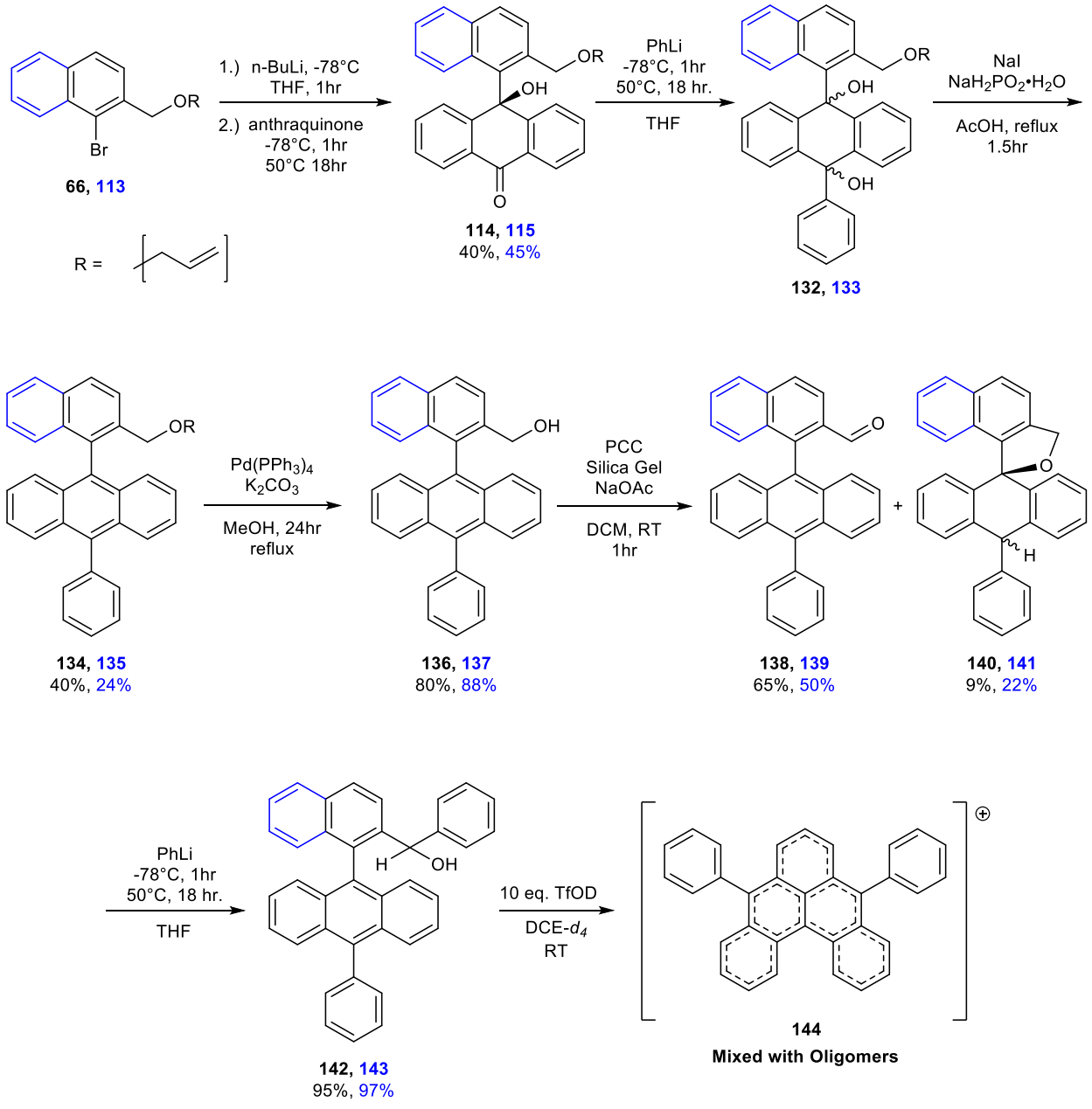

Scheme 47: Synthesis of diphenyl substituted victorenes.

cation as well as some form of oligomer. The representative cation peaks were, a pair of doublets at 9.0 and 9.3 ppm that integrate in a 1:1 ratio. These protons are located on carbons

1, 3, 8, and 9 (Figure 40, left), and agree very well with their predicted values of 9.0 and 9.2 ppm. The large degree of oligomerization observed in this experiment indicates that performing the cyclization and cation formation in one step is not an optimal route to observing a clean victorenium cation spectrum. Instead, initial cyclization of the benzyl alcohols affords hydro[3]victorenes which could be used as cation precursors.

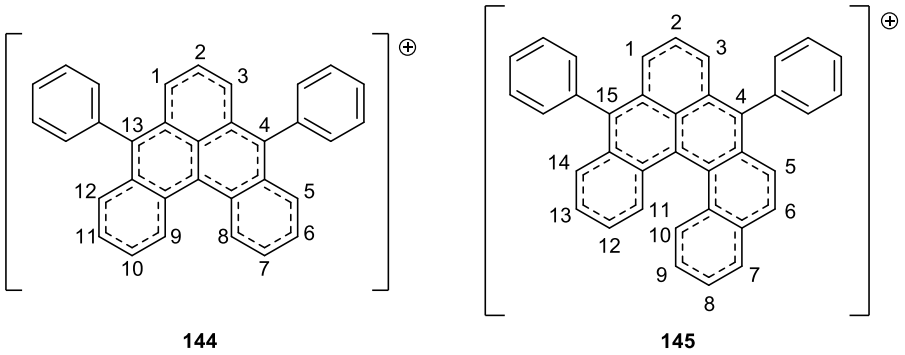

Figure 40: Numbering scheme for substituted [3]victorene (**144**) and benzo[3]victorene (**145**).

This type of intramolecular cyclization of benzyl cations is known to occur effectively using $BF_3{\cdot}Et_2O$ in similar polycyclic aromatic systems.[46,91] Under these cyclization conditions, the [3]victorene alcohol precursor (**142**) afforded two hydro[3]victorene isomers (**146** and **147**) in a 3:1 ratio, respectively and 53% isolated yield (Scheme 48). The expected product from immediate intramolecular cyclization is the 4-hydro product (**146**), which is observed as the major product. DFT computations predict the 1-hydro isomer (**147**) as being 0.7 kcal/mol lower

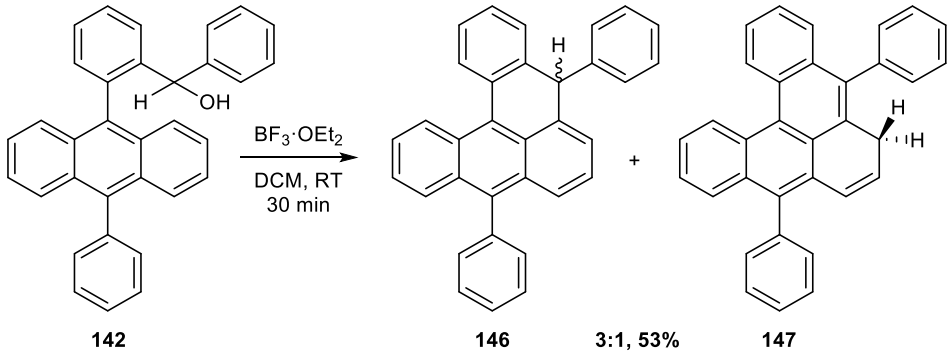

Scheme 48: Intramolecular cyclization of [3]victorene precursor (**142**).

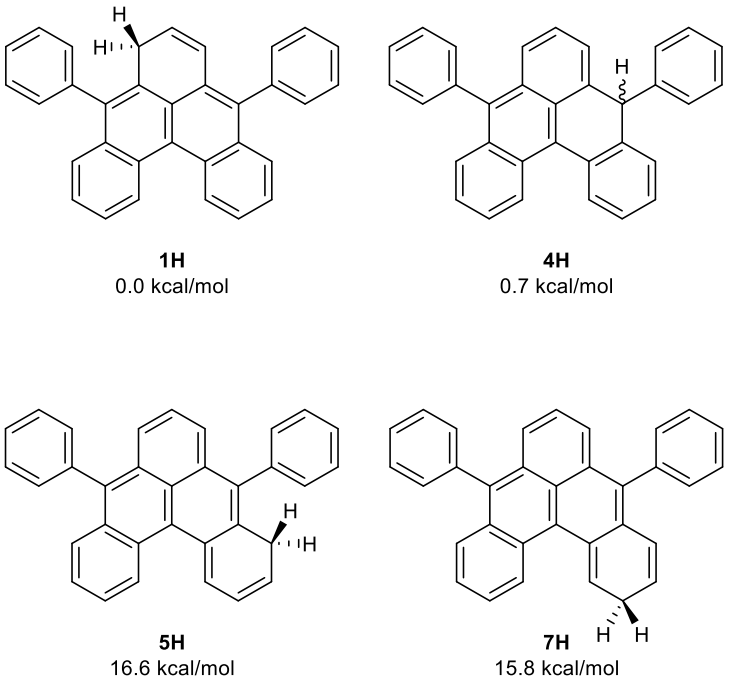

Figure 41: Relative free energies of hydro[3]victorene isomers [IEFPCM(DCE)/B3LYP/6-31+G(d,p)].

in energy than the 4-hydro isomer, so it is not surprising that some rearrangement is observed. The other potential hydro isomers (Figure 41) are ca. 16 kcal/mol higher in energy and are therefore not likely to be observed under these conditions.

For the benzohydro[3]victorene isomers, the addition of the extra benzene ring breaks the symmetry of the molecule giving rise to more theoretical hydro isomers (Figure 42). DFT computations predict the lowest energy isomer as the 15H isomer; however, the expected product from immediate cyclization is the 4H isomer, which is only 1.9 kcal/mol higher in energy. Other isomers that are similar in energy include 1H and 3H, which are now different isomers due to the broken symmetry. The remaining isomers have calculated free energies that are 17 – 27 kcal/mol higher in energy and are unlikely to be observed under the reaction conditions. When the benzo[3]victorene was subjected to the cyclization conditions, a mixture of three hydro isomers was isolated in 70% yield. These were the 4H (**148**), 3H (**149**), and 1H (**150**) isomers in a 16:1:1 ratio as determined by ^{1}H NMR. The observed experimental results match

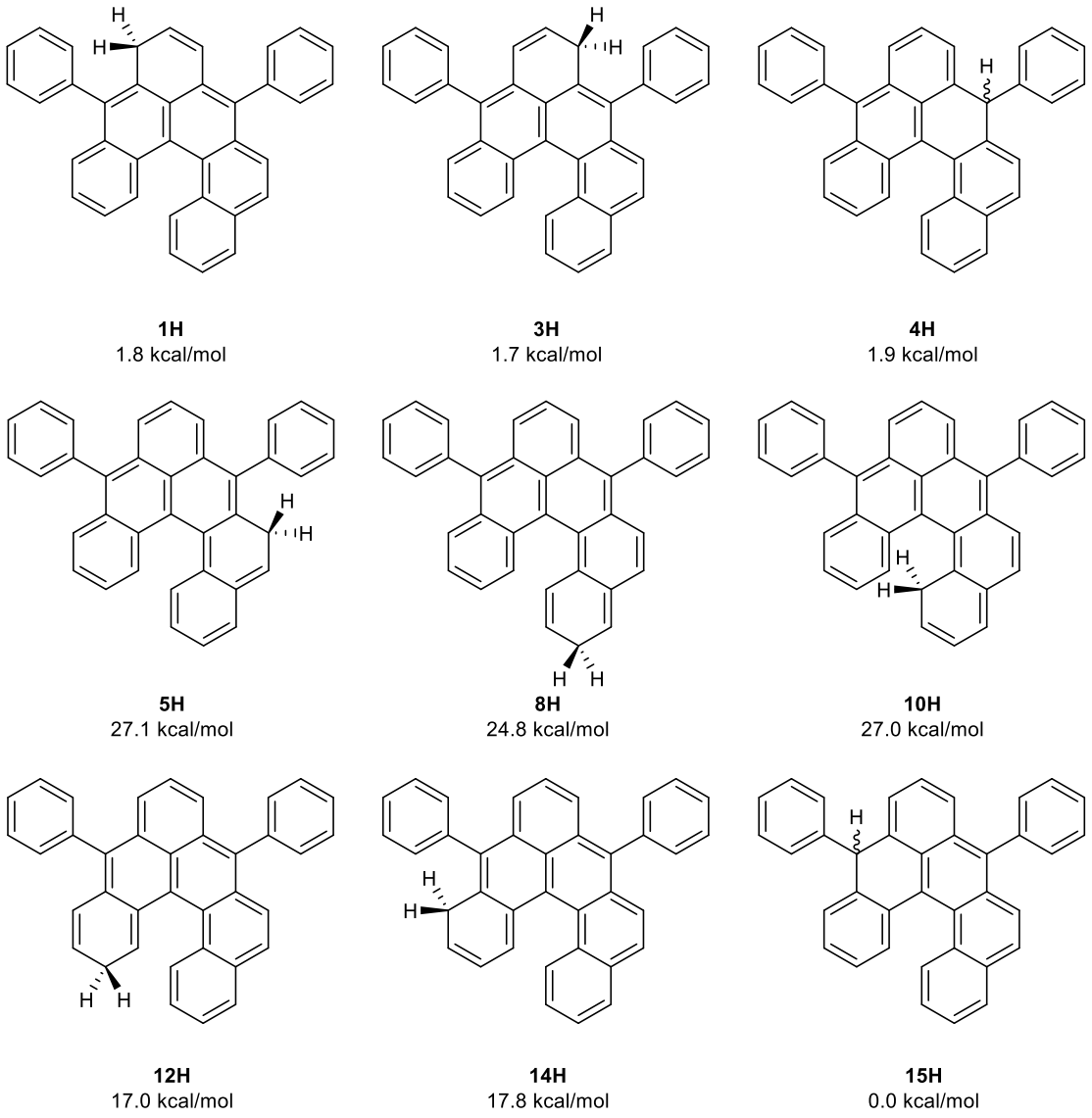

Figure 42: Relative free energies of hydrobenzo[3]victorene isomers [IEFPCM(DCE)/B3LYP/6-31+G(d,p)].

well with computations in terms of which isomers are favored with the exception of the 15H isomer, which was not observed.

When each mixture of hydro isomers was subjected to the triflic acid NMR conditions, complete conversion to the [3]victorene cations was observed (Schemes 50 and 51). Very little oligomerization was observed in these experiments, confirming that the hydro[3]victorenes are better cation precursors. ^{1}H NMRs of the hydro[3]victorenes and resultant victorenium cations are provided in Figures 43 – 46, with predicted NMR values of relevant peaks at the ωB97X-D/

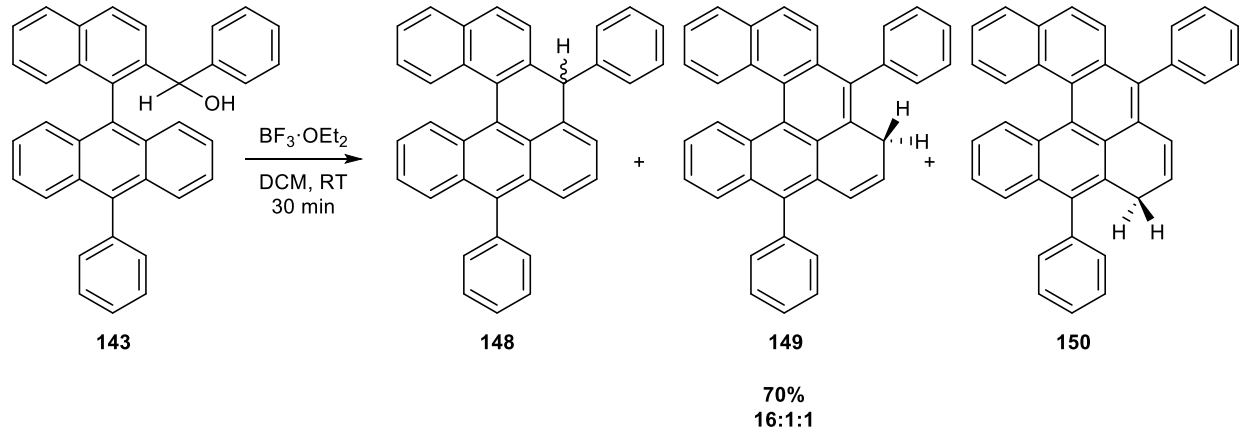

Scheme 49: Intramolecular cyclization of benzo[3]victorene precursor.

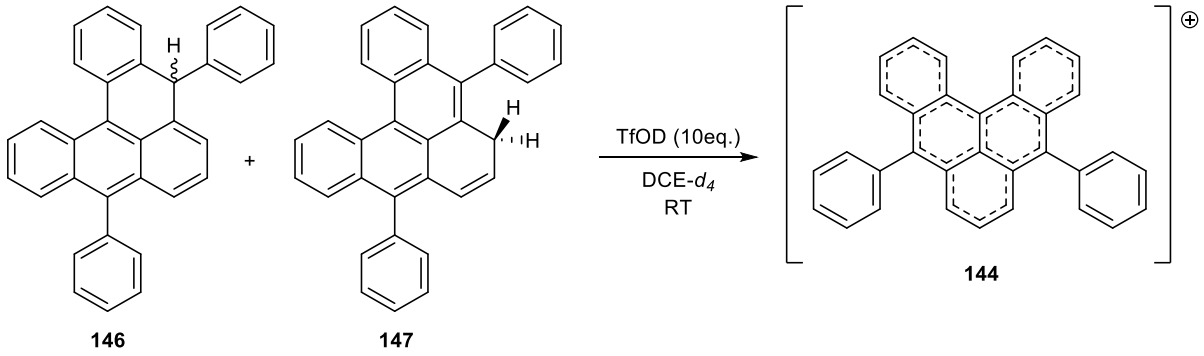

Scheme 50: Generation of the diphenyl[3]victorenium cation (**144**).

6-31G* level of theory. In each NMR, the predicted values agree with the observed experimental values. A mixture of isomers is clearly seen in both hydro[3]victorene spectra, but these consolidate to one single isomer when TfOD is added, which is expected for the cationic species. Furthermore, the methylene protons around 3.5 ppm disappear and a clear downfield shift is observed for all protons indicating an electron-poor environment. Additionally, the peaks that were attributed to the [3]victorenium cation (**144**) matched the ones previously observed in the TfOD cyclization experiment (Scheme 47). This confirmed that the cation was indeed formed in this experiment, albeit with a higher degree of oligomerization.

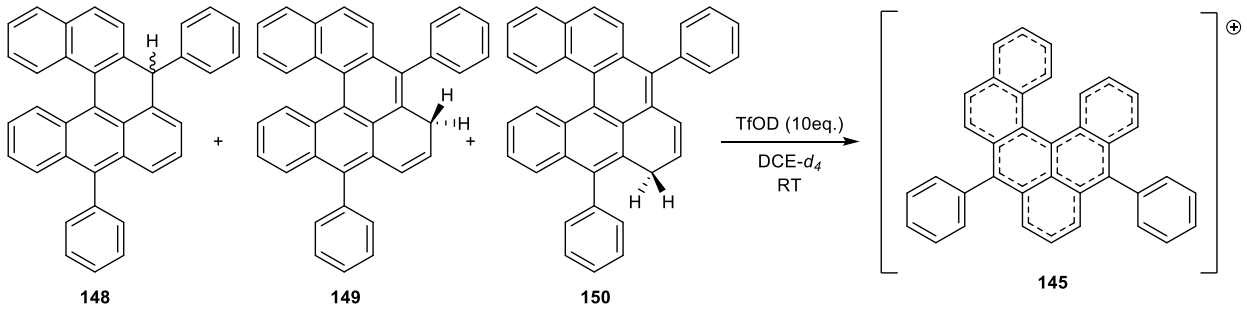

Scheme 51 Generation of the diphenylbenzo[3]victorenium cation (**145**).

Conclusions

The synthesis of novel diphenyl-substituted [3]victorenes was possible by cyclization of an alcohol precursor with BF_3•Et_2O. This chemistry was performed on both [3]victorene and a benzo[3]victorene derivative to yield a variety of hydro[3]victorene isomers. The presence and relative amounts of these hydro isomers are supported by DFT computations, which confirms that only low-energy species are generated. The synthetic route can easily be modulated to incorporate other functional groups at the 4- and 13-positions of [3]victorene, including unsymmetrical versions that have two different functional groups. In this way, the victorenes electrochemical properties can be readily tuned without changing the overall synthetic route. The victoreneium cations can be formed directly by cyclization of their alcohol precursors in triflic acid; however, a significant amount of oligomeric byproducts are formed using this method. This oligomerization is avoided when the cyclization is performed as a separate step, and the hydro[3]victorene is used as the cation precursor.

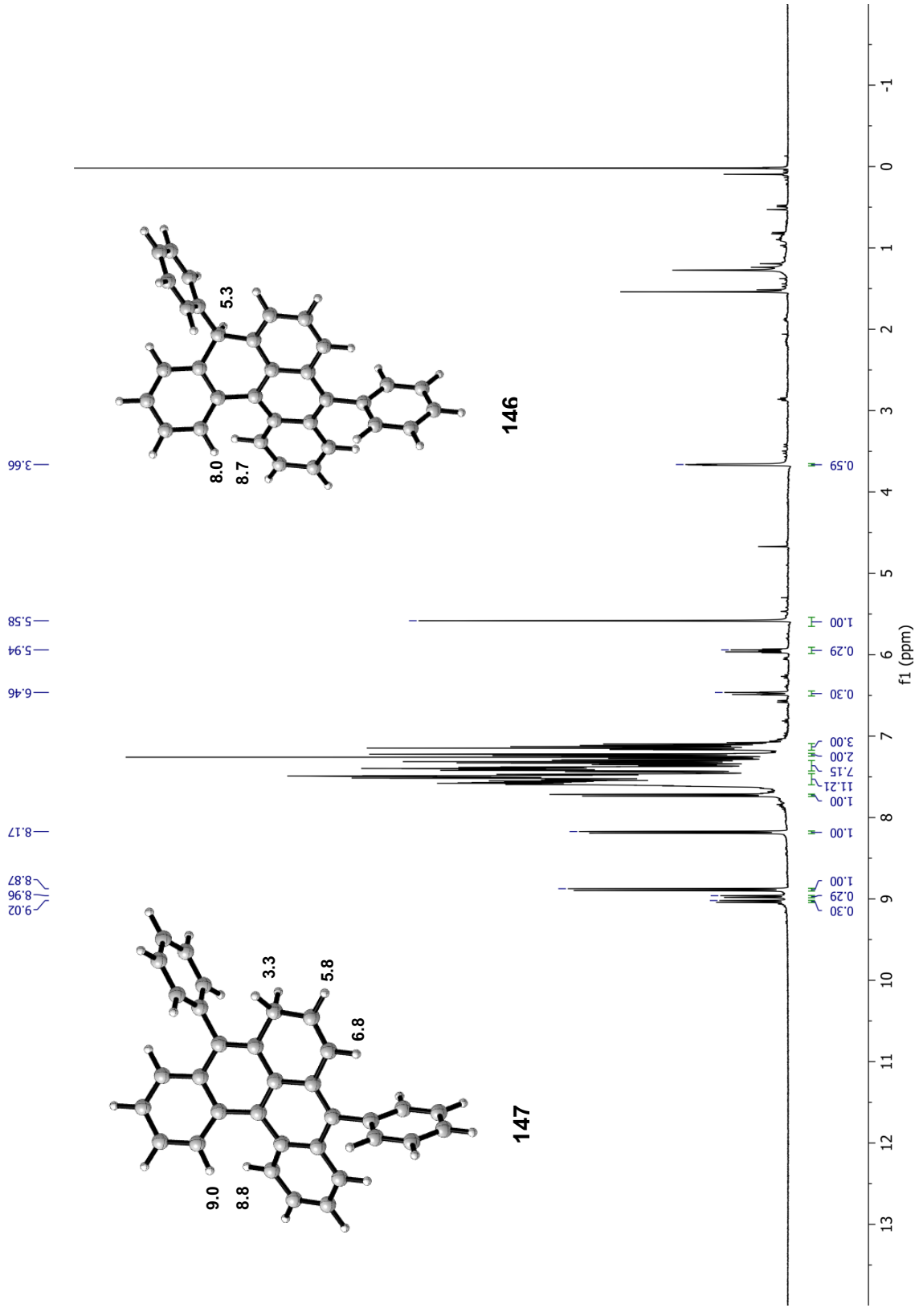

Figure 43: ^{1}H NMR of hydro[3]victorenes and predicted values.

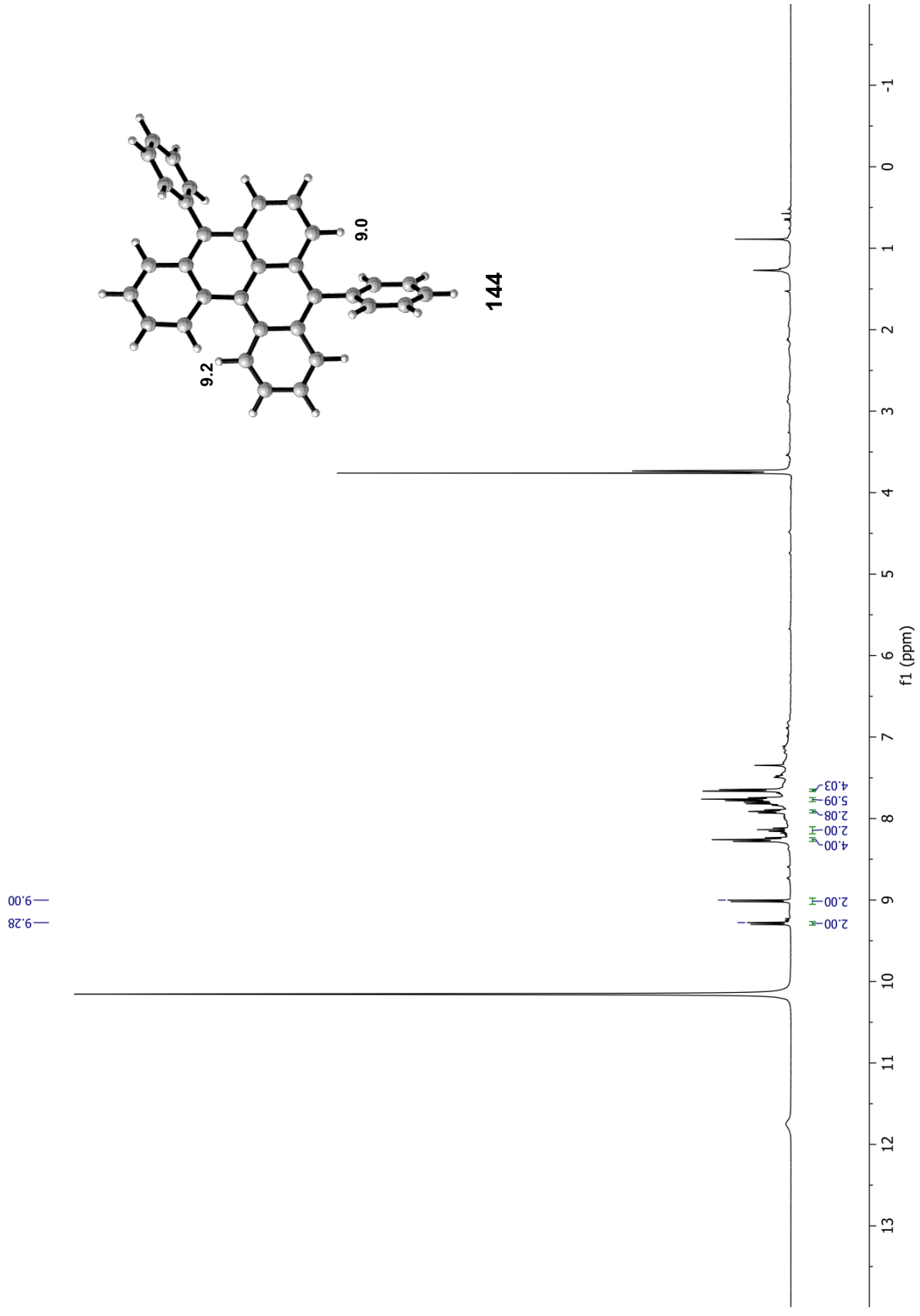

Figure 44: ^{1}H NMR of diphenyl[3]victorene cation (**144**) and predicted values.

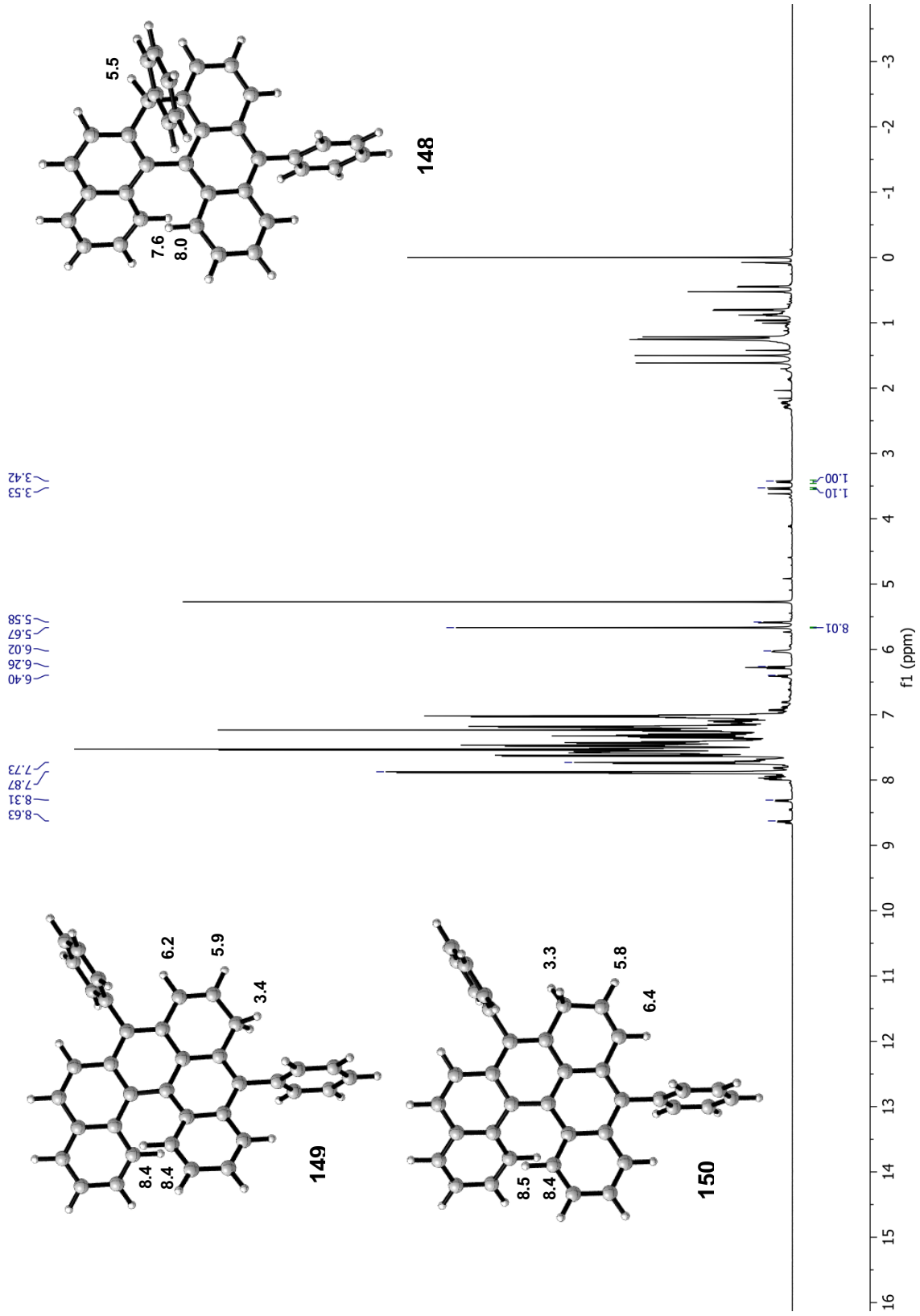

Figure 45: ^{1}H NMR of hydrobenzo[3]victorenes and predicted values.

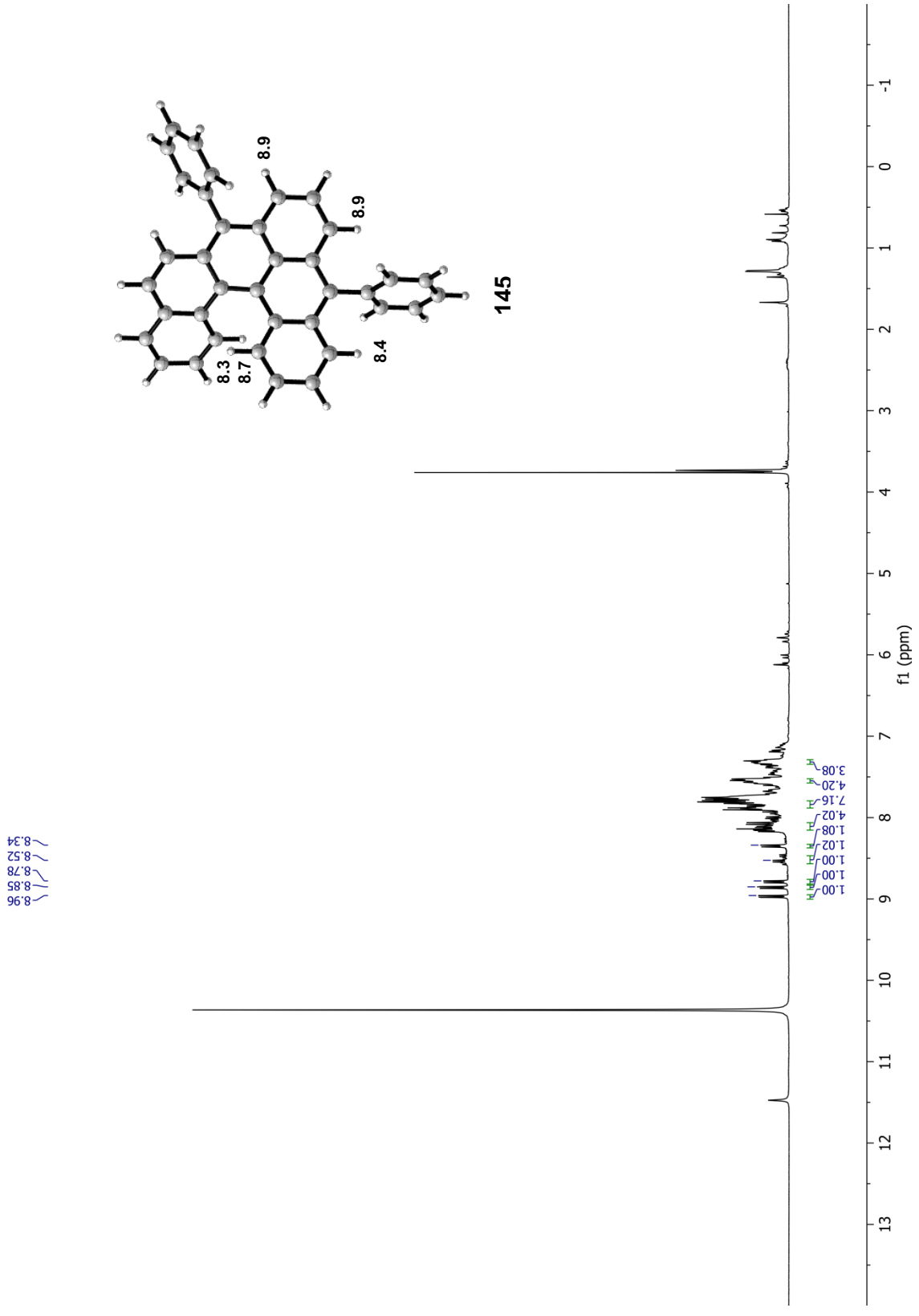

Figure 46: ^{1}H NMR of diphenylbenzo[3]victorene cation (**145**) and predicted values.

Chapter IV. Experimental

General Experimental Section

Solvents

Anhydrous solvents [diethyl ether, dichloromethane (DCM), and tetrahydrofuran (THF)], passed through drying agent with nitrogen pressure, were obtained from an Innovative Technology, Inc. Solvent Delivery System before use and stored over 4 Å molecular sieves. THF was purified further by distillation over sodium metal and benzophenone. Other solvents, including 1,2-dichloroethane (DCE), hexanes, ethyl acetate, cyclohexane, benzene, and methanol were purchased from EMD Serono, Inc. or Pharmco-AAPER.

Reagents

All reagents were received from commercial sources and were used as received unless otherwise noted. Reagents were obtained from the following sources: Fisher Scientific (Acros), Alfa Aesar, TCI America, Sigma-Aldrich, and Cambridge Isotope Laboratories. *Note:* Many of the polycyclic aromatic hydrocarbons used here have some level of carcinogenicity. All reactions were carefully conducted in a hood to limit exposure.

Reactions

Glassware and Teflon coated magnetic stir bars were dried in an oven at 110 ^{o}C before use. Sigma-Aldrich natural rubber septa were used. Unless otherwise noted, nitrogen gas was introduced to the reaction vessel through a Tygon® tube with a needle or glass inlet adapter. Henke Sass Wolf Norm-ject® plastic syringes were used for volumetric addition of reagents with oven-dried Popper & Sons needles, Precision Glide sterile needles, or Sterican® sterile needles unless otherwise noted.

Chromatography

Flash column chromatography was performed with Silicycle SiliaFlash P60 Flash Silica Gel or with a Teledyne Isco CombiFlash Rf 200 purification system. Purifications using CombiFlash Rf used RediSep® pre-packed silica gel columns (20-70 μm particle size). Thin Layer Chromatography (TLC) analysis used Whatman polyester-backed Silica Gel, 60 Å, 250 μm thickness, on flexible plates with a fluorescent indicator. Mobile phases were prepared per-use.

Instrumentation

Nuclear Magnetic Resonance (NMR) spectra were measured on a Varian Mercury Plus 400 FT-NMR operating at 400 MHz for ^{1}H and 100 MHz for ^{13}C spectroscopy, a Bruker 500 FT-NMR operating at 500 MHz for ^{1}H and 126 MHz for ^{13}C spectroscopy, or a Bruker 700 FT-NMR operating at 700 MHz for ^{1}H and 176 MHz for ^{13}C spectroscopy. Deuterated solvents for NMR analysis were purchased from Cambridge Isotope Laboratory and stored over 4 Å molecular sieves. All ^{1}H resonances were reported relative to an internal standard tetramethylsilane (TMS, δ 0 ppm) unless otherwise noted. Microwave-assisted reactions were conducted in a CEM Discover single-mode microwave reactor in capped 10 mL or 35 mL vessels. HRMS was performed at the University of Illinois using a Micromass 70-VSE and ESI/Q-TOF methods.

Detailed Experimental Section

Chapter I

Mono Addition of 2-bromo-m-xylene to Anthraquinone (45)

To an oven-dried 100 mL RBF was added a solution of 2-bromo-m-xylene (1.3 mL, 10 mmol) in anhydrous THF (62 mL). The colorless solution was cooled to -78 °C and n-BuLi (2.65M, 3.8 mL, 10 mmol) was added and stirred at -78°C for 1hr to give a pale-yellow solution. This was slowly transferred *via* cannula over the course of 2h to a solution of 9,10-anthraquinone (4.16 g, 20 mmol) in anhydrous THF (125 mL) at -78 °C, then stirred at room temperature overnight. The reaction mixture was quenched with 1 M HCl, extracted with DCM, then condensed to give an orange solid. The crude mixture was suspended in acetone to give a yellow ppt. that was filtered off and identified as residual anthraquinone (0.91 g). The filtrate was dried with $MgSO_4$, gravity filtered, and condensed to give an orange solid. The crude product was purified *via* CombiFlash (Hex:DCM) to give ketone **45** as an off-white solid (0.83 g, 26% yield). ^{1}H NMR (400 MHz, $CDCl_3$) δ 8.23 -8.26 (m, 2H), 7.55 – 7.48 (m, 2H), 7.45 – 7.39 (m, 2H), 7.26 – 7.21 (m, 2H), 7.13 (t, *J* = 7.45 Hz, 1H), 7.02 (s, 1H), 2.93 (s, 1H), 2.80 (s. 6H).

Reduction to Give Diol 46

To an oven-dried 10 mL RBF was added a suspension of $LiAlH_4$ (0.083 g, 2.2 mmol) in anhydrous THF (3 mL) at 0 °C. A solution of ketone **45** (0.20 g, 0.64 mmol) in anhydrous THF (8 mL) was added drop-wise and kept at 0°C for 10 min, then held at room temperature for 2h. The bright yellow suspension was cooled to 0°C then quenched with 1 M NaOH, H_2O, and 1 M HCl. The orange suspension was filtered through a silica plug with EtOAc, extracted with EtOAc, dried with $MgSO_4$, gravity filtered, and condensed to give diol **46** as an orange solid (0.17 g, 85% yield).

Aromatization to Give Compound 40

To a 50 mL RBF was added a solution of diol **46** (0.162 g, 0.51 mmol), NaI (0.53 g, 3.6 mmol), and $NaH_2PO_2•H_2O$ (0.50 g, 4.7 mmol) in glacial acetic acid (13 mL). The dark red solution was heated to reflux for 1.5 h to give a bright yellow solution. The reaction mixture was cooled to room temperature, quenched with water, extracted with DCM, dried with $MgSO_4$, gravity filtered, and condensed to give a reddish solid. The crude product was purified *via* CombiFlash (Hex:DCM) to give the aromatic product (**40**) as a yellow solid (0.043 g, m.p. 130 – 132 ^oC, 30% yield).

Bromination to Compound 48

To an oven-dried 25 mL RBF was added a solution of biaryl **40** (0.20 g, 0.75 mmol), NBS (0.13 g, 0.75 mmol), and BPO (1 mg, 0.002 mmol) in benzene (7.5 mL). The yellow solution was heated to reflux, the irradiated with a 100W lamp for 3h to give an orange solution. The reaction mixture was hot filtered with benzene then condensed to give a yellow solid identified as the 10-bromo product (0.23 g, 90%)

Synthesis of 2-bromo-1,3-benzene dicarboxylic acid (49)[37]

To a 500 mL RBF was added a solution of 2-bromo-m-xylene (10.9 mL, 82 mmol) in t-BuOH (63mL) and water (63 mL). $KMnO_4$ (16.20 g, 103 mmol) was added slowly, and the dark purple solution was heated ton 70 °C. After 2h, a second portion of $KMnO_4$ (16.20 g, 103 mmol) was added, and the solution was stirred at 70 °C overnight. The resulting brown sludge was refluxed with formaldehyde (37% w/w, 90 mL) until to solution turned light brown (ca. 1h). The crude reaction mixture was then filtered through a Celite plug with boiling water. The filtrate was condensed to 1/3 its original volume then acidified with con. HCl to give a white ppt. which was collected *via* vacuum filtration. The crude product was purified by recrystallization in water to give 2-bromo-1,3-benzene dicarboxylic acid as white crystals (19.53 g, m.p. 213 - 215 ^oC, *lit* 218 ^oC 98% yield). ^1H NMR (400 MHz, DMSO-d_6): δ 13.58 (s, 2H), 7.69 (d, J = 7.62 Hz, 2H), 7.52

(dd, J = 7.93, 7.33 Hz, 1H); ^{13}C NMR (101 MHz, DMSO-d_6): δ 168.20, 137.17, 131.17, 128.26, 116.64.

Synthesis of 1,3-dimethyl 2-bromobenzene-1,3-dicarboxylate (50)[37]

To an oven-dried 100mL RBF was added a solution of 2-bromo-1,3-benzene dicarboxylic acid (4.77 g, 19.5 mmol) in thionyl chloride (33 mL). The reaction mixture was heated to 100 °C over 5h (15 °C/hr), then held at this temperature for an additional 4h. The pale-yellow solution was condensed to give an off-white solid then cooled to 0 °C. MeOH (22 mL) and Et_3N (11 mL) were added dropwise, and the solution was stirred for 2h at room temperature. The brown solution was condensed, suspended in water, extracted with EtOAc, dried with $MgSO_4$, gravity filtered, and condensed to give 1,3-dimethyl 2-bromobenzene-1,3-dicarboxylate as a brown oil (5.08 g, 97% yield). ^{1}H NMR (400 MHz, $CDCl_3$): δ 7.70 (dd, J = 7.68, 0.98 Hz, 2H), 7.45 – 7.39 (m, 1H), 3.94 (s, 6H); ^{13}C NMR (101 MHz, $CDCl_3$): δ 166.95, 135.42, 132.32, 127.19, 119.11, 52.84.

Synthesis of 2-bromo-1,3-benzenedimethanol (51)[37]

To an oven-dried 100 mL RBF was added a suspension of $LiBH_4$ (0.38 mL, 18 mmol) in anhydrous THF (10 mL) at 0 °C. A solution of 1,3-dimethyl 2-bromobenzene-1,3-dicarboxylate (2.17 g, 8.0 mmol) in anhydrous THF (20 mL) was added dropwise then stirred at room temperature overnight to give a white suspension. The reaction mixture was acidified with 1 M HCl, extracted with EtOAc, dried with $MgSO_4$, gravity filtered, and condensed to give 2-bromo-1,3-benzenedimethanol as a white solid (1.69 g, m.p. 166 – 169 °C, *lit.* 167 – 169 °C, 98% yield). ^{1}H NMR (400 MHz, DMSO-d_6): δ 7.44 – 7.36 (m, 3H), 5.41 (s, 2H), 4.53 (s, 4H); ^{13}C NMR (101 MHz, DMSO-d_6): δ 140.95, 127.06, 126.22, 120.32, 62.83.

THP-Ether Protection of 2-bromobenzyl alcohol (52)

To an oven-dried 100 mL RBF was added a solution of 2-bromobenzyl alcohol (3.45 g, 18.4 mmol), p-TsOH (0.070 g, 0.37 mmol), and 3,4-dihydropyran (6.2 mL, 74 mmol) in DCM (37 mL).

The reaction mixture was stirred at room temperature overnight then neutralized with sat. $NaHCO_3$, extracted with DCM, dried with $MgSO_4$, gravity filtered, and condensed to give a viscous red oil. The crude product was purified *via* CombiFlash (Hex:EtOAc) to give the protected alcohol as a colorless oil (4.32 g, 86% yield). ^{1}H NMR (400 MHz, $CDCl_3$) δ 7.53 (ddd, *J* = 7.42, 2.77, 1.07 Hz, 2H), 7.31 (td, *J* = 7.58 1.20 Hz, 1H), 7.16 – 7.11 (m, 1H), 4.84 (d, *J* = 13.31 Hz, 1H), 4.79 (t, *J* = 3.46 Hz, 1H), 4.58 (d, *J* = 13.31 Hz, 1H), 3.93 (ddd, *J* = 11.36, 8.95, 3.18 Hz, 1H), 3.60 – 3.54 (m, 1H), 1.93 – 1.57 (m, 6H).

THP-Ether Protection of 2-bromo-1,3-benzenedimethanol (56)

To an oven-dried 100 mL RBF was added a solution of 2-bromo-1,3-benzenedimethanol (2.63 g, 12.1 mmol), p-TsOH (0.046 g, 0.24 mmol), and 3,4-dihydropyran (8.2 mL, 97 mmol) in DCM (26 mL). The reaction mixture was stirred at room temperature overnight then neutralized with sat. $NaHCO_3$, extracted with DCM, dried with $MgSO_4$, gravity filtered, and condensed to give a viscous red oil. The crude product was purified *via* CombiFlash (Hex:EtOAc) to give the protected diol as a colorless oil (4.60 g, 99% yield). ^{1}H NMR (400 MHz, $CDCl_3$) δ 7.43 (d, *J* = 7.53 Hz, 2H), 7.35 – 7.27 (m, 1H), 4.83 (d, 13.39 Hz, 2H), 4.76 (t, *J* = 3.43 Hz, 2H), 4.58 (d, *J* = 13.40 Hz, 2H), 3.90 (ddd, *J* = 11.35, 8.95, 3.15, 2H), 3.54 (dtd, *J* = 8.66, 4.84, 4.09, 1.56 Hz, 2H), 1.89 – 1.56 (m, 12H).

Organolithium Addition of THP-Protected 2-bromobenzyl alcohol to Anthraquinone (53)

To an oven-dried 250 mL RBF was added a solution of THP-protected benzyl alcohol (**52**) (3.98 g, 14.7 mmol) in anhydrous THF (92 mL). The colorless solution was cooled to -78 °C, and *n*-BuLi (2.65 M, 4.6 mL, 12 mmol) was added dropwise and stirred at -78°C for 1h to give a pale-yellow solution. To this reaction mixture was added a solution of 9,10-anthraquinone (0.509 g, 2.4 mmol) in anhydrous THF (15 mL) and the resulting orange solution was stirred at room temperature overnight. The reaction mixture was acidified with 1 M HCl and stirred with MeOH (30 mL) for 2 hr. The resultant yellow solution was extracted with DCM, dried with $MgSO_4$,

gravity filtered, and condensed to give a yellow oil. The crude product was purified *via* CombiFlash (Hex:EtOAc) to give a mixture of cis/trans spirocycles as an off-white in a 1:3 ratio (0.40 g, 38% yield). **Spirocycle-Cis:** ^{1}H NMR (400 MHz, $CDCl_3$) δ 7.42 – 7.39 (m, 2H), 7.37 – 7.32 (m, 2H), 7.25 – 7.24 (m, 12H), 5.60 (s, 4H); ^{13}C NMR (101 MHz, $CDCl_3$): δ 146.25, 139.82, 138.61, 128.43, 128.30, 127.86, 127.69, 124.30, 120.88, 87.93, 73.90. **Spirocycle-Trans:** ^{1}H NMR (400 MHz, $CDCl_3$) δ 7.51 – 7.44 (m, 4H), 7.37 (ddd, *J* = 7.64, 6.58, 2.15 Hz, 2H), 7.22 (dd, *J* = 5.98, 3.34 Hz, 4H), 7.07 (d, *J* = 7.64 Hz, 2H), 7.04 (dd, *J* = 5.91, 3.40 Hz, 4H), 5.48 (s, 4H); ^{13}C NMR (101 MHz, $CDCl_3$): δ 145.27, 140.60, 139.20, 128.51, 128.27, 128.16, 128.07, 123.88, 120.98, 87.22, 72.91.

Reaction of Spirocycle 53 with PPA (54)

Spirocycle **53** (0.050 g, 0.13 mmol) and PPA (1.8 mL) were placed in a Pyrex tube then manually stirred with a spatula until the mixture became brightly colored. The reaction mixture was then transferred to the microwave reactor (100 °C, 15 min). The crude reaction mixture was quenched with sat. $NaHCO_3$, extracted with DCM, dried with $MgSO_4$, gravity filtered, and condensed to give a black solid. The crude product was purified *via* CombiFlash (Hex) to give acene **54** (0.009 g, 20% yield). ^{1}H NMR (400 MHz, $CDCl_3$) δ 9.25 (d, *J* = 8.34 Hz, 2H), 9.16 (dd, *J* = 6.25, 3.44 Hz, 2H), 8.38 (s, 2H), 8.30 – 8.22 (m, 2H), 7.81 (s, 2H), 7.78 – 7.71 (m, 6H).

Benzyl-Ether Protection of 2-bromo-1,3-benzenedimethanol (57)

To an oven-dried 100 mL RBF was added a suspension of NaH (60% w/w, 1.10 g, 28 mmol) in anhydrous THF (8 mL) at 0 °C. A solution of 2-bromo-1,3-benzenedimethanol (1.00 g, 4.6 mmol) in anhydrous THF (12 mL) was added, and the solution was sonicated at room temperature for 2h. Benzyl bromide (3.3 mL, 28 mmol) was added dropwise, and the solution was sonicated overnight to give a chalky-white suspension. The crude reaction mixture was cooled to 0 °C, quenched with water, extracted with EtOAc, dried with $MgSO_4$, gravity filtered, and condensed to give a yellow oil. The crude product was purified *via* CombiFlash

(Hex:EtOAc) to give the protected alcohol **57** as a yellow oil (1.15 g, 63% yield). ^{1}H NMR (400 MHz, $CDCl_3$) δ 7.52 – 7.29 (m, 13H), 4.66 (d, *J* = 4.23 Hz).

Mono Addition of Benzyl-Protected Diol 57 to Anthraquinone (60)

To an oven-dried 100 mL RBF was added a solution of benzyl-ether protected diol **57** (1.00 g, 2.5 mmol) in anhydrous THF (16 mL). The colorless solution was cooled to -78 °C and n-BuLi (2.65M, 0.94 mL, 2.5 mmol) was added and stirred at -78°C for 1hr to give a pale-yellow solution. This was slowly transferred *via* cannula for 2h to a solution of 9,10-anthraquinone (1.04 g, 5.0 mmol) in anhydrous THF (32 mL) at -78 °C, then stirred at room temperature overnight. The reaction mixture was quenched with 1 M HCl, extracted with DCM, then condensed to give an orange solid. The crude mixture was suspended in acetone to give a yellow ppt. that was filtered off and identified as residual anthraquinone (0.14 g). The filtrate was dried with $MgSO_4$, gravity filtered, and condensed to give an orange solid. The crude product was purified *via* CombiFlash (Hex:DCM) to give ketone **60** as a yellow solid (0.42 g, 32% yield). ^{1}H NMR (400 MHz, $CDCl_3$) δ 8.33 – 8.31 (m, 2H), 7.63 (d, *J* = 6.86 Hz, 1H), 7.42 (dtd, *J* = 9.55, 7.42, 4.90 Hz, 7H), 7.31 – 7.28 (m, 4H), 7.22 – 7.17 (m, 3H), 7.13 – 7.11 (m, 2H), 6.95 – 6.83 (m, 2H), 5.95 (s, 1H), 5.18 (s, 2H), 4.69 (s, 2H), 3.69 (s, 2H), 3.56 (s, 2H).

Reduction to Give Diol (62)

To an oven-dried 10 mL RBF was added a suspension of $LiAlH_4$ (0.104 g, 2.7 mmol) in anhydrous THF (3 mL) at 0 °C. A solution of ketone **60** (0.44 g, 0.83 mmol) in anhydrous THF (10 mL) was added drop-wise and kept at 0°C for 10 min, then held at room temperature for 2h. The lime-green suspension was cooled to 0°C then quenched with 1 M NaOH, H_2O, and 1 M HCl. The orange suspension was filtered through a silica plug with EtOAc, extracted with EtOAc, dried with $MgSO_4$, gravity filtered, and condensed to give diol **62** as an orange oil (0.44 g, 100 % yield).

Aromatization to Give Compound 64

To a 100 mL RBF was added a solution of diol **62** (0.57 g, 1.1 mmol), NaI (1.15 g, 7.7 mmol), and $NaH_2PO_2•H_2O$ (1.07 g, 10.1 mmol) in glacial acetic acid (27 mL). The dark red solution was heated to reflux for 1.5 h to give a bright orange solution. The reaction mixture was cooled to room temperature, quenched with water, extracted with DCM, dried with $MgSO_4$, gravity filtered, and condensed to give a reddish solid. The crude product was purified *via* CombiFlash (Hex:DCM) to give the aromatic product (**64**) as an orange oil (0.12 g, 22% yield).

Allyl-Ether Protection of 2-bromo-1,3-benzenedimethanol (58)

To an oven-dried 100 mL RBF purged with nitrogen and cooled to 0 °C was added NaH (60% w/w, 0.42 g, 10 mmol) and anhydrous THF (2 mL) to give a grey suspension. A solution of 2-bromo-1,3-benzenedimethanol (0.57 g, 2.6 mmol) in anhydrous THF (8 mL) was added dropwise via addition funnel, and the mixture was sonicated at 0 °C for 1h. Allyl bromide (0.9 mL, 10 mmol) was added dropwise, followed by sonication at room temperature overnight to give a chalky-white suspension. This was cooled to 0 °C, quenched with water, extracted with DCM, washed with brine, dried with $MgSO_4$, gravity filtered, and condensed to give an orange oil. The crude product was purified via vacuum distillation to give a colorless oil (0.77 g, 100% yield. ^{1}H NMR (400 MHz, $CDCl_3$): δ 7.48 – 7.40 (m, 2H), 7.33 (dd, *J* = 8.21, 6.90 Hz, 1H), 5.99 (ddt, *J* = 17.24, 10.42, 5.57 Hz, 2H), 5.36 (dq, *J* = 17.24, 1.65 Hz, 2H), 5.29 – 5.18 (m, 2H), 4.61 (s, 4H), 4.12 (dt, *J* = 5.57, 1.44 Hz, 4H).

Mono Addition of Allyl-Protected Diol 58 to Anthraquinone (61)

To an oven-dried 50 mL RBF was added a solution of allyl-protected diol **58** (0.50 g, 1.7 mmol) in anhydrous THF (10 mL). The solution was cooled to -78 °C and n-BuLi (2.5M, 0.67 mL, 1.7 mmol) was added and stirred at -78°C for 1hr to give a pale-yellow solution. This was slowly transferred *via* cannula over the course of 2h to a solution of 9,10-anthraquinone (0.70 g, 3.4 mmol) in anhydrous THF (40 mL) at -78 °C, then stirred at room temperature overnight. The

reaction mixture was quenched with 1 M HCl, extracted with DCM, then condensed to give an orange solid. The crude mixture was suspended in acetone to give a yellow ppt. that was filtered off and identified as residual anthraquinone (0.14 g). The filtrate was dried with $MgSO_4$, gravity filtered, and condensed to give an orange solid. The crude product was purified *via* CombiFlash (Hex:DCM) to give ketone **61** as a yellow oil (0.35 g, 48% yield). ^{1}H NMR (400 MHz, $CDCl_3$) δ 8.40 – 8.30 (m, 2H), 7.58 – 7.37 (m, 7H), 5.98 (s, 1H), 5.97 – 5.80 (m, 1H), 5.33 -5.08 (m, 5H), 4.97 – 4.72 (m, 2H), 4.21 – 4.12 (m, 2H), 3.51 (s, 2H), 3.18 (s, 1H).

Reduction to Give Diol (63)

To an oven-dried 25 mL RBF was added a suspension of $LiAlH_4$ (0.032 g, 0.85 mmol) in anhydrous THF (1 mL) at 0 °C. A solution of ketone **61** (0.11 g, 0.25 mmol) in anhydrous THF (3 mL) was added drop-wise and kept at 0°C for 10 min, then held at room temperature for 2h. The bright yellow suspension was cooled to 0°C then quenched with 1 M NaOH, H_2O, and 1 M HCl. The orange suspension was filtered through a silica plug with EtOAc, extracted with EtOAc, dried with $MgSO_4$, gravity filtered, and condensed to give diol **63** as a red oil (0.11 g, 100 % yield).

Aromatization to Give Compound 65

To a 50 mL RBF was added a solution of diol **63** (1.06 g, 2.5 mmol), NaI (2.62 g, 18 mmol), and $NaH_2PO_2•H_2O$ (2.44 g, 23 mmol) in glacial acetic acid (63 mL). The dark red solution was heated to reflux for 1.5 h to give a bright yellow solution. The reaction mixture was cooled to room temperature, quenched with water, extracted with DCM, dried with $MgSO_4$, gravity filtered, and condensed to give a reddish oil. The crude product was purified *via* CombiFlash (Hex:DCM) to give the aromatic product (**65**) as an orange oil (0.33 g, 33% yield). ^{1}H NMR (400 MHz, $CDCl_3$) δ 8.52 (s, 1H), 8.08 – 8.04 (m, 2H), 7.71 (d, *J* = 7.78 Hz, 2H), 7.61 (dd, *J* = 8.34, 6.96 Hz, 1H), 7.49 – 7.41 (m, 4H), 7.32 (ddd, *J* = 8.80, 6.40, 1.20 Hz, 2H), 5.57 – 5.43 (m, 2H), 5.03 – 4.77 (m, 4H), 3.88 (s, 4H), 3.53 (dt, *J* = 5.56 1.41 Hz, 4H).

Deprotection of Aromatic Diol (42)

To an oven-dried 50 mL flask purged with nitrogen was added $Pd(PPh_3)_4$ (16 mg, 0.013 mmol) and MeOH (9 mL). A solution of aromatic diol **65** (0.26 g, 0.67 mmol) in MeOH (10 mL) was added, and the mixture was stirred at room temperature for 15 min. K_2CO_3 (10.6 g, 75.6 mmol) was added, and the yellow suspension was heated to reflux overnight. The reaction mixture was cooled to room temperature, condensed to remove MeOH, washed with sat. NH4Cl, extracted with DCM, and flushed through a silica plug with ethyl acetate. The filtrate was condensed to give an orange slurry, which was dissolved in minimal DCM, then hexanes was added to give a white precipitate. This was vacuum filtered and rinsed with cold hexanes to give the desired product as a yellow solid (0.18 g, 83 % yield, m.p. 182 – 184 °C).

Allyl-Protection of 2-bromobenzyl alcohol (66)

To an oven-dried 500 mL RBF purged with nitrogen and cooled to 0 °C was added NaH (60% w/w, 7.04 g, 176 mmol) and anhydrous THF (50 mL) to give a grey suspension. A solution of 2-bromobenzyl alcohol (16.5 g, 88 mmol) in anhydrous THF (126 mL) was added dropwise via addition funnel, and the mixture was sonicated at 0 °C for 1 h. Allyl bromide (15.2 mL, 176 mmol) was added dropwise, followed by sonication at room temperature overnight to give a chalky-white suspension. This was cooled to 0 °C, quenched with water, extracted with DCM, washed with brine, dried with $MgSO_4$, gravity filtered, and condensed to give an orange oil. The crude product was purified via vacuum distillation to give a colorless oil (19.4 g, 97% yield, bp 58 °C at 0.17 torr). ^{1}H NMR (500 MHz, $CDCl_3$): δ 7.56 - 7.51 (m, 2H), 7.32 (td, *J* = 7.53, 1.18 Hz, 1H), 7.17 – 7.12 (m, 1H), 6.00 (ddt, *J* = 17.21, 10.43, 5.55 Hz, 1H), 5.37 (dq, *J* = 17.24, 1.65 Hz, 1H) 5.27 – 5.23 (m, 1H), 4.60 (s, 2H), 4.13 (dt, *J* = 5.56, 1.44 Hz, 2H); ^{13}C NMR (500 MHz, CDCl3): δ 137.8, 134.6, 132.6, 129.1, 128.9, 127.5, 122.7, 117.3, 71.8, 71.48.

Synthesis of Allyl-Protected Triarylmethanol (67)

To an oven-dried 500 mL flask purged with nitrogen was added a solution of allyl-protected bromobenzyl alcohol **66** (18.3 g, 81 mmol) in anhydrous THF (208 mL). The mixture was cooled to - 78 °C. n-BuLi (2.5 M, 35.6 mL, 89 mmol) was added dropwise over 30 min and the mixture was stirred at -78 °C for 1 h to give a pale-yellow solution. Freshly distilled diethyl carbonate (3.28 mL, 27 mmol) was added dropwise followed by stirring at -78 °C for 1 h to give a bright orange solution. This was heated to 50 °C and stirred overnight to give a yellow suspension. The crude product was cooled to 0 °C, quenched with sat. NH_4Cl, extracted with DCM, dried with $MgSO_4$, gravity filtered, and condensed to give an orange oil. Volatile impurities were removed by vacuum distillation to give the desired product as a viscous orange oil (12.0 g, 95% yield). ^{1}H NMR (500 MHz, $CDCl_3$): δ 7.65 (d, *J* = 6.70 Hz, 3H), 7.33 (td, *J* = 7.49, 1.23 Hz, 3H), 7.09 (td, *J* = 7.69, 1.33 Hz, 3H), 6.68 (d, *J* = 7.67 Hz, 3H), 6.33 (s, 1H), 5.79 (ddt, *J* = 17.16, 10.56, 5.31 Hz, 3H), 5.17 (dq, *J* = 17.24, 1.62 Hz, 3H), 5.10 (dq, *J* = 10.40, 1.33 Hz, 3H), 4.64 (d, *J* = 13.21, 3H), 4.39 (d, *J* = 13.23, 3H), 3.81 (dddt, *J* = 41.37, 12.70, 5.58, 1.37 Hz, 6H); ^{13}C NMR (126 MHz, $CDCl_3$): δ 144.6, 138.2, 134.4, 129.9, 129.0, 127.8, 126.8, 117.0, 85.5, 71.3, 71.0; HRMS (ESI/Q-TOF) m/z: $[M + Na]^+$ Calcd for $C_{31}H_{34}O_4Na$ 493.2355; Found 493.2351.

Deprotection to Tetraol (68)

To an oven-dried 250 mL flask purged with nitrogen was added $Pd(PPh_3)_4$ (21 mg, 0.018 mmol) and MeOH (8 mL). A solution of allyl-protected triarylmethanol **67** (1.0 g, 2.1 mmol) in MeOH (50 mL) was added, and the mixture was stirred at room temperature for 15 min. K_2CO_3 (5.24 g, 38 mmol) was added, and the yellow suspension was heated to reflux. After 1 h, a second equivalent of $Pd(PPh_3)_4$ was added, and this process was repeated twice more for a total of four equivalents (84 mg, 0.072 mmol, 4 mol%). The reaction was stirred at reflux overnight to give a yellow suspension. This was cooled to room temperature, condensed to remove MeOH, washed with sat. NH_4Cl, extracted with DCM, and flushed through a silica plug with ethyl acetate. The

filtrate was condensed to give an orange slurry, which was dissolved in minimum DCM, then hexanes was added to give a white precipitate. This was vacuum filtered and rinsed with cold hexanes to give the desired product as a white solid (0.62 g, m.p. 182 – 184 °C, 85% yield). ^{1}H NMR (400 MHz, DMSO-d_6): δ 7.69 - 7.62 (m, 3H), 7.33 (td, *J* = 7.50, 1.18 Hz, 3H), 7.16 (s, 1H), 7.09 (td, *J* = 7.74, 1.30 Hz, 3H), 6.56 (d, *J* = 7.73 Hz, 3H), 5.31 (t, *J* = 5.26 Hz, 3H), 4.34 (ddd, *J* = 52.82, 14.18, 4.90 Hz, 6H); ^{13}C NMR (101 MHz, DMSO-d_6): δ 143.48, 141.71, 128.03, 128.03, 127.44, 126.04, 84.99, 62.11; HRMS (ESI/Q-TOF) m/z: $[M + Na]^+$ Calcd for $C_{22}H_{22}O_4Na$ 373.1400; Found 373.1404.

Reduction to Triarylmethane (69)

To an oven-dried 100 mL RBF was added a solution of allyl-protected triarylmethanol (**68**) (5.00 g, 11 mmol) and NaI (3.51 g, 23 mmol) in CH_3CN (50 mL) at 0°C. Dichlorodimethylsilane (2.6 mL, 21 mmol) was added dropwise, and the dark red solution was stirred at 0°C for 1 h. The reaction mixture was diluted with EtOAc, washed with water, sat. $NaHCO_3$, NaS_2O_3, and brine, then the organic fraction was dried with $MgSO_4$, gravity filtered, and condensed to give a dark red oil. The crude product was purified *via* CombiFlash (Hex:DCM) to give the allyl-protected triarylmethane as a yellow oil (3.27 g, 70% yield). ^{1}H NMR (500 MHz, $CDCl_3$): δ 7.46 (dd, *J* = 7.55, 1.02 Hz, 3H), 7.26 (td, *J* = 7.47, 1.31 Hz, 3H), 7.16 (td, *J* = 7.56, 1.44 Hz, 3H), 6.74 (dd, *J* = 7.72, 1.22 Hz, 3H), 6.28 (s, 1H), 5.88 (ddt, *J* = 17.24, 10.45, 5.53 Hz, 3H), 5.24 (dq, *J* = 17.25, 1.67 Hz, 3H), 5.16 – 5.13 (m, 3H), 4.40 (s, 6H), 3.93 (dt, *J* = 5.53, 1.46 Hz, 6H); ^{13}C NMR (126 MHz, $CDCl_3$): δ 141.16, 136.61, 134.78, 139.52, 128.79, 127.53, 126.62, 116.82, 71.39, 70.04, 44.27.

Deprotection to Triol (70)

To an oven-dried 250 mL flask purged with nitrogen was added $Pd(PPh_3)_4$ (6 mg, 0.005mmol) and MeOH (4 mL). A solution of allyl-protected triarylmethane **69** (0.22 g, 0.49 mmol) in MeOH (10 mL) was added, and the mixture was stirred at room temperature for 15 min. K_2CO_3 (1.23 g,

8.8 mmol) was added, and the yellow suspension was heated to reflux. After 1 h, a second equivalent of $Pd(PPh_3)_4$ was added, and this process was repeated twice more for a total of four equivalents (24 mg, 0.02 mmol, 4 mol%). The reaction was stirred at reflux overnight to give a yellow suspension. This was cooled to room temperature, condensed to remove MeOH, washed with sat. NH_4Cl, extracted with DCM, and flushed through a silica plug with ethyl acetate. The filtrate was condensed to give an orange slurry, which was dissolved in minimum DCM, then hexanes was added to give a white precipitate. This was vacuum filtered and rinsed with cold hexanes to give the desired product as a white solid (0.11 g, 67% yield). ^{1}H NMR (400 MHz, DMSO-d_6) δ 7.47 (d, *J* = 6.87 Hz, 3H), 7.25 (td, *J* = 7.47, 1.21 Hz, 3H), 7.13 (td, *J* = 7.52, 1.29 Hz, 3H), 6.59 (dd, *J* = 7.65 1.05 Hz, 3H), 5.98 (s, 1H), 5.20 (t, *J* = 5.38 Hz, 3H), 4.35 (d, *J* = 5.22 Hz, 6H); ^{13}C NMR (101 MHz, DMSO-d_6): δ 140.21, 139.38, 128.15, 126.70, 126.40, 126.36, 60.40, 54.93.

Cyclization of Tetraol 68 with PPA (73)

To a 50 mL flask was added water (2.8 mL), polyphosphoric acid (0.28 mL) and DCE (20 mL). The colorless solution was heated to reflux and a solution of tetraol (**68**) (0.100 g, 0.280 mmol) in DCE (8 mL) was added followed by reflux overnight (18 h). The resultant opaque solution was cooled to room temperature, diluted with water, extracted with DCM, dried with MgSO4, gravity filtered, and condensed to give pure spirocycle (**73**) as an off-white solid (0.090 g, m.p. 126 – 130 °C, 97% yield). ^{1}H NMR (400 MHz, $CDCl_3$): δ 7.51 (d, *J* = 7.12 Hz, 2H), 7.40 - 7.27 (m, 5H), 7.14 (td, *J* = 7.66, 1.42 Hz), 6.89 (d, *J* = 7.52 Hz, 1H), 6.83 (d, *J* = 7.63 Hz, 2H) 5.10 (s, 2H), 4.38 (s, 4H), 2.96 (s, 2H) ^{13}C NMR (101 MHz, $CDCl_3$): δ 142.67, 141.46, 140.27, 138.84, 131.63, 128.84, 128.38, 128.06, 127.65, 127.22, 124.96, 121.39, 96.26, 70.64, 63.84; HRMS (ESI/Q-TOF) m/z: $[M + Na]^+$ Calcd for $C_{22}H_{20}O_3Na$ 355.1310; Found 355.1311.

Cyclization of Tetraol 68 with TfOD: NMR Experiment (74)

To a nitrogen-flushed NMR tube was added a solution of tetraol (**68**) (0.02 g, 0.05 mmol) in 1,2-dichloroethane-d_4 (1.0 mL) and triflic acid-*d* (0.09 mL, 1.0 mmol) to give a dark green solution. This was identified as the triangulene cation (**74**). These results were also observed when the same reaction conditions were used starting from triol (**70**) and internally cyclized product (**73**). ^{1}H NMR (400 MHz, 1,2-dichloroethane-d_4): δ 8.11 (t, *J* = 7.65 Hz, 3H), 7.89 (d, *J* = 7.71 Hz, 6H), 5.03 (s, 6H); ^{13}C NMR (101 MHz, 1,2-dichloroethane-d_4): δ 168.65, 147.03, 139.25, 128.96, 123.32, 120.16, 116.99, 113.83, 36.93.

Triangulene Cation Neutralization with Triethylsilane (71)

To an oven-dried 100 mL flask purged with nitrogen was added tetraol **68** (0.06 g, 0.16 mmol) and DCM (33 mL) to give a colorless solution. Triflic acid (2.9 mL, 32.8 mmol) was added turning the solution dark green. This was transferred to an addition funnel and slowly added to a solution of triethylsilane (10.0 mL, 62.6 mmol) in DCM (28 mL) over 30 min at 0 °C to give a yellow solution. Water was added (100mL) to give a bright yellow-green solution, then extracted with DCM, dried with $MgSO_4$, gravity filtered, and condensed to give a yellow oil. The crude product was purified by CombiFlash (100% hexanes) to afford 1,2,3,8-tetrahydrotriangulene (**76**) (0.004 g, 9% yield), 1,8-dihydrotriangulene (**16**) (0.022 g, 49% yield), and 4,8,12,12C-tetrahydro-triangulene (**71**) as an orange solid (0.017 g, 38% yield). ^{1}H NMR (400 MHz, $CDCl_3$): δ 7.25 - 7.23 (m, 9H), 7.21 - 7.63 (m, 1H), 4.18 (dd, *J* = 18.08, 4.69 Hz, 3H), 4.06 (d, *J* = 17.92 Hz); ^{13}C NMR (101 MHz, $CDCl_3$): δ 135.61, 133.95, 126.75, 125.61, 36.43, 35.99; HRMS (EI$^+$/Q-TOF) m/z: $[M]^+$ Calcd for $C_{22}H_{16}$ 280.1252; Found 280.1255.

Triangulene Cation Neutralization with $NaHCO_3$ (76)

To an oven-dried 50 mL flask was added a solution of added tetraol **68** (0.10 g, 0.28 mmol) in DCM (28 mL). TfOH (1.0 mL, 11.3 mmol) was carefully added and the resultant dark green solution was stirred at room temperature for 5 min. This was transferred to an addition funnel

and slowly added to a solution of sat. aqueous $NaHCO_3$ (100 mL) held at 0 °C over the course of 30 min to give a dark green solution. This was extracted with DCM, dried with MgSO4, gravity filtered and condensed to give a dark green solid. The crude product was purified by CombiFlash (Hexanes) to afford 1,2,3,8-tetrahydrotriangulene (**76**) as a bright yellow solid (0.02 g, 27% yield) and 1,8-dihydrotriangulene (**16**) as a bright yellow solid (0.04 g 53% yield). ^{1}H NMR (500 MHz, $CDCl_3$): δ 7.66 - 7.63 (m, 2H), 7.57 (s, 2H), 7.49 - 7.45 (m, 2H), 7.39 (dq, *J* = 7.15, 1.45 Hz, 2H), 4.94 (s, 2H), 3.24 - 3.18 (m, 4H), 2.16 - 2.11 (m, 2H); ^{13}C NMR (101 MHz, $CDCl_3$): δ 133.96, 133.25, 130.90, 126.48, 125.56, 125.34, 124.92, 123.90, 123.53, 123.44, 33.44, 31.06, 22.47; HRMS (ESI/FTMS) m/z: $[M - H]^+$ Calcd for $C_{22}H_{15}$ 279.117; Found 279.1172.

Triangulene Cation Neutralization with Triethylamine (16)

To an oven-dried 250 mL flask was added a solution of tetraol (**68**) (0.50 g, 1.4 mmol) in DCM (140 mL). TfOH (6.2 mL, 70 mmol) was carefully added and the resultant dark green solution was stirred at room temperature for 5 min. This was transferred to an addition funnel and slowly added to a solution of triethylamine (19.5 mL, 140 mmol) in DCM (280 mL) at 0 °C over the course of 2 hours to give a brown-yellow solution. The reaction mixture was diluted with water (200 mL), extracted with DCM, dried with MgSO4, gravity filtered, and condensed to give a brown solid. The crude product was purified by flash chromatography (hexane elution) to afford 1,8-dihydrotriangulene (**16**) as a bright yellow solid (0.26 g, 66% yield). ^{1}H NMR (400 MHz, $CDCl_3$): δ 7.64 - 7.58 (m, 3H), 7.45 (dt, *J* = 13.16, 7.53 Hz, 2H), 7.40 - 7.33 (m, 3H), 6.74 – 6.69 (m, 1H), 6.15 (dt, *J* = 10.07, 4.01 Hz), 4.90 (s, 2H), 4.11 (s, 2H); ^{13}C NMR (101 MHz, $CDCl_3$): δ 134.20, 134.13, 132.55, 132.14, 132.05, 130.47, 128.07, 127.91, 127.75, 126.98, 126.81, 126.63, 125.99, 125.47, 125.23, 125.03, 124.79, 124.52, 124.45, 123.25, 34.25, 31.91; HRMS (EI^+/Q-TOF) m/z: $[M]^+$ Calcd for $C_{22}H_{14}$ 278.1096; Found 278.1100.

Air Oxidation of 1,2,3,8-tetrahydrotriangulene (10)

To a scintillation vial was added a solution of 1,2,3,8-tetrahydrotriangulene (**76**) (0.014 g, 0.05 mmol) in DCE (5 mL) to give a bright yellow-green solution. This was allowed to stir under air for 24 h to give a dark red solution. This was condensed and found to be a mixture of starting material and triangulene ketone (**10**) in a 4.6:1 ratio. Pure samples of **10** were isolated by chromatography in a separate experiment. ^{1}H NMR (500 MHz, $CDCl_3$): δ 8.78 (d, *J* = 7.40 Hz, 2H), 8.20 (d, *J* = 7.83, 2H), 7.86 - 7.79 (m, 4H), 3.32 - 3.26 (m, 4H), 2.21 (q, *J* = 6.16 Hz, 2H). HRMS (ESI/FTMS) m/z: $[M]^+$ Calcd for $C_{22}H_{15}O$ 295.1161; Found 295.1121.

TEMPO Oxidation of 1,8-dihydrotriangulene (79)

To an oven-dried 25 mL round bottom flask was added a solution of 1,8-dihydrotriangulene (**16**) (0.030 g, 0.11 mmol) in benzene (10 mL) to give a bright yellow-green solution. TEMPO (0.17 g, 1.1 mmol was added and the solution turned orange. This was stirred at room temperature for 1 h until an orange precipitate formed. The crude product was condensed and purified by CombiFlash (Hex:EtOAc) to afford dione (**76**) as a dark red solid (0.015 g, 44% yield). ^{1}H NMR (400 MHz, $CDCl_3$): δ 8.91 (s, 1H), 8.80 (d, *J* = 7.42 Hz, 1H), 8.72 (d, *J* = 7.12 Hz, 1H), 8.38 (d, *J* = 7.84 Hz, 1H), 8.24 (d, *J* = 7.67 Hz, 1H), 8.06 (s, 1H), 7.90 - 7.78 (m, 3H), 6.75 (d, *J* = 9.81 Hz, 1H); ^{13}C NMR (126 MHz, $CDCl_3$): δ 184.99, 183.01, 142.39, 135.50, 132.01, 131.95, 130.78, 130.58, 130.17, 129.56, 126.42, 129.28, 128.93, 128.46, 127.81, 127.76, 127.46, 126.55, 125.99, 120.18; HRMS (EI^+/Q-TOF) m/z: $[M]^+$ Calcd for $C_{22}H_{10}O_2$ 306.0692; Found 306.0681.

Reaction of 1,8-dihydrotriangulene with TfOD (50 eq.): NMR Experiment (80)

To a nitrogen-flushed NMR tube was added a solution of 1,8-dihydrotriangulene (**16**) (0.010 g, 0.04 mmol) in 1,2-dichloroethane-d_4 (0.7 mL) and triflic acid-d (0.18 mL, 2.0 mmol) to give a dark green solution. This was characterized as a mixture of protonated triangulene (**80**, 9%), olympicenium cation (**82**, 3%), and triangulenium cation (**74**, 88%) as the major product. After three days at room temperature, the product mixture changed to protonated triangulene (**80**,

0%), olympicenium cation (**82**, 8%), and triangulenium cation (**74**, 92%) as the major product. Protonated triangulene (**80**) ^{1}H NMR (400 MHz, 1,2-dichloroethane-d_4): δ 9.54 (s, 2H), 9.40 (d *J* = 7.75 Hz, 2H), 8.45 (t, *J* = 7.74 Hz, 1H), 8.37 (d, *J* = 8.20 Hz, 2H), 5.23 (s, 2H).

Reaction of 1,8-dihydrotriangulene with TfOD (5 eq.): NMR Experiment (82)

To a nitrogen-flushed NMR tube was added a solution of 1,8-dihydrotriangulene (**16**) (0.022 g, 0.08 mmol) in 1,2-dichloroethane-d_4 (0.5 mL) and triflic acid-*d* (0.035 mL, 0.4 mmol) to give a dark green solution. This was identified as a mixture of olympicenium cation (**82**, 60%), and trianuglenium cation (**74**, 40%). After three days at room temperature the product mixture changed to give solely the olympicenium cation (**82**). Pure olympicenium cation was formed directly by reaction of 1,2,3,8-tetrahydrotriangulene (**76**) with triflic acid-*d* (5 eq). ^{1}H NMR (400 MHz, 1,2-dichloroethane-d_4): δ 10.12 (s, 1H), 9.23 (dd, J = 7.66, 2.40 Hz, 4H), 8.63 (s, 2H), 8.48 (dt, *J* = 7.39, 3.77 Hz, 2H), 3.55 - 3.50 (m, 4H), 2.37 (p, *J* = 6.24 Hz, 2H); ^{13}C NMR (101 MHz, 1,2-dichloroethane-d_4): δ 157.17, 149.67, 145.62, 140.75, 138.95, 135.17, 131.17, 130.78, 130.16, 128.66, 123.26, 120.10, 116.94, 113.78, 30.93, 22.36.

Oxidation of 1,8-dihydrotriangulene with *p*-Chloranil

To a nitrogen flushed NMR tube was added a solution of 1,8-dihydrotriangulene (**16**) (0.010 g, 0.036 mmol) in $CDCl_3$ (0.5 mL) to give a fluorescent green solution. A solution of *p*-chloranil (0.018 g, 0.072 mmol) in $CDCl_3$ (0.5 mL) was added giving a dark blue solution instantaneously. The sample was then immediately analyzed by ^{1}H NMR to show the complete disappearance of starting material and the formation of reduced *p*-chloranil. This was condensed to give a black solid, which was subsequently analyzed by LDI-TOF spectrometry. The sample was dissolved at 1 mg/mL in dichloromethane and deposited neat on a polished steel MALDI plate. The LDI analysis was carried out on a rapifleX TOF/TOF mass spectrometer (Bruker Scientific, LLC, Billerica, MA). The spectra were acquired in reflector mode with 4000 laser shots per spectrum

in the mass range 0 – 2200 Da to give a complex spectrum containing higher-order oligomers of triangulene. ^{1}H NMR (400 MHz, $CDCl_3$) δ 5.69 (s, 2H).

Synthesis of Bianthrone (86)[52]

To a 500 mL RBF was added a solution of 9-anthrone (10.0 g, 52 mmol) in glacial acetic acid. The dark brown solution was heated to reflux, and a solution of $FeCl_3$ (17.5g, 108 mmol) and NaOAc (1.52 g, 19 mmol) in water (52 mL) was added dropwise then refluxed for an additional hour. The reaction mixture was cooled to room temperature, diluted with water, extracted with DCM, washed with water, dried with $MgSO_4$, gravity filtered, and condensed to give a brown solid. EtOH (286 mL) and KOH (41.9 g, 747 mmol) were added, and the dark red solution was heated to reflux for 30 min. The reaction mixture was hot filtered into a solution of $K_2S_2O_8$ (11.8 g, 44 mmol) in water (1.2 L). The resulting bright green solution was stirred at room temperature for 2 h covered with foil to give a bright yellow suspension. This was cooled to 0 °C and vacuum filtered to give bianthrone as a bright yellow solid (5.331 g, 53% yield). ^{1}H NMR (400 MHz, $CDCl_3$) δ 8.10 (d, *J* = 7.71 Hz, 4H), 7.40 (t, *J* = 7.51 Hz, 4H), 7.18 – 7.13 (m, 4H), 7.07 (d, *J* = 7.84 Hz, 4H).

Organolithium Addition of Allyl-Protected Diol to Bianthrone (87)

To an oven-dried 100 mL RBF was added a solution of allyl-protected diol (**56**) (2.00 g, 6.7 mmol) in anhydrous THF (42 mL). The solution was cooled to -78 °C and n-BuLi (2.5 M, 2.2 mL, 5.6 mmol) was added dropwise and stirred at -78°C for 1 h to give a pale-yellow solution. To this reaction mixture was added a solution of bianthrone (0.0.429 g, 1.1 mmol) in anhydrous THF (10 mL) and the resulting dark orange solution was stirred at room temperature for 1 h then heated to 50 °C overnight. The reaction mixture was cooled to 0 °C, acidified with sat NH_4Cl, extracted with DCM, dried with $MgSO_4$, gravity filtered, and condensed to give an orange oil identified as the diol. This was used as a crude product in the following reaction.

Aromatization to give Allyl-Protected Tetraol (88)

To a 100 mL RBF was added a solution of diol **87** (0.90 g, 1.1 mmol), NaI (1.15 g, 7.7 mmol), and $NaH_2PO_2•H_2O$ (1.07 g, 10.1 mmol) in glacial acetic acid (27 mL). The dark red solution was heated to reflux for 1.5 h to give a bright orange solution. The reaction mixture was cooled to room temperature, quenched with water, extracted with DCM, dried with $MgSO_4$, gravity filtered, and condensed to give a reddish solid. The crude product was purified *via* CombiFlash (Hex:DCM) to give the aromatic product (**88**) as a red oil (0.37 g, 43% yield). ^{1}H NMR (500 MHz, $CDCl_3$): δ 7.80 (d, *J* = 7.63 Hz, 4H), 7.72 – 7.68 (m, 2H), 7.62 (d, *J* = 8.81 Hz, 4H), 7.35 – 7.31 (m, 4H), 7.22 – 7.17 (m, 8H), 5.54 (ddd, *J* = 22.76, 10.79, 5.57 Hz, 4H), 4.99 – 4.90 (m, 8H), 4.14 (s, 8H), 3.69 (dt, *J* = 5.56, 1.31 Hz, 8H); ^{13}C NMR (126 MHz, $CDCl_3$): δ 138.47, 136.05, 134.53, 133.66, 133.50, 131.42, 130.15, 128.71, 127.57, 127.08, 126.76, 125.92, 125.84, 116.77, 71.59, 70.06.

Deprotection to Give Tetraol (89)

To an oven-dried 50 mL flask purged with nitrogen was added $Pd(PPh_3)_4$ (5 mg, 0.005 mmol) and MeOH (3 mL). A solution of allyl-protected tetraol **88** (0.37 g, 0.67 mmol) in MeOH (10 mL) was added, and the mixture was stirred at room temperature for 15 min. K_2CO_3 (1.18 g, 8.5 mmol) was added, and the yellow suspension was heated to reflux. After 1 h, a second equivalent of $Pd(PPh_3)_4$ was added, and this process was repeated twice more for a total of four equivalents (20 mg, 0.020 mmol, 4 mol%). The reaction was stirred at reflux overnight to give a yellow suspension. This was cooled to room temperature, condensed to remove MeOH, washed with sat. NH_4Cl, extracted with DCM, and flushed through a silica plug with ethyl acetate. The filtrate was condensed to give an orange slurry, which was dissolved in minimum DCM, then hexanes was added to give a white precipitate. This was vacuum filtered and rinsed with cold hexanes to give the desired product as a tan solid (0.14 g, 46% yield). ^{1}H NMR (400 MHz,

Acetone-d_6) δ 7.97 (d, *J* = 7.68 Hz, 4H), 7.84 – 7.78 (m, 2H), 7.68 (d, *J* = 8.78 Hz, 4H), 7.48 (ddd, *J* = 8.79, 6.21, 1.41 Hz, 4H), 7.35 – 7.27 (m, 8H), 4.31 (d, *J* = 5.65 Hz, 8H), 2.96 (s, 4H).

Chapter II

A pure sample of 1,8-dihydrotriangulene was prepared inside a glovebox to avoid oxidation. The sample was diluted to 1 mM in degassed anhydrous acetonitrile with 0.1 M n-Bu_4PF_6 as the supporting electrolyte under an atmosphere of N_2. The electrochemical apparatus contained a glassy carbon working electrode, sheathed platinum wire counter electrode, and a 0.01 M Ag/Ag+ pseudo reference electrode with ferrocene added as an internal reference.

Chapter III

Suzuki-Miyaura Coupling to form 2-(1-Naphthyl)benzyl alcohol (105)

1-Naphthaleneboronic acid (0.64 g, 3.7 mmol) and 1 M K_2CO_3 (6.0 mL) were added to a 25 mL Pyrex tube and purged with nitrogen. 2-Bromobenzyl alcohol (0.32 g, 1.7 mmol), EtOH (9.2 mL), and $Pd(PPh_3)_4$ (0.083 g, 0.072 mmol) were then added and the head-space was purged with nitrogen. The reaction mixture was then transferred to the microwave reactor (150 °C, 30 min). The reaction mixture was quenched with 1M NaOH, extracted with DCM, dried with $MgSO_4$, gravity filtered, and condensed to give an off-white solid. The crude product was purified *via* CombiFlash (Hex:EtOAc) to give 2-(1-Naphthyl)benzyl alcohol **105** as a white solid (0.49g, 82% yield). ^{1}H NMR (400 MHz, $CDCl_3$) δ 7.90 (t, *J* = 8.15 Hz, 2H), 7.68 – 7.61 (m, 1H), 7.55 – 7.36 (m, 7H), 7.29 (dd, *J* = 7.51, 1.33 Hz, 1H), 4.37 (s, 2H), 1.37 (s, 1H).

Cyclization of 2-(1-Naphthyl)benzyl alcohol with $FeCl_3$/$AgSbF_6$ (98 and 106)

To an oven-dried 50 mL RBF was added a solution of 2-(1-Naphthyl)benzyl alcohol (0.062g, 0.26 mmol) and $FeCl_3$ (6 mg, 0.37 mmol) in DCE (10 mL). The reaction vessel was purged with nitrogen then $AgSbF_6$ (0.044g, 0.13 mmol) was added and the green solution was immediately placed in an oil bath (50 °C, 24 h). The reaction mixture was quenched with 1 M HCl, extracted with DCM, dried with $MgSO_4$, gravity filtered, and condensed to give a yellow-green solid. The crude product was purified *via* CombiFlash (Hex) to give a mixture of regioisomers **98** and **106** in a 2.4:1 ratio (0.030 g, 53% yield).

Cyclization of 2-(1-Naphthyl)benzyl alcohol with PPA (106)

2-(1-Naphthyl)benzyl alcohol (0.33g, 1.4 mmol) and PPA (20 mL) were placed in a Pyrex tube then manually stirred with a spatula until the mixture became brightly colored. The reaction mixture was then transferred to the microwave reactor (60 °C, 10 min). The crude reaction mixture was quenched with sat. $NaHCO_3$, extracted with DCM, dried with $MgSO_4$, gravity

filtered, and condensed to give a green solid. The crude product was purified *via* CombiFlash (Hex) to give only regio isomer **106** as a white solid (0.11g, 36% yield). ^{1}H NMR (400 MHz, $CDCl_3$) δ 8.79 (d, *J* = 8.48 Hz, 1H), 8.42 (d, *J* = 7.84 Hz, 1H), 8.01 – 7.95 (m, 1H), 7.84 (d, *J* = 8.24 Hz, 1H), 7.71 (d, *J* = 8.26 Hz, 1H), 7.66 (ddd, *J* = 8.33, 6.90, 1.32 Hz, 3H), 7.57 – 7.49 (m, 2H), 7.37 (td, *J* = 7.42, 0.95 Hz, 1H), 4.03 (s, 2H).

Synthesis of 1-bromo-2-(bromomethyl)naphthalene (111)

To an oven-dried 50 mL RBF was added a solution of 1-bromo-2-methylnaphthalene (3.5 mL, 23 mmol), NBS (4.02 g, 23 mmol), and benzoyl peroxide (17 mg, 0.07 mmol) in benzene (28 mL). The yellow solution was heated to reflux then irradiated with a100W lamp for 3 h. The crude reaction mixture was hot filtered with benzene and then condensed to give an off-white solid. The crude product was purified *via* recrystallization with hexanes to give 1-bromo-2-(bromomethyl)naphthalene as a white crystalline solid (0.68 g, m.p. 100 - 103 °C, *lit.* 103 – 105 °C, 75% yield). ^{1}H NMR (400 MHz, $CDCl_3$) δ 8.37 – 8.30 (m, 1H), 7.84 – 7.79 (m, 2H), 7.62 (ddd, *J* = 8.48, 6.88, 1.40 Hz, 1H), 7.57 – 7.53 (m, 1H), 7.52 (d, *J* = 8.41 Hz, 1H).

Synthesis of 1-bromo-2-naphthalenemethanol (112)

To an oven-dried 250 mL RBF was added 1-bromo-2-(bromomethyl)naphthalene (4.11 g, 13.7 mmol), $CaCO_3$ (7.09 g, 71 mmol), dioxane (45mL), and water (45 mL). The chalky-white suspension was heated to reflux and held at this temperature overnight. The crude reaction mixture was cooled to 0 °C, acidified with 1 M HCl, extracted with DCM, washed with sat. $NaHCO_3$, dried with $MgSO_4$, gravity filtered, and condensed to give a white solid identified as 1-bromo-2-naphthalenemethanol (3.13 g, m.p. 92 – 94 °C, *lit* 101 – 102, 96% yield). ^{1}H NMR (400 MHz, $CDCl_3$) δ 8.32 (dd, *J* = 8.56, 1.02 Hz, 1H), 7.84 (ddd, *J* = 8.11, 2.07, 1.42 Hz, 2H), 7.64 (d, *J* = 8.53 Hz, 1H), 7.60 (dd, *J* = 8.48, 1.41 Hz, 1H), 7.53 (ddd, *J* = 8.07, 6.87, 1.23 Hz, 1H), 5.00 (d, *J* = 6.36 Hz, 2H), 2.08 (t, *J* = 6.42 Hz, 1H).

Synthesis of Allyl-Protected 1-bromo-2-naphthalenemethanol (113)

To an oven-dried 100 mL RBF was added a suspension of NaH (60% w/w, 1.06 g, 26 mmol) in anhydrous THF (10 mL) at 0 °C. A solution of 1-bromo-2-naphthalenemethanol (3.13 g, 13.2 mmol) in anhydrous THF (16 mL) was added dropwise *via* addition funnel and the suspension was sonicated at 0 °C for 1 h. Allyl bromide (2.3 mL, 26 mmol) was added and the suspension was sonicated at room temperature overnight to give a chalky-white suspension. The crude reaction mixture was cooled to 0 °C and slowly quenched with water. This was then extracted with DCM, washed with brine, dried with $MgSO_4$, gravity filtered, and condensed to give a yellow oil. The crude product was purified *via* CombiFlash (liquid load, hexanes) to give the allyl-protected alcohol as a yellow oil (3.66 g, 100% yield). ^{1}H NMR (500 MHz, $CDCl_3$): δ 8.34 (d, *J* = 8.49 Hz, 1H), 7.83 (d, *J* = 8.42 Hz, 2H), 7.67 (d, *J* = 8.45 Hz, 1H), 7.60 (ddd, *J* = 8.41, 6.84, 1.18 Hz, 1H), 7.55 – 7.50 (m, 1H), 6.04 (ddd, *J* = 11.56, 10.42, 5.20 Hz, 1H), 5.40 (dq, *J* = 17.24, 1.61 Hz, 1H), 5.27 (dq, *J* = 10.40, 1.31 Hz, 1H), 4.86 (s, 2H), 4.17 (dt, *J* = 5.58, 1.39 Hz, 2H); ^{13}C NMR (126 MHz, $CDCl_3$): δ 136.08, 134.67, 134.10, 132.28, 128.24, 127.80, 127.47, 127.10, 126.52, 126.05, 122.50, 117.44, 72.28, 71.79.

Mono Addition of Allyl-Protected 2-bromobenzyl alcohol to Anthraquinone (114)

To an oven-dried 100 mL RBF was added a solution of allyl-protected 2-bromobenzyl alcohol (2.00 g, 8.8 mmol) in anhydrous THF (55 mL). The solution was cooled to -78 °C and n-BuLi (2.5M, 3.9 mL, 9.7 mmol) was added and stirred at -78°C for 1hr to give a pale-yellow solution. This was slowly transferred *via* cannula over the course of 2h to a solution of 9,10-anthraquinone (3.66 g, 17.6 mmol) in anhydrous THF (110 mL) at -78 °C, then stirred at this temperature for 1h and finally heated to 50 °C overnight. The reaction mixture was cooled to 0 °C, quenched with sat. NH_4Cl, extracted with DCM, then condensed to give an orange solid. The crude mixture was suspended in acetone to give a yellow ppt. that was filtered off and identified as residual anthraquinone. The filtrate was dried with $MgSO_4$, gravity filtered, and

condensed to give an orange solid. The crude product was purified *via* CombiFlash (Hex:DCM) to give ketone **114** as an orange solid (1.50 g, m.p. 80 – 83 ºC 48% yield). ^{1}H NMR (700 MHz, $CDCl_3$) δ 8.28 (d, *J* = 7.80 Hz, 2H), 7.14 – 7.04 (m, 1H), 7.51 (t, *J* = 7.49 Hz, 2H), 7.44 (dt, *J* = 12.90, 7.64 Hz, 3H), 7.40 (d, *J* = 7.50 Hz, 1H), 7.35 (t, *J* = 7.41 Hz, 1H), 7.24 (d, *J* = 7.83 Hz, 2H) 5.52 (td, *J* = 10.55, 5.06 Hz, 1H), 4.99 – 4.92 (m, 2H), 3.82 (s, 2H), 3.51 (s, 1H), 3.44 (d, *J* = 4.67 Hz, 2H); ^{13}C NMR (176 MHz, $CDCl_3$): δ 183.47, 146.78, 142.51, 134.80, 134.41, 133.97, 130.01, 129.55, 129.03, 128.62, 128.10, 127.58, 127.50, 127.40, 117.54, 73.17, 71.16, 69.37.

Reduction to Give Diol (116)

To an oven-dried 100 mL RBF was added a suspension of $LiAlH_4$ (0.44 g, 11.5 mmol) in anhydrous THF (25 mL) at 0 °C. A solution of ketone **114** (1.20 g, 3.4 mmol) in anhydrous THF (43 mL) was added drop-wise and kept at 0 °C for 10 min, then held at room temperature for 2h. The yellow suspension was cooled to 0°C then quenched with 1 M NaOH, H_2O, and 1 M HCl. The orange suspension was filtered through a silica plug with EtOAc, extracted with EtOAc, dried with $MgSO_4$, gravity filtered, and condensed to give an orange oil. The crude product was purified *via* CombiFlash (Hex:DCM) to give diol **116** as an orange oil (1.050g, 87%). ^{1}H NMR (500 MHz, $CDCl_3$) δ 8.34 (dd, *J* = 7.91, 1.11 Hz, 1H), 7.77 (d, *J* = 7.77 Hz, 2H), 7.51 (td, *J* = 7.70, 1.40 Hz, 1H), 7.35 (qd, *J* = 7.62, 1.25 Hz, 3H), 7.27 – 7.25 (m, 1H), 7.23 – 7.19 (m, 2H), 7.07 (dd, *J* = 7.90, 0.98 Hz, 2H), 5.75 (d, *J* = 10.22 Hz, 1H), 5.30 (ddt, *J* = 16.28, 10.40, 5.88 Hz, 1H), 4.91 (dd, *J* = 10.35, 1.54 Hz, 1H), 4.83 (dd, *J* = 17.20, 1.60 Hz, 1H), 3.71 – 3.65 (m, 3H), 3.06 (dt, *J* = 5.86, 1.18 Hz, 2H), 2.79 (s, 1H).

Aromatization to Give 118

To a 250 mL RBF was added a solution of diol **116** (1.21 g, 3.4 mmol), NaI (3.55 g, 24 mmol), and NaH_2PO_2•H_2O (3.30 g, 31 mmol) in glacial acetic acid (85 mL). The dark red solution was heated to reflux for 1.5 h to give a yellow-orange solution. The reaction mixture was cooled to room temperature, quenched with water, extracted with DCM, dried with $MgSO_4$, gravity filtered,

and condensed to give a reddish oil. The crude product was purified *via* CombiFlash (Hex) to give the aromatic product (**118**) as a yellow solid (0.37 g, 34% yield). ^{1}H NMR (400 MHz, $CDCl_3$) δ 8.52 (s, 1H), 8.06 (d, *J* = 8.46 Hz, 2H), 7.81 – 7.78 (m, 1H), 7.59 (td, 7.59, 1.17 Hz, 1H), 7.53 – 7.45 (m, 5H), 7.37 – 7.29 (m, 3H), 5.54 (ddd, *J* = 17.12, 10.71, 5.24 Hz, 1H), 5.00 – 4.89 (m, 2H), 4.03 (s, 2H), 3.61 – 3.58 (m, 2H).

Deprotection of Aromatic Alcohol (120)

To an oven-dried 100 mL flask purged with nitrogen was added $Pd(PPh_3)_4$ (13 mg, 0.01 mmol) and MeOH (10 mL). A solution of allyl-protected alcohol **118** (0.37 g, 1.15 mmol) in MeOH (22 mL) was added and the mixture was stirred at room temperature for 15 min. K_2CO_3 (0.95 g, 6.9 mmol) was added and the yellow suspension was heated to reflux. After two hours a second equivalent of $Pd(PPh_3)_4$ was added and the suspension was held at reflux overnight. The reaction mixture was cooled to room temperature, condensed to remove MeOH, washed with sat. NH_4Cl, extracted with DCM, and flushed through a silica plug with ethyl acetate. The filtrate was condensed to give an orange solid, which was dissolved in minimal DCM, then hexanes was added but no precipitate was observed. Instead the crude product was purified *via* CombiFlash (Hex:DCM) to give the alcohol as a yellow solid (0.26 g, mp 112-114 °C, 78% yield). ^{1}H NMR (500 MHz, $CDCl_3$) δ 8.53 (s, 1H), 8.06 (d, *J* = 8.47 Hz, 2H), 7.78 – 7.73 (m, 1H), 7.60 (td, *J* = 7.60 1.33 Hz, 1H), 7.53 – 7.45 (m, 5H), 7.35 (ddd, *J* = 8.70, 6.54, 1.22 Hz, 2H), 7.30 (dd, *J* = 7.47 1.15 Hz, 1H), 4.18 (s, 2H), 1.26 (s, 1H); ^{13}C NMR (126 MHz, $CDCl_3$): δ 140.49, 137.05, 134.72, 131.51, 131.50, 130.37, 128.70, 128.54, 127.96, 127.86, 127.09, 126.32, 126.01, 125.42, 63.36.

Monoaddition of Allyl-Protected 1-bromo-2-naphthalenemethanol to Anthraquinone (115)

To an oven-dried 100 mL RBF was added a solution of allyl-protected 1-bromo-2-naphthalenemethanol (3.60 g, 13 mmol) in anhydrous THF (80 mL). The solution was cooled to -78 °C and n-BuLi (2.5M, 5.7 mL, 14.3 mmol) was added and stirred at -78°C for 1hr to give a

pale-yellow solution. This was slowly transferred *via* cannula over the course of 2h to a solution of 9,10-anthraquinone (5.41 g, 26 mmol) in anhydrous THF (160 mL) at -78 °C, then stirred at this temperature for 1h and finally heated to 50 °C overnight. The black-green reaction mixture was cooled to 0 °C, quenched with sat. NH_4Cl, extracted with DCM, then condensed to give an orange solid. The crude mixture was suspended in acetone to give a yellow ppt. that was filtered off and identified as residual anthraquinone. The filtrate was dried with $MgSO_4$, gravity filtered, and condensed to give an orange solid. The crude product was purified *via* CombiFlash (Hex:DCM) to give ketone **115** as a tan solid (2.37 g, m.p. 145 – 150 ^oC, 45% yield). ^1H NMR (700 MHz, $CDCl_3$) δ 8.43 (d, *J* = 7.71 Hz, 2H), 7.88 (d, *J* = 8.35 Hz, 1H), 7.73 (d, *J* = 7.98 Hz, 1H), 7.54 (d, *J* = 8.37 Hz, 1H), 7.43 (t, *J* = 7.30 Hz, 2H), 7.34 (t, *J* = 7.35 Hz, 2H), 7.20 (d, *J* = 6.90 Hz, 2H), 7.02 (d, *J* = 7.69 Hz, 2H), 6.87 (t, *J* = 7.58 Hz, 1H), 6.01 – 5.84 (m, 2H), 5.32 – 5.19 (m, 4H), 4.21 (d, *J* = 4.65 Hz, 2H); ^{13}C NMR (176 MHz, $CDCl_3$): δ 184.02 148.93, 139.22, 134.84, 134.69, 134.30, 133.60, 130.65, 130.60, 129.92, 129.47, 128.55, 128.34, 128.14, 127.69, 127.66, 125.98, 125.57, 118.18, 77.70, 74.86, 71.61.

Reduction to Give Diol (117)

To an oven-dried 250 mL RBF was added a suspension of $LiAlH_4$ (0.71 g, 18.6 mmol) in anhydrous THF (30 mL) at 0 °C. A solution of ketone **115** (2.23 g, 5.5 mmol) in anhydrous THF (70 mL) was added drop-wise and kept at 0°C for 10 min, then held at room temperature for 2h. The orange suspension was cooled to 0°C then quenched with 1 M NaOH, H_2O, and 1 M HCl. The yellow-green solution was filtered through a silica plug with EtOAc, extracted with EtOAc, dried with $MgSO_4$, gravity filtered, and condensed to give diol **117** as a viscous red oil (2.29 g). This was used in the following reaction without further purification.

Aromatization to Give Compound (119)

To a 250 mL RBF was added a solution of diol **117** (2.24 g, 5.5 mmol), NaI (5.77 g, 39 mmol), and $NaH_2PO_2•H_2O$ (5.36 g, 51 mmol) in glacial acetic acid (140 mL). The dark red solution was

heated to reflux for 1.5 h to give a yellow-orange solution. The reaction mixture was cooled to room temperature, quenched with water, extracted with DCM, dried with $MgSO_4$, gravity filtered, and condensed to give a dark red oil. The crude product was purified *via* CombiFlash (Hex:DCM) to give the aromatic product (**119**) as a yellow solid (0.41 g, 20% yield). ^{1}H NMR (400 MHz, $CDCl_3$) δ 8.62 (s, 1H), 8.13 (d, *J* = 8.40 Hz, 3H), 8.00 (dd, *J* = 8.34, 3.52 Hz, 2H), 7.46 (q, *J* = 7.27 Hz, 3H), 7.34 (d, *J* = 8.81 Hz, 2H), 7.28 – 7.23 (m, 2H), 7.15 (t, *J* = 7.64 Hz, 1H), 6.93 (d, *J* = 8.51 Hz, 1H), 5.62 (ddd, *J* = 11.43, 10.47, 5.20 Hz, 1H), 5.07 – 4.90 (m, 2H), 4.13 (s, 2H), 3.66 (dd, *J* = 5.56, 1.20 Hz, 2H).

Deprotection of Aromatic Alcohol (121)

To an oven-dried 50 mL flask purged with nitrogen was added $Pd(PPh_3)_4$ (12 mg, 0.01 mmol) and MeOH (5 mL). A solution of allyl-protected alcohol **119** (0.35 g, 0.93 mmol) in MeOH (15 mL) was added and the mixture was stirred at room temperature for 15 min. K_2CO_3 (0.78 g, 5.6 mmol) was added and the yellow suspension was heated to reflux. After 1 h, a second equivalent of $Pd(PPh_3)_4$ was added and this process was repeated twice more for a total of four equivalents (46 mg, 0.04 mmol, 4 mol%). The reaction was stirred at reflux overnight to give a brown-yellow suspension. This was cooled to room temperature, condensed to remove MeOH, washed with sat. NH_4Cl, extracted with DCM, and flushed through a silica plug with ethyl acetate. The filtrate was condensed to give a brown solid. The crude product was purified *via* CombiFlash (Hex:DCM) to give the alcohol as an off-white solid (0.29 g, 46% yield). ^{1}H NMR (400 MHz, $CDCl_3$) δ 8.62 (s, 1H), 8.12 (d, *J* = 8.66 Hz, 3H), 7.99 (d, *J* = 8.17 Hz, 1H), 7.91 (d, *J* = 8.52 Hz, 1H), 7.48 – 7.43 (m, 3H), 7.30 – 7.27 (m, 3H), 7.24 (dd, *J* = 5.94, 1.09 Hz, 1H), 7.15 (ddd, *J* = 8.23, 6.79, 1.26 Hz, 1H), 6.94 – 6.85 (m, 1), 4.24 (d, *J* = 6.11 Hz, 2H), 1.33 (t, *J* = 6.16 Hz, 1H).

PCC Oxidation of Benzyl Alcohol 120

To an oven-dried 25 mL RBF was added a suspension of PCC (0.13 g, 0.53 mmol), NaOAc (0.01 g, 0.11 mmol) and silica gel (0.13 g) in DCM (3 mL). The orange suspension was stirred under nitrogen at room temperature for 5 min then a solution of benzyl alcohol (**120**) (0.10 g, 0.35 mmol) in DCM (4 mL) was added and the suspension immediately turned dark brown. This was stirred at room temperature for an additional hour. The crude reaction mixture was flushed through a silica plug with EtOAc and condensed to give a yellow-green oil. The crude product was purified *via* CombiFlash (Hex:DCM) to give benzaldehyde (**122**) as an orange solid (0.067 g, 67% yield) as well as spirocycle (**124**) as an off-white solid (0.033 g, 30% yield). **Benzaldehyde (122):** ^{1}H NMR (400 MHz, $CDCl_3$) δ 9.32 (s, 1H), 8.59 (s, 1H), 8.24 (dd, *J* = 7.84, 1.33 Hz, 1H), 8.09 (d, *J* = 8.50 Hz, 2H), 7.81 (td, *J* = 7.48, 1.42 Hz, 1H), 7.70 (t, *J* = 7.60 Hz, 1H), 7.51 – 7.45 (m, 5H), 7.38 (ddd, *J* = 8.84, 6.35, 1.22 Hz, 2H). **Spirocycle (124):** ^{1}H NMR (400 MHz, $CDCl_3$) δ 8.34 – 8.27 (m, 2H), 7.54 (td, *J* = 7.51, 1.49 Hz, 2H), 7.47 – 7.40 (m, 4H), 7.37 (d, *J* = 7.62 Hz, 1H), 7.29 – 7.26 (m, 1H), 7.12 – 7.08 (m, 1H), 6.63 (d, *J* = 7.75 Hz, 1H), 5.76 (s, 2H).

PCC Oxidation of Naphthyl Alcohol 121

To an oven-dried 25 mL RBF was added a suspension of PCC (0.26 g, 1.0 mmol), NaOAc (0.02 g, 0.21 mmol) and silica gel (0.26 g) in DCM (5 mL). The orange suspension was stirred under nitrogen at room temperature for 5 min then a solution of naphthyl alcohol (**121**) (0.23 g, 0.70 mmol) in DCM (9 mL) was added and the suspension immediately turned dark brown. This was stirred at room temperature for an additional hour. The crude reaction mixture was flushed through a silica plug with EtOAc and condensed to give a yellow oil. The crude product was purified *via* CombiFlash (Hex:DCM) to give naphthaldehyde (**123**) as bright yellow solid (0.16 g, 65% yield) as well as spirocycle (**125**) as an off-white solid (0.085 g, 35% yield). **Naphthaldehyde (123):** ^{1}H NMR (500 MHz, $CDCl_3$) δ 9.38 (s, 1H), 8.68 (s, 1H), 8.26 (d, *J* =

8.65 Hz, 1H), 8.41 (d, *J* = 8.68 Hz, 3H), 8.03 (d, *J* = 8.22 Hz, 1H), 7.62 -7.58 (m, 1H), 7.48 (ddd, *J* = 8.28, 6.24, 1.18 Hz, 2H), 7.30 – 7.27 (m, 2H), 7.23 (ddd, *J* = 8.15, 5.74, 1.10 Hz, 3H), 7.08 (d, *J* = 8.48 Hz, 1H). **Spirocycle (125):** ^{1}H NMR (500 MHz, $CDCl_3$) δ 8.41 (dd, *J* = 7.51, 1.75 Hz, 2H), 7.96 (d, *J* = 8.42 Hz, 1H), 7.86 (d, *J* = 8.22 Hz, 1H), 7.57 (d, *J* = 8.42 Hz, 1H), 7.48 – 7.42 (m, 4H), 7.32 (t, *J* = 7.50 Hz, 1H), 7.10 (dt, *J* = 6.81, 2.12 Hz, 3H), 6.97 (d, *J* = 8.42 Hz, 1H), 5.68 (s, 2H).

Cyclization of Benzaldehyde 122 with TBHP (126)

To an oven-dried 10 mL RBF was added a solution of benzaldehyde (**122**) (0.067 g, 0.24 mmol), ferrocene (5 mM in CH_3CN, 48 µL, 0.24 µM), and t-butyl hydrogen peroxide (70% v/v, 72 µL, 0.53 mmol) in CH_3CN (2 mL). The solution was stirred at room temperature for 5 min and then heated to 90 °C overnight. The crude reaction was filtered through a silica plug with DCM and condensed to give a red solid. The crude product was purified *via* CombiFlash (Hex:DCM) to give the cyclized product as a red solid (0.015 g, 36% yield). ^{1}H NMR (500 MHz, $CDCl_3$) δ 8.41 – 8.35 (m, 2H), 8.03 (dd, *J* = 6.12, 2.09 Hz, 1H), 7.57 – 7.53 (m, 4H), 7.51 (ddd, *J* = 6.45, 4.19, 1.28 Hz 2H), 7.22 (dd, *J* = 7.24, 1.70 Hz, 2H), 6.88 (dd, *J* = 6.08, 1.83 Hz, 1H).

Cyclization of Naphthaldehyde 123 with TBHP (127)

To an oven-dried 10 mL RBF was added a solution of naphthaldehyde (**123**) (0.16 g, 0.47 mmol), ferrocene (5 mM in CH_3CN, 94 µL, 0.47 µM), and t-butyl hydrogen peroxide (70% v/v, 14 µL, 1.0 mmol) in CH_3CN (5 mL). The solution was stirred at room temperature for 5 min and then heated to 90 °C overnight. The crude reaction was filtered through a silica plug with DCM and condensed to give a red solid. The crude product was purified *via* CombiFlash (Hex:DCM) to give the cyclized product as a red solid (0.050 g, 32% yield). ^{1}H NMR (500 MHz, $CDCl_3$) δ 8.48 (dd, *J* = 7.87, 1.10 Hz, 2H), 8.12 – 8.06 (m, 2H), 7.97 (d, *J* = 8.33 Hz, 1H), 5.57 – 7.51 (m, 3H), 7.48 – 7.44 (m, 2H), 7.34 (dd, *J* = 8.54, 5.52 Hz, 1H), 7.13 (d, *J* = 8.29 Hz, 1H), 6.96 (d, *J* = 7.86 Hz, 2H).

Mono Addition of Phenyl Lithium to Anthraquinone (129)

To an oven-dried 100 mL RBF was added a solution of bromobenzene (1.8 mL, 17 mmol) in anhydrous THF (100 mL). The solution was cooled to -78 °C and n-BuLi (2.5M, 7.7 mL, 19.1 mmol) was added and stirred at -78 °C for 1 h to give a pale-yellow solution. This was slowly transferred *via* cannula over the course of 2 h to a solution of 9,10-anthraquinone (7.25 g, 35 mmol) in anhydrous THF (200 mL) at -78 °C, then stirred at this temperature for 1h and finally heated to 50 °C overnight. The black reaction mixture was cooled to 0 °C, quenched with sat. NH_4Cl, extracted with DCM, then condensed to give a red solid. The crude mixture was suspended in acetone to give a yellow ppt. that was filtered off and identified as residual anthraquinone. The filtrate was dried with $MgSO_4$, gravity filtered, and condensed to give an red solid. The crude product was purified *via* CombiFlash (Hex:DCM) to give ketone **129** as an off-white solid (0.36 g, 7.2% yield) as well as diol **130** (0.42 g, 11% yield) and 9,10-diphenyl anthracene (0.40 g, 15% yield). ^{1}H NMR (400 MHz, $CDCl_3$) δ 7.71 (dd, *J* = 6.82, 3.28 Hz, 2H), 7.64 -7.56 (m, 3H), 7.50 (dd, *J* = 6.66, 1.49 Hz, 2H), 7.34 (dd, *J* = 6.90, 3.23 Hz, 2H), 1.27 (s, 1H).

Reaction of Ketone 114 with Phenyl Lithium (132)

To an oven-dried 50 mL RBF was added a solution of bromobenzene (1.0 mL, 9.5 mmol) in anhydrous THF (27 mL). The solution was cooled to -78 °C and n-BuLi (2.5M, 3.8 mL, 9.5 mmol) was added and stirred at -78°C for 1 h to give a pale-yellow solution. This was slowly transferred *via* cannula over the course of 30 min to a solution of ketone (**114**) (1.54 g, 4.3 mmol) in anhydrous THF (27 mL) at -78 °C, then stirred at this temperature for 1h and finally heated to 50 °C overnight. The yellow suspension was cooled to 0 °C, quenched with sat. NH_4Cl, extracted with DCM, dried with $MgSO_4$, gravity filtered, and condensed to give the diol as a yellow solid (1.88 g). This was used without purification in the reductive aromatization.

Reaction of Ketone (115) with Phenyl Lithium (133)

To an oven-dried 50 mL RBF was added a solution of bromobenzene (0.7 mL, 6.6 mmol) in anhydrous THF (19 mL). The solution was cooled to -78 °C and n-BuLi (2.5M, 2.6 mL, 6.6 mmol) was added and stirred at -78°C for 1 h to give a pale-yellow solution. This was slowly transferred *via* cannula over the course of 30 min to a solution of ketone (**115**) (1.24 g, 3.0 mmol) in anhydrous THF (19 mL) at -78 °C, then stirred at this temperature for 1h and finally heated to 50 °C overnight. The red solution was cooled to 0 °C, quenched with sat. NH_4Cl, extracted with DCM, dried with $MgSO_4$, gravity filtered, and condensed to give the diol as an orange solid (1.48 g). This was used without purification in the reductive aromatization.

Aromatization to Give Compound 134

To a 250 mL RBF was added a solution of diol **132** (1.88 g, 4.3 mmol), NaI (4.54 g, 30 mmol), and $NaH_2PO_2•H_2O$ (4.22 g, 40 mmol) in glacial acetic acid (108 mL). The dark red solution was heated to reflux for 1.5 h to give a yellow solution. The reaction mixture was cooled to room temperature, quenched with water, extracted with DCM, dried with $MgSO_4$, gravity filtered, and condensed to give a dark red oil. The crude product was purified *via* CombiFlash (Hex:DCM) to give the aromatic product (**134**) as a yellow solid (0.69 g, 40% yield). ^{1}H NMR (700 MHz, $CDCl_3$) δ 7.84 (d, *J* = 7.75 Hz, 1H), 7.73 (d, *J* = 8.00 Hz, 2H), 7.64 – 7.61 (m, 3H), 7.58 (t, *J* = 7.88 Hz, 3H), 7.55 – 7.51 (m, 3H), 7.35 – 7.32 (m, 5H), 5.59 (ddt, *J* = 16.10, 10.64, 5.49 Hz, 1H), 4.98 (dd, *J* = 29.80, 13.82 Hz, 2H), 4.12 (s, 2H), 3.67 (d, *J* = 5.41 Hz, 2H); ^{13}C NMR (176 MHz, $CDCl_3$): δ 139.14, 138.57, 137.44, 137.41, 135.10, 134.57, 131.53, 131.50, 131.46, 129.99, 129.96, 128.56, 128.51, 128.26, 127.80, 127.63, 127.62, 127.18, 126.77, 125.36, 125.20, 116.71, 71.41, 69.84.

Aromatization to Give Compound 135

To a 250 mL RBF was added a solution of diol **133** (1.48 g, 3.0 mmol), NaI (3.15 g, 21 mmol), and $NaH_2PO_2•H_2O$ (2.93 g, 28 mmol) in glacial acetic acid (75 mL). The dark red solution was

heated to reflux for 1.5 h to give an orange solution. The reaction mixture was cooled to room temperature, quenched with water, extracted with DCM, dried with $MgSO_4$, gravity filtered, and condensed to give a dark red oil. The crude product was purified *via* CombiFlash (Hex:DCM) to give the aromatic product (**135**) as a yellow solid (0.32 g, 24% yield). ^{1}H NMR (700 MHz, $CDCl_3$) δ 8.12 (d, *J* = 8.53 Hz, 1H), 7.98 (dd, *J* = 17.61, 8.37, 2H), 7.76 (d, *J* = 8.77 Hz, 2H), 7.67 – 7.63 (m, 2H), 7.58 (dt, *J* = 14.52, 7.06 Hz, 3H), 7.46 (t, *J* = 7.38 Hz, 1H), 7.35 – 7.31 (m, 4H), 7.22 (t, *J* = 7.48 Hz, 2H), 7.18 (t, *J* = 7.54 Hz, 1H), 6.99 (d, *J* = 8.50 Hz, 1H), 5.61 (ddt, *J* = 16.21, 10.62, 5.48 Hz, 1H), 4.97 (dd, *J* = 24.37, 13.83 Hz, 2H), 4.16 (s, 2H), 3.68 (d, *J* = 5.39 Hz, 2H); ^{13}C NMR (176 MHz, $CDCl_3$): δ 139.13, 137.81, 136.36, 134.62, 134.12, 133.64, 133.24, 132.68, 131.58, 131.54, 130.57, 130.11, 128.59, 128.57, 128.56, 128.14, 127.70, 127.34, 136.81, 126.69, 126.48, 125.93, 125.64, 125.62, 125.34, 116.80, 71.45, 70.03.

Deprotection of Aromatic Alcohol (136)

To an oven-dried 100 mL flask purged with nitrogen was added $Pd(PPh_3)_4$ (15 mg, 0.013 mmol) and MeOH (10 mL). A solution of allyl-protected alcohol **134** (0.52 g, 1.3 mmol) in MeOH (26 mL) was added and the mixture was stirred at room temperature for 15 min. K_2CO_3 (1.08 g, 7.7 mmol) was added and the yellow suspension was heated to reflux. After 1 h, a second equivalent of $Pd(PPh_3)_4$ was added and this process was repeated twice more for a total of four equivalents (60 mg, 0.05 mmol, 4 mol%). The reaction was stirred at reflux overnight to give a brown-yellow suspension. This was cooled to room temperature, condensed to remove MeOH, washed with sat. NH_4Cl, extracted with DCM, and flushed through a silica plug with ethyl acetate. The filtrate was condensed to give a grey solid. The crude product was purified *via* CombiFlash (Hex:DCM) to give the alcohol as a bright yellow solid (0.38 g, m.p. 276 – 280 °C, 83% yield). ^{1}H NMR (700 MHz, $CDCl_3$) δ 7.79 (d, *J* = 7.70 Hz, 1H), 7.73 – 7.70 (m, 2H), 7.62 (q, *J* = 7.25 Hz, 3H), 7.58 – 7.51 (m, 5H), 7.48 (d, *J* = 7.29 Hz, 1H), 7.37 – 7.32 (m, 5H), 4.26 (d, *J* = 3.79 Hz, 2H), 1.26 (d, *J* = 6.02 Hz, 1H); ^{13}C NMR (176 MHz, $CDCl_3$): δ 140.58, 138.99,

137.72, 137.38, 134.74, 131.65, 131.47, 131.45, 130.05, 128.58, 128.06, 127.96, 127.70, 127.39, 126.44, 125.70, 125.31, 63.50.

Deprotection of Aromatic Alcohol (137)

To an oven-dried 100 mL flask purged with nitrogen was added $Pd(PPh_3)_4$ (8 mg, 0.006 mmol) and MeOH (5 mL). A solution of allyl-protected alcohol **135** (0.30 g, 0.66 mmol) in MeOH (13 mL) was added and the mixture was stirred at room temperature for 15 min. K_2CO_3 (0.55 g, 4.0 mmol) was added and the yellow suspension was heated to reflux. After 1 h, a second equivalent of $Pd(PPh_3)_4$ was added and this process was repeated twice more for a total of four equivalents (32 mg, 0.03 mmol, 4 mol%). The reaction was stirred at reflux overnight to give a black suspension. This was cooled to room temperature, condensed to remove MeOH, washed with sat. NH_4Cl, extracted with DCM, and flushed through a silica plug with ethyl acetate. The filtrate was condensed to give an orange oil. The crude product was purified *via* CombiFlash (Hex:DCM) to give the alcohol as a bright yellow solid (0.24 g, m.p. 224 – 228 °C, 88% yield). ^{1}H NMR (700 MHz, $CDCl_3$) δ 8.14 (d, *J* = 8.47 Hz, 1H), 8.01 (d, *J* = 8.18 Hz, 1H), 7.94 (d, *J* = 8.51 Hz, 1H), 7.77 (d, *J* = 8.92 Hz, 2H), 7.65 (t, *J* = 7.22 Hz, 2H), 7.58 (dq, *J* =12.18, 7.42 Hz, 3H), 7.47 (t, *J* = 7.34 Hz, 1H), 7.33 (d, *J* = 8.37 Hz, 4H), 7.25 – 7.22 (m, 2H), 7.20 (t, *J* = 7.48 Hz, 1H), 7.01 (d, *J* = 8.48 Hz, 1H), 4.32 (d, *J* = 3.92 Hz, 2H), 1.36 (s, 1H); ^{13}C NMR (176 MHz, $CDCl_3$): δ 138.97, 138.07, 138.05, 134.15, 133.62, 133.34, 132.46, 131.53, 131.51, 130.68, 130.15, 128.92, 128.62, 128.60, 128.19, 128.76, 127.55, 126.88, 126.64, 126.34, 126.11, 126.10, 125.98, 125.43, 63.79.

PCC Oxidation of Benzyl Alcohol (138)

To an oven-dried 50 mL RBF was added a suspension of PCC (0.37 g, 1.5 mmol), NaOAc (0.024 g, 0.29 mmol) and silica gel (0.37 g) in DCM (5 mL). The orange suspension was stirred under nitrogen at room temperature for 5 min then a solution of benzyl alcohol **136** (0.35 g, 0.97

mmol) in DCM (15 mL) was added and the suspension immediately turned dark brown. This was stirred at room temperature for an additional hour. The crude reaction mixture was flushed through a silica plug with EtOAc and condensed to give a yellow solid. The crude product was purified *via* CombiFlash (Hex:DCM) to give benzaldehyde (**138**) as a bright yellow solid (0.23 g, m.p. 250 – 253 °C, 65% yield) as well as spirocycle (**140**) as an off-white solid (0.033g, 9% yield). **Benzaldehyde (138):** ^{1}H NMR (700 MHz, $CDCl_3$) δ 9.41 (s, 1H), 8.26 (d, *J* = 7.82 Hz, 1H), 7.84 (t, *J* = 7.38 Hz, 1H), 7.75 – 7.72 (m, 3H), 7.63 (q, *J* = 7.37 Hz, 2H), 7.58 (t, *J* = 7.36 Hz, 1H), 7.50 (dt, *J* = 18.33, 5.52 Hz, 5H), 7.37 – 7.34 (m, 4H); ^{13}C NMR (176 MHz, $CDCl_3$): δ 192.21, 143.33, 138.78, 138.52, 135.98, 134.28, 132.87, 131.77, 131.44, 131.34, 130.88, 129.84, 128.75, 128.66, 128.60, 127.83, 127.44, 127.43, 126.46, 126.11, 125.39. **Spirocycle (140):** ^{1}H NMR (400 MHz, $CDCl_3$) δ 7.61 – 7.57 (m, 2H), 7.50 – 7.34 (m, 5H), 7.31 – 7.27 (m, 3H), 7.25 – 7.16 (m, 6H), 7.03 – 6.97 (m, 3H), 5.50 (s, 2H), 2.77 (s, 1H).

PCC Oxidation of Naphthyl Alcohol (139)

To an oven-dried 50 mL RBF was added a suspension of PCC (0.20 g, 0.81 mmol), NaOAc (0.013 g, 0.16 mmol) and silica gel (0.20 g) in DCM (3 mL). The orange suspension was stirred under nitrogen at room temperature for 5 min then a solution of naphthyl alcohol **137** (0.22 g, 0.54 mmol) in DCM (8 mL) was added and the suspension immediately turned dark brown. This was stirred at room temperature for an additional hour. The crude reaction mixture was flushed through a silica plug with EtOAc and condensed to give an orange solid. The crude product was purified *via* CombiFlash (Hex:DCM) to give naphthaldehyde (**139**) as a yellow solid (0.11 g, m.p. 302 – 304 °C, 50% yield) as well as spirocycle (**141**) as an off-white solid (0.033 g, m.p. 278 – 281 °C, 22% yield). **Naphthaldehyde (139):** ^{1}H NMR (700 MHz, $CDCl_3$) δ 9.46 (s, 1H), 8.27 (d, *J* = 8.61 Hz, 1H), 8.15 (d, *J* = 8.61 Hz, 1H), 8.05 (d, *J* = 8.19 Hz, 1H), 7.78 (d, *J* = 8.93 Hz, 2H), 7.66 (t, *J* = 7.36 Hz, 2H), 7.60 (dt, *J* = 15.03, 7.71 Hz, 3H), 7.55 (d, *J* = 7.24 Hz, 1H), 7.36 – 7.33 (m, 2H), 7.28 (t, *J* = 7.70 Hz, 5H), 7.20 (d, *J* = 8.45 Hz, 1H); ^{13}C NMR (176 MHz, $CDCl_3$): δ

192.51, 143.99, 138.82, 138.59, 136.41, 133.47, 133.18, 131.52, 131.37, 131.23, 129.68, 129.13, 129.06, 128.57, 128.47, 128.40, 127.78, 127.75, 127.39, 127.30, 126.42, 126.21, 125.36, 122.34. **Spirocycle (141):** ^{1}H NMR (400 MHz, $CDCl_3$) δ 7.99 (d, *J* = 8.35 Hz, 1H), 7.91 (d, *J* = 8.25 Hz, 1H), 7.73 – 7.67 (m, 4H), 7.58 (d, *J* = 8.38 Hz, 1H), 7.38 – 7.24 (m, 7H), 7.18 – 7.11 (m, 2H), 7.08 – 7.00 (m, 3H), 6.83 (dd, *J* = 7.97, 1.30 Hz, 2H), 5.52 (s, 2H), 2.87 (s, 1H).

Reaction of Benzaldehyde 138 with Phenyl Lithium (142)

To an oven-dried 25 mL RBF was added a solution of bromobenzene (0.13 mL, 1.3 mmol) in anhydrous THF (5 mL). The solution was cooled to -78 °C and n-BuLi (2.5M, 0.48 mL, 1.3 mmol) was added and stirred at -78°C for 1 h to give a pale-yellow solution. A solution of benzaldehyde **138** (0.21 g, 0.58 mmol) in anhydrous THF (5 mL) was added dropwise then stirred at -78 °C for 1h then room temperature overnight. The orange solution was cooled to 0 °C, quenched with sat. NH_4Cl, extracted with DCM, dried with $MgSO_4$, gravity filtered, and condensed to give a yellow oil. The crude product was purified *via* CombiFlash (Hex:DCM) to give a mixture of phenyl-substituted benzyl alcohol enantiomers as a yellow solid (0.241 g, 95% yield).

Reaction of Naphthaldehyde 139 with Phenyl Lithium (143)

To an oven-dried 25 mL RBF was added a solution of bromobenzene (0.05 mL, 0.5 mmol) in anhydrous THF (2 mL). The solution was cooled to -78 °C and n-BuLi (2.5M, 0.20 mL, 0.5 mmol) was added and stirred at -78°C for 1 h to give a pale-yellow solution. A solution of naphthaldehyde **139** (0.10 g, 0.25 mmol) in anhydrous THF (3 mL) was added dropwise then stirred at -78 °C for 1h then room temperature overnight. The yellow solution was cooled to 0 °C, quenched with sat. NH_4Cl, extracted with DCM, dried with $MgSO_4$, gravity filtered, and condensed to give a yellow oil. The crude product was purified *via* CombiFlash (Hex:DCM) to give the phenyl-substituted naphthyl alcohol as a yellow solid (0.12 g, m.p. 190 – 193 °C, 97% yield). ^{1}H NMR (400 MHz, $CDCl_3$) δ 8.07, (d, *J* = 8.67 Hz, 1H), 7.96 (d, *J* = 8.18 Hz, 1H), 7.83

(d, *J* = 8.67 Hz, 1H), 7.80 (d, *J* = 8.27 Hz, 1H), 7.73 (d, *J* = 7.73 Hz, 1H), 7.68 – 7.64 (m, 2H), 7.62 – 7.55 (m, 3H), 7.50 – 7.45 (m, 2H), 7.38 – 7.28 (m, 3H), 7.22 – 7.16 (m, 2H), 7.13 – 7.03 (m, 5H), 6.97 (dd, *J* = 6.85, 2.70 Hz, 2H), 5.38 (d, *J* = 3.23 Hz, 1H), 1.95 (d, *J* = 3.29 Hz, 1H).

Synthesis of Diphenyl[3]victorenium Cation with TfOD: An NMR Experiment (144)

To an NMR tube purged with nitrogen was added a solution of phenyl-substituted benzaldehyde **142** (0.025 g, 0.06 mmol) in DCE-d_4 (1 mL). TfOD (50 µL, 0.6 mmol) was added and the solution immediately turned dark green. The ^{1}H NMR was taken and the resulting spectrum showed the formation of the [3]victorenium cation as well as oligomeric byproducts. The reaction mixture was purified *via* CombiFlash to give a mixture of hydro[3]victorene isomers.

Synthesis of Hydro[3]victorenes with BF_3•Et_2O (146 and 147)

To an oven-dried 50 mL RBF was added a solution of phenyl-substituted benzyl alcohol **142** (0.050 g, 0.11 mmol) in DCM (22 mL). The purple solution was stirred under nitrogen for 15 min, then BF_3•Et_2O (41 µL, 0.33 mmol) was added, and the solution turned bright green immediately. The reaction mixture was stirred at room temperature for 30 min then quenched with water, extracted with DCM, dried with $MgSO_4$, gravity filtered, and condensed to give a green solid. The crude product was purified *via* CombiFlash (Hex:DCM) to give a mixture of hydrocarbons **146** and **147** in a 1:3 ratio (0.025 g, 53% yield). **Hydrocarbon (146):** ^{1}H NMR (400 MHz, $CDCl_3$) δ 9.03 (d, *J* = 8.46 Hz, 1H), 8.97 (d, *J* = 8.31 Hz, 1H), 7.60 – 7.08 (m, 16H), 6.48 (dt, *J* = 10.14, 2.13 Hz, 1H), 5.95 (dt, *J* = 10.06, 4.14 Hz, 1H), 3.66 (dd, *J* = 3.93, 2.17 HZ, 2H); **Hydrocarbon (147):** ^{1}H NMR (400 MHz, $CDCl_3$) δ 8.89 (d, *J* = 8.82 Hz, 1H), 8.18 (d, *J* = 7.84 Hz, 1H), 7.73 (d, *J* = 8.73 Hz, 1H), 7.60 – 7.08 (m, 18H), 5.58 (s, 1H).

Synthesis of Benzohydro[3]victorenes with BF_3•Et_2O (148 – 150)

To an oven-dried 50 mL RBF was added a solution of phenyl-substituted naphthyl alcohol **143** (0.050 g, 0.10 mmol) in DCM (20 mL). The purple solution was stirred under nitrogen for 15 min,

then BF_3•Et_2O (37 µL, 0.30 mmol) was added, and the solution turned bright green immediately. The reaction mixture was stirred at room temperature for 30 min then quenched with water, extracted with DCM, dried with $MgSO_4$, gravity filtered, and condensed to give a green solid. The crude product was purified *via* CombiFlash (Hex:DCM) to give a mixture of hydrocarbons **148**, **149**, and **150** in a 16:1:1 ratio (0.038 g, 77% yield).

Synthesis of Diphenyl[3]victorenium Cation with TfOD: An NMR Experiment (144)

To an NMR tube purged with nitrogen was added a solution of hydro[3]victorenes (**146** and **147**) (0.023 g, 0.06 mmol) in DCE-d_4 (0.5 mL). TfOD (50 µL, 0.6 mmol) was added and the solution immediately turned dark green. The ^{1}H NMR was taken and the resulting spectrum showed the formation of the diphenyl[3]victorenium cation (**144**) without excess oligomer formation. ^{1}H NMR (400 MHz, 1,2-dichloroethane-d_4): δ 9.29 (d, *J* = 8.54 Hz, 2H), 9.01 (d, *J* = 7.94 Hz, 2H), 8.29 – 8.24 (m, 4H), 8.14 (t, *J* = 7.97 Hz, 2H), 7.93 – 7.89 (m, 2H), 7.78 (dt, *J* = 14.66, 7.22 Hz, 5H), 7.65 (d, *J* = 7.64 Hz, 4H); ^{13}C NMR (101 MHz, 1,2-dichloroethane-d_4): δ 163.40, 154.09, 137.43, 136.89, 134.29, 133.98, 133.54, 131.79, 130.47, 130.26, 129.88, 129.67, 128.62, 128.42, 120.14, 116.98.

Synthesis of Diphenylbenzo[3]victorenium Cation with TfOD: An NMR Experiment (145)

To an NMR tube purged with nitrogen was added a solution of hydro[3]victorenes (**148** - **150**) (0.025 g, 0.05 mmol) in DCE-d_4 (0.5 mL). TfOD (47 µL, 0.5 mmol) was added and the solution immediately turned dark green. The ^{1}H NMR was taken and the resulting spectrum showed the formation of the diphenylbenzo[3]victorenium cation (**145**) without excess oligomer formation. ^{1}H NMR (400 MHz, 1,2-dichloroethane-d_4): δ 8.97 (dd, *J* = 8.00, 1.21 Hz, 1H), 8.86 (dd, *J* = 7.81, 1.17 Hz, 1H), 8.79 (d, *J* = 7.94 Hz, 1H), 8.54 (d, *J* = 8.50 Hz, 1H), 8.35 (d, *J* = 8.36 Hz, 1H), 8.16 – 8.06 (m, 4H), 7.88 – 7.80 (m, 7H), 7.57 – 7.52 (m, 4H), 7.35 – 7.29 (m, 3H).

LIST OF REFERENCES

(1) Clar, E.; Macpherson, I. A. The Significance of Kekulé Structures for the Stability of Aromatic Systems. *Tetrahedron* **1962**, *18* (12), 1411–1416.

(2) Longuet-Higgins, H. C. Some Studies in Molecular Orbital Theory. I. Resonance Structures and Molecular Orbitals in Unsaturated Drocarbons. *J. Chem. Phys.* **1950**, *18* (3), 265–274.

(3) Raman, K. V.; Kamerbeek, A. M.; Mukherjee, A.; Atodiresei, N.; Sen, T. K.; Lazić, P.; Caciuc, V.; Michel, R.; Stalke, D.; Mandal, S. K.; et al. Interface-Engineered Templates for Molecular Spin Memory Devices. *Nature* **2013**, *493* (7433), 509–513.

(4) Bullard, Z.; Giraõ, E. C.; Owens, J. R.; Shelton, W. A.; Meunier, V. Improved All-Carbon Spintronic Device Design. *Sci. Rep.* **2015**, *5*, 1–7.

(5) Stamp, P. C. E.; Gaita-Ariño, A. Spin-Based Quantum Computers Made by Chemistry: Hows and Whys. *J. Mater. Chem.* **2009**, *19* (12), 1718–1730.

(6) Ratera, I.; Veciana, J. Playing with Organic Radicals as Building Blocks for Functional Molecular Materials. *Chem. Soc. Rev.* **2012**, *41*, 303–349.

(7) Morita, Y.; Suzuki, S.; Sato, K.; Takui, T. Synthetic Organic Spin Chemistry for Structurally Well-Defined Open-Shell Graphene Fragments. *Nat. Chem.* **2011**, *3* (3), 197–204.

(8) Reid, B. D. H. The Chemistry of the Phenalenes. *Q. Rev. Chem. Soc.* **1965**, *19*, 274–302.

(9) Mishra, S.; Beyer, D.; Eimre, K.; Liu, J.; Berger, R.; Gröning, O.; Pignedoli, C. A.; Müllen, K.; Fasel, R.; Feng, X.; et al. Synthesis and Characterization of π-Extended Triangulene. *J. Am. Chem. Soc.* **2019**, *141*, 10621–10625.

(10) Su, J.; Telychko, M.; Hu, P.; Macam, G.; Mutombo, P.; Zhang, H.; Bao, Y.; Cheng, F.; Huang, Z.; Qiu, Z. Atomically Precise Bottom-Up Synthesis of π-Extended [5]Triangulene. *Sci. Adv.* **2019**, *5*, 1–6.

(11) Weiß, R.; Korczyn, J. Über Triphenylmethane, Deren Benzolkerne Miteinander Verbunden Sind. **1924**, *45*, 207–214.

(12) Allinson, G.; Bushby, R. J.; Paillaud, J.-L.; Thorton-Pett, M. Synthesis of a Derivative of Triangulene; the First Non-Kekule Polynuclear Aromatic. *J. Chem. Soc. Perkin. Trans. 1* **1995**, 385–390.

(13) Pavliček, N.; Mistry, A.; Majzik, Z.; Moll, N.; Meyer, G.; Fox, D. J.; Gross, L. Synthesis and Characterization of Triangulene. *Nat. Nanotechnol.* **2017**, *12* (4), 308–311.

(14) Clar, E.; Stewart, D. G. Aromatic Hydrocarbons. LXV. Triangulene Derivatives. *J. Am. Chem. Soc.* **1953**, *75* (11), 2667–2672.

(15) Clar, E.; Stewart, D. G. Aromatic Hydrocarbons. LXVIII. Triangulene Derivatives. Part II. *J. Am. Chem. Soc.* **1954**, *76* (13), 3504–3507.

(16) Sogo, P. B.; Nakazaki, M.; Calvin, M. Free Radical from Perinaphthene. *J. Chem. Phys.* **1958**, *26*, 1343–1345.

(17) Hara, O.; Tanaka, K.; Yamamoto, K.; Nakazawa, T.; Murata, I. The Chemistry of Phenalenium Systems. XXV. The Triangulenyl Dianion. *Tetrahedron Lett.* **1977**, *18* (28), 2435–2436.

(18) Allinson, G.; Bushby, R. J.; Jesudason, M. V.; Paillaud, J. L.; Taylor, N. The Synthesis of Singlet Ground State Derivatives of Non-Kekulé Polynuclear Aromatics. *J. Chem. Soc. Perkin Trans. 2* **1997**, No. 2, 147–156.

(19) Morita, Y.; Murata, T.; Ueda, A.; Yamada, C.; Kanzaki, Y.; Shiomi, D.; Sato, K.; Takui, T. Trioxotriangulene: Air- and Thermally Stable Organic Carbon-Centered Neutral π-Radical without Steric Protection. *Bull. Chem. Soc. Jpn.* **2018**, *91* (6), 922–931.

(20) Morita, Y.; Nishida, S.; Murata, T.; Moriguchi, M.; Ueda, A.; Satoh, M.; Arifuku, K.; Sato, K.; Takui, T. Organic Tailored Batteries Materials Using Stable Open-Shell Molecules

with Degenerate Frontier Orbitals. *Nat. Mater.* **2011**, *10* (12), 947–951.
(21) Inoue, J.; Fukui, K.; Kubo, T.; Nakazawa, S.; Sato, K.; Shiomi, D.; Morita, Y.; Yamamoto, K.; Takui, T.; Nakasuji, K. The First Detection of a Clar's Hydrocarbon, 2,6,10-Tri-Tert-Butyltriangulene: A Ground-State Triplet of Non-Kekulé Polynuclear Benzenoid Hydrocarbon. *J. Am. Chem. Soc.* **2001**, *123* (50), 12702–12703.
(22) Morita, Y.; Ohba, T.; Haneda, N.; Maki, S.; Kawai, J.; Hatanaka, K.; Sato, K.; Shiomi, D.; Takui, T.; Nakasuji, K. New Persistent Radicals: Synthesis and Electronic Spin Structure of 2,5- Di-Tert-Butyl-6-Oxophenalenoxyl Derivatives. *J. Am. Chem. Soc.* **2000**, *122* (19), 4825–4826.
(23) Hellwinkel, D.; Melan, M.; Aulmich, G. Polycyclen Vom Triangulentyp. *Tetrahedron Lett.* **1976**, *17* (46), 4137–4138.
(24) Delgado, I. H.; Pascal, S.; Besnard, C.; Voci, S.; Bouffier, L.; Sojic, N.; Lacour, J. C-Functionalized Cationic Diazaoxatriangulenes: Late-Stage Synthesis and Tuning of Physicochemical Properties. *Chem. - A Eur. J.* **2018**, *24* (40), 10186–10195.
(25) Nakatsuka, S.; Gotoh, H.; Kinoshita, K.; Yasuda, N.; Hatakeyama, T. Divergent Synthesis of Heteroatom-Centered 4,8,12-Triazatriangulenes. *Angew. Chemie - Int. Ed.* **2017**, *56* (18), 5087–5090.
(26) Field, J. E.; Venkataraman, D. Heterotriangulenes-Structure and Properties. *Chem. Mater.* **2002**, *14* (3), 962–964.
(27) Rosenberg, M.; Santella, M.; Bogh, S. A.; Muñoz, A. V.; Andersen, H. O. B.; Hammerich, O.; Bora, I.; Lincke, K.; Laursen, B. W. Extended Triangulenium Ions: Syntheses and Characterization of Benzo-Bridged Dioxa- and Diazatriangulenium Dyes. *J. Org. Chem.* **2018**, *84* (5), 2556–2567.
(28) Martin, J. C.; Smith, R. G. Factors Influencing the Basicities of Triarylcarbinols. The Synthesis of Sesquixanthydrol. *J. Am. Chem. Soc.* **1964**, *86* (11), 2252–2256.
(29) Laursen, B. W.; Krebs, F. C. Synthesis, Structure, and Properties of Azatriangulenium Salts. *Chem. Eur. J.* VCH Verlagsgesellschaft: [Weinheim, Germany : 2001, pp 1773–1783.
(30) Ball, P. Elusive Triangulene Created by Moving Atoms One at a Time. *Nature* **2017**, *542*, 284–285.
(31) Gross, L.; Mohn, F.; Moll, N.; Liljeroth, P.; Meyer, G. The Chemical Structure of a Molecule Resolved by Atomic Force Microscopy. *Science (80-.).* **2009**, *325*, 1110–1114.
(32) Mistry, A.; Moreton, B.; Schuler, B.; Mohn, F.; Meyer, G.; Gross, L.; Williams, A.; Scott, P.; Costantini, G.; Fox, D. J. The Synthesis and STM/AFM Imaging of "Olympicene" Benzo[Cd]Pyrenes. *Chem. - A Eur. J.* **2015**, *21* (5), 2011–2018.
(33) Altenhoff, G.; Goddard, R.; Lehmann, C. W.; Glorius, F. Sterically Demanding, Bioxazoline-Derived N-Heterocyclic Carbene Ligands with Restricted Flexibility for Catalysis. *J. Am. Chem. Soc.* **2004**, *126* (46), 15195–15201.
(34) Wu, L.; Drinkel, E.; Gaggia, F.; Capolicchio, S.; Linden, A.; Falivene, L.; Cavallo, L.; Dorta, R. Room-Temperature Synthesis of Tetra-Ortho-Substituted Biaryls by NHC-Catalyzed Suzuki-Miyaura Couplings. *Chem. - A Eur. J.* **2011**, *17* (46), 12886–12890.
(35) Lu, D. D.; He, X. X.; Liu, F. S. Bulky Yet Flexible Pd-PEPPSI-IPentAn for the Synthesis of Sterically Hindered Biaryls in Air. *J. Org. Chem.* **2017**, *82* (20), 10898–10911.
(36) Kaur, I.; Miller, G. P. [60]Fullerene Cycloaddition Across Hindered Acenes. *New J. Chem.* **2008**, *32* (3), 459–463.
(37) Ye, L.; Ding, D.; Feng, Y.; Xie, D.; Wu, P.; Guo, H.; Meng, Q.; Zhou, H. Convenient and Versatile Synthesis of Formyl-Substituted Benzoxaboroles. *Tetrahedron* **2009**, *65* (42), 8738–8744.
(38) Greene, T. W. *Protective Groups in Organic Synthesis*; John Wiley & Sons, Inc., 1981.
(39) Clar, E.; Holker, J. R. Aromatic Hydrocarbons Part LXII: 1:2-3:4-9:10-Tribenzopyrene. *J. Chem. Soc.* **1951**, 3252–3259.

(40) Harvey, R. G.; Yang, D. T. C.; Yang, C. Syntheses of Dibenzo[h,Rst]Pentaphene and Naphtho[l,2,3,4-Rst]Pentaphene. *Polycycl. Aromat. Compd.* **1994**, *4* (3), 127–133.
(41) Cristau, H. J.; Hervé, A.; Loiseau, F.; Virieux, D. Synthesis of New Arylhydroxymethylphosphinic Acids and Derivatives. *Synthesis (Stuttg).* **2003**, No. 14, 2216–2220.
(42) Hon, Y. S.; Hsu, Y. C.; Cheng, C. Y. Intramolecular Heck Reaction of Aryl Halide Tethered with Dienes as Acceptors: Studies of Their 6-Endo-Trig Versus 6-Exo-Trig Selectivities. *J. Chinese Chem. Soc.* **2006**, *53* (6), 1447–1462.
(43) Vutukuri, D. R.; Bharathi, P.; Yu, Z.; Rajasekaran, K.; Tran, M. H.; Thayumanavan, S. A Mild Deprotection Strategy for Allyl-Protecting Groups and Its Implications in Sequence Specific Dendrimer Synthesis. *J. Org. Chem.* **2003**, *68* (3), 1146–1149.
(44) Iovel, I.; Mertins, K.; Kischel, J.; Zapf, A.; Beller, M. An Efficient and General Iron-Catalyzed Arylation of Benzyl Alcohols and Benzyl Carboxylates. *Angew. Chemie - Int. Ed.* **2005**, *44* (25), 3913–3917.
(45) Jefferies, L. R.; Cook, S. P. Iron-Catalyzed Arene Alkylation Reactions with Unactivated Secondary Alcohols. *Org. Lett.* **2014**, *16* (7), 2026–2029.
(46) Liu, J.; Ravat, P.; Wagner, M.; Baumgarten, M.; Feng, X.; Müllen, K. Tetrabenzo[a,f,j,o]Perylene: A Polycyclic Aromatic Hydrocarbon with An Open-Shell Singlet Biradical Ground State. *Angew. Chemie - Int. Ed.* **2015**, *54*, 12442–12446.
(47) Bank, S.; Ehrlich, C. L.; Mazur, M.; Zubieta, J. A. Substituent Effect on the Electrochemical Oxidation of Trityl Anions. 2. Effect of an Electron-Withdrawing Group. *J. Org. Chem.* **1981**, *46* (7), 1243–1247.
(48) Dominikowska, J.; Domagala, M.; Palusiak, M. UV-Vis Spectra of Singlet State Cationic Polycyclic Aromatic Hydrocarbons: Time-Dependent Density Functional Theory Study. *J. Chem. Phys.* **2014**, *140* (4).
(49) Durham, L. J.; Studebaker, J.; Perkins, M. J. Long-Range Coupling in the Proton Magnetic Resonance Spectra of 1,4-Dihydrobenzenes. *Chem. Commun.* **1965**, No. 19, 456–457.
(50) Spartan 18, Version 1.20, Wavefunction Inc., Irvine, California.
(51) Gaussian 09, R. D. 0.; Frisch, M. J. .; Trucks, G. W. .; Schlegel, H. B. .; Scuseria, G. E. .; Robb, M. A. .; Cheeseman, J. R. .; Scalmani, G. .; Barone, V. .; Mennucci, B. .; et al. Gaussian, Inc., Wallingford CT, 2009.
(52) Konishi, A.; Hirao, Y.; Matsumoto, K.; Kurata, H.; Kubo, T. Facile Synthesis and Lateral π-Expansion of Bisanthenes. *Chem. Lett.* **2013**, *42*, 592–594.
(53) Reid, D. H. Stable π-Electron Systems and New Aromatic Structures. *Tetrahedron* **1958**, *3*, 339–352.
(54) Uchida, K.; Ito, S.; Nakano, M.; Abe, M.; Kubo, T. Biphenalenylidene: Isolation and Characterization of the Reactive Intermediate on the Decomposition Pathway of Phenalenyl Radical. *J. Am. Chem. Soc.* **2016**, *138* (7), 2399–2410.
(55) Zaitsev, V.; Rosokha, S. V.; Head-Gordon, M.; Kochi, J. K. Steric Modulations in the Reversible Dimerizations of Phenalenyl Radicals via Unusually Weak Carbon-Centered π- and σ-Bonds. *J. Org. Chem.* **2006**, *71* (2), 520–526.
(56) Suzuki, S.; Morita, Y.; Fukui, K.; Sato, K.; Shiomi, D.; Takui, T.; Nakasuji, K. Aromaticity on the Pancake-Bonded Dimer of Neutral Phenalenyl Radical as Studied by MS and NMR Spectroscopies and NICS Analysis. *J. Am. Chem. Soc.* **2006**, *128* (8), 2530–2531.
(57) Cui, Z. H.; Lischka, H.; Beneberu, H. Z.; Kertesz, M. Rotational Barrier in Phenalenyl Neutral Radical Dimer: Separating Pancake and van Der Waals Interactions. *J. Am. Chem. Soc.* **2014**, *136*, 5539–5542.
(58) Mou, Z.; Uchida, K.; Kubo, T.; Kertesz, M. Evidence of σ- and Π-Dimerization in a Series of Phenalenyls. *J. Am. Chem. Soc.* **2014**, *136* (52), 18009–18022.
(59) Bachman, J. C.; Kavian, R.; Graham, D. J.; Young Kim, D.; Noda, S.; Nocera, D. G.;

Shao-Horn, Y.; Lee, S. W. Electrochemical Polymerization of Pyrene Derivatives on Functionalized Carbon Nanotubes for Pseudocapacitive Electrodes. *Nat. Commun.* **2015**, *6*, 3–4.
(60) Mou, Z.; Kertesz, M. Pancake Bond Orders of a Series of π-Stacked Triangulene Radicals. *Angew. Chemie - Int. Ed.* **2017**, *56*, 10188–10191.
(61) Mou, Z.; Kertesz, M. Sigma- versus Pi-Dimerization Modes of Triangulene. *Chem. - A Eur. J.* **2018**, *24* (23), 6140–6147.
(62) Bhattacharyya, K.; Surendran, A.; Chowdhury, C.; Datta, A. Steric and Electric Field Driven Distortions in Aromatic Molecules: Spontaneous and Non-Spontaneous Symmetry Breaking. *Phys. Chem. Chem. Phys.* **2016**, *18* (45), 31160–31167.
(63) Ravat, P.; Ribar, P.; Rickhaus, M.; Häussinger, D.; Neuburger, M.; Juríček, M. Spin-Delocalization in a Helical Open-Shell Hydrocarbon. *J. Org. Chem.* **2016**, *81* (24), 12303–12317.
(64) Shen, Y.; Chen, C. F. Helicenes: Synthesis and Applications. *Chem. Rev.* **2012**, *112* (3), 1463–1535.
(65) Rao, M. R.; Black, H. T.; Perepichka, D. F. Synthesis and Divergent Electronic Properties of Two Ring-Fused Derivatives of 9,10-Diphenylanthracene. *Org. Lett.* **2015**, *17* (17), 4224–4227.
(66) Scholl, R.; Dehnert, H.; Wanka, L. Die Tautomerie Der Anthrachinon-a-Carbonsgure-Chloride Und Der Aufbau Yon Ringgebilden Der Coeranthren-Reihe. *Justus Liebigs Ann. Chem.* **1931**, *493*, 56–96.
(67) Clar, E.; Stewart, D. G. Aromatic Hydrocarbons. LXIII. Resonance Restriction and the Absorption Spectra of Aromatic Hydrocarbons. *J. Am. Chem. Soc.* **1952**, *74* (24), 6235–6238.
(68) Bergman, I. The Polarography of Polycyclic Aromatic Hydrocarbons; The Relationship Between Their Half-Wave Potentials and Absorption Spectra: Part 2. - Recently Synthesized and “Odd” Hydrocarbons. *Trans. Faraday Soc.* **1956**, *52*, 690–696.
(69) Lee, G. E.; Choi, J. S.; Ahn, Y. H.; Kim, U. S.; Lee, Y. S.; Lee, J. D.; Kim, D. J.; Noh, Y. S. Preparation of Aromatic Compounds for Organic Electroluminescent Device and Organic Solar Cell. **2014**, KR 2014021969 A 20140221.
(70) Zahradnik, R.; Tichy, M.; Hochmann, P.; Reid, D. Physical Properties and Chemical Reactivity of Alternant Hydrocarbons and Related Compounds. XIII. An Experimental and Theoretical Study of Phenalenyl. *J. Phys. Chem.* **1967**, *71* (9), 3040–3046.
(71) Sato, I.; Yamashima, R.; Kadowaki, K.; Yamamoto, J.; Shibata, T.; Soai, K. Asymmetric Induction by Helical Hydrocarbons: [6]-and [5]Helicenes. *Angew. Chemie - Int. Ed.* **2001**, *40* (6), 1096–1098.
(72) Reetz, M. T.; Beuttenm̈ller, E. W.; Goddard, R. First Enantioselective Catalysis Using a Helical Diphosphane. *Tetrahedron Lett.* **1997**, *38* (18), 3211–3214.
(73) Tang, Y.; Cook, T. A.; Cohen, A. E. Limits on Fluorescence Detected Circular Dichroism of Single Helicene Molecules. *J. Phys. Chem. A* **2009**, *113* (22), 6213–6216.
(74) Hassey, R.; McCarthy, K.; Swain, E.; Basak, D.; Venkataraman, D.; Barnes, M. Single-Molecule Chiroptical Spectroscopy: Fluorescence Excitation of Individual Helicene Molecules in Polymer-Supported Thin-Films. **2011**, *43* (March 2010), 34–43.
(75) Cohen, Y. S.; Xiao, S.; Steigerwald, M. L.; Nuckolls, C.; Kagan, C. R. Enforced One-Dimensional Photoconductivity in Core-Cladding Hexabenzocoronenes. *Nano Lett.* **2006**, *6* (12), 2838–2841.
(76) Bhattacharyya, K.; Mukhopadhyay, T. K.; Datta, A. Controlling Electronic Effects and Intermolecular Packing in Contorted Polyaromatic Hydrocarbons (c-PAHs): Towards High Mobility Field Effect Transistors. *Phys. Chem. Chem. Phys.* **2016**, *18* (22), 14886–14893.
(77) Solà, M. Forty Years of Clar’s Aromatic π-Sextet Rule. *Front. Chem.* **2013**, *1*, 4–11.
(78) Vasudevan, K.; Laidlaw, W. G. Energetics and Bond-Lengths of Some Polynuclear

Aromatic Hydrocarbons. *Tetrahedron* **1969**, *25* (3), 591–604.
(79) Boschi, R.; Clar, E.; Schmidt, W. Photoelectron Spectra of Polynuclear Aromatics. III. the Effect of Nonplanarity in Sterically Overcrowded Aromatic Hydrocarbons. *J. Chem. Phys.* **1974**, *4406* (1974), 4406–4418.
(80) Clar, E.; Schmidt, W. Correlations Between Photoelectron and UV Absorption Spectra of Polycyclic Hydrocarbons: The Pyrene Series. *Tetrahedron* **1977**, *35*, 1037–1032.
(81) Khan, Z. H. Electronic Spectra of Radical Cations and Their Correlation with Photoelectron Spectra. *Spectrochim. Acta Part A Mol. Spectrosc.* **1988**, *44A* (11), 1125–1128.
(82) Nakayama, N.; Nagashima, U. Semiempirical Calculation of Electronic Spectra of Organic Compounds by Using the Improved Method of New-γ Electron Repulsion Integral. Part 2. Polycyclic Aromatic Hydrocarbons (PAHs). *J. Mol. Struct. THEOCHEM* **2003**, *640* (1–3), 25–37.
(83) Wornat, M. J.; Sarofim, A. F.; Lafleur, A. L. The Pyrolysis of Anthracene as a Model Coal-Derived Compound. **1992**, 955–963.
(84) Lebon, F.; Longhi, G.; Gangemi, F.; Abbate, S.; Priess, J.; Juza, M.; Bazzini, C.; Caronna, T.; Mele, A. Chiroptical Properties of Some Monoazapentahelicenes. *J. Phys. Chem. A* **2004**, *108* (52), 11752–11761.
(85) Grimme, S.; Peyerimhoff, S. D. Theoretical Study of the Structures and Racemization Barriers of [n]Helicenes (n = 3-6, 8). *Chem. Phys.* **1996**, *204* (2-3 SPEC. ISS.), 411–417.
(86) Huang, M.; Li, X.; Huang, S.-J. Methods of Producing Polyanthracene and Uses Thereof. **2016**, *US 9,290,6*.
(87) Wertz, S.; Leifert, D.; Studer, A. Cross Dehydrogenative Coupling via Base-Promoted Homolytic Aromatic Substitution (BHAS): Synthesis of Fluorenones and Xanthones. *Org. Lett.* **2013**, *15* (4), 928–931.
(88) Shi, Z.; Glorius, F. Synthesis of Fluorenones via Quaternary Ammonium Salt-Promoted Intramolecular Dehydrogenative Arylation of Aldehydes. *Chem. Sci.* **2013**, *4* (2), 829–833.
(89) Barluenga, J.; Trincado, M.; Rubio, E.; González, J. M. Direct Intramolecular Arylation of Aldehydes Promoted by Reaction with IPy2BF4/HBF4: Synthesis of Benzocyclic Ketones. *Angew. Chemie - Int. Ed.* **2006**, *45* (19), 3140–3143.
(90) Yamazaki, S. . *Tetrahedron Lett.* **2001**, *42*, 3355–3357.
(91) Li, Y.; Huang, K. W.; Sun, Z.; Webster, R. D.; Zeng, Z.; Zeng, W.; Chi, C.; Furukawa, K.; Wu, J. A Kinetically Blocked 1,14:11,12-Dibenzopentacene: A Persistent Triplet Diradical of a Non-Kekulé Polycyclic Benzenoid Hydrocarbon. *Chem. Sci.* **2014**, *5* (5), 1908–1914.

Appendices

Appendix A: Spectra

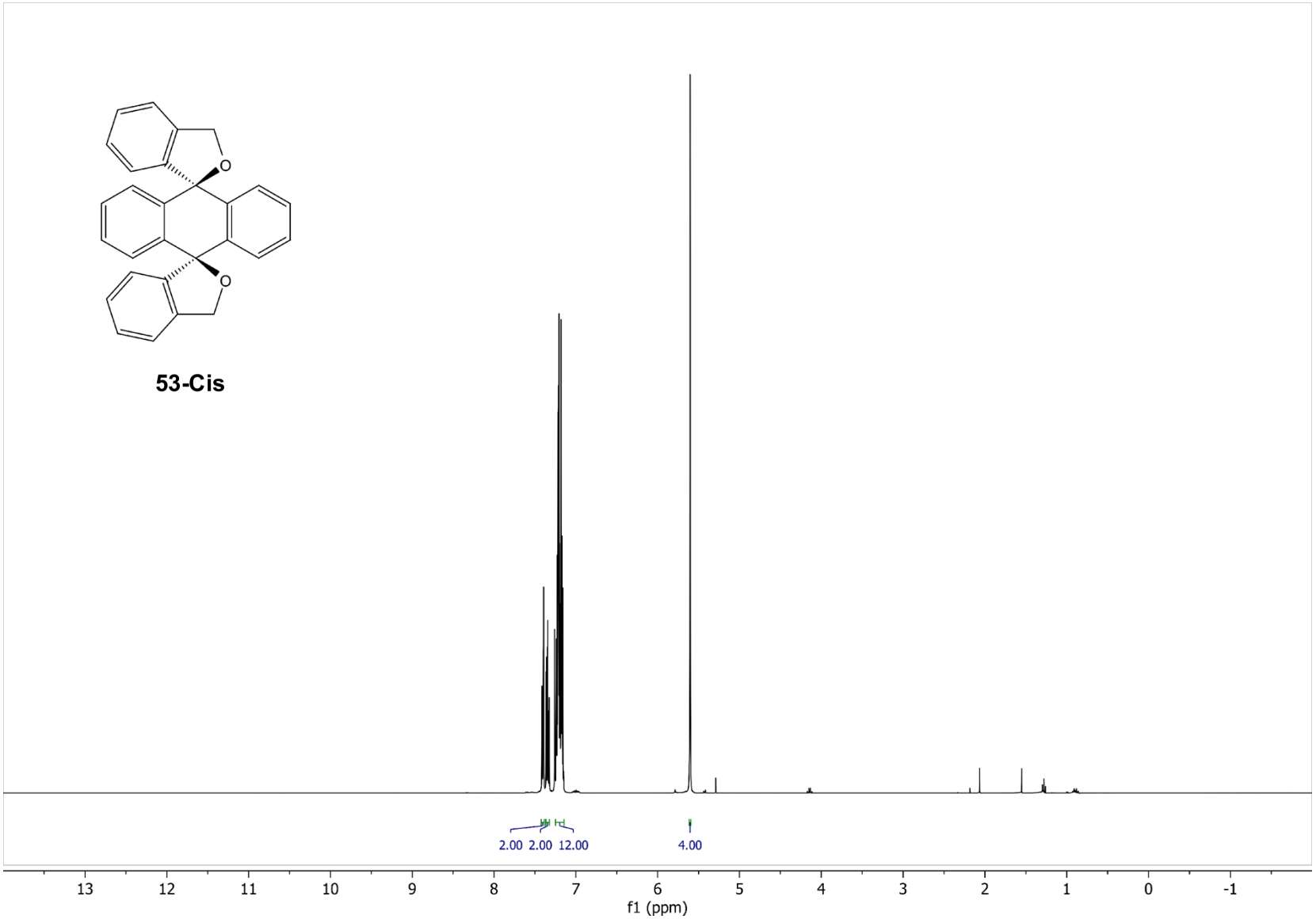
53-Cis
2.00 2.00 12.00
4.00
13 12 11 10 9 8 7 6 5 4 3 2 1 0 -1
f1 (ppm)

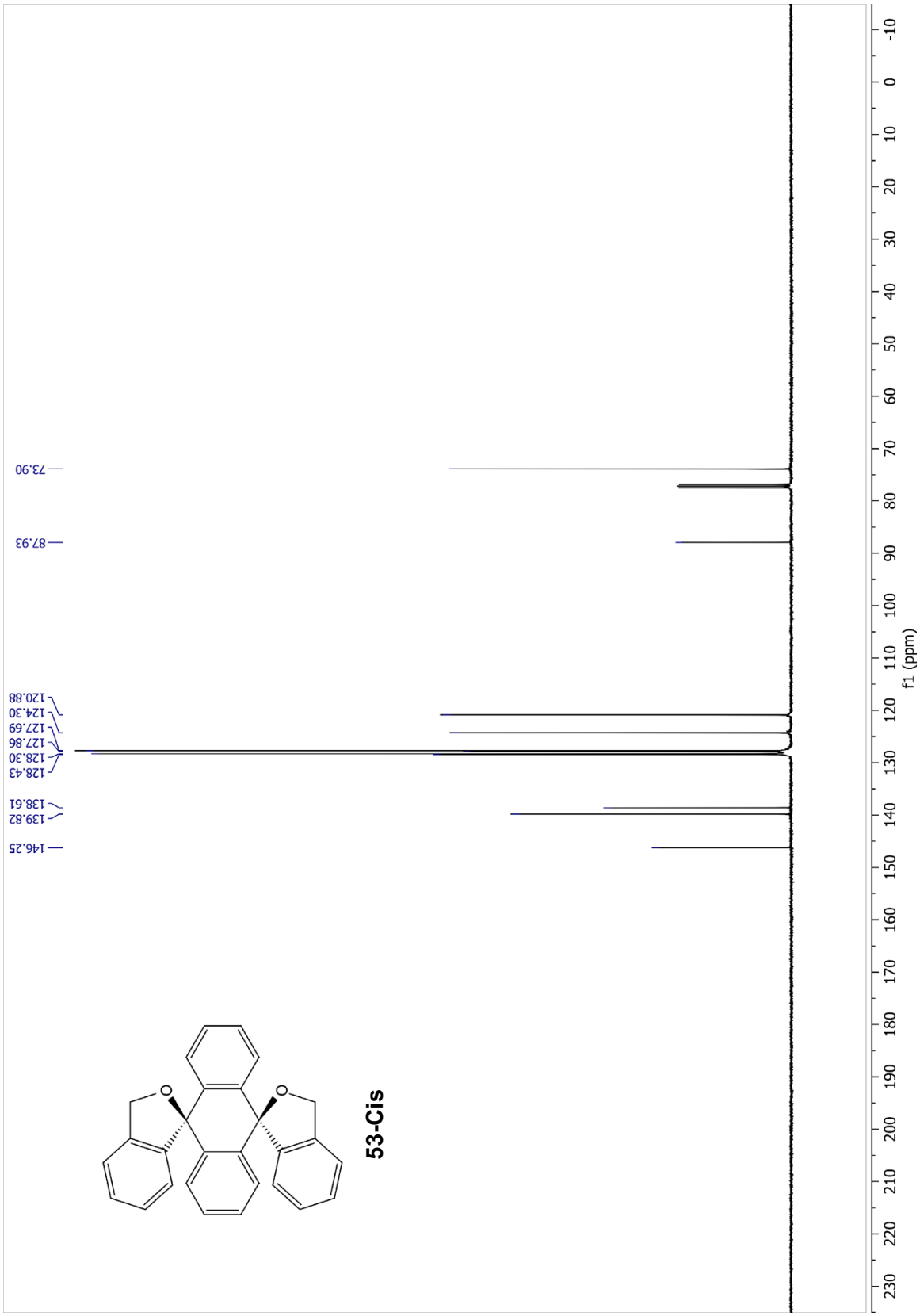
73.90
87.93
120.88
124.30
127.69
127.86
128.30
128.43
138.61
139.82
146.25
f1 (ppm)
53-Cis

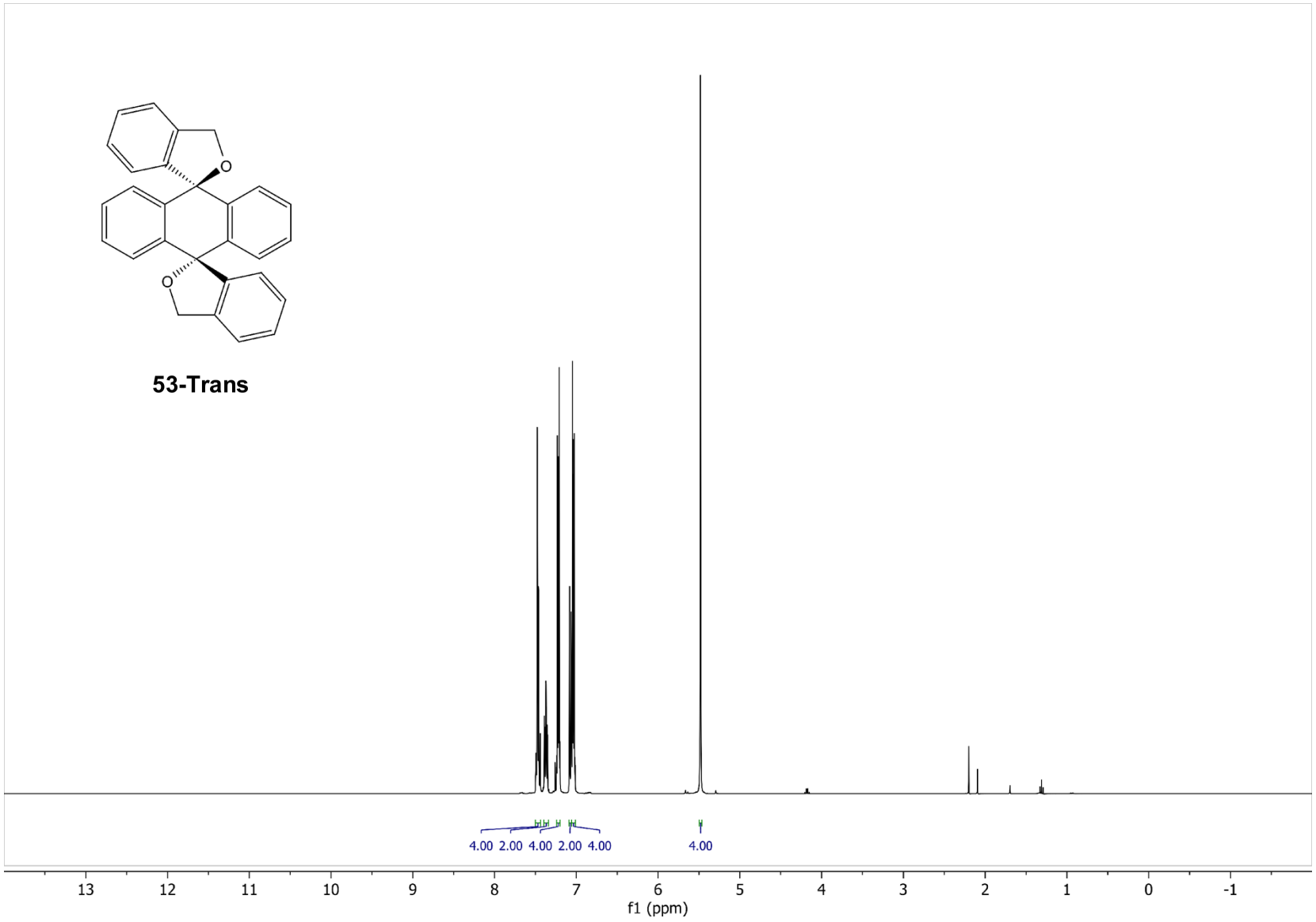
53-Trans
4.00 2.00 4.00 2.00 4.00
4.00
13 12 11 10 9 8 7 6 5 4 3 2 1 0 -1
f1 (ppm)

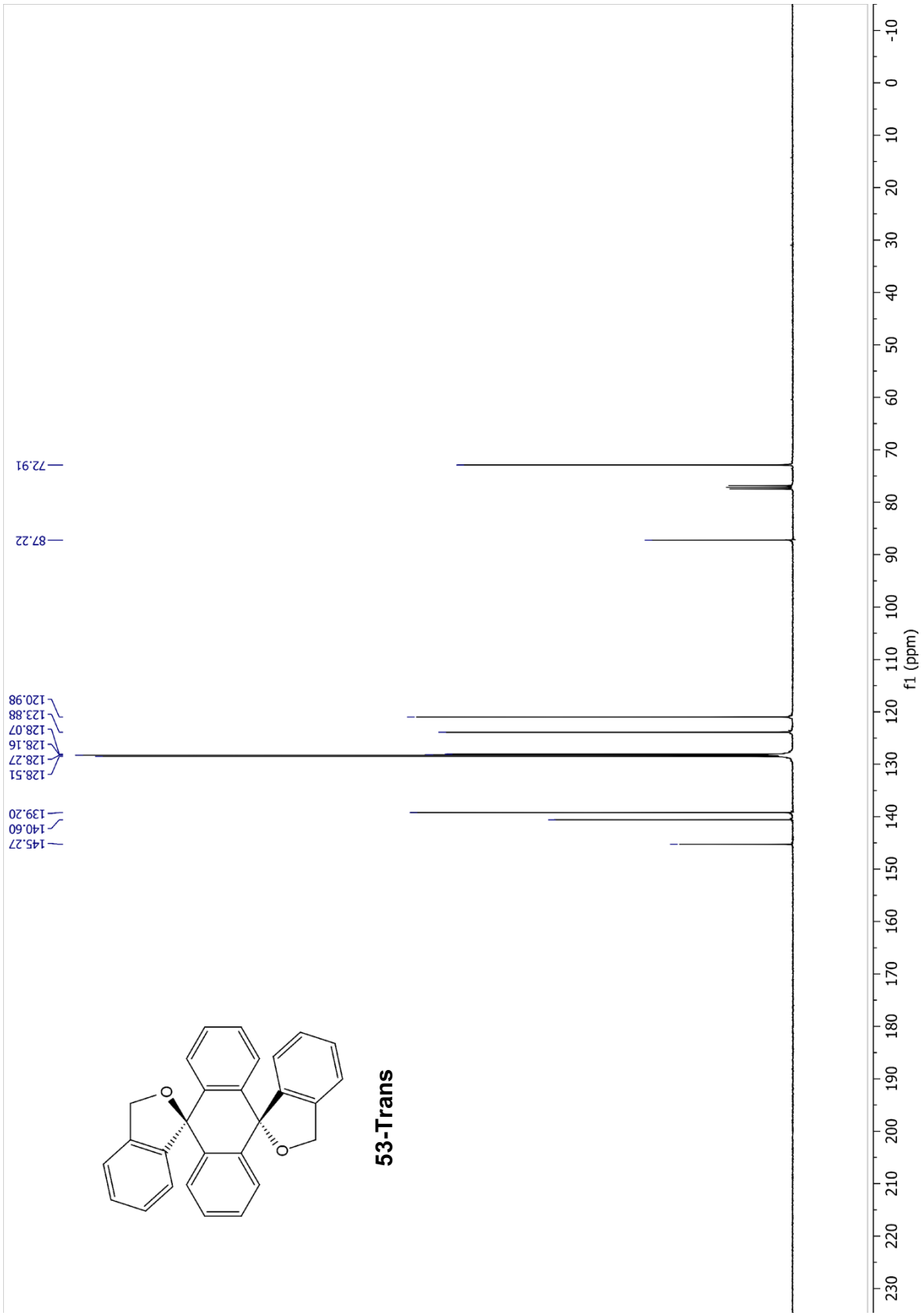
145.27
140.60
139.20
128.51
128.27
128.16
128.07
123.88
120.98
87.22
72.91
f1 (ppm)

53-Trans

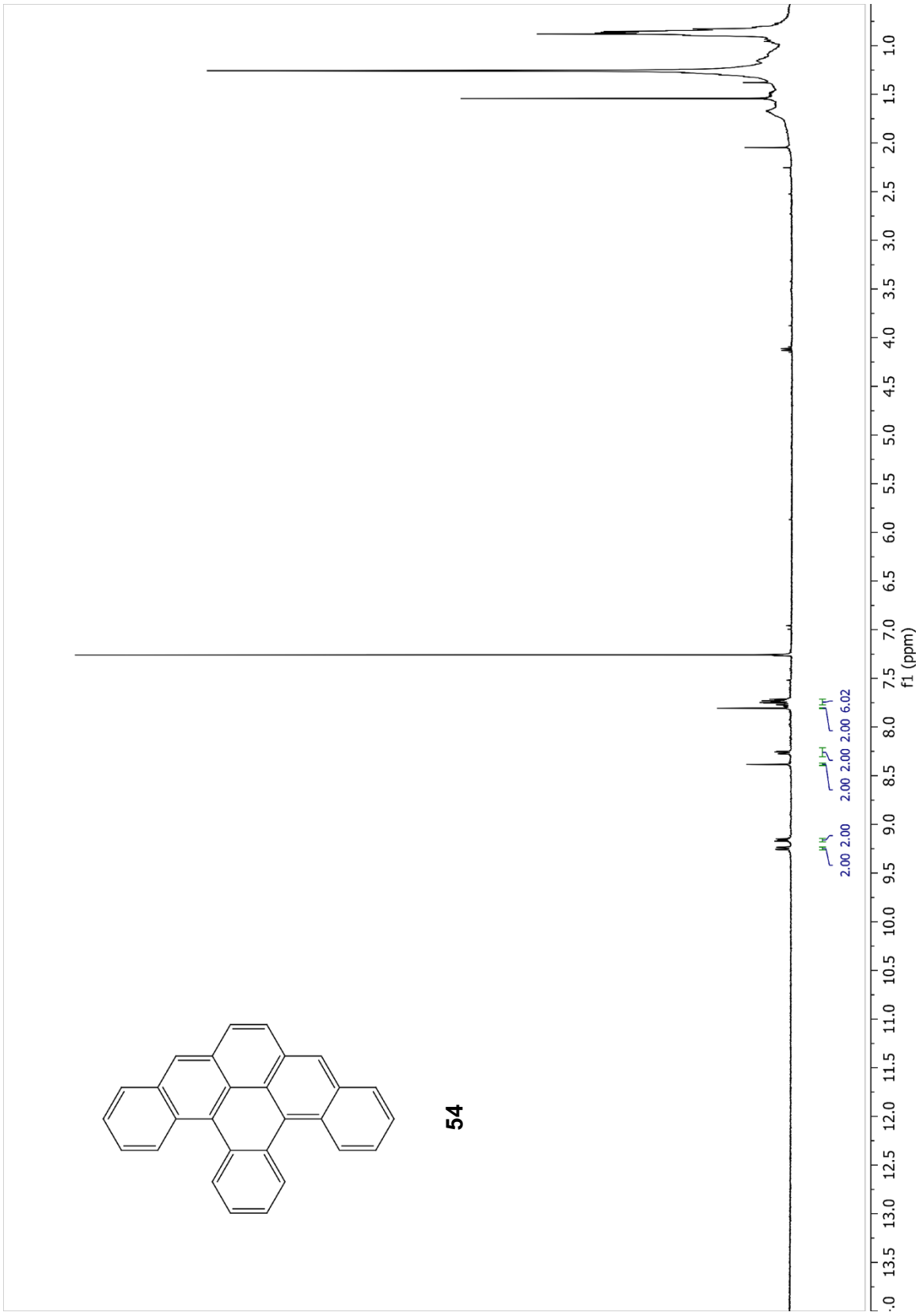
54
2.00 2.00
2.00 2.00 2.00 6.02
f1 (ppm)

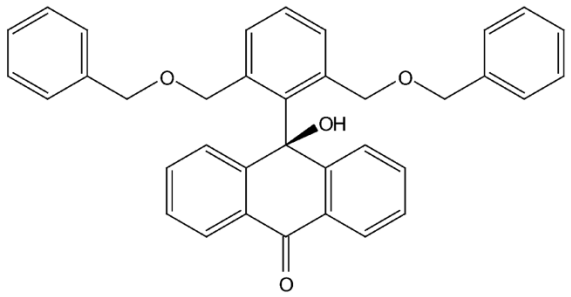
O
O
OH
O

60

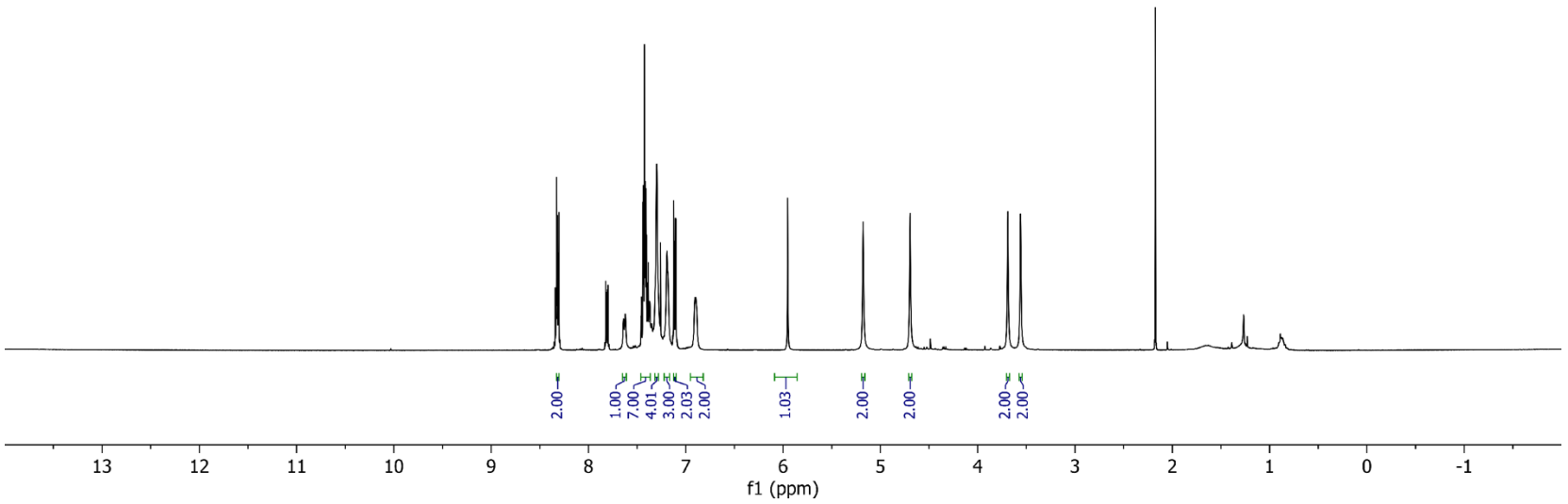
2.00
1.00
7.00
4.01
3.00
2.03
2.00
1.03
2.00
2.00
2.00
2.00
13
12
11
10
9
8
7
6
5
4
3
2
1
0
-1
f1 (ppm)

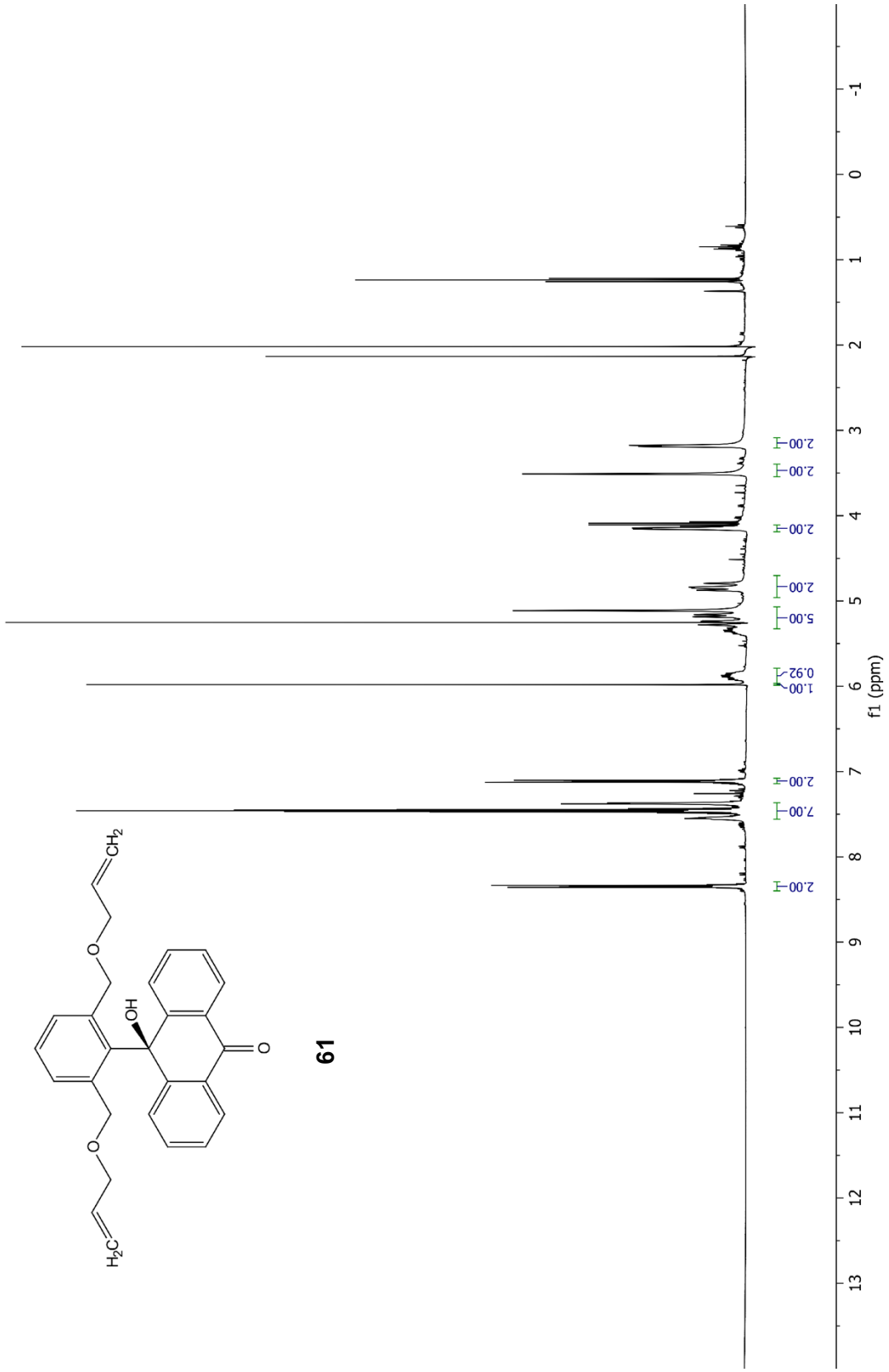
OH
O
O
O
H_2C
CH_2
61
2.00
7.00
2.00
1.00
0.92
5.00
2.00
2.00
f1 (ppm)

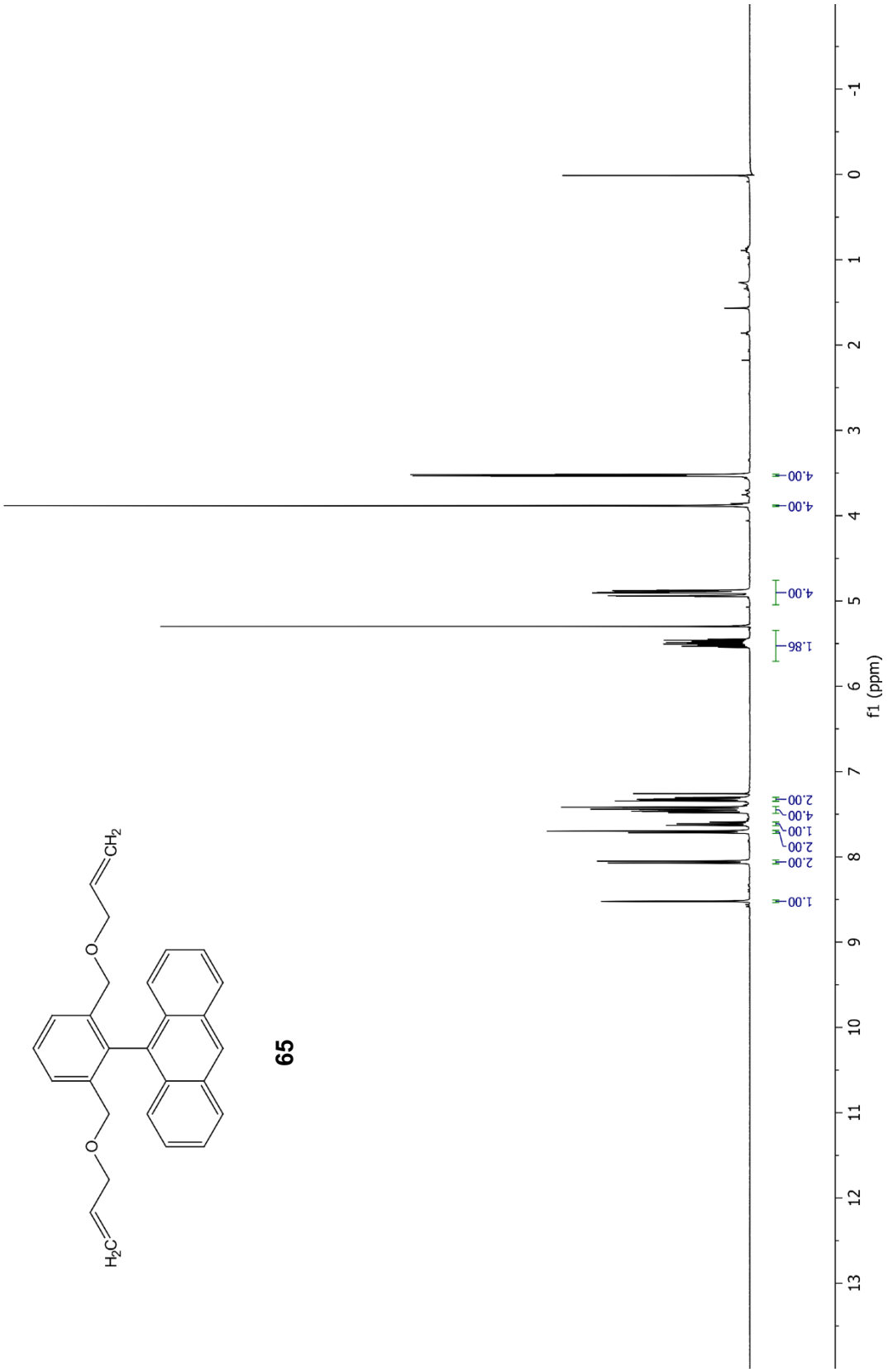
O
O
CH2
H2C
65
1.00
2.00
2.00
1.00
4.00
2.00
1.86
4.00
4.00
f1 (ppm)

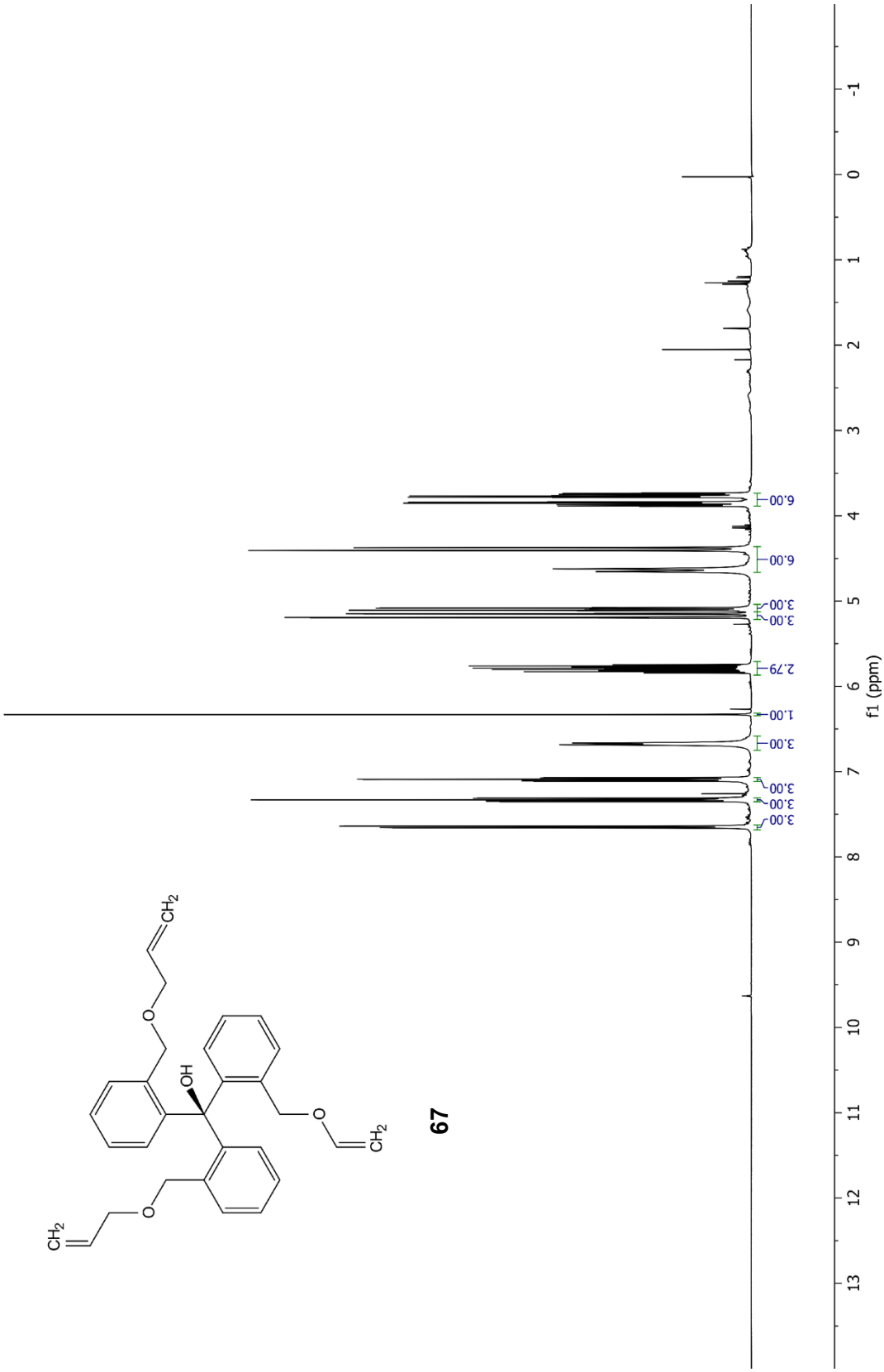

67

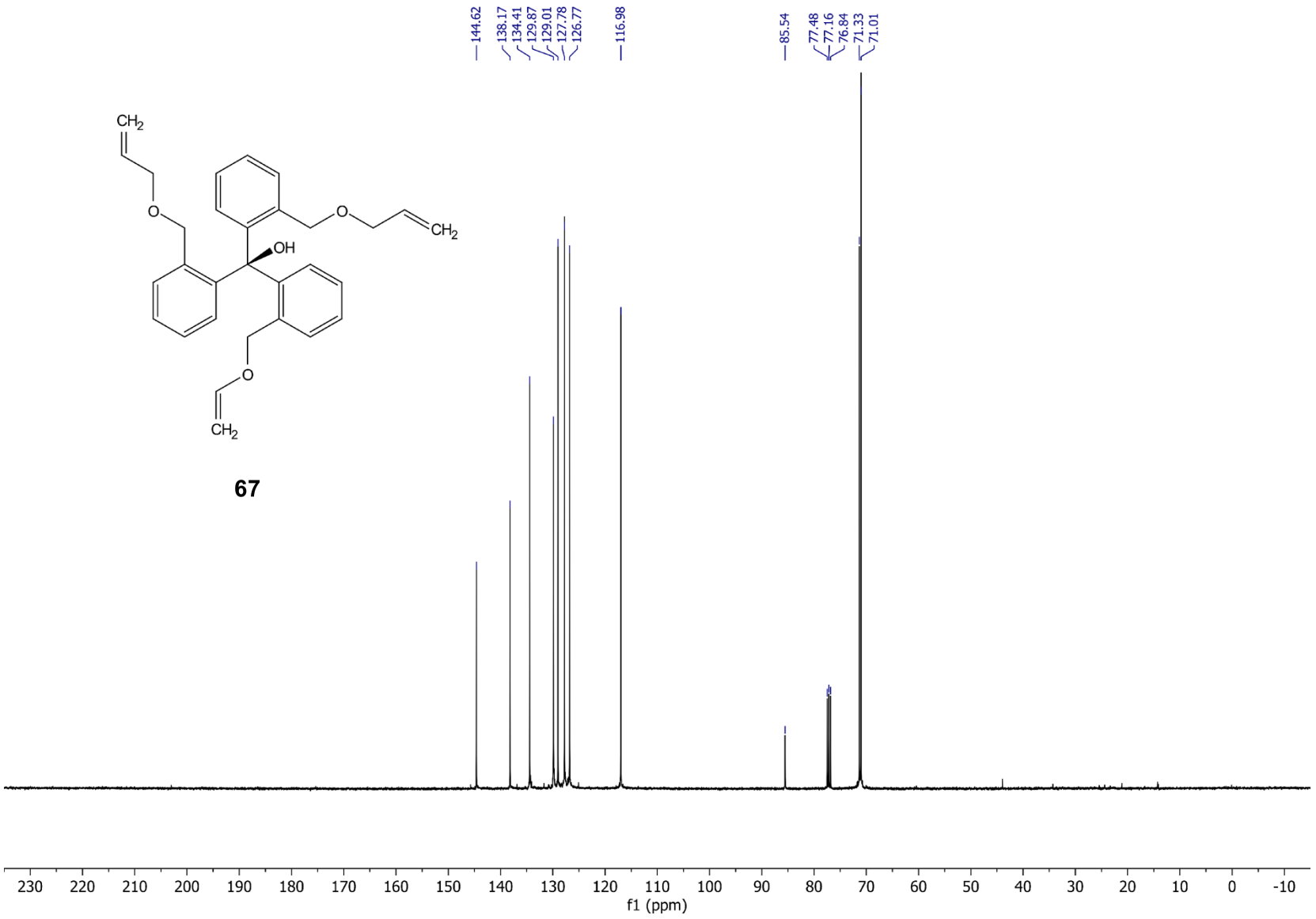
144.62
138.17
134.41
129.87
129.01
127.78
126.77
116.98
85.54
77.48
77.16
76.84
71.33
71.01
CH2
O
O
CH2
OH
O
CH2
230 220 210 200 190 180 170 160 150 140 130 120 110 100 90 80 70 60 50 40 30 20 10 0 -10
f1 (ppm)

67

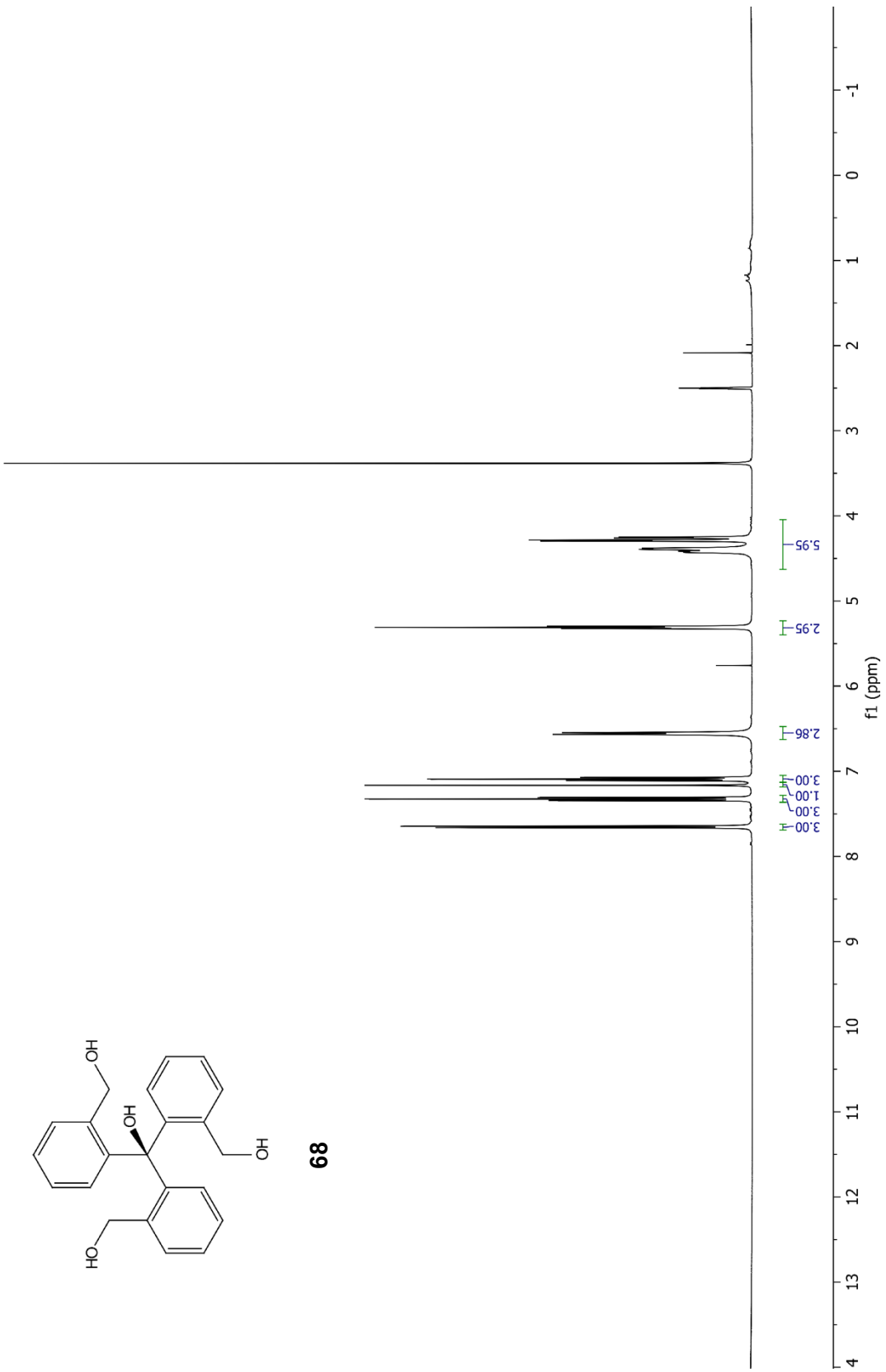

68

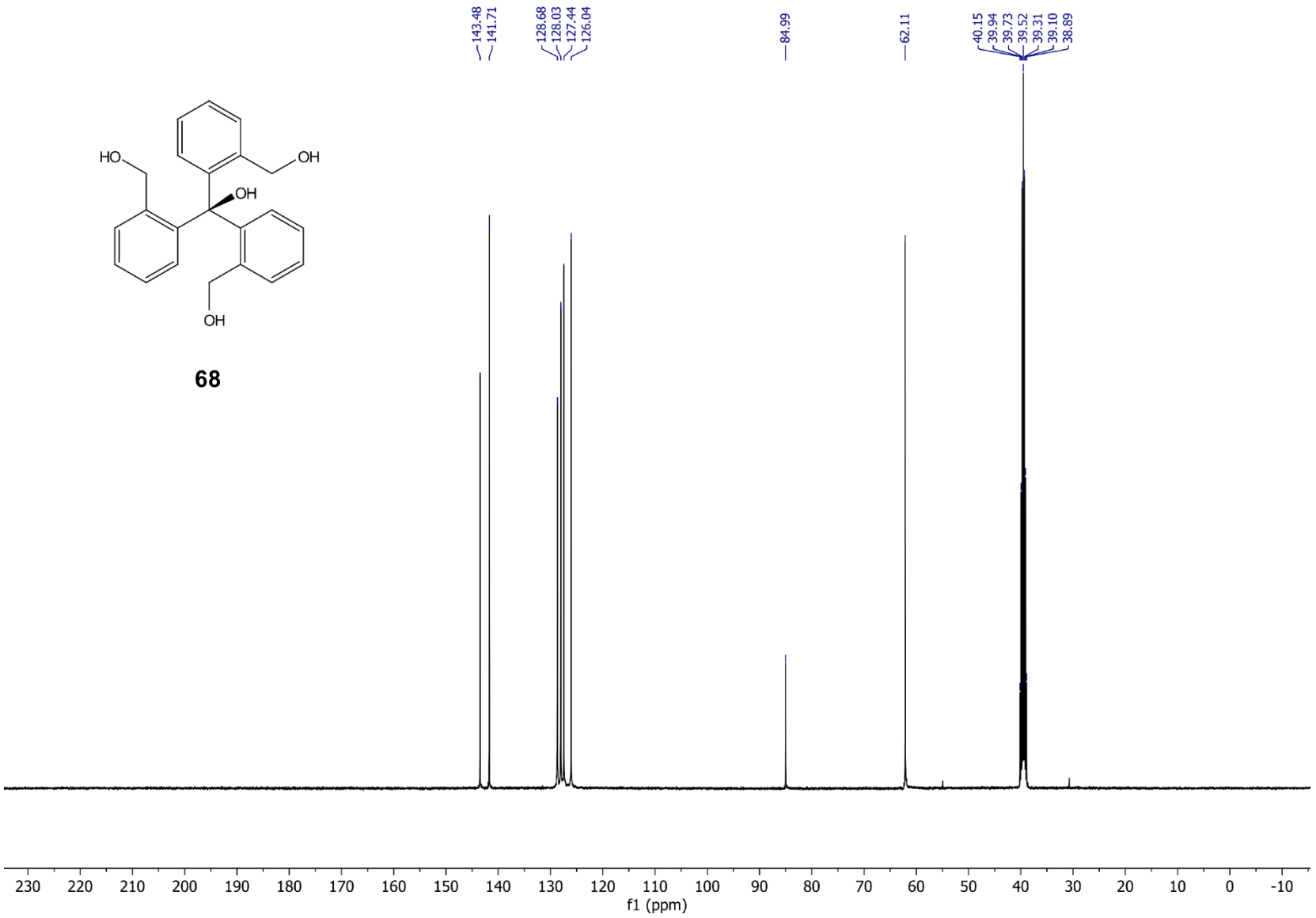
143.48
141.71
128.68
128.03
127.44
126.04
84.99
62.11
40.15
39.94
39.73
39.52
39.31
39.10
38.89
HO
OH
OH
OH
68
230 220 210 200 190 180 170 160 150 140 130 120 110 100 90 80 70 60 50 40 30 20 10 0 -10
f1 (ppm)

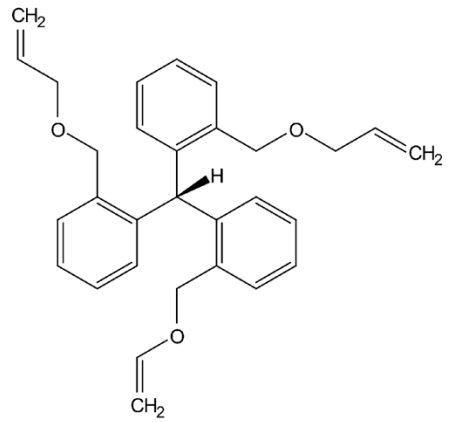
CH2
O
O
CH2
H
O
CH2

69

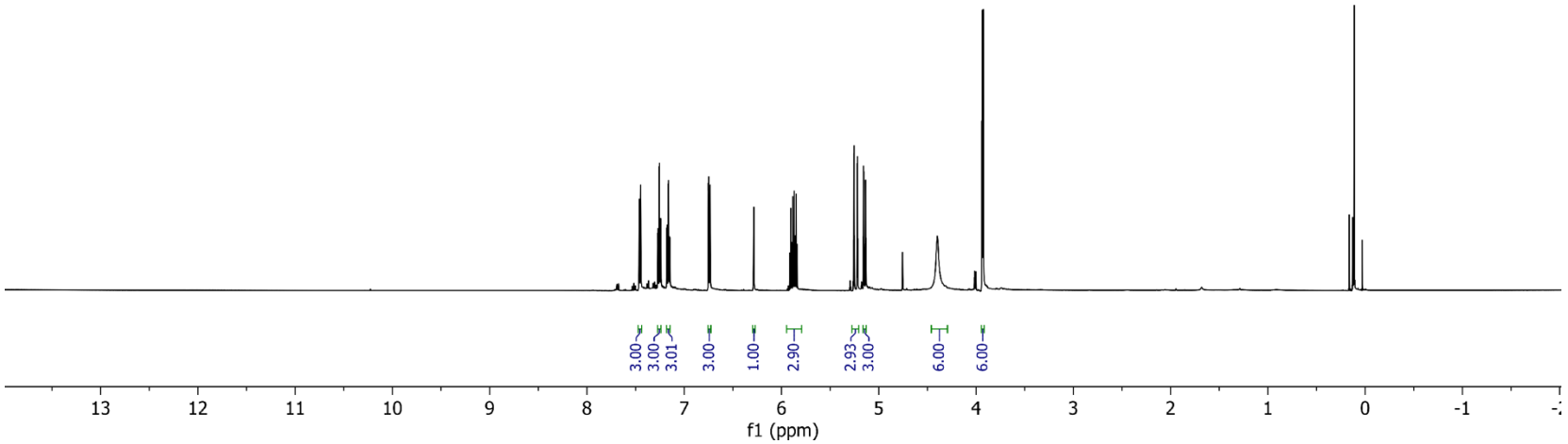
3.00
3.00
3.01
3.00
1.00
2.90
2.93
3.00
6.00
6.00
13
12
11
10
9
8
7
6
5
4
3
2
1
0
-1
f1 (ppm)

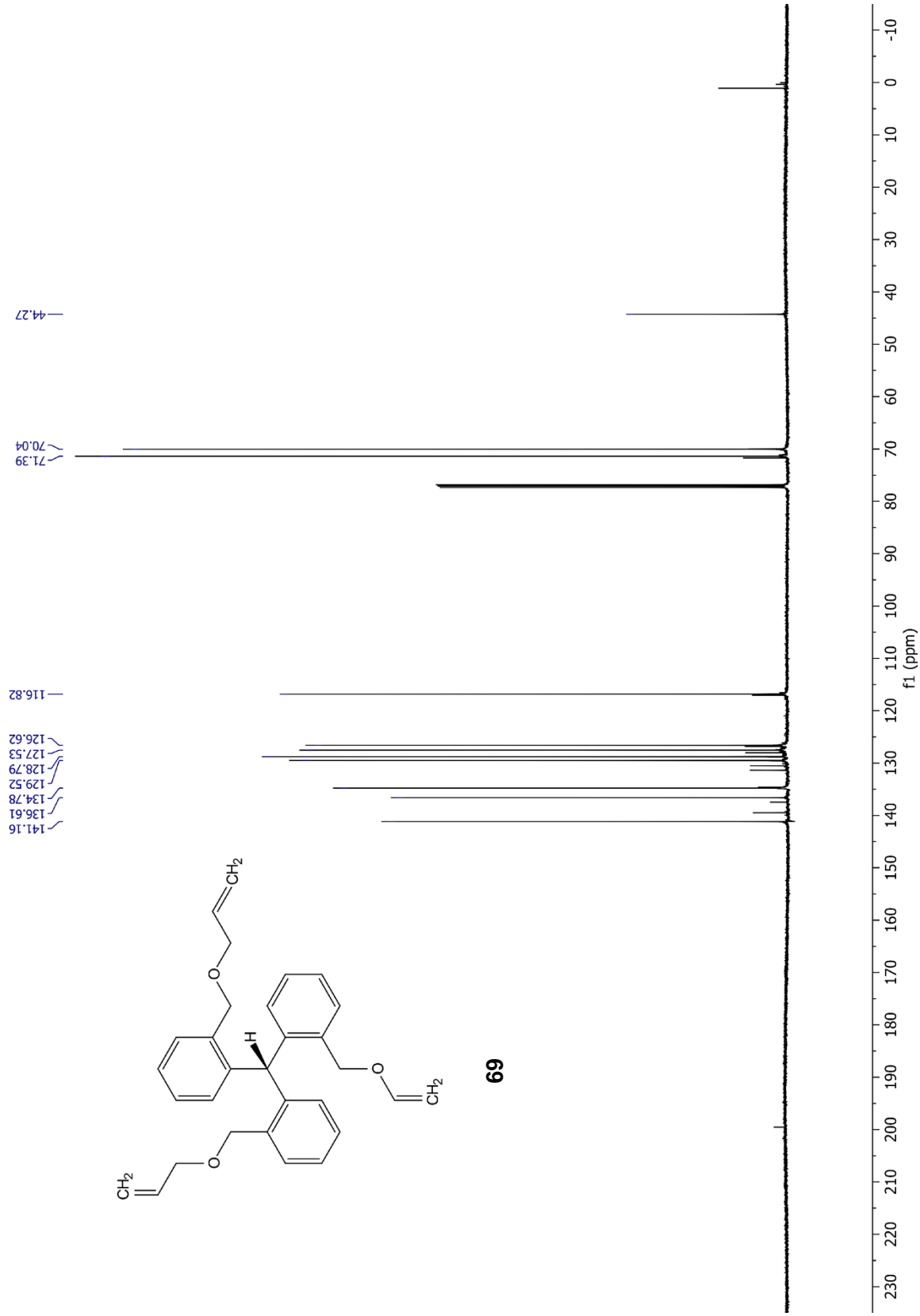
141.16
136.61
134.78
129.52
128.79
127.53
126.62
116.82
71.39
70.04
44.27
f1 (ppm)
69

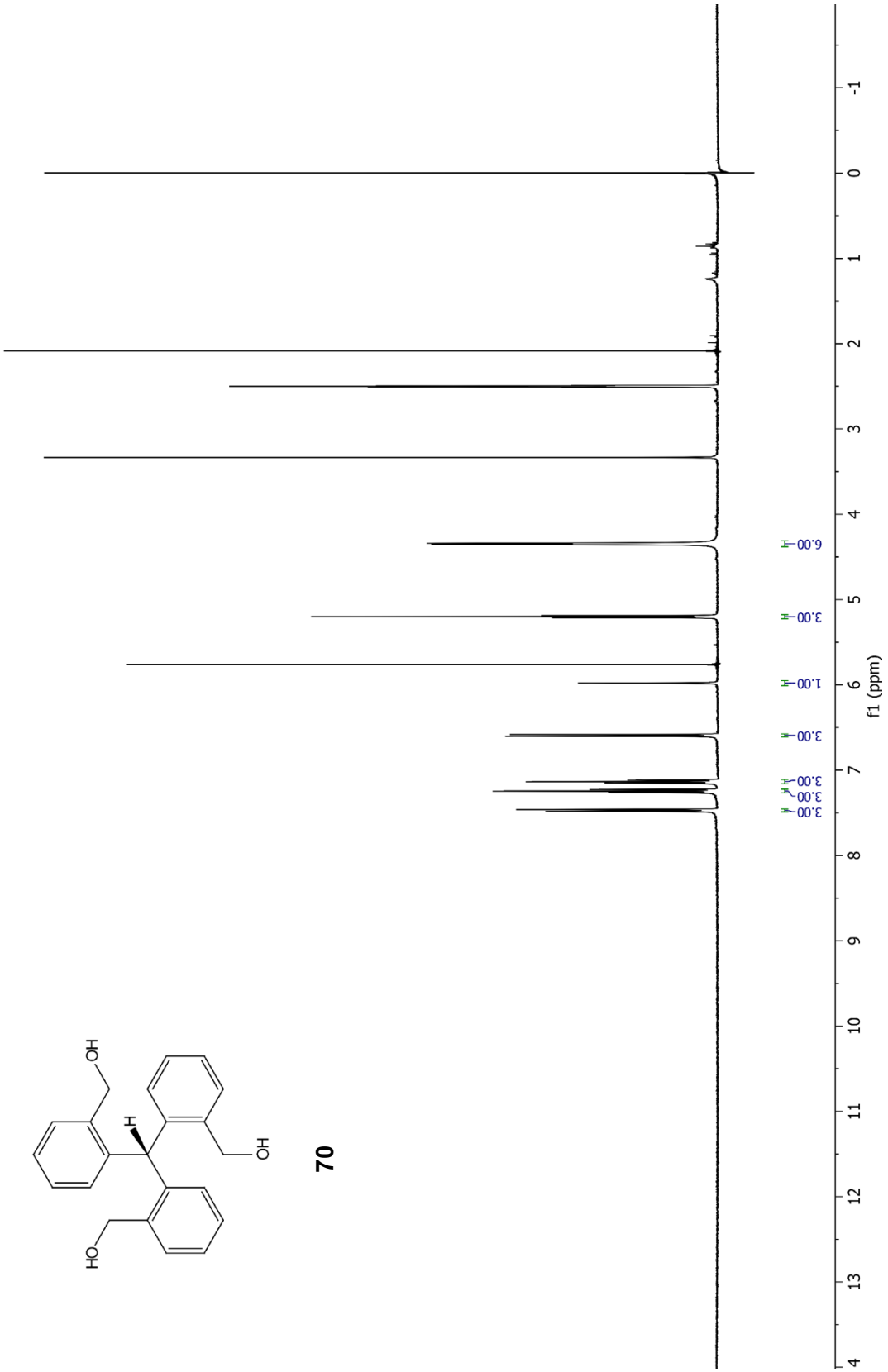
OH
H
OH
HO
70
6.00
3.00
1.00
3.00
3.00
3.00
f1 (ppm)

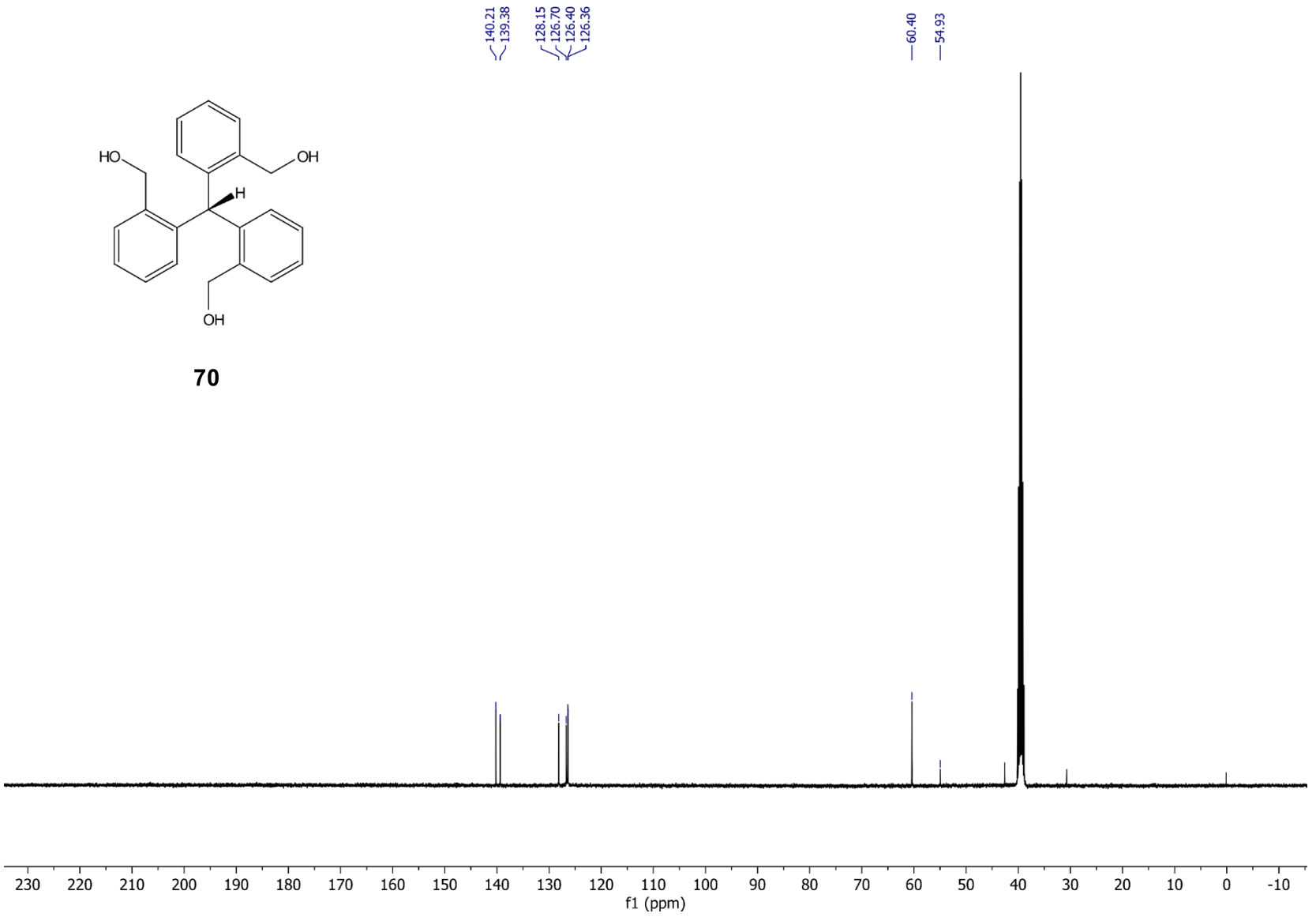
140.21
139.38
128.15
126.70
126.40
126.36
60.40
54.93
HO
OH
H
OH
230 220 210 200 190 180 170 160 150 140 130 120 110 100 90 80 70 60 50 40 30 20 10 0 -10
f1 (ppm)

70

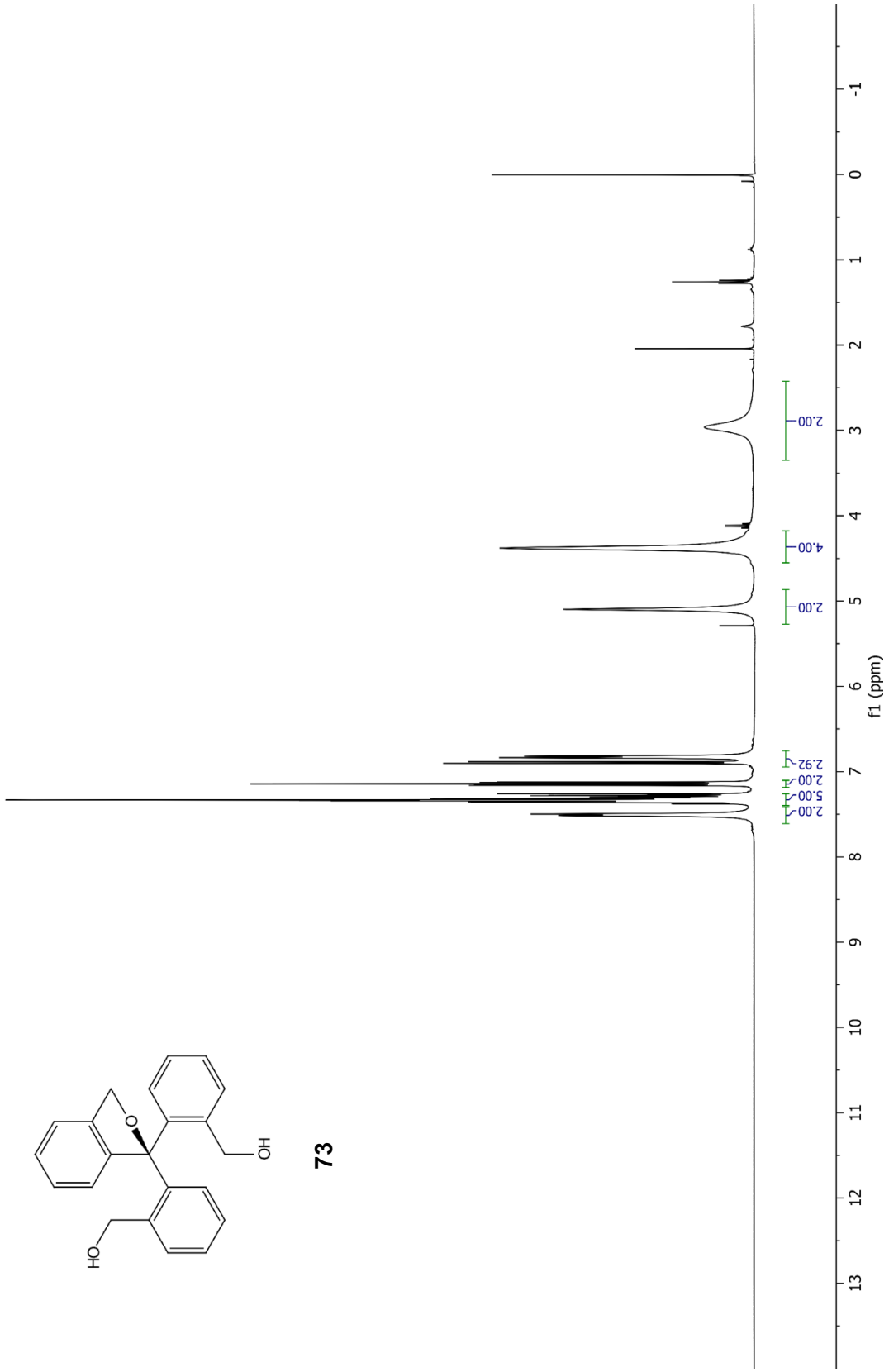
HO
O
OH
73
2.00
4.00
2.00
2.92
2.00
5.00
2.00
f1 (ppm)

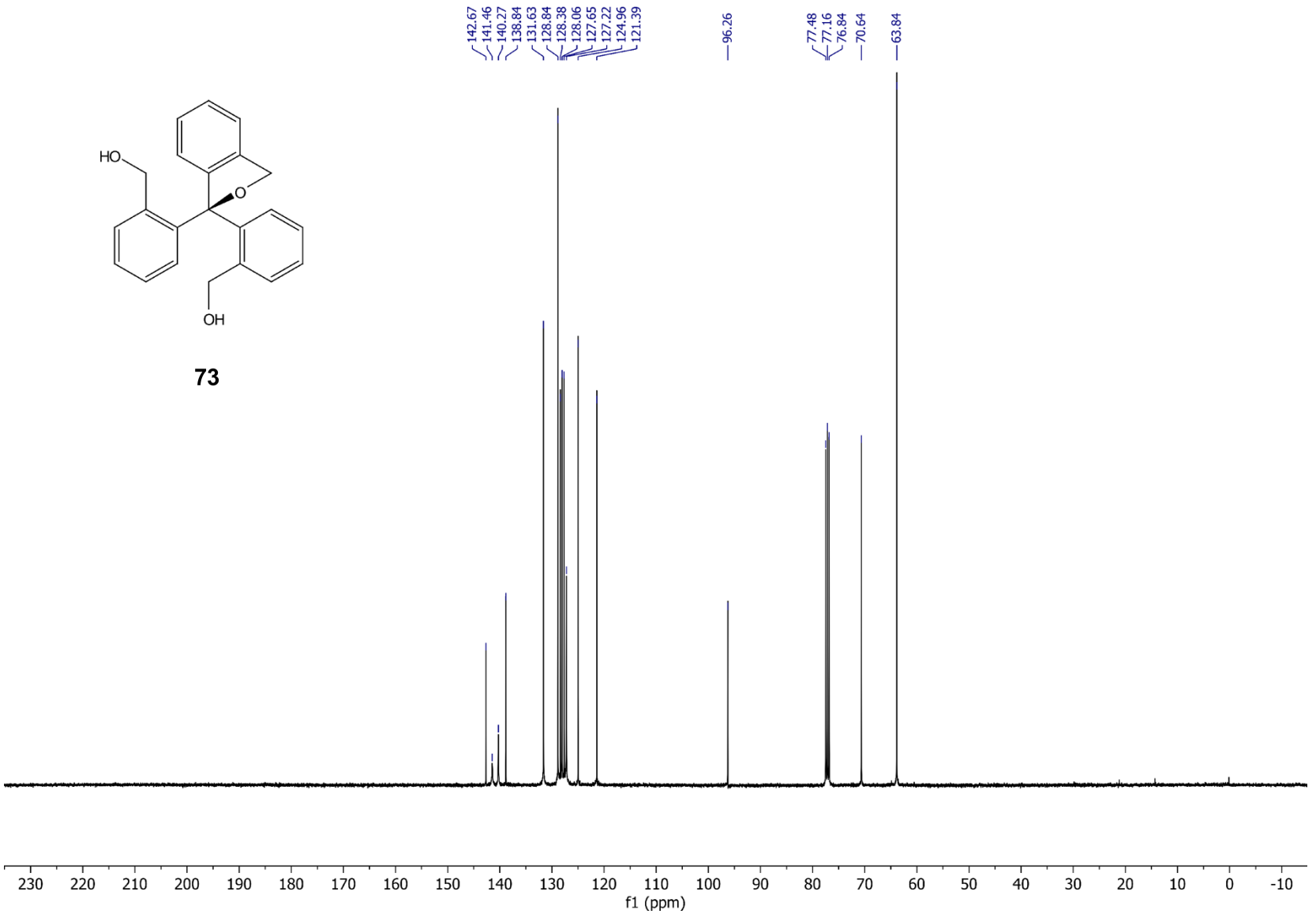
142.67
141.46
140.27
138.84
131.63
128.84
128.38
128.06
127.65
127.22
124.96
121.39
96.26
77.48
77.16
76.84
70.64
63.84
HO
O
OH
73
230 220 210 200 190 180 170 160 150 140 130 120 110 100 90 80 70 60 50 40 30 20 10 0 -10
f1 (ppm)

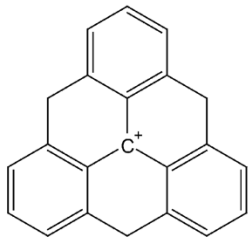

74

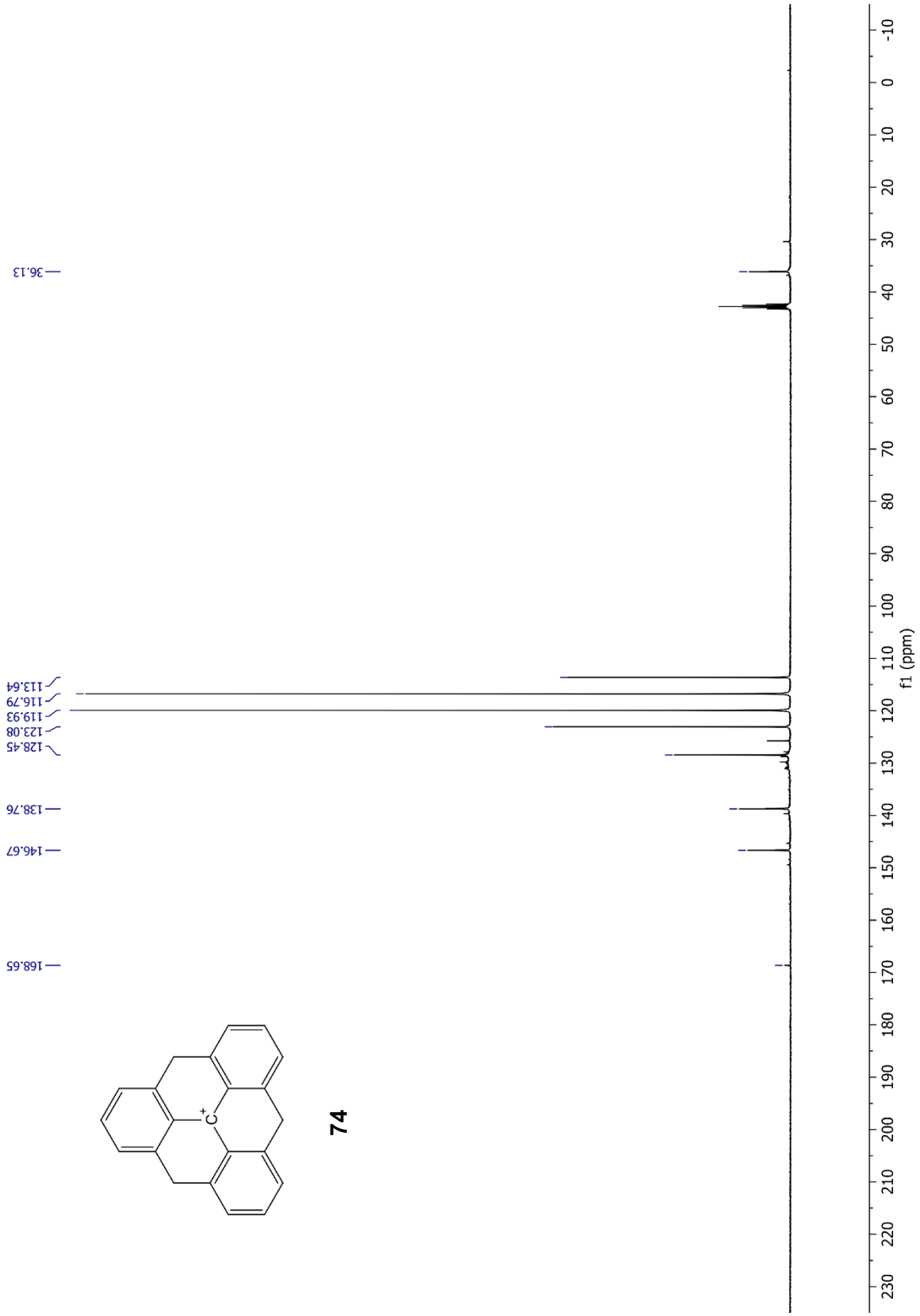

74

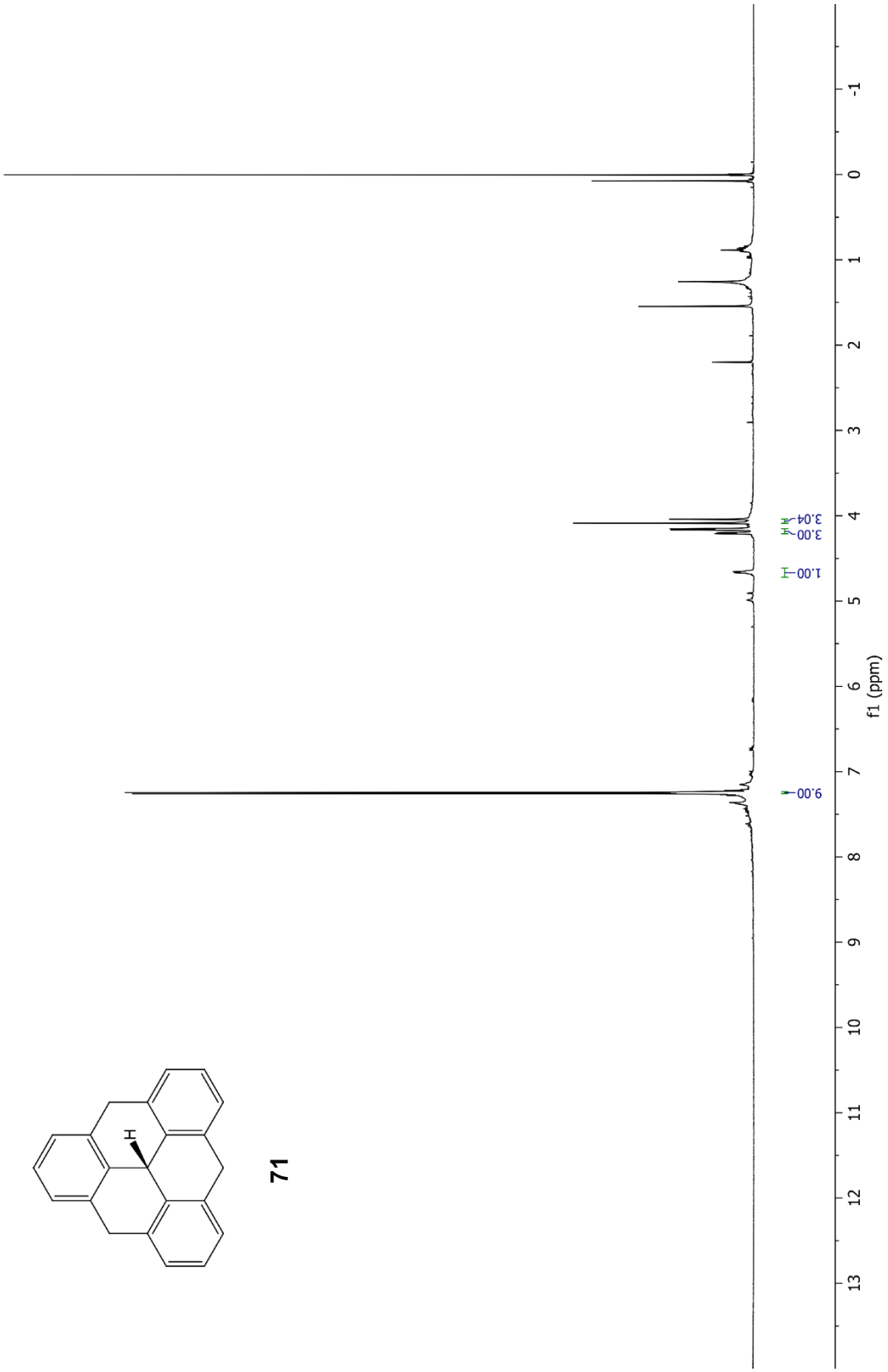

71

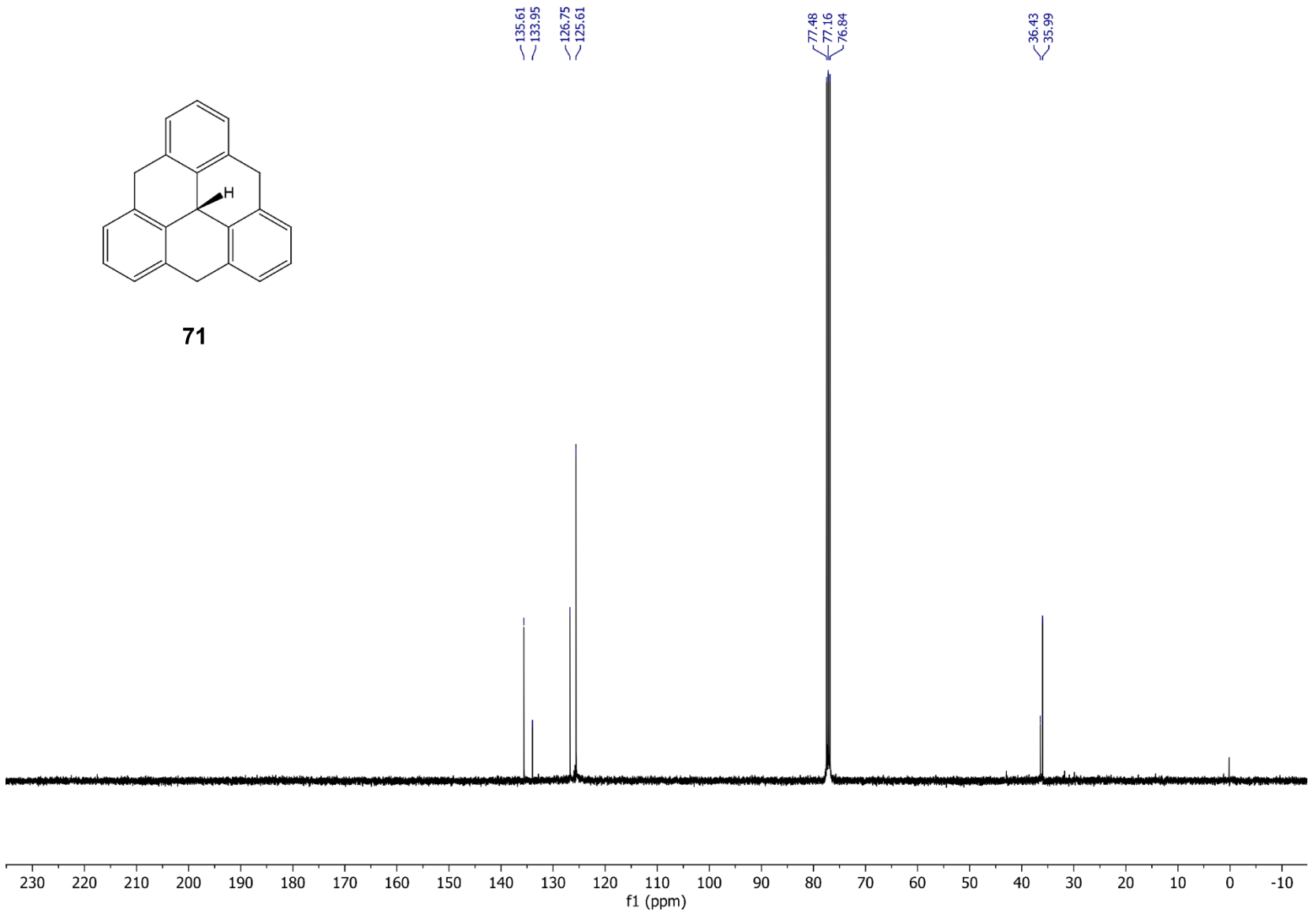
135.61
133.95
126.75
125.61
77.48
77.16
76.84
36.43
35.99
H
71
230 220 210 200 190 180 170 160 150 140 130 120 110 100 90 80 70 60 50 40 30 20 10 0 -10
f1 (ppm)

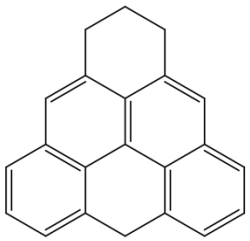

76

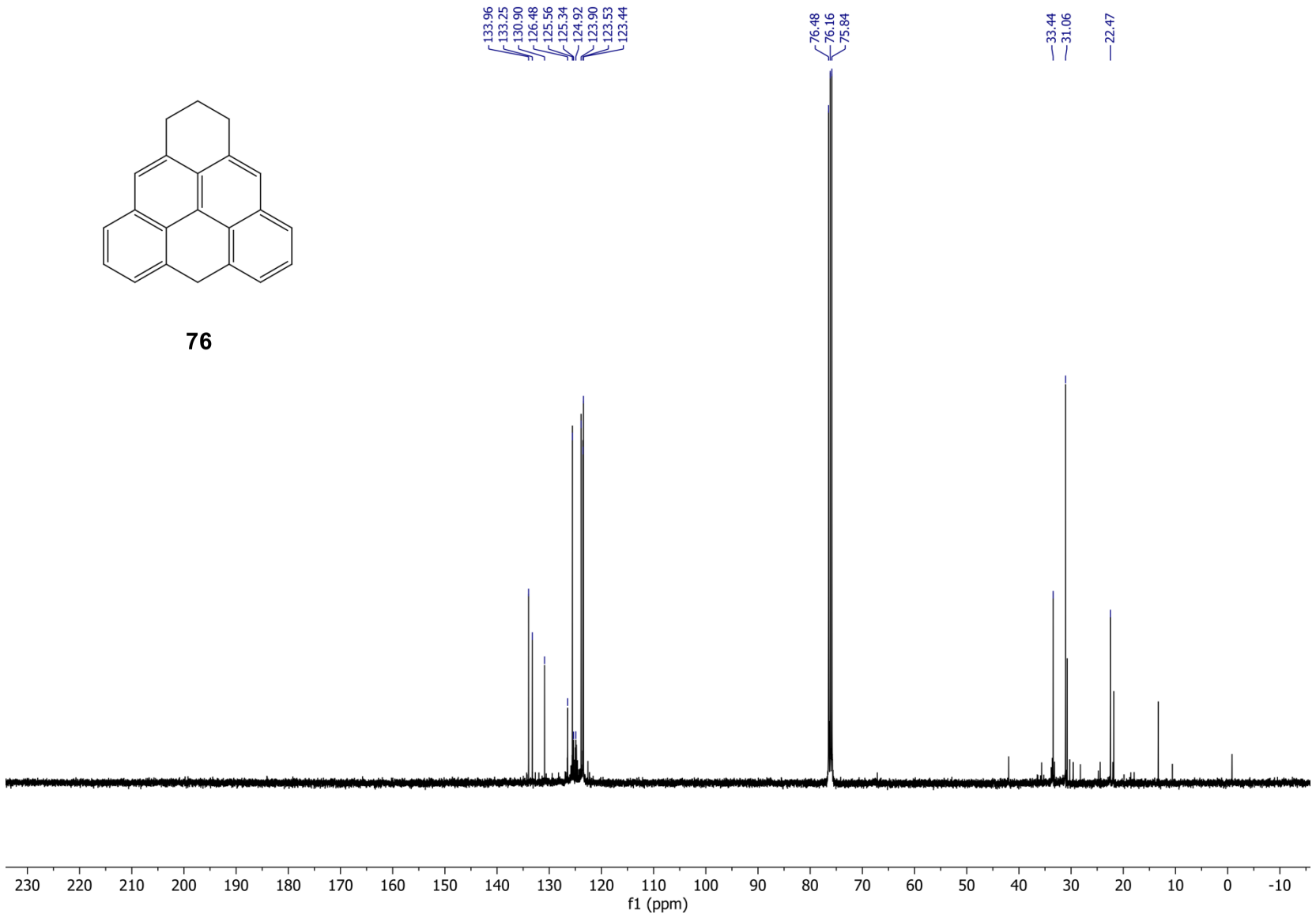
133.96
133.25
130.90
126.48
125.56
125.34
124.92
123.90
123.53
123.44
76.48
76.16
75.84
33.44
31.06
22.47
230 220 210 200 190 180 170 160 150 140 130 120 110 100 90 80 70 60 50 40 30 20 10 0 -10
f1 (ppm)

76

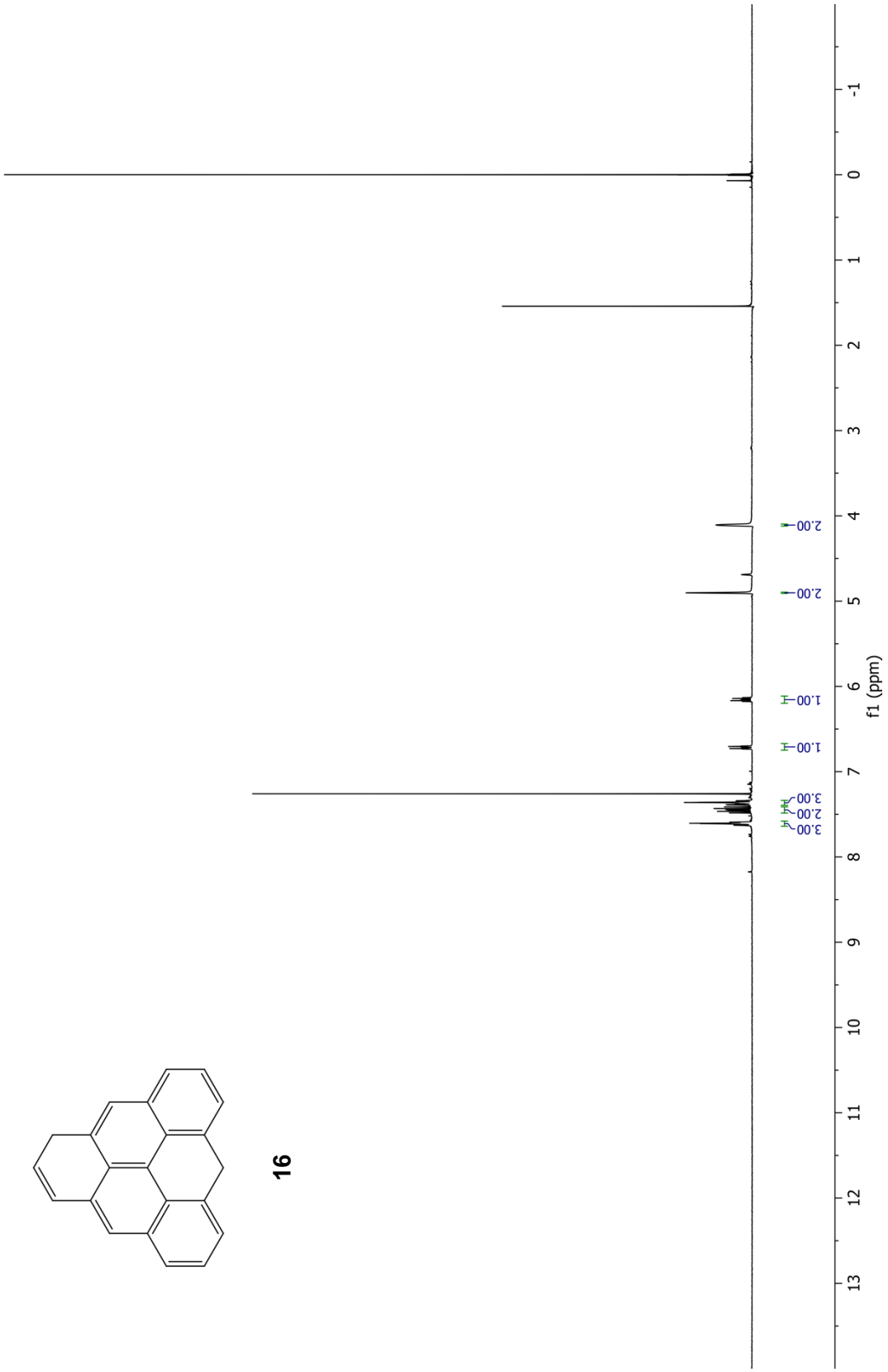

16

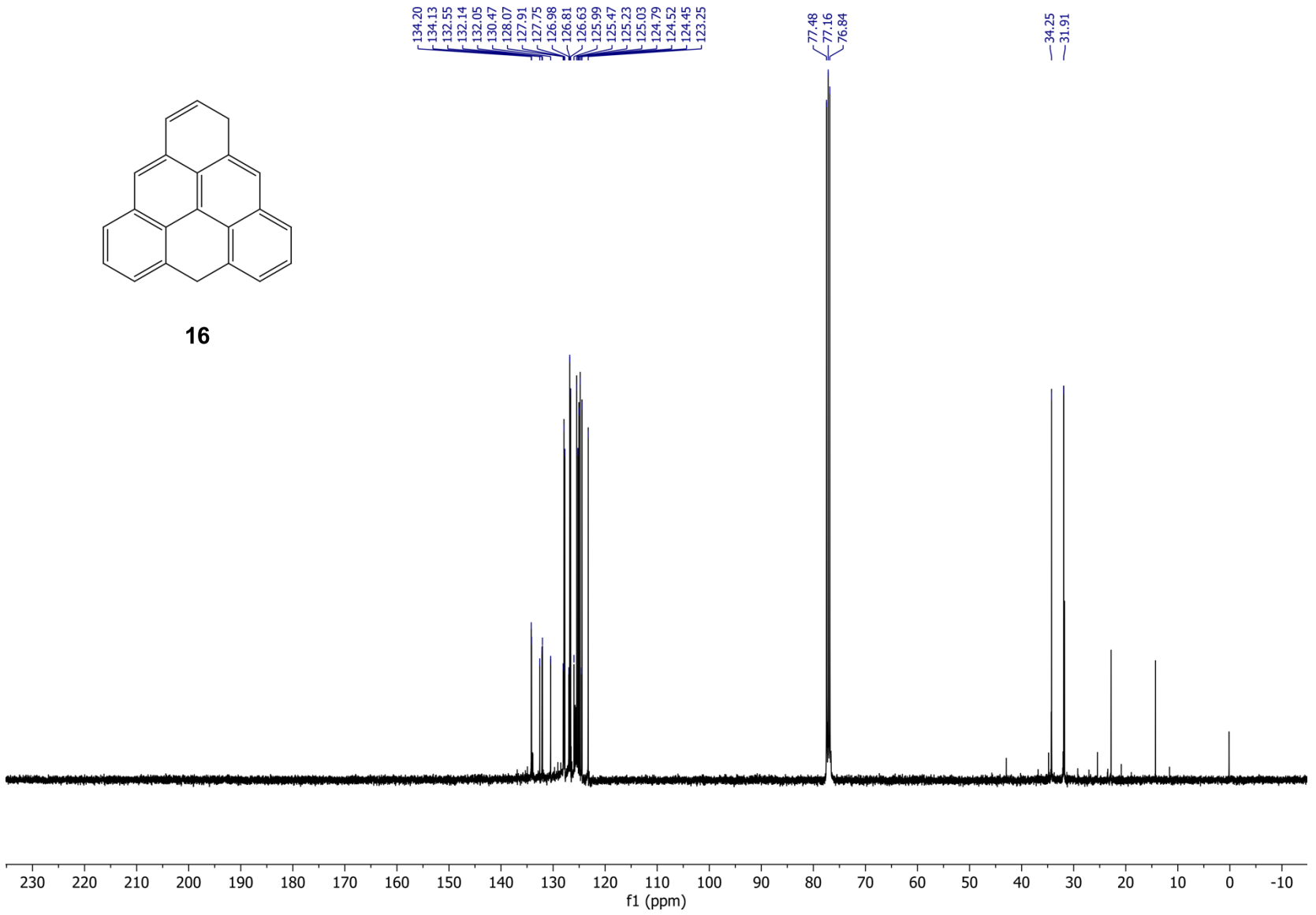
134.20
134.13
132.55
132.14
132.05
130.47
128.07
127.91
127.75
126.98
126.81
126.63
125.99
125.47
125.23
125.03
124.79
124.52
124.45
123.25
77.48
77.16
76.84
34.25
31.91
16
230 220 210 200 190 180 170 160 150 140 130 120 110 100 90 80 70 60 50 40 30 20 10 0 -10
f1 (ppm)

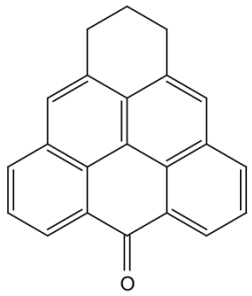

10

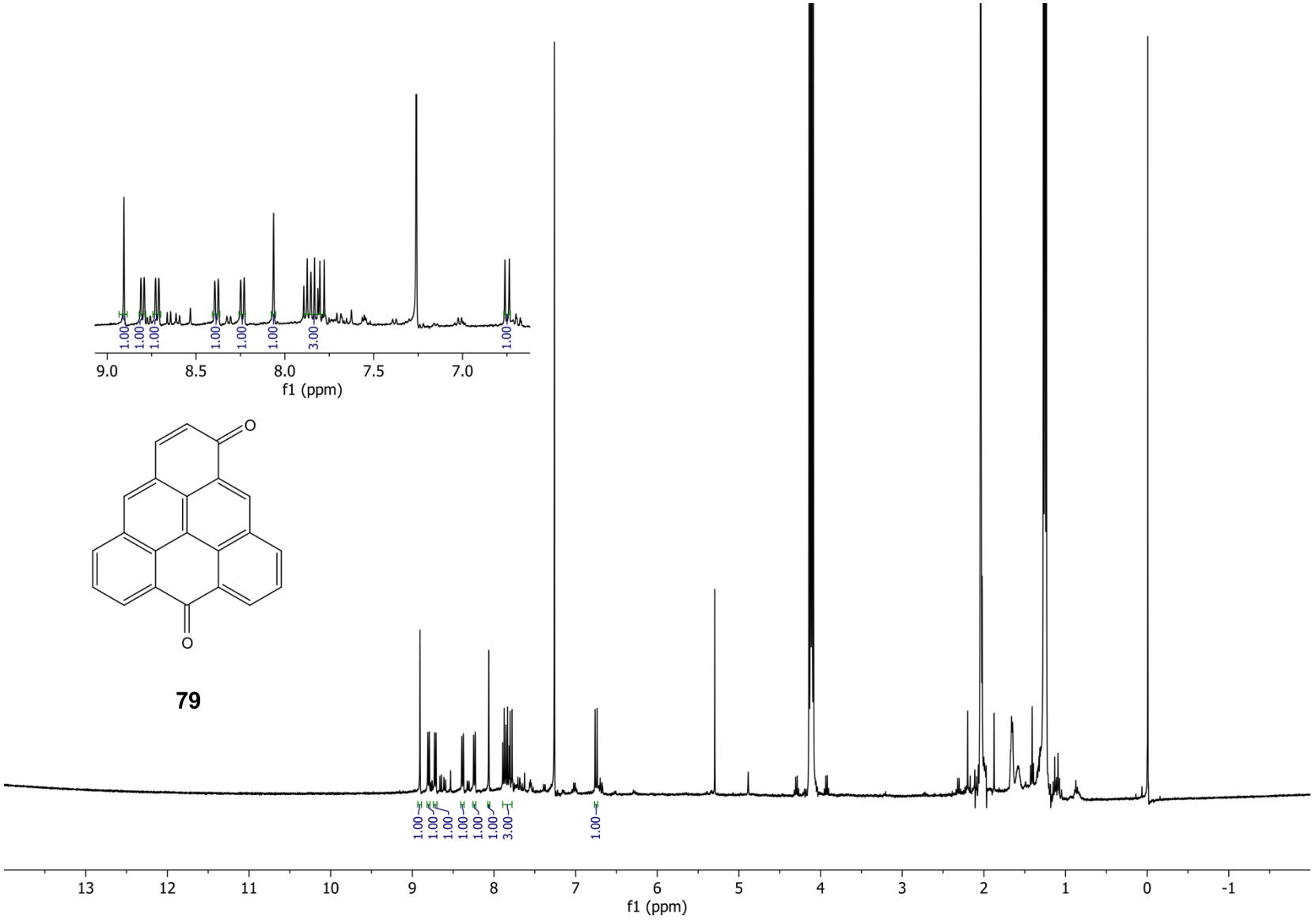
1.00
1.00
1.00
1.00
1.00
1.00
3.00
1.00
9.0
8.5
8.0
7.5
7.0
f1 (ppm)
O
O
79
1.00
1.00
1.00
1.00
1.00
3.00
1.00
13
12
11
10
9
8
7
6
5
4
3
2
1
0
-1
f1 (ppm)

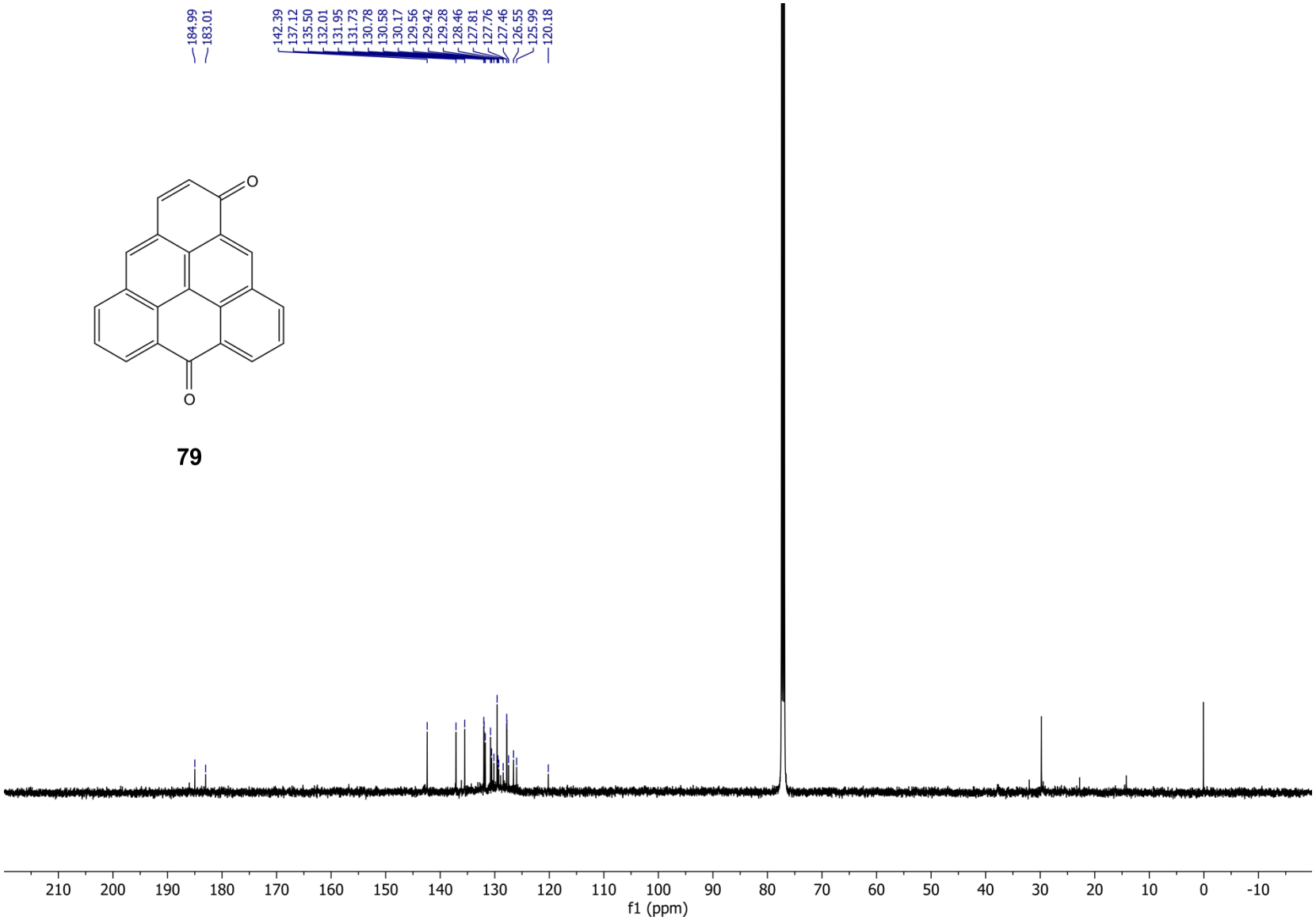
184.99
183.01
142.39
137.12
135.50
132.01
131.95
131.73
130.78
130.58
130.17
129.56
129.42
129.28
128.46
127.81
127.76
127.46
126.55
125.99
120.18
O
O
210 200 190 180 170 160 150 140 130 120 110 100 90 80 70 60 50 40 30 20 10 0 -10
f1 (ppm)

79

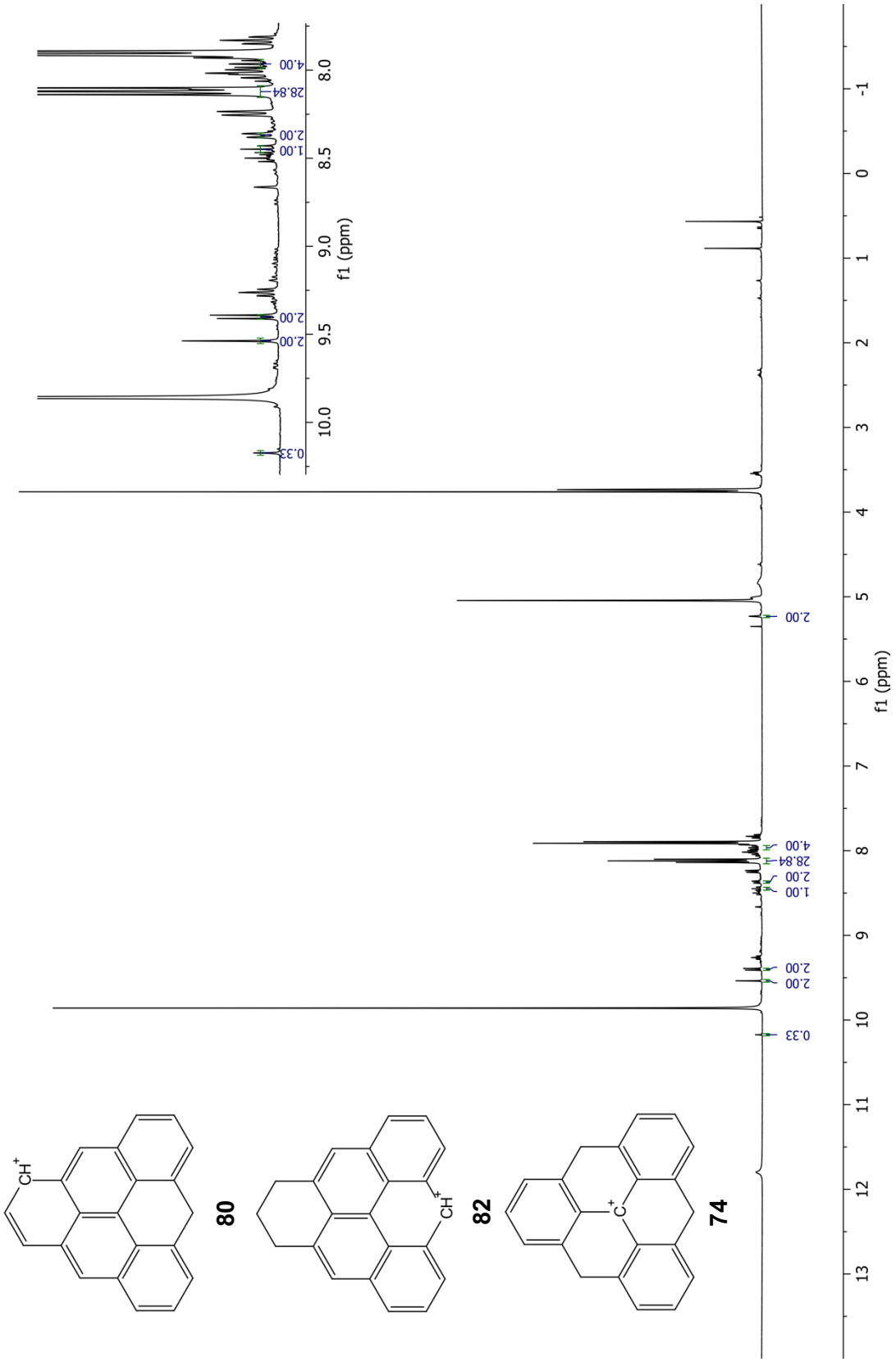
80
82
74
f1 (ppm)

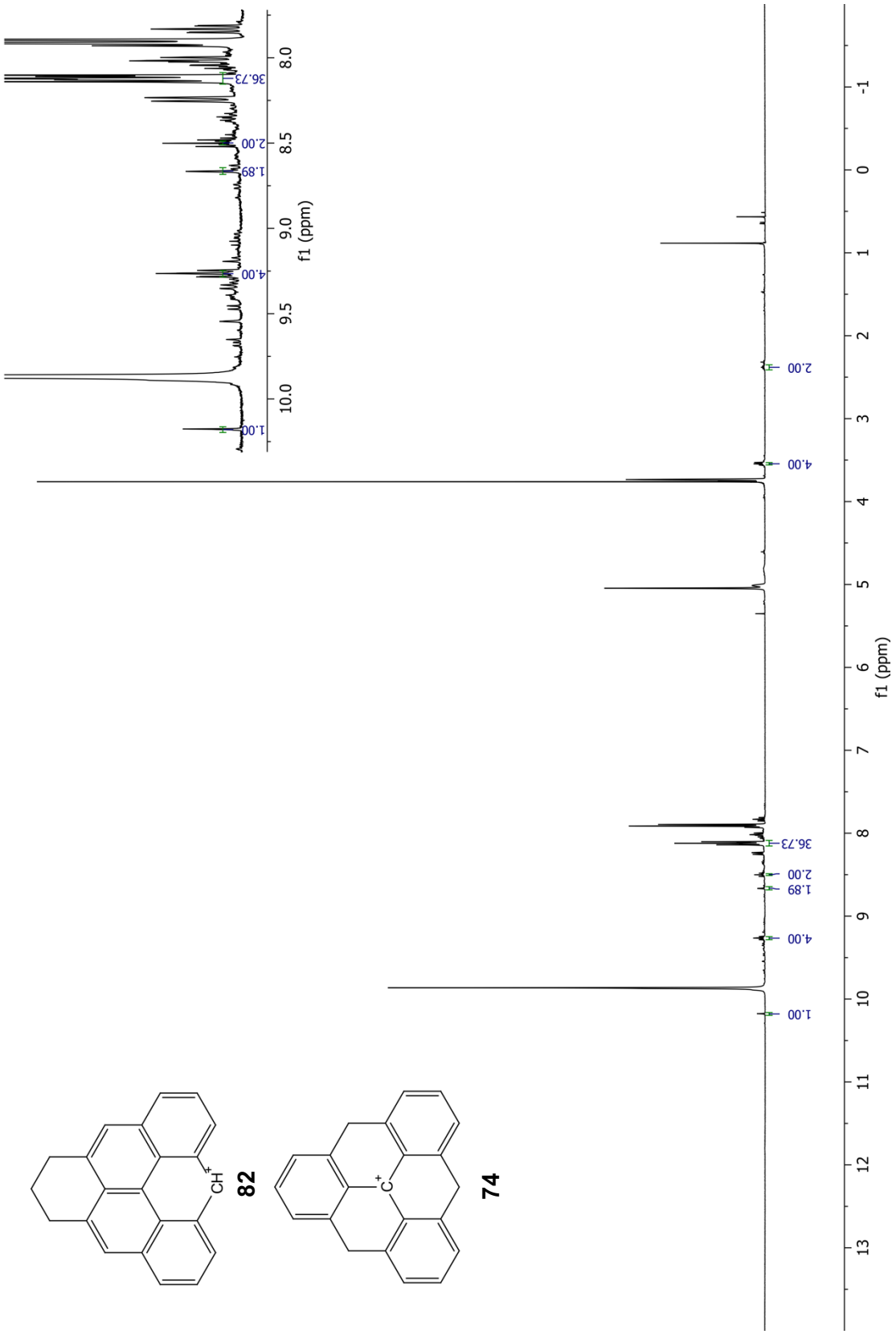
f1 (ppm)
1.00
4.00
2.00
36.73
1.89
2.00
4.00
1.00
f1 (ppm)
1.00
4.00
1.89
2.00
36.73
CH
82
C
74

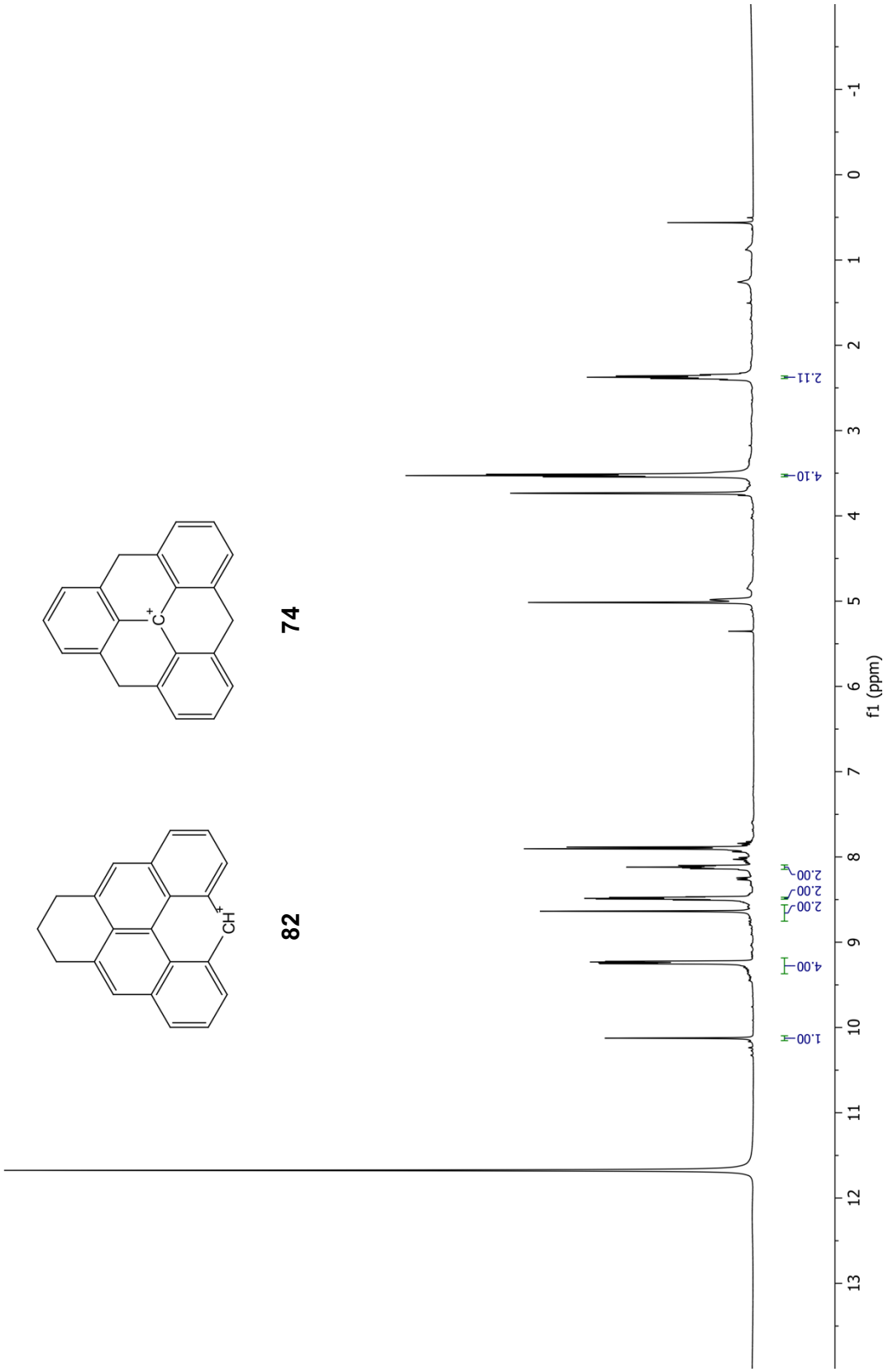
74
82
2.11
4.10
2.00
2.00
2.00
4.00
1.00
f1 (ppm)

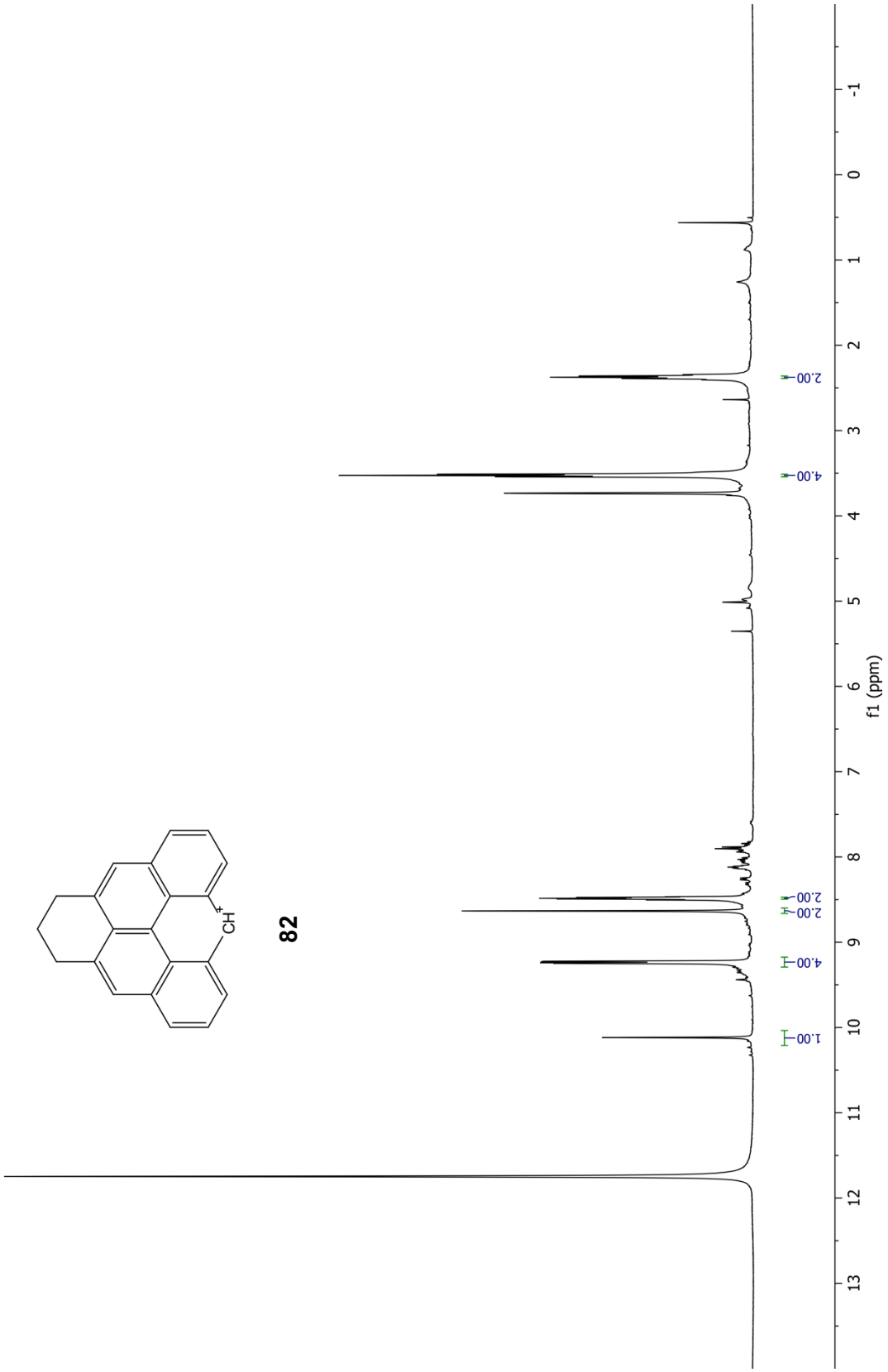
CH+
82
2.00
4.00
2.00
2.00
4.00
1.00
f1 (ppm)

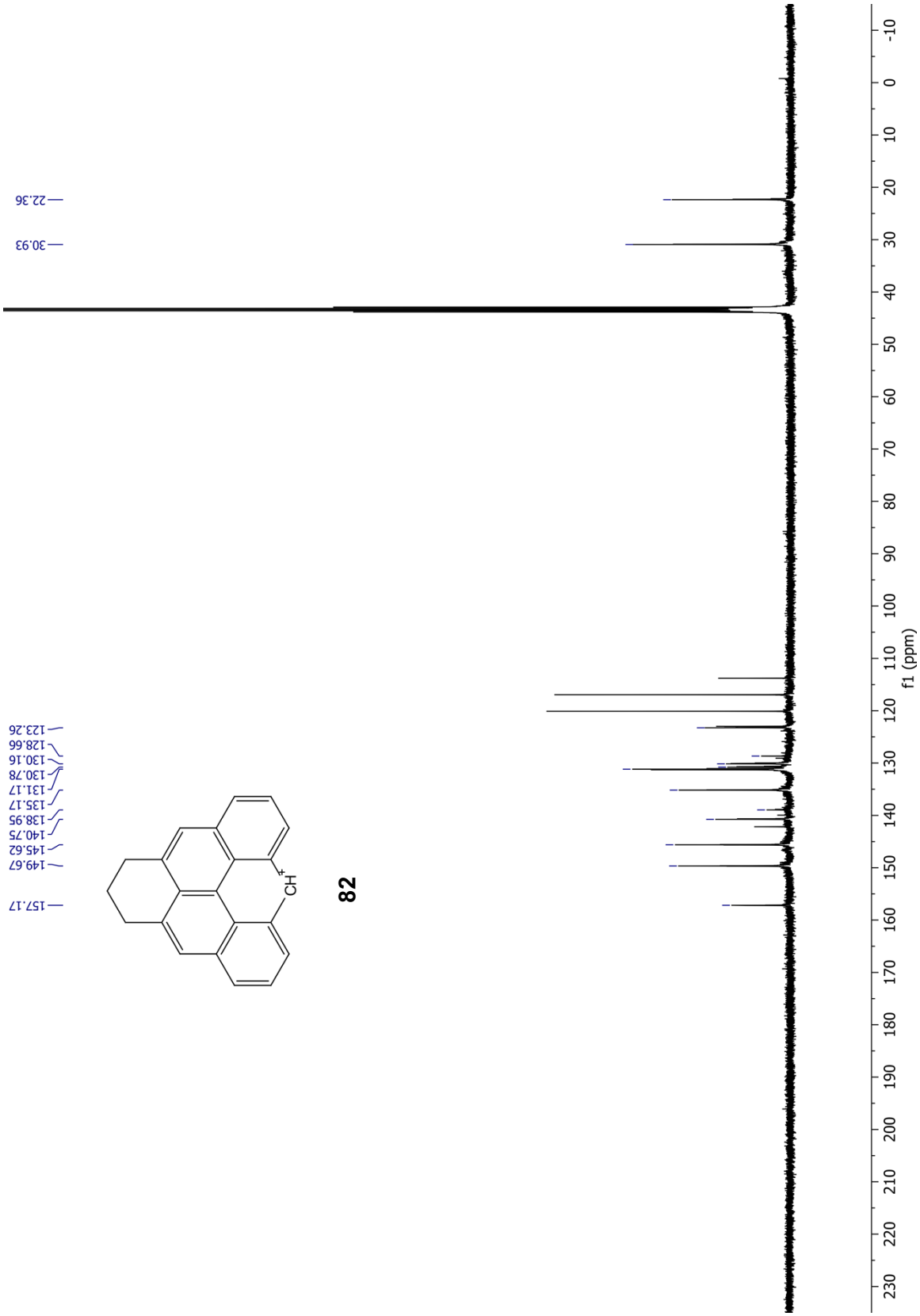
22.36
30.93
123.26
128.66
130.16
130.78
131.17
135.17
138.95
140.75
145.62
149.67
157.17
CH
82
-10
0
10
20
30
40
50
60
70
80
90
100
110
120
130
140
150
160
170
180
190
200
210
220
230
f1 (ppm)

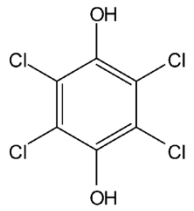

83

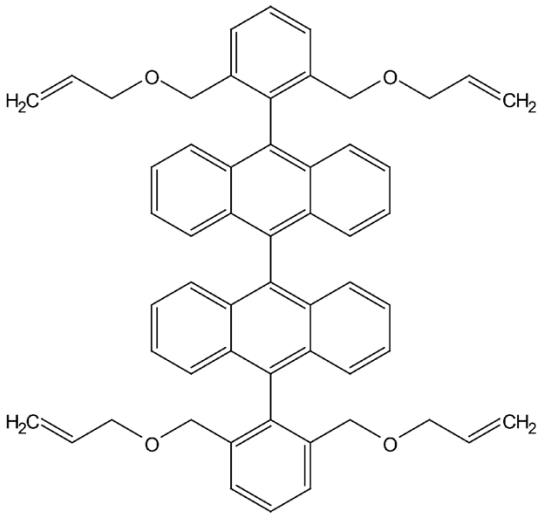
H2C
O
O
CH2
H2C
O
O
CH2

88

4.00
2.00
4.00
4.00
8.00
4.00
8.00
8.00
8.00
4
13
12
11
10
9
8
7
6
5
4
3
2
1
0
-1
f1 (ppm)

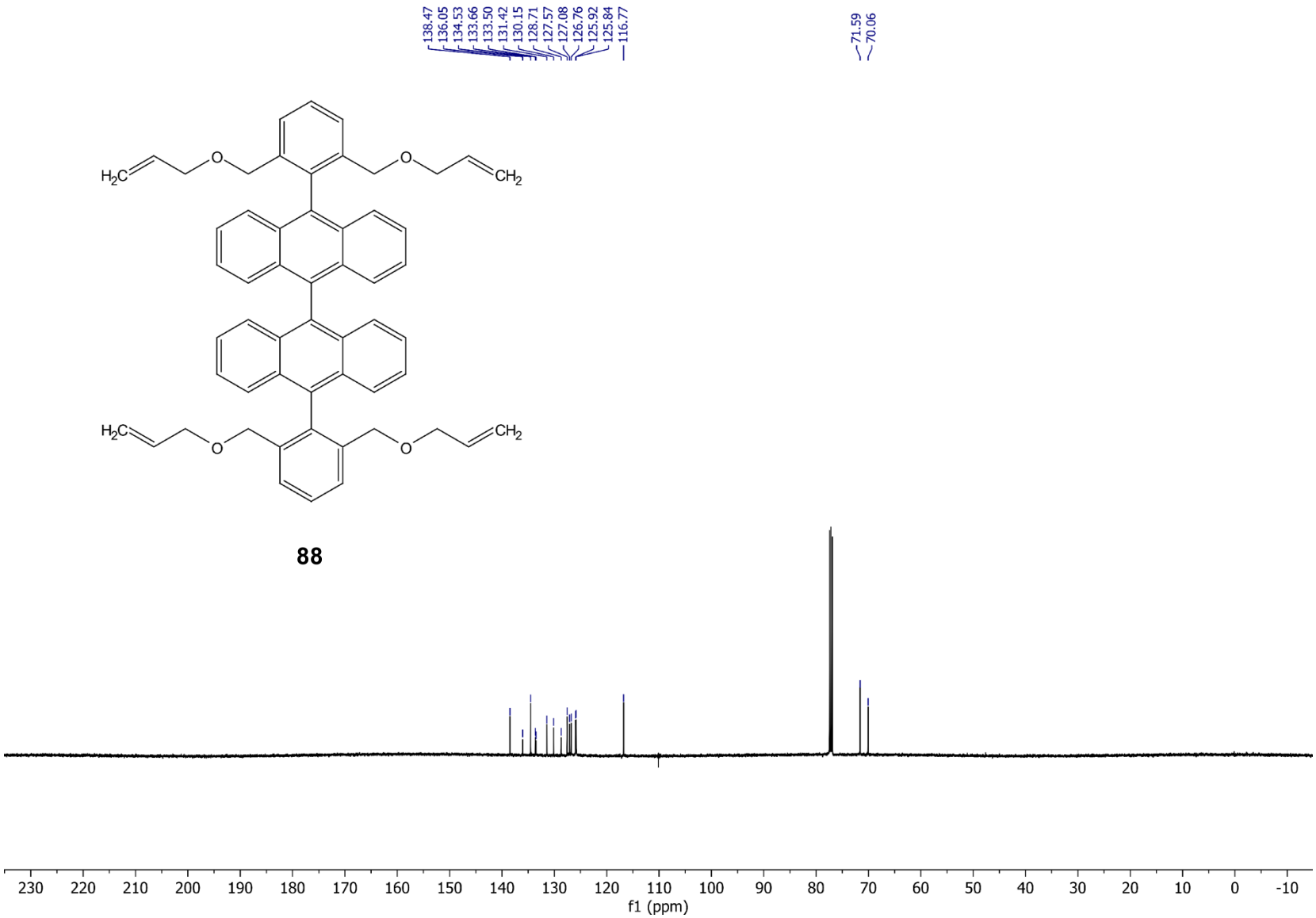
138.47
136.05
134.53
133.66
133.50
131.42
130.15
128.71
127.57
127.08
126.76
125.92
125.84
116.77
71.59
70.06
H2C
O
O
CH2
H2C
O
O
CH2
230
220
210
200
190
180
170
160
150
140
130
120
110
100
90
80
70
60
50
40
30
20
10
0
-10
f1 (ppm)

88

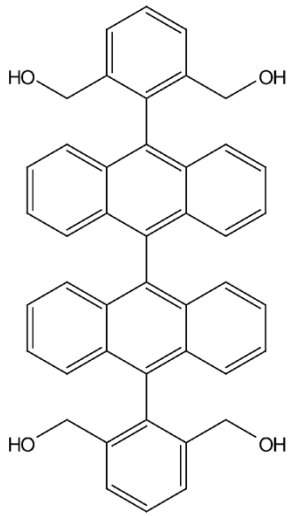
HO
OH
HO
OH

89

4.00
2.00
4.00
4.01
8.00
8.00
4.00
14
13
12
11
10
9
8
7
6
5
4
3
2
1
0
-1
f1 (ppm)

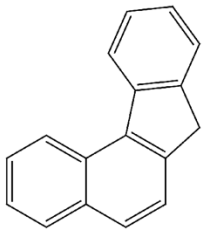

106

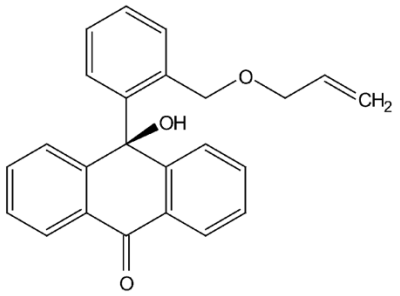
O
CH2
OH
O

114

2.00
1.00
2.00
4.00
1.00
2.00
1.00
2.00
2.00
1.00
2.00
16
15
14
13
12
11
10
9
8
7
6
5
4
3
2
1
0
-1
-2
-3
f1 (ppm)

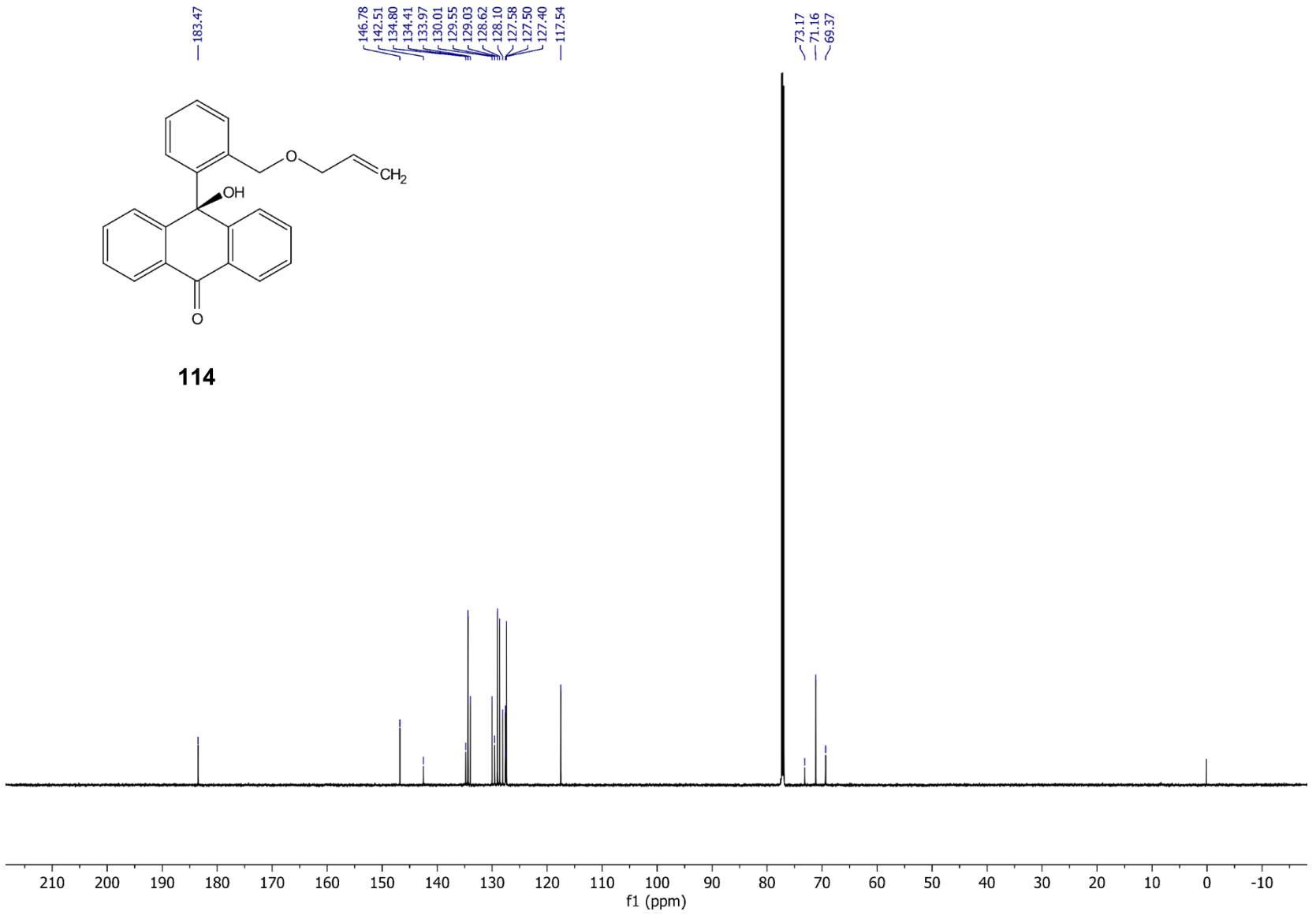
183.47
146.78
142.51
134.80
134.41
133.97
130.01
129.55
129.03
128.62
128.10
127.58
127.50
127.40
117.54
73.17
71.16
69.37
O
CH2
OH
O
210
200
190
180
170
160
150
140
130
120
110
100
90
80
70
60
50
40
30
20
10
0
-10
f1 (ppm)

114

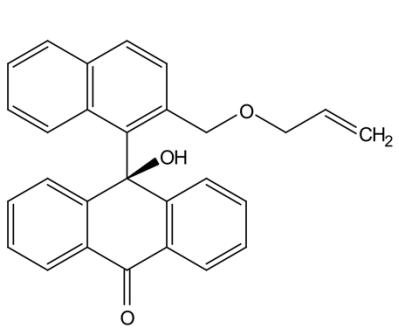
O
CH2
OH
O

115

2.00
1.00
1.00
1.00
2.00
2.00
2.00
2.00
1.00
2.00
4.00
2.00
16
15
14
13
12
11
10
9
8
7
6
5
4
3
2
1
0
-1
-2
-3
f1 (ppm)

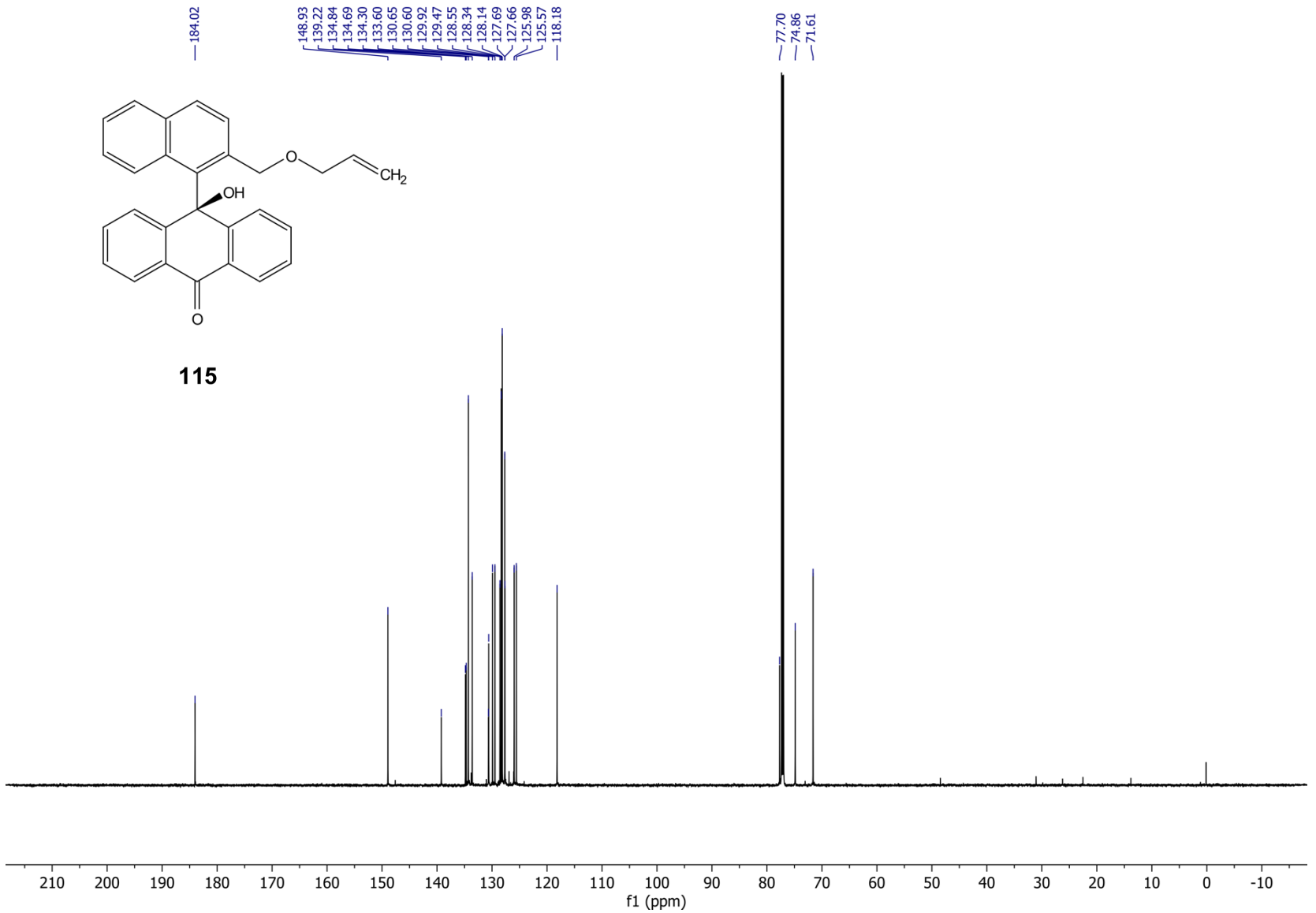
184.02
148.93
139.22
134.84
134.69
134.30
133.60
130.65
130.60
129.92
129.47
128.55
128.34
128.14
127.69
127.66
125.98
125.57
118.18
77.70
74.86
71.61
OH
O
CH2
O
210
200
190
180
170
160
150
140
130
120
110
100
90
80
70
60
50
40
30
20
10
0
-10
f1 (ppm)

115

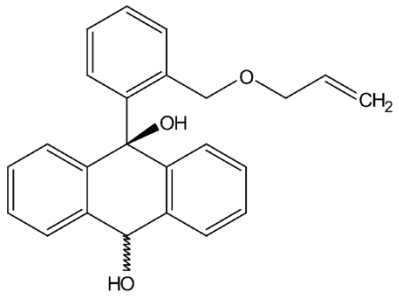
O
CH2
OH
HO

116

1.00
2.00
1.00
3.01
1.06
2.00
2.00
1.00
1.00
2.00
3.00
2.00
1.00
16
15
14
13
12
11
10
9
8
7
6
5
4
3
2
1
0
-1
-2
-3
f1 (ppm)

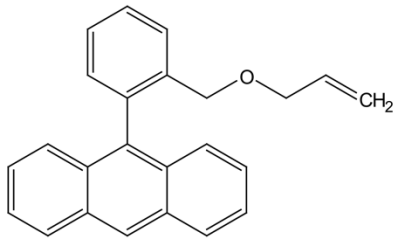
O
CH2

118

1.00
2.00
1.00
1.00
5.01
3.00
0.92
2.00
2.00
2.00
13
12
11
10
9
8
7
6
5
4
3
2
1
0
-1
f1 (ppm)

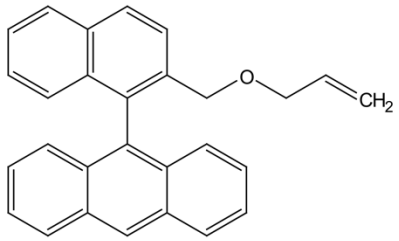
O
CH2

119

1.00
3.00
2.00
3.00
2.00
2.00
1.00
1.00
0.92
2.00
2.00
2.00
13
12
11
10
9
8
7
6
5
4
3
2
1
0
-1
f1 (ppm)

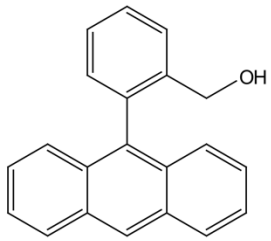
OH

120

1.00
2.00
1.00
1.00
5.00
2.00
1.00
2.00
1.00
13
12
11
10
9
8
7
6
5
4
3
2
1
0
-1
f1 (ppm)

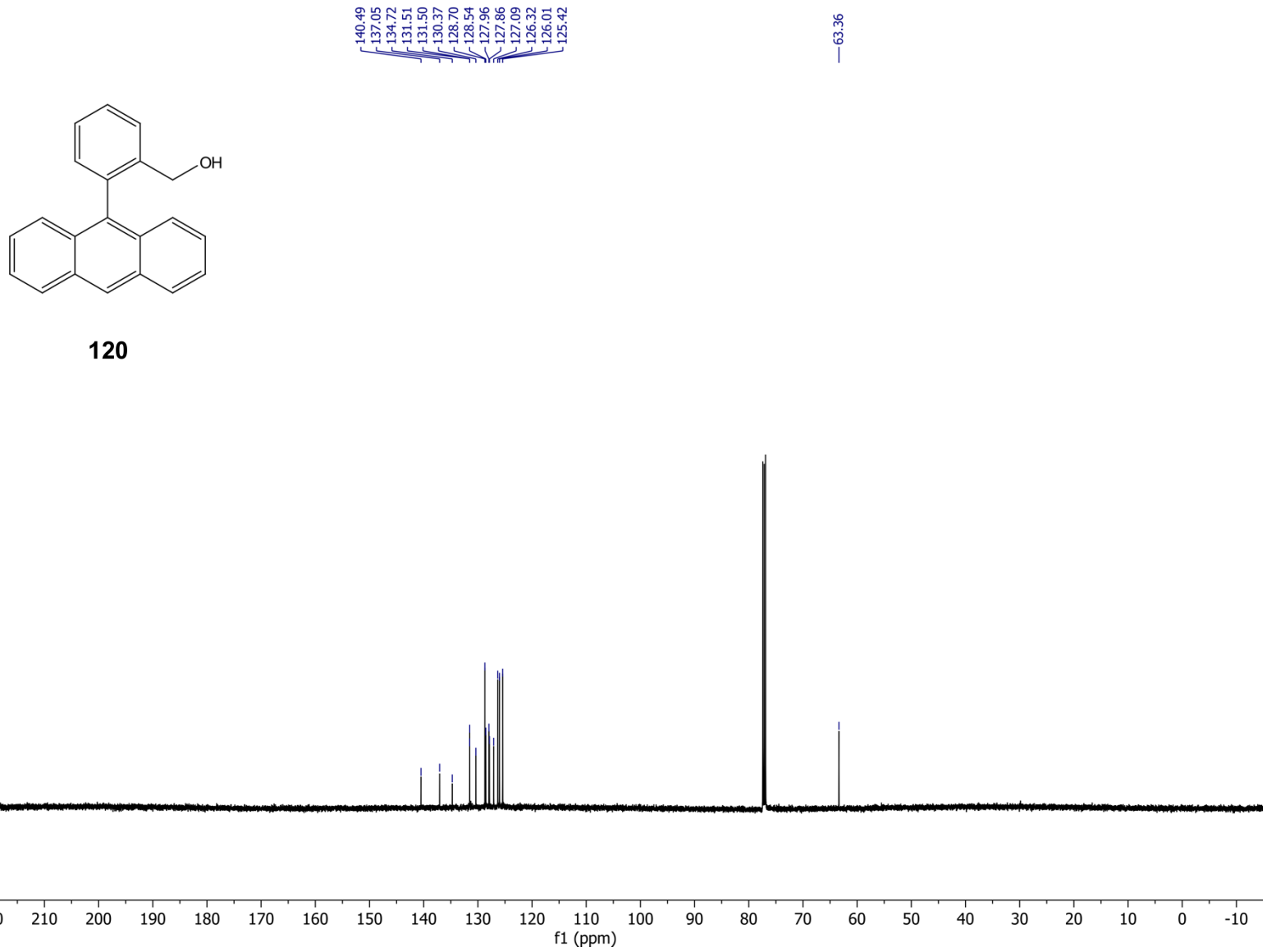
140.49
137.05
134.72
131.51
131.50
130.37
128.70
128.54
127.96
127.86
127.09
126.32
126.01
125.42
63.36
OH
230 220 210 200 190 180 170 160 150 140 130 120 110 100 90 80 70 60 50 40 30 20 10 0 -10
f1 (ppm)

120

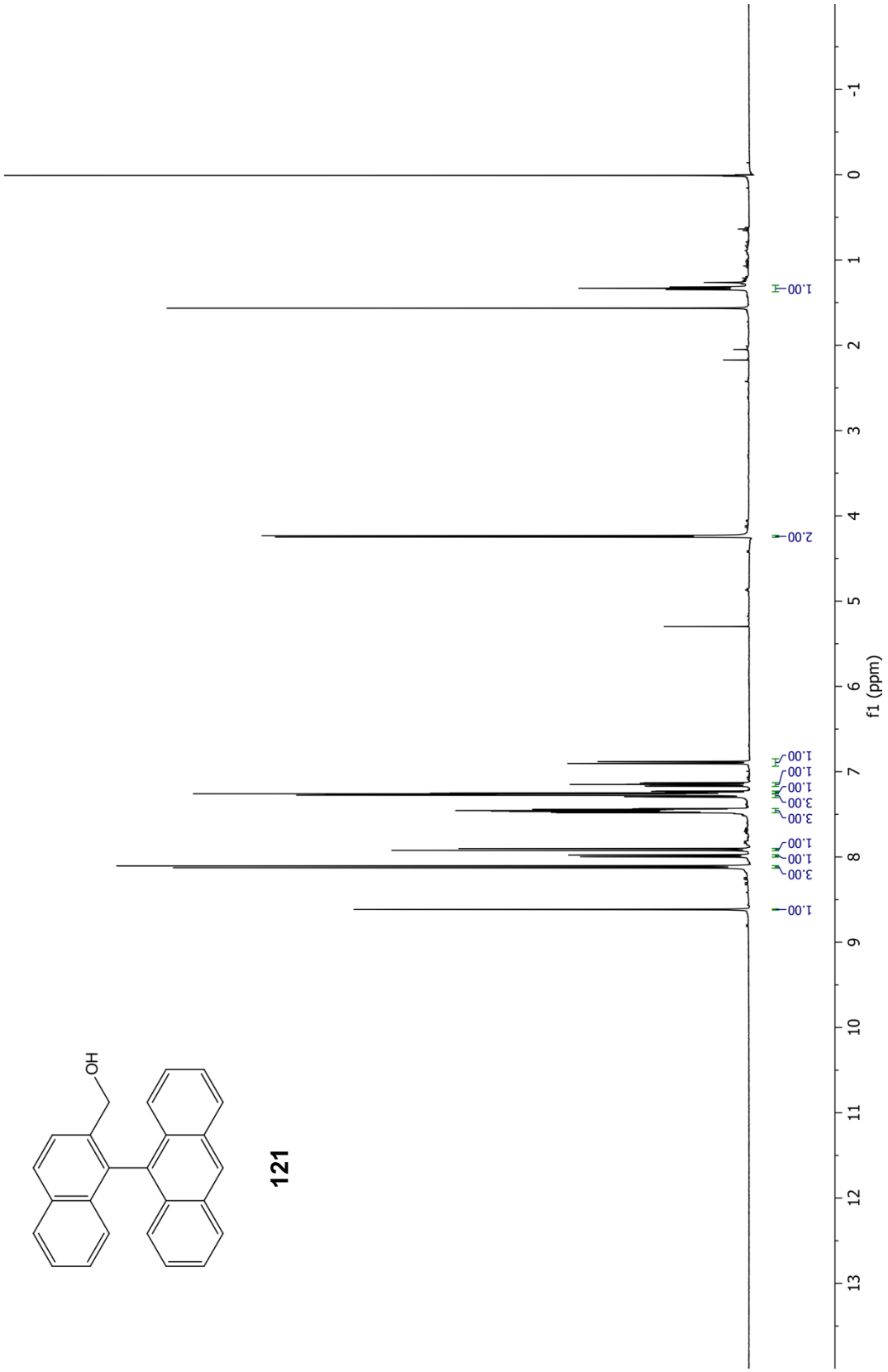
OH
121
1.00
2.00
1.00
3.00
1.00
1.00
1.00
3.00
1.00
3.00
1.00
1.00
f1 (ppm)

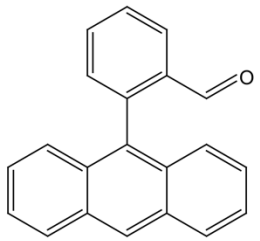

122

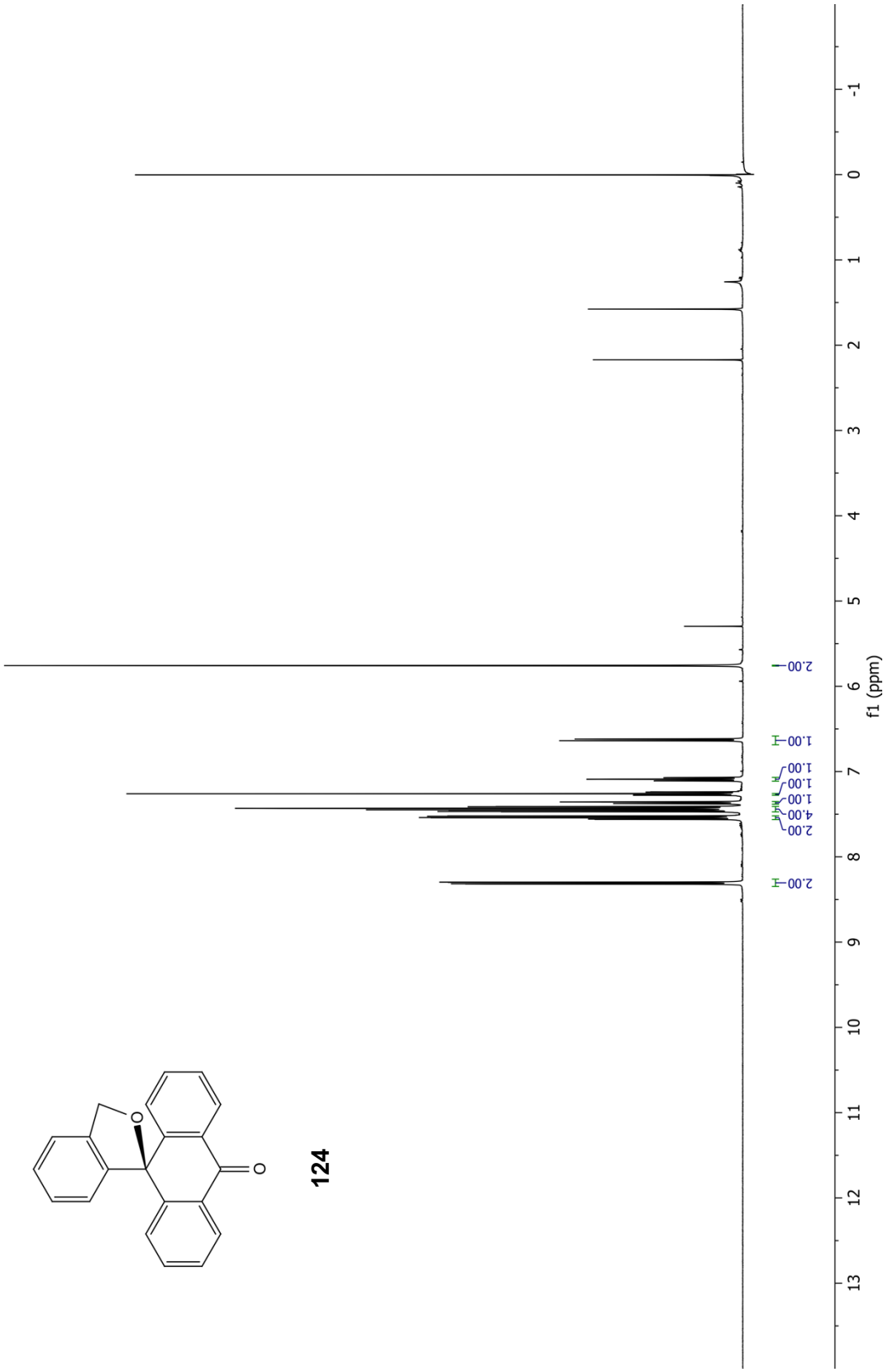

124

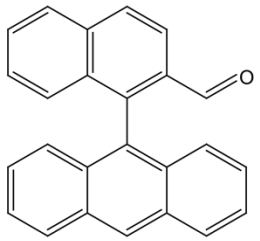
O

123

1.00
1.00
1.00
3.00
1.00
1.00
2.00
2.00
3.00
1.00
16
15
14
13
12
11
10
9
8
7
6
5
4
3
2
1
0
-1
-2
-3
f1 (ppm)

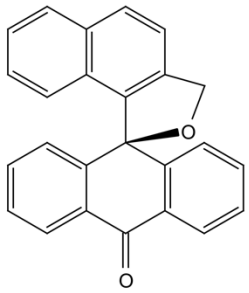

125

2.00
1.00
1.00
1.00
4.00
1.00
3.00
1.00
2.00
16
15
14
13
12
11
10
9
8
7
6
5
4
3
2
1
0
-1
-2
-3
f1 (ppm)

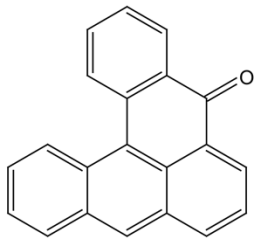
O

126

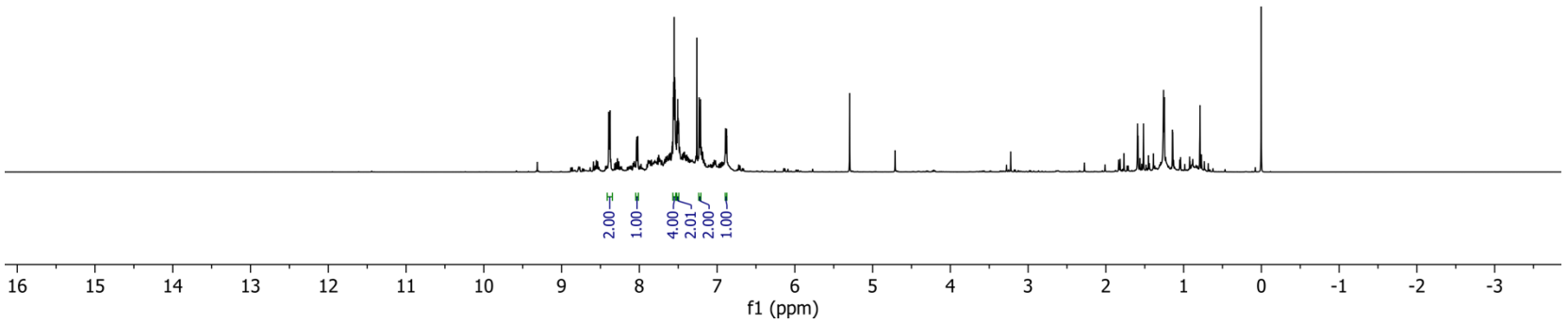
2.00
1.00
4.00
2.01
2.00
1.00
16
15
14
13
12
11
10
9
8
7
6
5
4
3
2
1
0
-1
-2
-3
f1 (ppm)

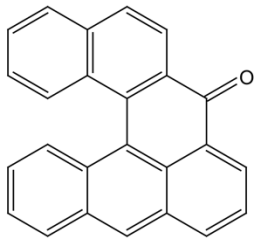
O

127

2.00
2.01
1.00
3.00
2.02
1.00
1.01
2.00
16
15
14
13
12
11
10
9
8
7
6
5
4
3
2
1
0
-1
-2
-3
f1 (ppm)

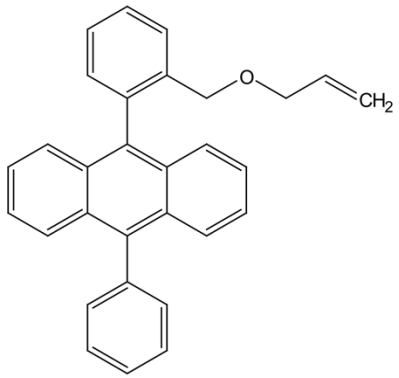
O
CH2

134

1.00
2.00
3.00
3.00
5.00
1.00
2.00
2.00
2.00
16
15
14
13
12
11
10
9
8
7
6
5
4
3
2
1
0
-1
-2
-3
f1 (ppm)

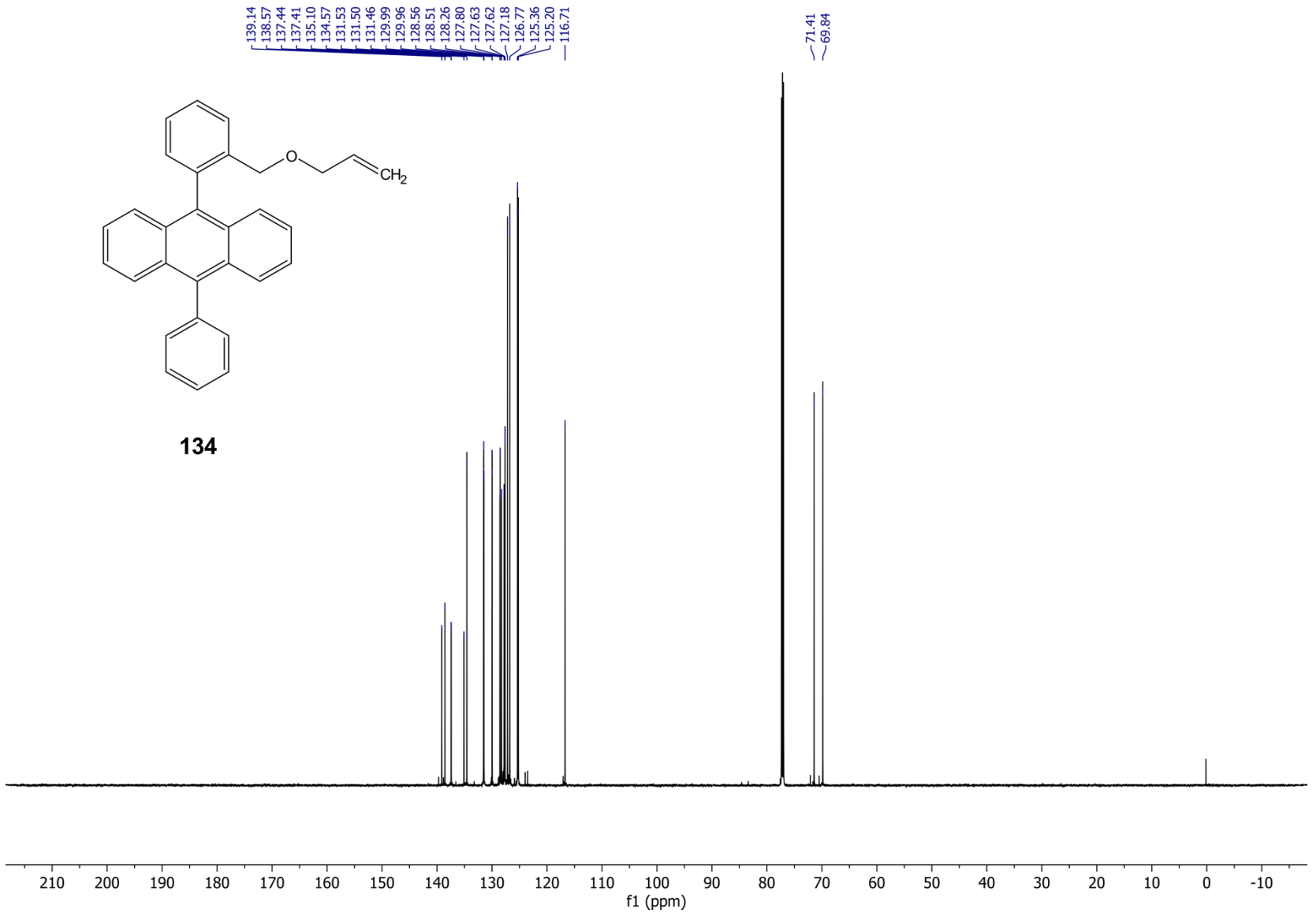
139.14
138.57
137.44
137.41
135.10
134.57
131.53
131.50
131.46
129.99
129.96
128.56
128.51
128.26
127.80
127.63
127.62
127.18
126.77
125.36
125.20
116.71
71.41
69.84
O
CH2
134
210 200 190 180 170 160 150 140 130 120 110 100 90 80 70 60 50 40 30 20 10 0 -10
f1 (ppm)

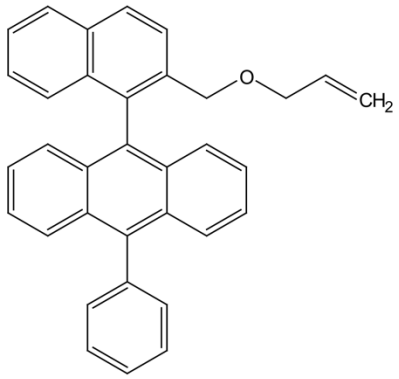
O
CH2

135

1.00
2.00
2.00
2.00
3.00
1.00
4.00
2.00
1.00
1.00
2.00
2.00
2.00
16
15
14
13
12
11
10
9
8
7
6
5
4
3
2
1
0
-1
-2
-3
f1 (ppm)

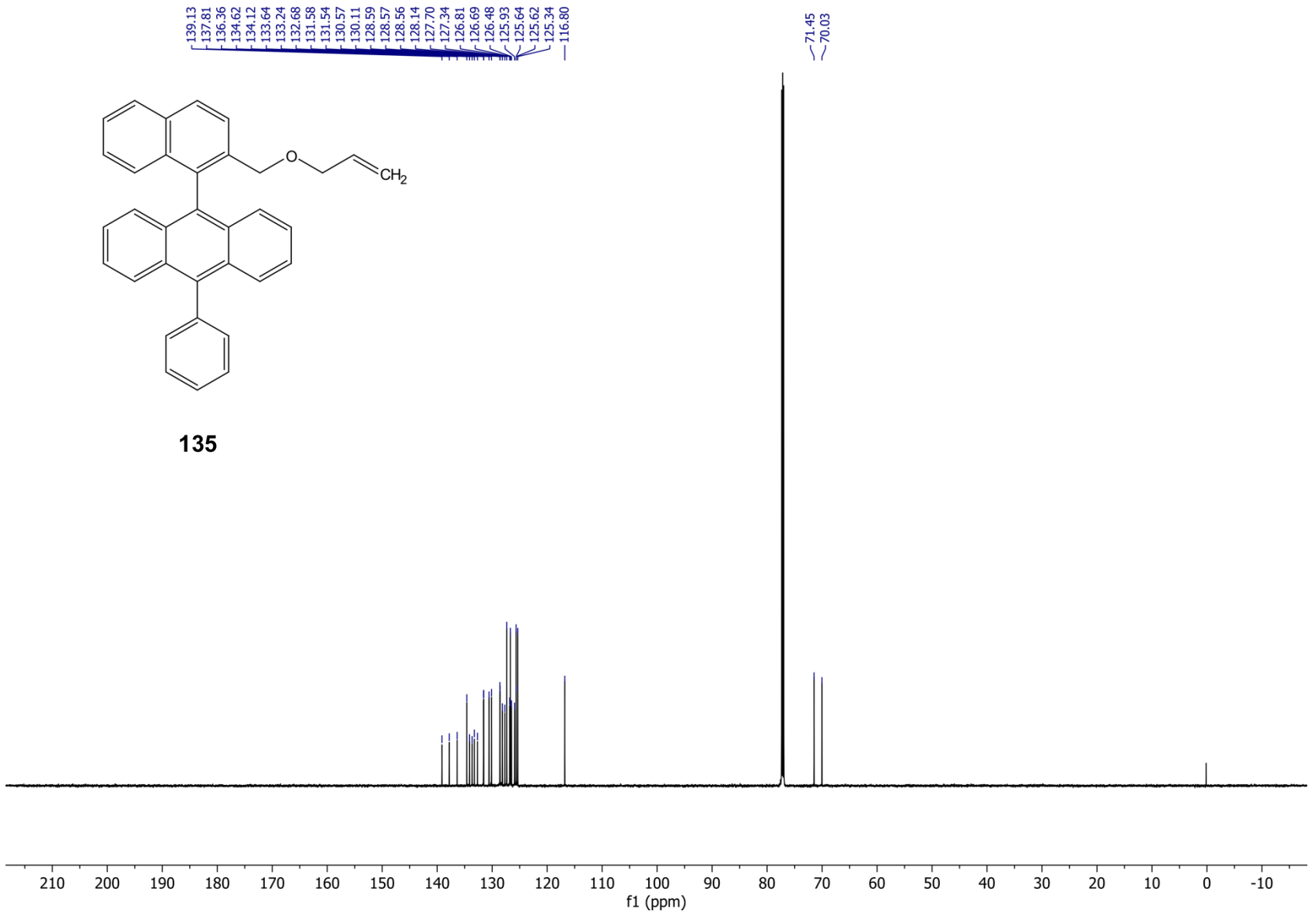
139.13
137.81
136.36
134.62
134.12
133.64
133.24
132.68
131.58
131.54
130.57
130.11
128.59
128.57
128.56
128.14
127.70
127.34
126.81
126.69
126.48
125.93
125.64
125.62
125.34
116.80
71.45
70.03
O
CH2
210
200
190
180
170
160
150
140
130
120
110
100
90
80
70
60
50
40
30
20
10
0
-10
f1 (ppm)

135

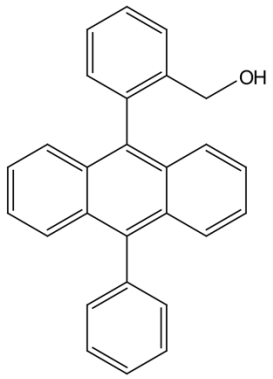
OH

136

1.00
2.00
3.00
5.00
1.00
5.00
2.00
1.00
16
15
14
13
12
11
10
9
8
7
6
5
4
3
2
1
0
-1
-2
-3
f1 (ppm)

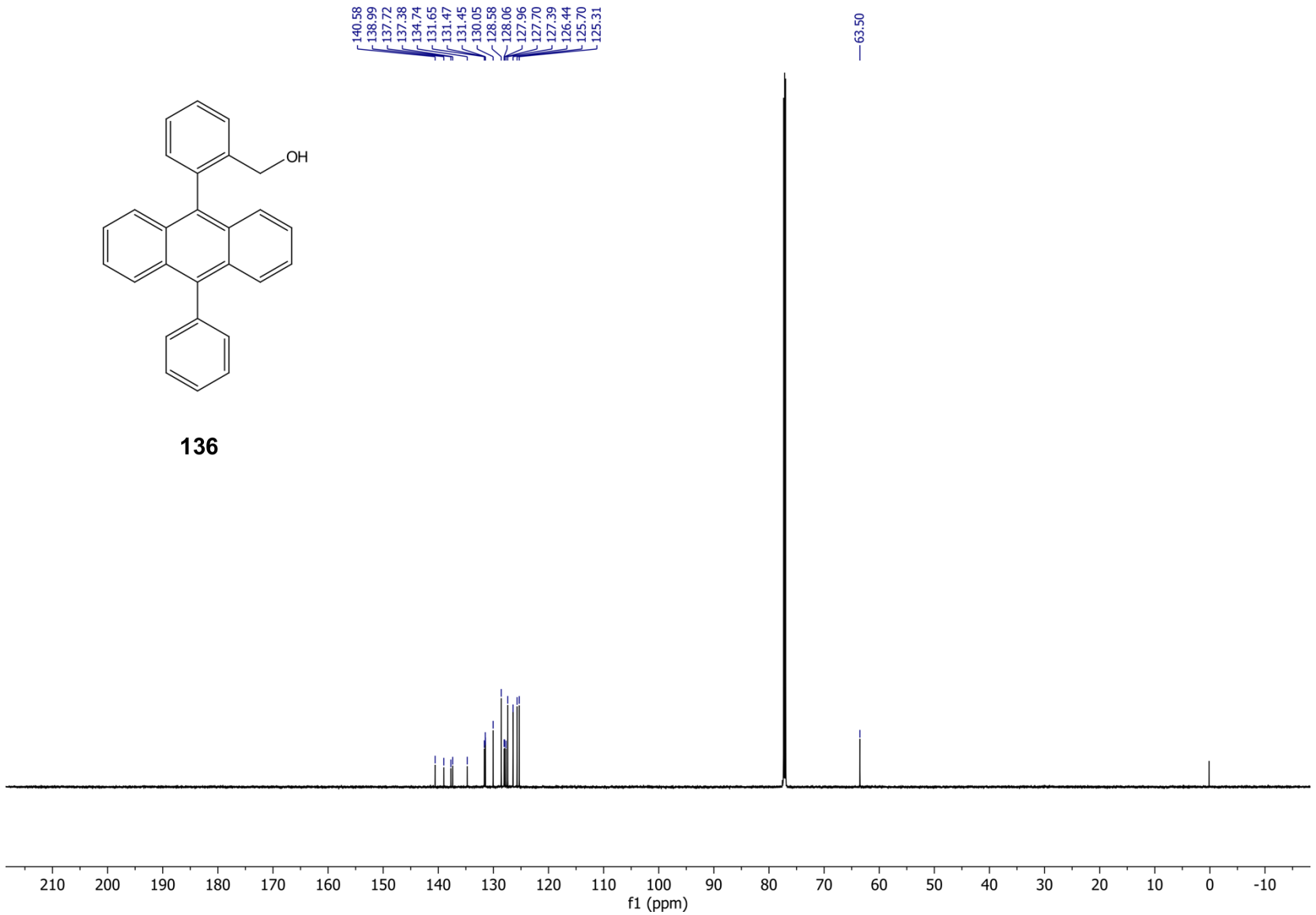
140.58
138.99
137.72
137.38
134.74
131.65
131.47
131.45
130.05
128.58
128.06
127.96
127.70
127.39
126.44
125.70
125.31
63.50
OH
210
200
190
180
170
160
150
140
130
120
110
100
90
80
70
60
50
40
30
20
10
0
-10
f1 (ppm)

136

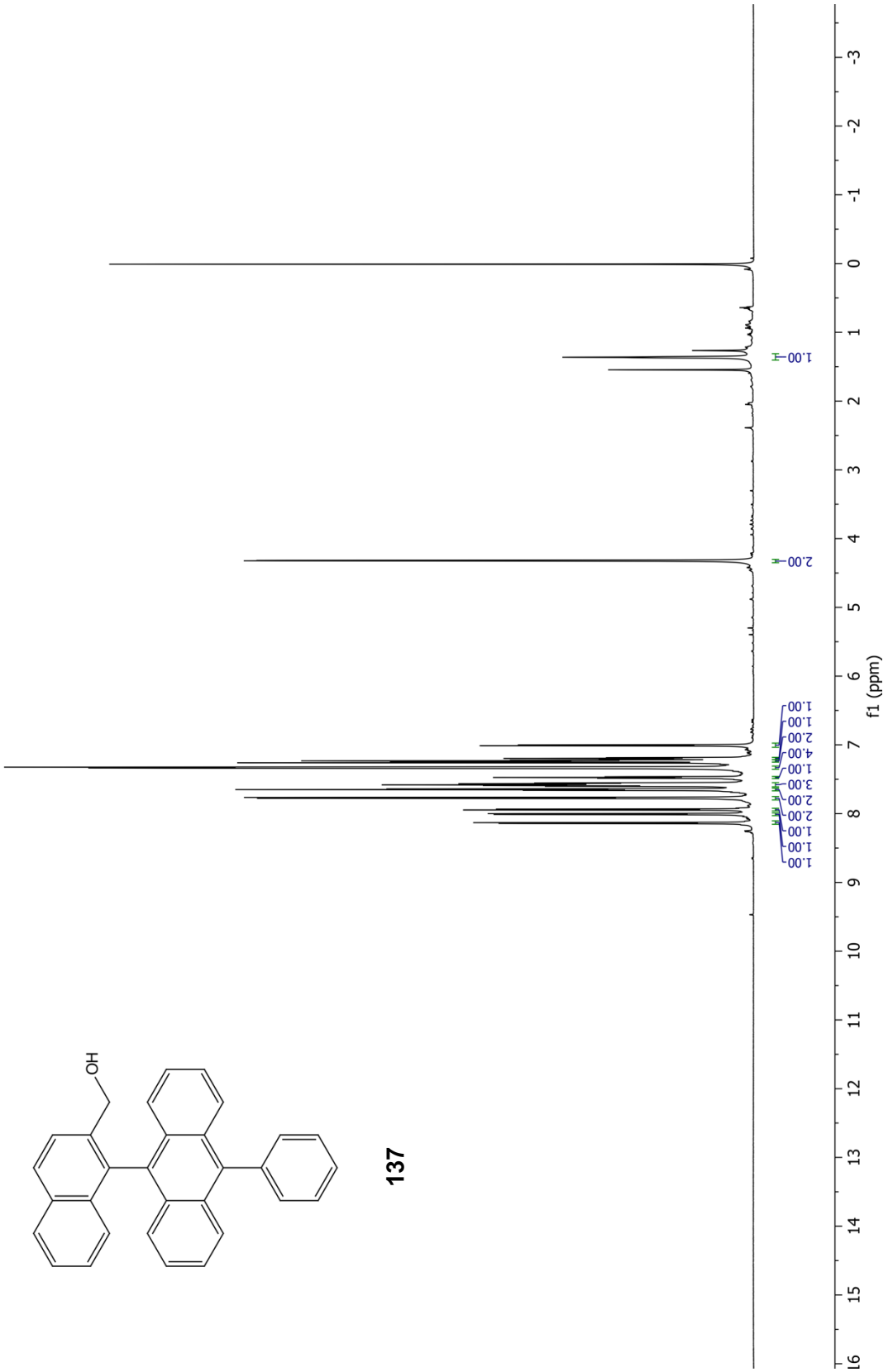
OH
137
1.00
2.00
1.00
1.00
1.00
2.00
4.00
1.00
3.00
2.00
2.00
1.00
1.00
1.00
f1 (ppm)

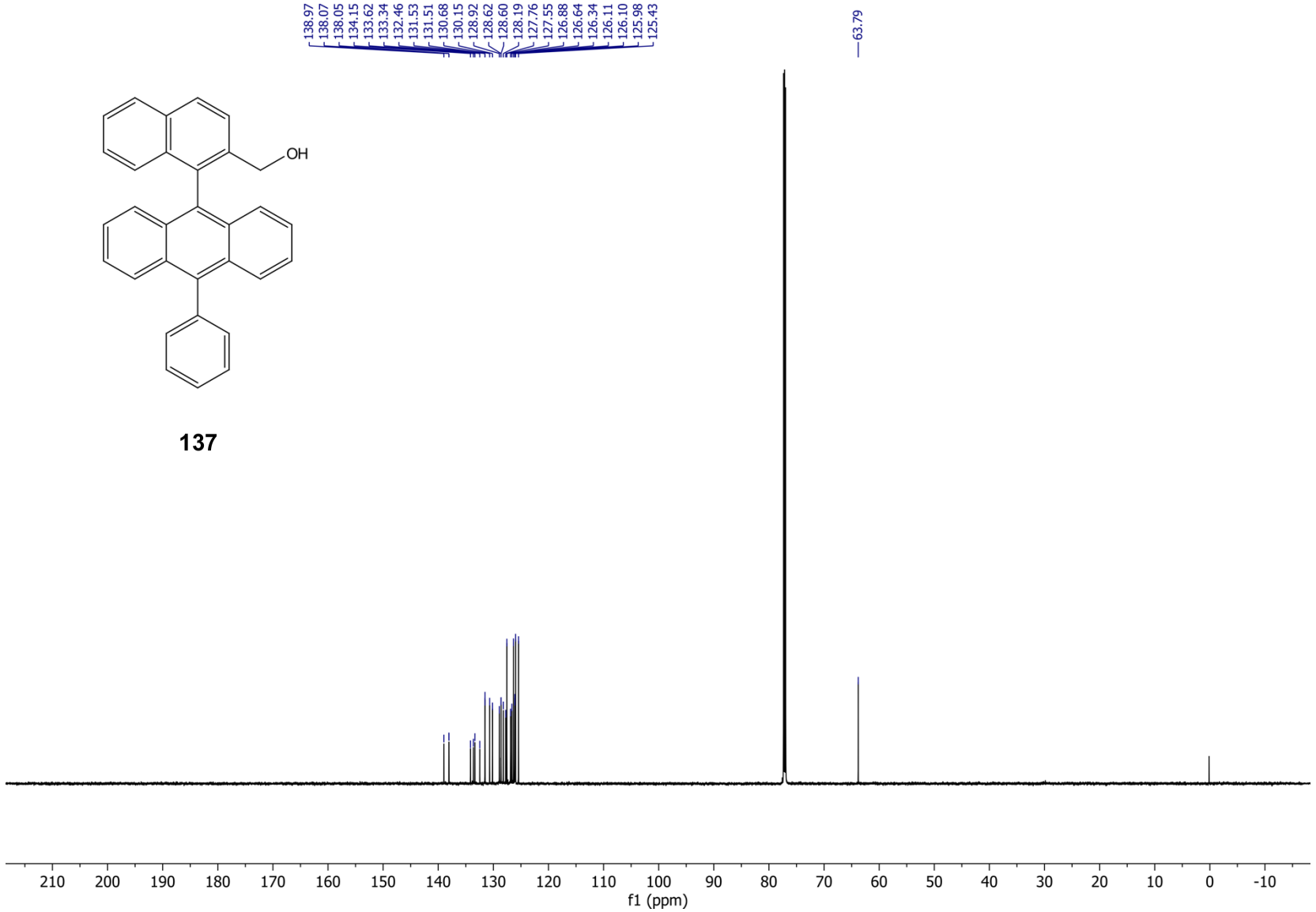
138.97
138.07
138.05
134.15
133.62
133.34
132.46
131.53
131.51
130.68
130.15
128.92
128.62
128.60
128.19
127.76
127.55
126.88
126.64
126.34
126.11
126.10
125.98
125.43
63.79
OH
210
200
190
180
170
160
150
140
130
120
110
100
90
80
70
60
50
40
30
20
10
0
-10
f1 (ppm)

137

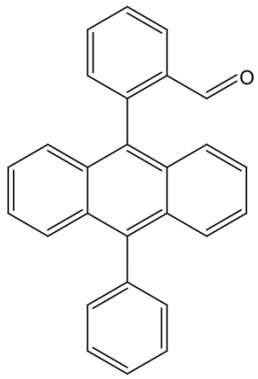
O

138

1.00
1.00
1.00
3.00
2.00
1.00
5.00
4.00
16
15
14
13
12
11
10
9
8
7
6
5
4
3
2
1
0
-1
-2
-3
f1 (ppm)

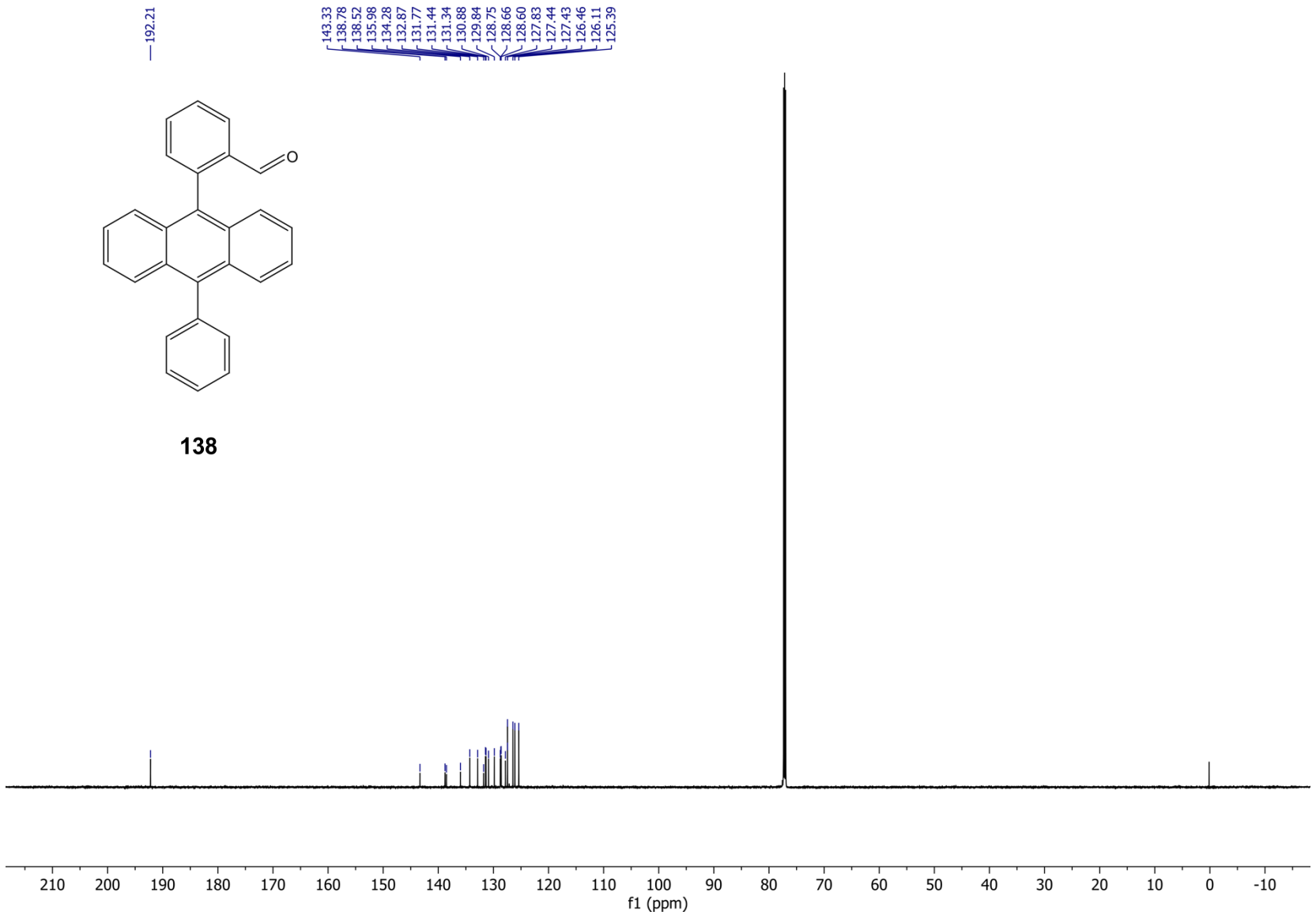
192.21
143.33
138.78
138.52
135.98
134.28
132.87
131.77
131.44
131.34
130.88
129.84
128.75
128.66
128.60
127.83
127.44
127.43
126.46
126.11
125.39
O
138
210
200
190
180
170
160
150
140
130
120
110
100
90
80
70
60
50
40
30
20
10
0
-10
f1 (ppm)

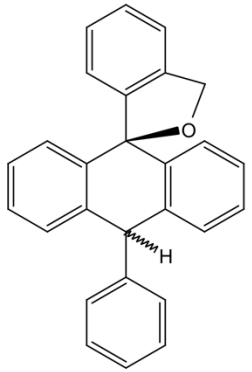

140

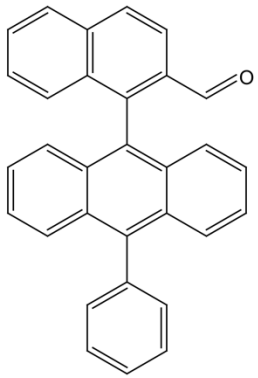
O

139

1.00
1.00
1.00
1.00
2.00
5.00
1.00
2.00
5.00
1.00
16
15
14
13
12
11
10
9
8
7
6
5
4
3
2
1
0
-1
-2
-3
f1 (ppm)

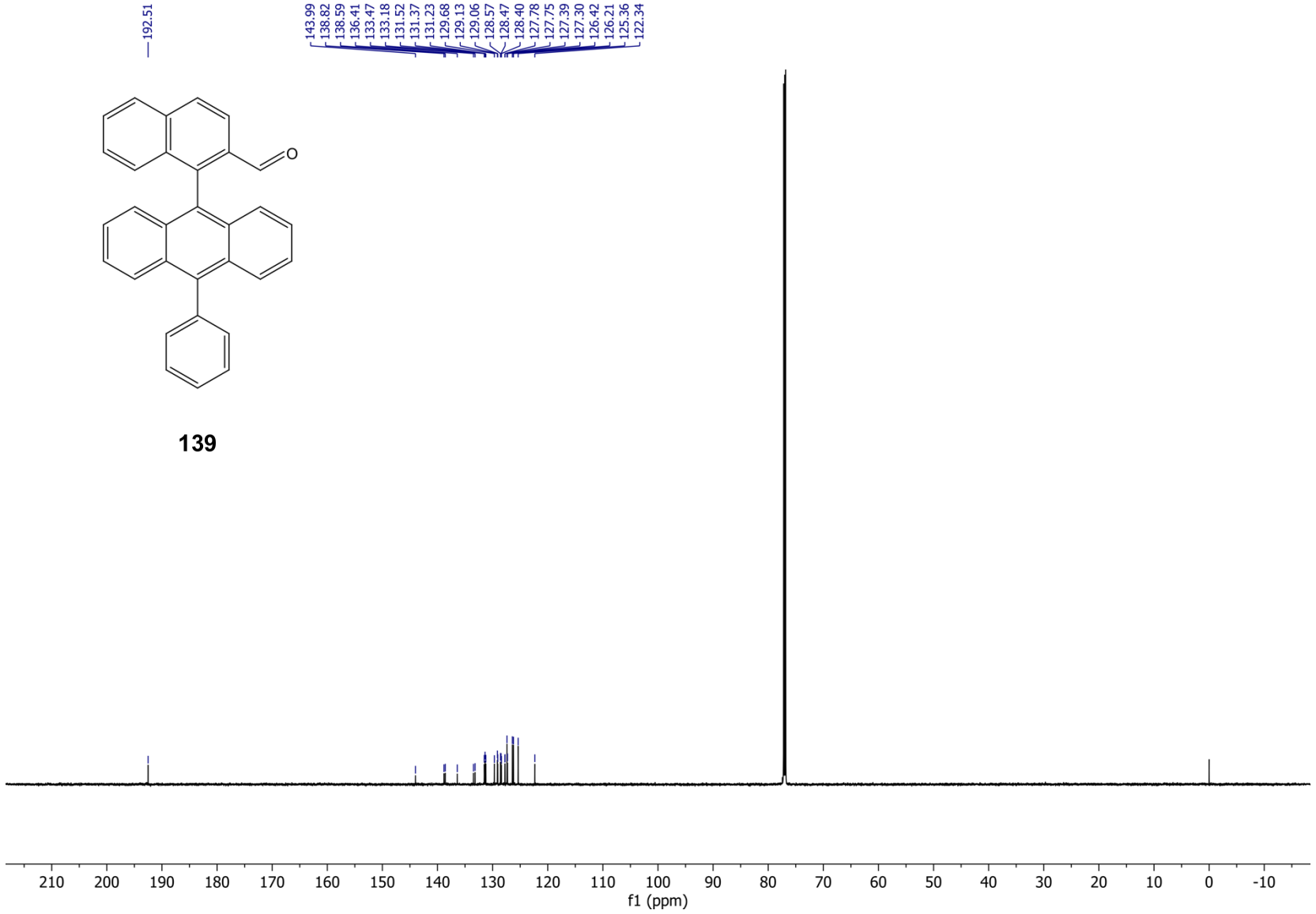
192.51
143.99
138.82
138.59
136.41
133.47
133.18
131.52
131.37
131.23
129.68
129.13
129.06
128.57
128.47
128.40
127.78
127.75
127.39
127.30
126.42
126.21
125.36
122.34
O
210
200
190
180
170
160
150
140
130
120
110
100
90
80
70
60
50
40
30
20
10
0
-10
f1 (ppm)

139

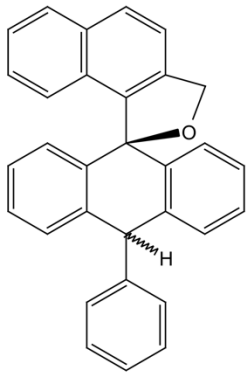
O
H

141

1.00
1.00
4.00
1.00
6.51
2.00
3.00
2.00
2.00
1.00
13
12
11
10
9
8
7
6
5
4
3
2
1
0
-1
f1 (ppm)

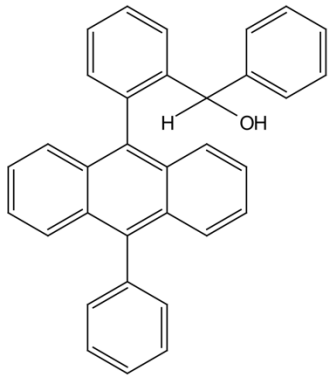

142

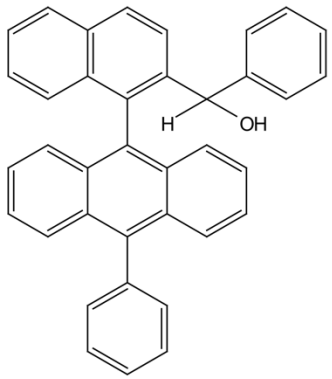
H
OH

143

1.00
1.00
1.00
1.00
2.00
3.00
2.00
3.00
2.00
5.00
2.00
1.00
1.00
13
12
11
10
9
8
7
6
5
4
3
2
1
0
-1
f1 (ppm)

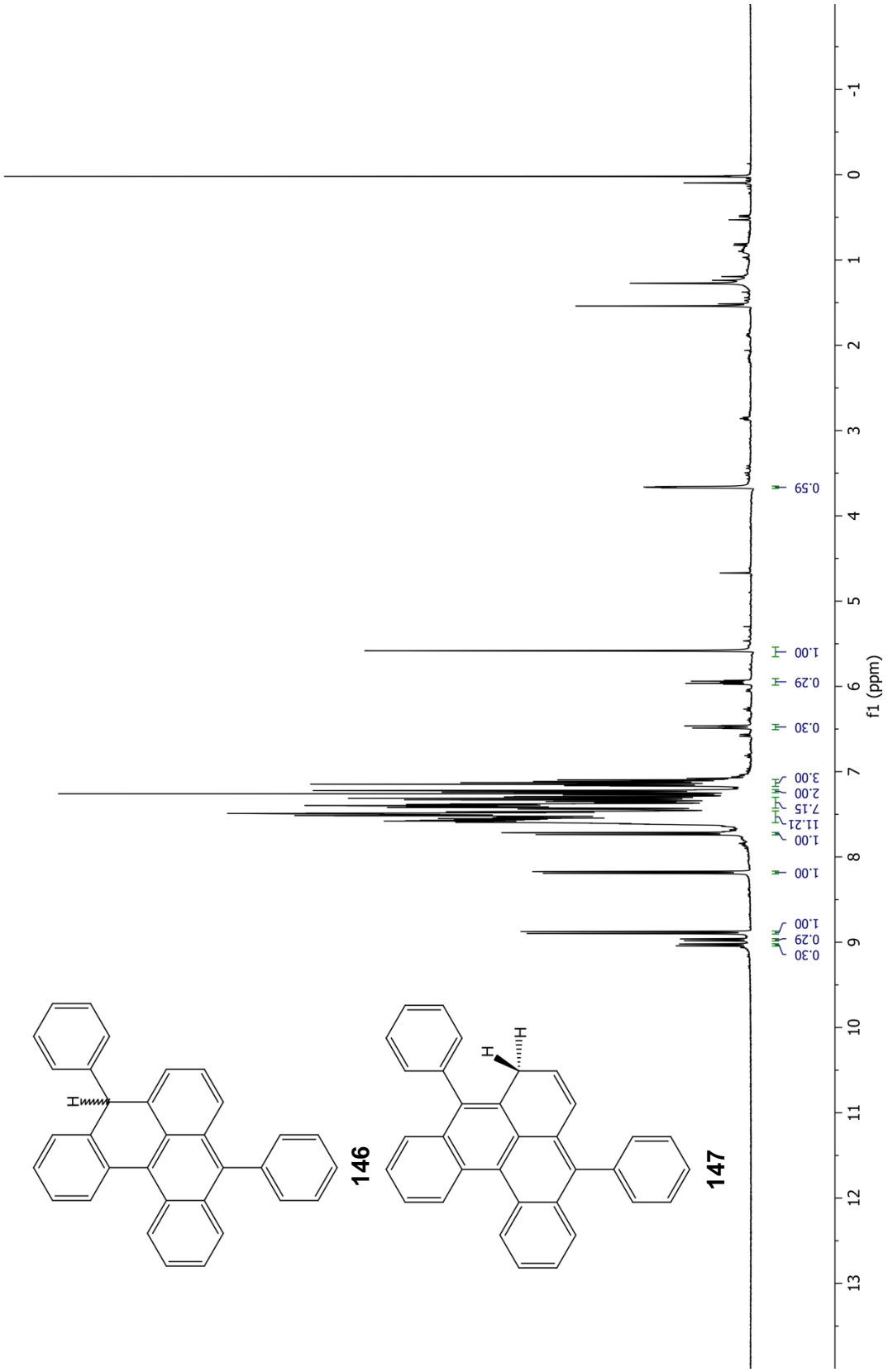
I
H
H
146
147
0.30
0.29
1.00
1.00
1.00
11.21
7.15
2.00
3.00
0.30
0.29
1.00
0.59
f1 (ppm)

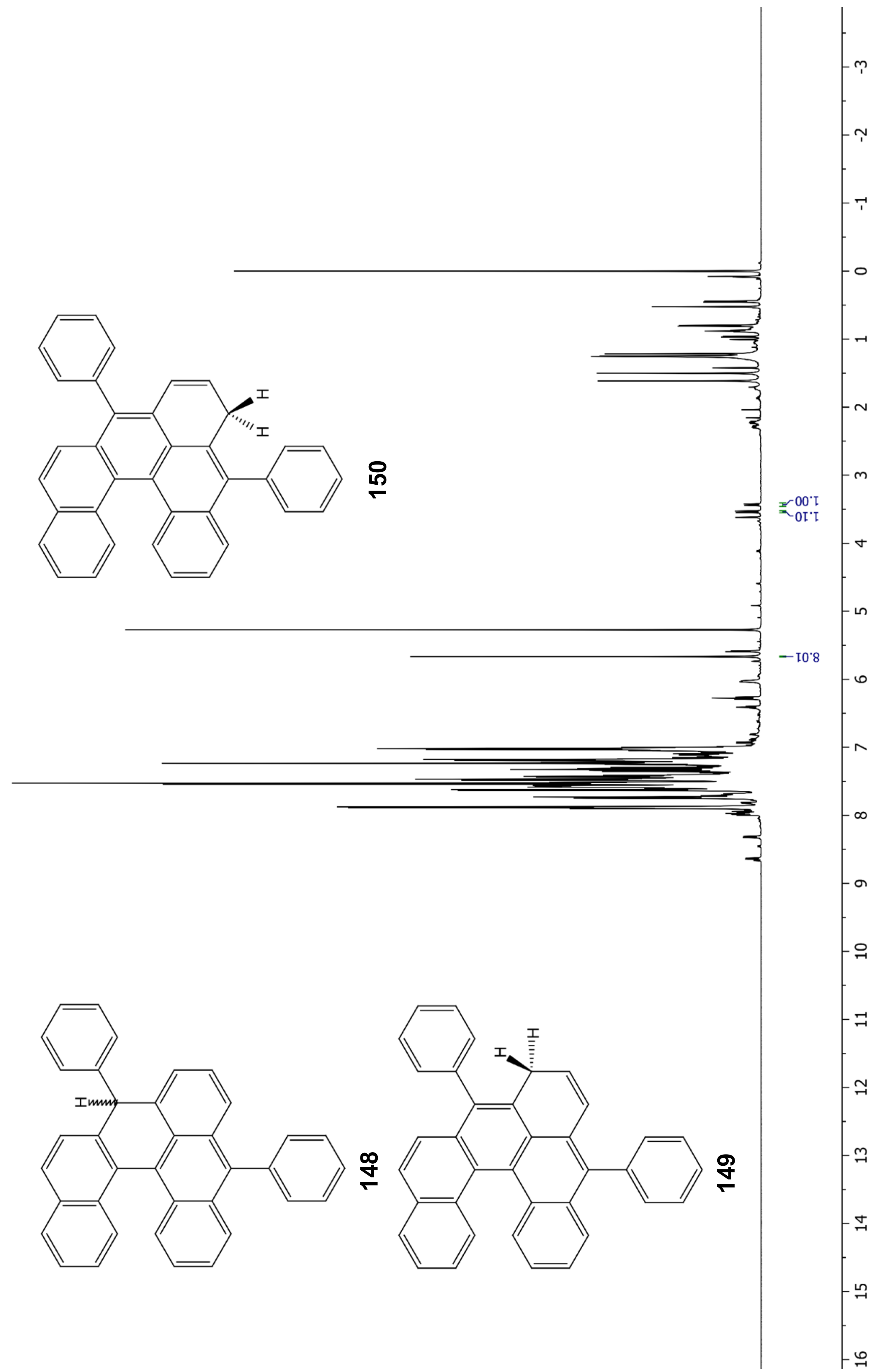
148
149
150
f1 (ppm)
8.01
1.10
1.00

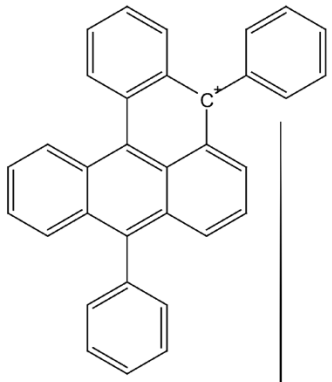

144

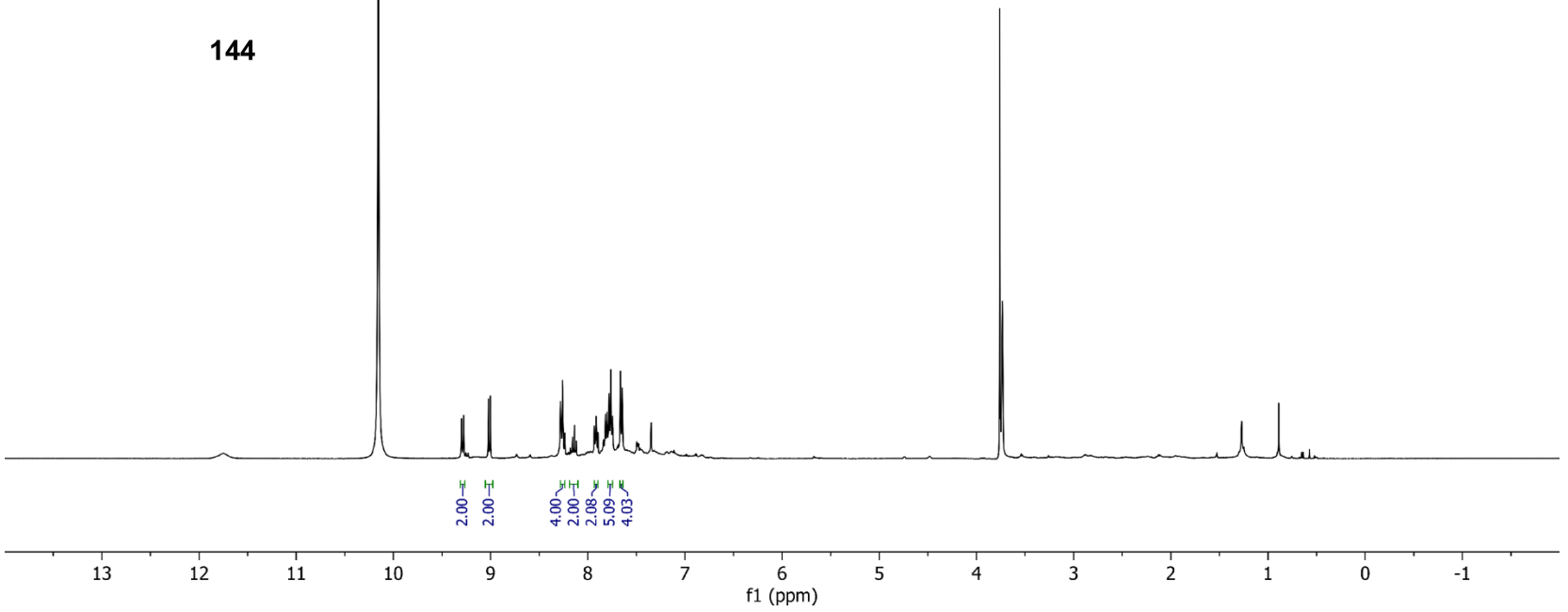

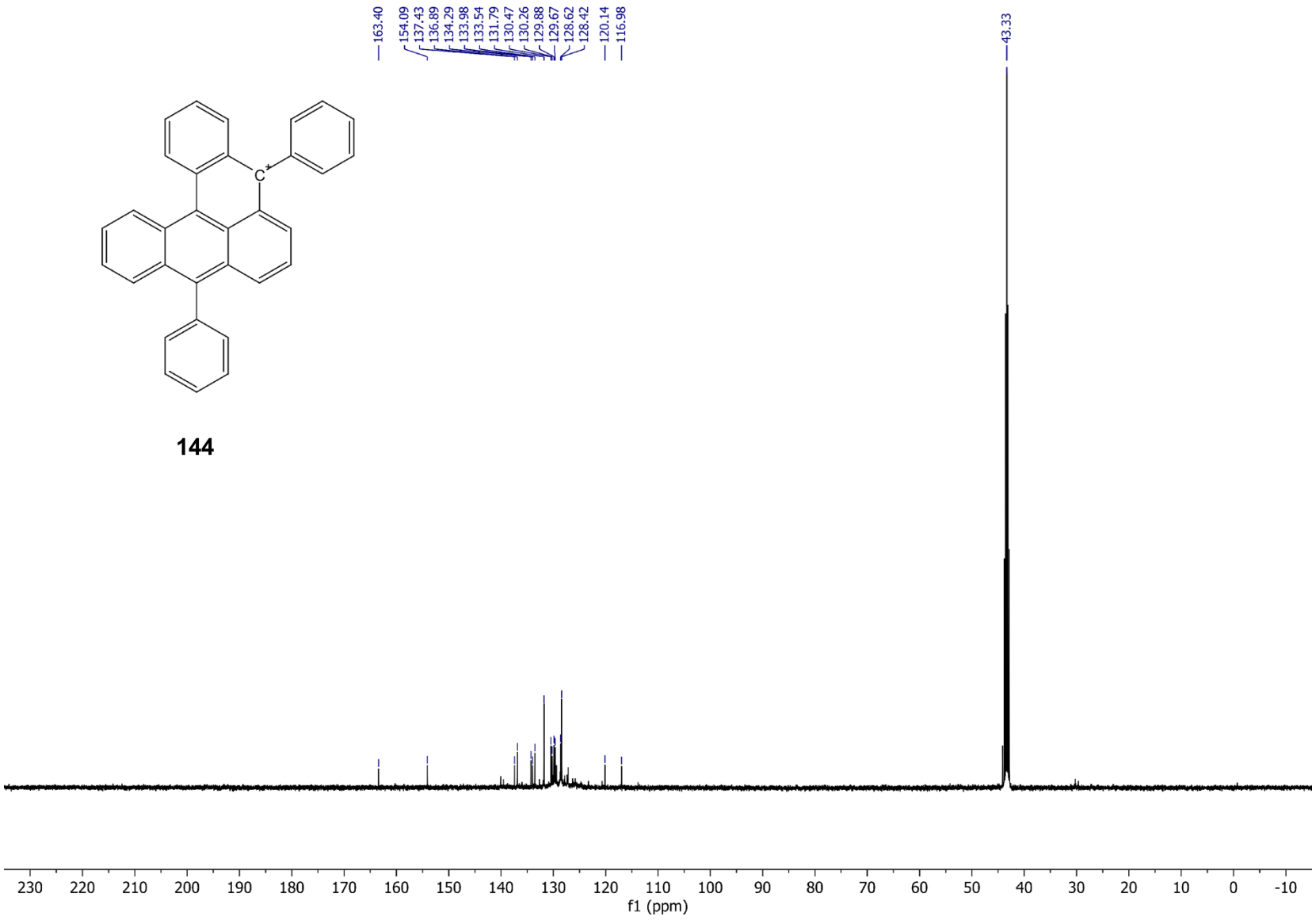
163.40
154.09
137.43
136.89
134.29
133.98
133.54
131.79
130.47
130.26
129.88
129.67
128.62
128.42
120.14
116.98
43.33
C+
230 220 210 200 190 180 170 160 150 140 130 120 110 100 90 80 70 60 50 40 30 20 10 0 -10
f1 (ppm)

144

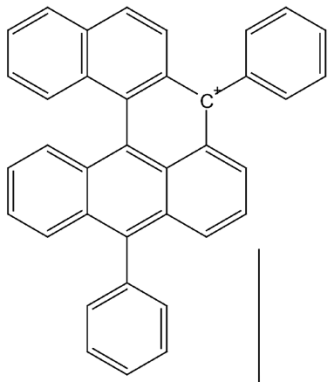

145

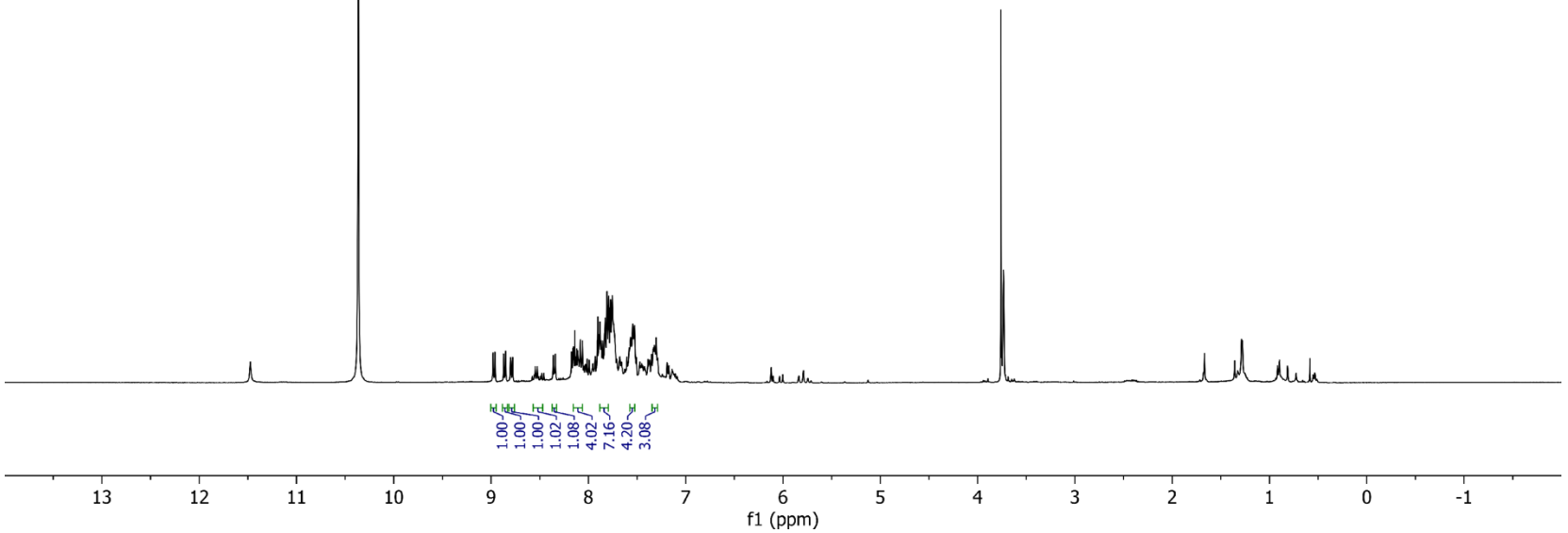
1.00
1.00
1.00
1.02
1.08
4.02
7.16
4.20
3.08
13
12
11
10
9
8
7
6
5
4
3
2
1
0
-1
f1 (ppm)

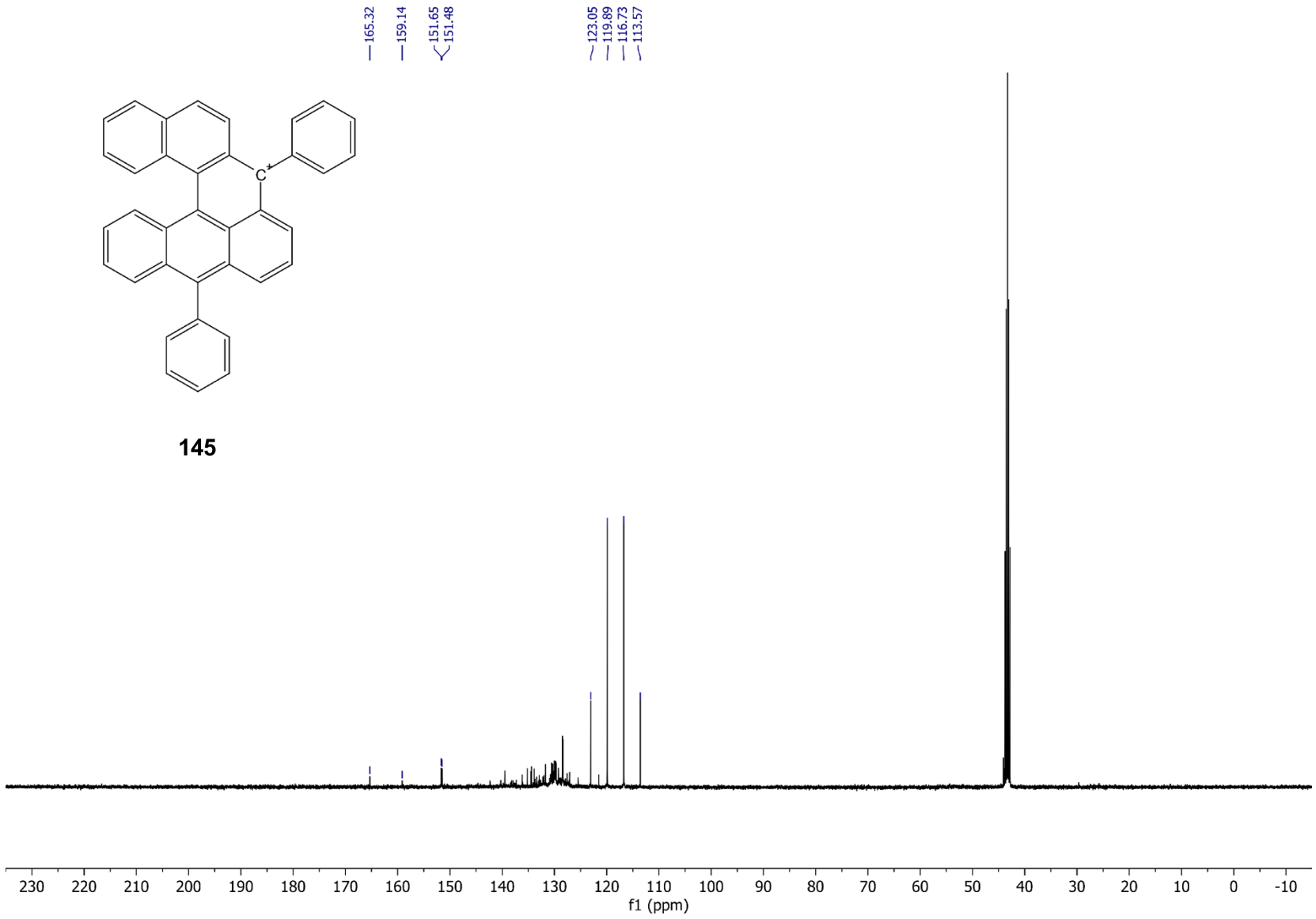
165.32
159.14
151.65
151.48
123.05
119.89
116.73
113.57
C+
230 220 210 200 190 180 170 160 150 140 130 120 110 100 90 80 70 60 50 40 30 20 10 0 -10
f1 (ppm)

145